Characterising the response to gliotoxin exposure in *Aspergillus fumigatus* Δ*gliT* and Δ*gliZ*

Stephen Hammel B.Sc.

Thesis is submitted to the

National University of Ireland

for the degree of

Doctor of Philosophy

October 2013

Supervisors

Dr. Gary Jones

Prof. Sean Doyle

National University of Ireland

Maynooth

Co. Kildare

Head of Department

Prof. Paul Moynagh

Table of Contents

Declaration of Authorship

This thesis has not been previously submitted in whole or part to this or any other University for any other degree. This thesis is the sole work of the author, with the exception of the creation of Δ*gliZ* which was carried out by Bok *et al*., (2006) and the *A. fumigatus* Δ*gliT* which was created by Schrettl *et al*., (2010).

Stephen Hammel B.Sc.

Acknowledgements

Firstly I would like to sincerely thank Dr. Gary Jones and Prof. Sean Doyle for giving me the opportunity to work on such an interesting project. I would also like to thank them for their guidance and help over the last number of years, which has been deeply appreciated and I has helped me learn a lot. Thanks to Dr. David Fitzpatrick for his help with the RNA Seq data.

I want to thank the many people who have helped me throughout my Ph.D., to everyone in the Biology Dept., especially my fellow 'yeasties' Jen and Naushie; Cindy, Gráinne and Rebecca who were very patient with the constant bombardment of questions I constantly threw at them. Lara for my new addiction; Kevin, Stephen No# 2, Niamh and Elizabeth for the craic and much needed coffee breaks. Nick for the many chats, and not so many repair jobs, and all the technicians in the Biology Dept. who were always there when I needed to borrow something and give it back months later when I remembered.

Thanks to my parents who supported me throughout my Ph.D., especially when they didn't understand what I was saying but still managing to say the right thing. I really appreciate all you have done for me. Jane, you have helped me so much, thank you for being so patient and supportive of something which took your boyfriend away from you and turned him into a hermit for the last few months. I promise to make it up to you.

Presentations

Oral Presentation

"Seq'n a Response". Irish Fungal Society Meeting, NUI Maynooth, Kildare, June 2013.

"Best Laid Plans of Mice and…Moths?" IGNITE, NUI Maynooth, May 2013

"Life of Gli: Analysis of key Gliotoxin Cluster Genes" Biology Department Research Day, NUI Maynooth, April 2013

"The redox-active fungal metabolite, gliotoxin, induces transcriptional remodelling in *Saccharomyces cerevisiae*". Irish Fungal Society Meeting, Queens University Belfast, Belfast, June 2012

"Examining the i*n vivo* Response to Gliotoxin in *Saccharomyces cerevisiae.*" Biology Departmental Talk, NUI Maynooth, May 2011

Poster Presentations

"Seq'ing a Response: A Transcriptomic Study of Gliotoxin Exposure in *Saccharomyces cerevisiae* and *Aspergillus fumigatus*." Biology Departmental Research Day, May 2013

"Using *Saccharomyces cerevisiae* to assess the *in vivo* cellular responses to gliotoxin exposure." European Conference of Fungal Genetics, Marburg Germany, March 2012.

"Using *Saccharomyces cerevisiae* to assess the *in vivo* cellular responses to gliotoxin exposure." FEBS Advanced Lecture Course: Human Fungal Pathogens, La Colle sure Loup, France, May 2011

Publications

Carberry, S. Molloy, E., **Hammel, S**., O'Keeffe, G., Jones, G.W., Kavanagh, K., Doyle, S.,(2012). Gliotoxin effects on fungal growth: mechanisms and exploitation. *Fungal genetics and biology: FG & B*, **49**(4), pp.302–12.

Abbreviations

2D-PAGE	Two dimensional polyacrylamide gel electrophoresis
aa	Amino acid
ABPA	Allergic bronchopulmonary aspergillosis
ADA	Adenosine deaminase deficiency
AMM	Aspergillus minimal media
AMP	Anti-microbial peptides
AmpB	Amphotericin B
AMT	*Agrobacterium*-mediated transformation
AP	Alkaline phosphatise
ATCC	American Type Cell Culture
ATP	Adenosine triphosphate
bp	Base pairs
BSA	Bovine serum albumin
bZIP	Basic leucine zipper
CADRE	Central *Aspergillus* Data Respository
cDNA	Complementary deoxyribonucleic acid
CDNB	1-chloro-2,4-nitrobenzene
cds	Coding sequence
CGD	Chronic granulomatous disease
CIAP	Calf intestine alkaline phosphate
CoA	Coenzyme A
CRD	Cysteine rich domain
CSPD	Chemiluminescent substrate phosphate detection
DIG	Digoxigenin

DIGE	Differential gel electrophoresis
DMSO	Dimethyl sulfoxide
DNA	Deoxyribonucleic acid
DTNB	5,5'-dithiobis-(2-nitrobenzoic acid)
ECL	Enhanced chemiluminescent
EDTA	Ethylenediaminetetraacetic acid
eEF1	Eukaryotic elongation factor 1
eIF	Eukaryotic initiation factor
EF	Elongation factor
ER	Endoplasmic reticulum
eRF	Eukaryotic termination release factor
ERAD	Endoplasmic reticulum associated degradation
gDNA	genomic deoxyribonucleic acid
GR	Glutathione reductase
GST	Glutathione *s*-transferase
GSH	Glutathione
GSSG	Glutathione disulphide
H_2O_2	Hydrogen peroxide
HCCA	α-cyano-4-hydroxycinnaminic acid
HR	Homologous recombination
IA	Invasive Aspergillosis
IEF	isoelectric focusing
IgE	Immunoglobulin
Kb	Kilobase
kDa	Kilodalton
LB	Luria Bertani

LC-MS	Liquid chromatography mass spectrometry
MALDI-ToF MS	Matrix assisted laser desorption time of flight mass spectrometry
MEA	Malt extract agar
MOPS	3-(N-morpholino)propanesulfonic acid
MRP	Multidrug resistance associated protein
NADH	Nicotinamide adenine dinucleotide
NADPH	Nicotinamide adenine dinucleotide phosphate
NHEJ	Non-homologous end joining
nm	Nanometer
NRP	Non ribosomal peptide
NRPS	Non ribosomal peptide synthetase
OD	Optical density
ORF	Open reading frame
PBS	Phosphate buffered saline
PBST	Phosphate buffered saline-Tween
PCR	Polymerase chain reaction
PEG	Polyethylene glycol
PMSF	Phenylmethylsulfonyl fluoride
RNA	Ribonucleic acid
ROS	Reactive oxygen species
RP-HPLC	Reverse-phase High performance liquid chromatography
RPM	Revolutions per minute
RT-PCR	Reverse-transcriptase polymerase chain reaction
SAM	s-adenosyl methionine
SDS	Sodium dodecyl sulphate

SDS-PAGE	Sodium dodecyl sulphate polyacrylamide gel electrophoresis
SSA	5’5-sulfosalicyclic acid
TAE	Tris:acetate:EDTA
TB	Tuberculosis
TCA	Trichloroacetic acid
TFA	Trifluroacetic acid
tRNA	transfer RNA
µM	Micro metre
UV	Ultraviolet
v/v	volume per volume
w/v	weight per volume

Summary

The non-ribosomal peptide gliotoxin, is a toxic fungal secondary metabolite produced by the filamentous fungus *Aspergillus fumigatus*. Previous work has implicated its potent anti-fungal properties and importance as a virulence factor in human infection. Availability of the *A. fumigatus* genome has allowed for the characterisation of the gliotoxin biosynthetic cluster *gli*, with previous work illustrating the importance of the thioredoxin reductase *gliT* in self protection against gliotoxin, regulation of which has been shown to be independent of the transcriptional role of *gliZ* in regulating the cluster. The work presented here characterises the creation of a double gene deletion strain lacking both *gliT* and *gliZ* (Δ*gliT*Δ*gliZ*) ultimately silencing the *gli* cluster. Phenotypic characterisation revealed that Δ*gliT*Δ*gliZ* is more sensitive to gliotoxin challenge when compared with Δ*gliZ*, yet is more resistant when compared with Δ*gliT*, highlighting the importance of *gliT* in protection against gliotoxin, especially when the cluster is still expressed.

An anti-oxidant role for gliotoxin is highlighted, with co-addition of gliotoxin and hydrogen peroxide resulting in a reduction in the production of reactive oxygen species in *A. fumigatus*, when compared with hydrogen peroxide only treated cells.

Additionally, proteomic and transcriptomic data indicate gliotoxin exposure dysregulates S-adenosyl-L-methionine biosynthesis with key enzymes of this pathway, i.e., S-adenosyl-L-homocysteinase and cobalmin-independent L-methionine synthase, eliciting significant changes in their respective expression in response to gliotoxin in *A. fumigatus* an also in *Saccharomyces cerevisiae*. Using a gene candidate approach, *S. cerevisiae* Δ*sod1* and Δ*yap1* sensitivity to exogenous gliotoxin suggest gliotoxin induces some form of oxidative stress on the cell. Furthermore, low to null levels of glutathione were seen to be advantageous to the *S. cerevisiae* mutant strain Δ*gsh1*, eliciting resistance to gliotoxin challenge. Similarly, glutathione levels were found to significantly altered in *A. fumigatus gliT* and *gliZ* mutant lysates and may be a factor in their respective gliotoxin sensitivity.

Overall this work highlights key factors which may contribute to gliotoxin toxicity. Highlighting the importance of gliotoxin biosynthetic genes and the pathways involved in the response to gliotoxin exposure.

Chapter 1

Introduction

1.1 *Aspergillus fumigatus*

The genus *Aspergillus* consists of approximately 200 species, 20 of which have been associated with some form of disease (Tomee & Werf 2001). The most pathogenic species *A. fumigatus*, was first described in 1863 after being isolated from avian lung tissue and is responsible for approximately 90 % of all invasive aspergillosis cases (Dagenais & Keller 2009). *A. fumigatus* is an omnipresent saprophytic fungus which naturally occupies niches within soil environments or decaying organic matter where it plays an important role in carbon and nitrogen recycling (Latge 2001).

The fungus produces thousands of airborne hydrophobic conidia which are released into the surrounding environment facilitated by their small size (2.5-3 μm) and aerodynamic nature (Dagenais & Keller 2009). *A. fumigatus* life cycle entails the asexual production of haploid conidia in chains known as conidiophores, release of conidia into the environment, conidia germination and hyphal growth from which the new conidiophores and haploid conidia will be produced (Latgé 1999). The identification of sexual reproduction and development genes in *A.* fumigatus suggested it held the potential to reproduce both asexually and sexually (Galagan *et al.,* 2005). This was later confirmed with the identification of a functional sexual cycle in certain *A. fumigatus* isolates of different mating types.

1.2 *Aspergillus fumigatus*, a pathogenic fungus

A. fumigatus is an opportunistic human pathogen whose small spore size allows for easy access into the alveoli of the lungs of mammals (Latgé 1999). It is estimated that the average human breathes up to 200 conidia, rarely resulting in any adverse affects due to the efficient elimination via the host immune system (Philippe *et al.*, 2003). However, in the case of immuno-compromised individuals, this is not always the case and in these situations, patients are vulnerable to the onset of Invasive Aspergillosis (IA) (Dagenais & Keller 2009). *A. fumigatus* infections are classed into three categories which affect patients who are severely immuno-compromised (Daly & Kavanagh 2001; Thomson & Patterson 2008; Tomee & Werf 2001). Allergic broncho-pulmonary aspergillosis (ABPA) is caused by a poorly controlled inflammatory

response primarily, but not limited to, patients who have already been suffering from some type of pulmonary disease such as cystic fibrosis or prolonged asthma (Daly & Kavanagh 2001; Sherif & Segal 2012). It can be differentiated from other types of IA by the elevated levels of IgE in the sera of patients (Moss 2002). The second category consists of the formation of masses of *A. fumigatus* hyphae and mucous known as Aspergillomas or fungal balls first described by Deve (1938). These masses form in pre-existing pulmonary cavities, usually caused by TB, pneumonia or carcinoma (Thomson & Patterson 2008) and can continue to grow in mass without invading any pulmonary tissue for months or even years (Daly & Kavanagh 2001).

IA is the most prevalent form of *A. fumigatus* infection, affecting immunocompromised individuals, and is particularly dangerous in recipients of solid organ and hematopoietic transplants, HIV patients and leukaemia patients (Pagano *et al.,* 2001; Post *et al.,* 2007; Holding *et al.,* 2000). In these cases a mortality rate of ~80 %, is not un-common and greatly depends on the point of entry, immune status of the patient, and time of diagnosis (S.-jane Lin *et al.,* 2001). *A. fumigatus* can produce an array of secondary metabolites which contribute to its pathogenicity as well as its anti-fungal activity such as fumagillin, fumitremorgin, helvolic acid and gliotoxin (Nierman *et al.,* 2005; Kamei & Watanabe 2005; Dhingra *et al.,* 2013)

1.3 *A.* fumigatus genome

The genome sequence of *A. fumigatus* strain AF293 was fully sequenced in 2005 (Nierman *et al.,* 2005). From this the total size of the genome was found to possess a total of 9,926 predicted genes in 8 chromosomes totalling 29.4 Mb in size (Nierman *et al.,* 2005). Only 451 (4.61 %) of the open reading frames (ORFs) have been characterised to date out of a total number of 9,783 ORFs (Arnaud *et al.,* 2011). The availability of this genome sequence data has facilitated large scale studies into further understanding the response of this fungus to various stimuli. These include the transcriptional response to anti-fungal drugs like amphotericin B (Gautam *et al.,* 2008) and voricanazole (Ferreira *et al.,* 2006; Zhao *et al.,* 2012); transcriptional response to hosts' cells including neutrophils (Sugui *et al.,* 2008) and epithelial cells (Oosthuizen *et*

al., 2011); and response to environmental factors including hypoxia (Barker *et al.,* 2012) and heat shock (Albrecht *et al.,* 2010). It has also allowed for direct comparison with the different genomes of other strains and *Aspergillus spp*. For example Fedorova *et al,* (2008) showed that a great translocation event had taken place between chromosomes 1 and 6 of AF293 when compared with the genome of *A. fumigatus* A1163, with 99.8 % similarity seen in core related genes at the nucleotide level. Similarly, when the size of the *A. fumigatus* genome is compared to the genome of *A. oryzae* it was found to be 34 % smaller, yet shares ~ 77 % identity with *A. oryzae* (Machida *et al.,* 2005; Galagan *et al.,* 2005). Additionally, when compared to *A. nidulans,* the *A. fumigatus* genome is 7% smaller and only shares ~66 % identity (Galagan *et al.,* 2005). Interestingly, > 70 % of each genome could be mapped onto conserved syntenic blocks of genes, even though they show re-arrangement (Galagan *et al.,* 2005). The regions where there is a loss of synteny occur near or within sub-telomeric regions, known for rapid re-arrangement and possible species-specific evolution of genes and is also where many secondary metabolite clusters have been shown to be located in *A. fumigatus* (Galagan *et al.,* 2005; Perrin *et al,* 2007a). This can be seen when the genes of *A. fumigatus*, *A. niger* and *A. nidulans* are compared, whereby there are 500 specific genes in *A. fumigatus* which share no homology with the other two species (Nierman *et al.,* 2005). Many of these are involved in secondary metabolite biosynthesis which will be discussed in more detail in the next section.

1.4 Secondary metabolite clusters and biosynthesis

Keller defines secondary metabolites as low molecular mass, bioactive molecules associated with secondary metabolism usually produced at specific morphological stages in the life cycle of the fungus but which are not essential for growth (Keller *et al.,* 2005). Secondary metabolism may refer to any process which is not directly linked to the primary growth of the organism. Secondary metabolites can be grouped into four broad categories: Alkaloids which include fumigclavines and fumitremorgins; terpenes which include gibberellin and asristolochene; polyketides which include fusarin C and aflatoxin and non-ribosomal peptides which include gliotoxin (Keller *et al.,* 2005; Fox & Howlett 2008)

The purpose of these secondary metabolites is to enable the fungus to adapt to its surroundings, improving its chance of survival by decreasing the fitness of competing microbes in their environment (Losada *et al.,* 2009). The effectiveness of these secondary metabolites and their uses against other microbes is exemplified in the use of the antibiotic penicillin or the cholesterol-reducing compound, lovastatin a.k.a. mevinolin (Demain & Elander 1999; Alberts *et al.,* 1980). However some secondary metabolites, known as mycotoxins, are quite toxic, and include aflatoxin which has been associated as a major risk factor for liver cancer in humans when it is ingested from certain contaminated food-stuff, and gliotoxin which will be discussed in more detail later (Groopman *et al.,* 1988; Jones & Hancock 1988).

Due to the many benefits secondary metabolites can have, much research has gone into the identification of new metabolites and fungi (Schulz *et al.,* 2002; Rateb & Ebel 2011). However, the production of many other secondary metabolites remain silenced under normal laboratory growth conditions, requiring specific conditions and stimuli in order for them to be expressed (Brakhage *et al.,* 2008; Hertweck 2009; Brakhage & Schroeckh 2011).

The biosynthesis of these secondary metabolites requires the presence of different 'backbone' enzymes which catalyse the initial biosynthetic step. These include non-ribosomal peptide syntethases (NRPS), polketide synthases (PKS), prenyl-transferases (DMATS) and terpene cyclises (Khaldi *et al.,* 2011). In the case of the NRPS and PKS enzymes, there exists particular domains which facilitate their function in the cell. In the *A. fumigatus* NRPS GliP (Figure 1.1), there exists two adenylation domains which are involved in amino acid activation, three thiolation domains which are involved in anchoring the growing polypeptide chain during biosynthesis and two condensation domains which help catalyse the formation of peptide bonds (Balibar & Walsh 2006; Brakhage & Schroeckh 2011). Other domains, also known as 'decorating' domains, can exist which further modify the metabolite, include methyltransferases and epimerisation domains which may also be present (Walsh *et al.,* 2001). PKS modules use slightly different domains such as an acyltransferase domain, acyl carrier protein and ketoacyl synthase (Brakhage & Schroeckh 2011). The final metabolite can then be

transported from the cell via a specific transporter which can be found within the cluster also (Khaldi *et al.,* 2011).

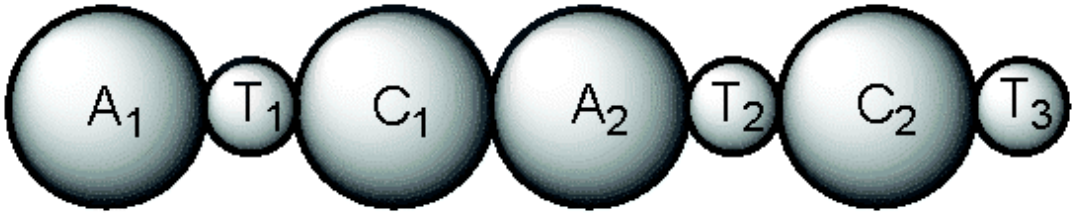

Figure 1.1 Schematic of the non-ribosomal synthetase GliP adapted from Balibar & Walsh 2006. Adenylation domain (A), Thiolation domain (T) and Condensation domain (C) are depicted in their respective positions along the NRPS

Certain clusters can be regulated by transcription factors which are encoded within their cluster such as GliZ of the gliotoxin biosynthetic cluster and ChaZ of the chaeotocin biosynthetic cluster (Gardiner & Howlett 2005; Gerken & Walsh 2013). Not all gene clusters are regulated by transcription factors encoded within the same cluster. Some are regulated by other external regulators such as the secondary metabolite global transcriptional regulators LaeA and VeA (Perrin *et al.,* 2007; Fox & Howlett 2008; Dhingra *et al.,* 2013). LaeA is a highly conserved, nuclear protein found to have global effects on the regulation of a plethora of different genes and pathways including secondary metabolite clusters in *A. fumigatus* (Bok & Keller 2004). LaeA was first characterised by Bok *et al.,* (2004) identifying its role as a global regulator of secondary metabolism with loss of LaeA in an *A. fumigatus* Δ*laeA* strain resulting in the abrogation of gene expression of several metabolic gene clusters. Additionally, Bok *et al.,* (2005) demonstrated that loss of *A. fumigatus laeA* resulted in abolition of gliotoxin biosynthesis and subsequent attenuation in virulence of mice hosts, further supporting gliotoxin as a virulence factor in IA. Additionally, Perrin *et al.,* (2007) highlighted that

loss of *laeA* in *A. fumigatus* resulted in 13 of 22 characterised secondary metabolite gene clusters to have significantly lower gene expression when compared to *A. fumigatus* wild-type. Furthermore, they identified that LaeA positively regulated 20-40 % of the major secondary metabolite biosynthesis classes. LaeA regulation of secondary metabolite gene clusters is facilitated by its SAM binding site and subsequent manipulation of chromatin re-modelling in the nucleus thus affecting expression (Bok *et al.*, 2006; Shwab *et al.*, 2007)

Similar to LaeA, VeA is a global regulator of gene expression effecting genes involved in sexual and asexual development in *Aspergillus spp*. Loss of VeA in *A. fumigatus* Δ*veA* strains resulted in conidiation being impaired (Krappmann & Braus 2005). Dhingra *et al.*, (2012) demonstrated that gliotoxin production in *A. fumigatus* Δ*veA* strains was significantly reduced highlighting VeA regulation of secondary metabolism. Interestingly, in *A. fumigatus* Δ*veA* there was a corresponding decrease in the expression of *gliZ* and *gliP*, both of which have been shown previously to be necessary for gliotoxin biosynthesis (Dhingra *et al.*, 2012; Bok *et al.*, 2006; Cramer *et al.*, 2006). Yet, loss of VeA in *A. fumigatus* does not affect virulence in mice, indicating that unlike LaeA, VeA is dispensable for virulence (Dhingra *et al.*, 2012).

Both LaeA and VeA are part of the *velvet* regulatory proteins which primarily regulate fungal development across the *Aspergillus spp.* (Bayram *et al.*, 2008). These proteins are involved in the regulation of the light response in *A. nidulans* whereby VeA expression, in the dark, interacts with VelB, another *velvet* associated regulatory protein primarily involved in sexual development, this interaction results in the bridging of VelB to LaeA and subsequent regulation of gene expression (Bayram *et al.*, 2008). In a recent study by Park *et al.*, (2012), the *velvet* proteins LaeA, VeA, VelB,VosB and BrlA of *A. fumigatus* were characterised. Δ*veA*, Δ*vosB* and Δ*velB A. fumigatus* strains all displayed dysregulation of asexual development, with a significant increase in the production of conidiophores (Park *et al.*, 2012). This study highlighted a similar regulatory role for these proteins which may prove to regulate important secondary metabolite gene clusters in *A. fumigatus* also.

Since the full genome sequencing of *A. fumigatus* a total of 26 gene clusters have been identified based on the presence of a PKS, NRPS or DMAT gene (Nierman

et al., 2005). One such cluster responsible for the biosynthesis of secondary metabolite gliotoxin will be discussed in more detail in the next section.

1.5 Gliotoxin biosynthesis

As mentioned, gliotoxin is a secondary metabolite produced by the filamentous fungus *A. fumigatus* which possesses a role as a virulence factor during IA (Sutton *et al.,* 1994). Gliotoxin is also produced in a number of other biologically and industrially relevant strains such as certain *Trichoderma* and *Penicillium spp* (Kamei & Watanabe 2005). It belongs to the epipolythiodioxopiperazine class of organic molecules, possessing an indicative piperazine ring and trans-molecular disulphide bridge as seen in figure 1.2 (Gross *et al.,* 2010). Presence of this disulphide bridge results in gliotoxin existing in either an oxidised disulphide form or reduced dithiol form (Waring *et al.,* 1995; Sutton & Waring 1996).

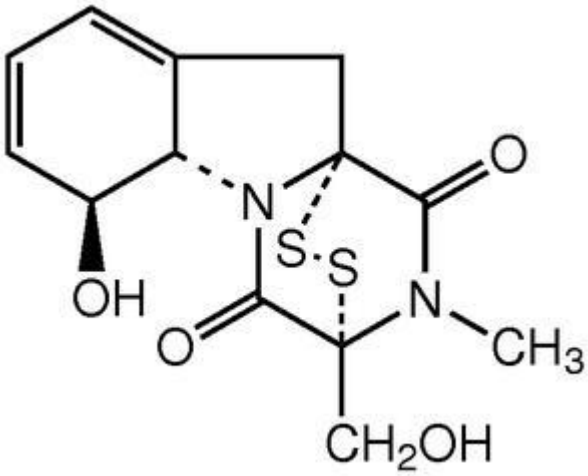

Figure 1.2 Chemical structure of the non-ribosomal peptide gliotoxin. Note the trans-molecular disulphide bridge shown here in its closed oxidised form. Source: http://www.abcam.com/ps/datasheet/images/142/ab142437/Gliotoxin-ab142437-ChemicalStructure-1.jpg

The gliotoxin biosynthetic cluster, *gli*, consists of a 13 gene cluster (figure 1.3) spanning 28 kb on chromosome six of *A. fumigatus* which is responsible for the biosynthesis of gliotoxin (Gardiner *et al.*, 2004; Gardiner & Howlett 2005). The functions of many of the genes of the *gli* cluster, have yet to be elucidated however some have been characterised. *GliZ* encodes a Zn_2Cys_6 transcription factor which regulates the *gli* cluster (Bok *et al.*, 2006). Loss of *gliZ* results in the subsequent abolition of gliotoxin biosynthesis (Bok *et al.*, 2006). It also results in the loss of *gliZ* dependant intermediates absent from Δ*gliZ* (Forseth *et al.*, 2011).

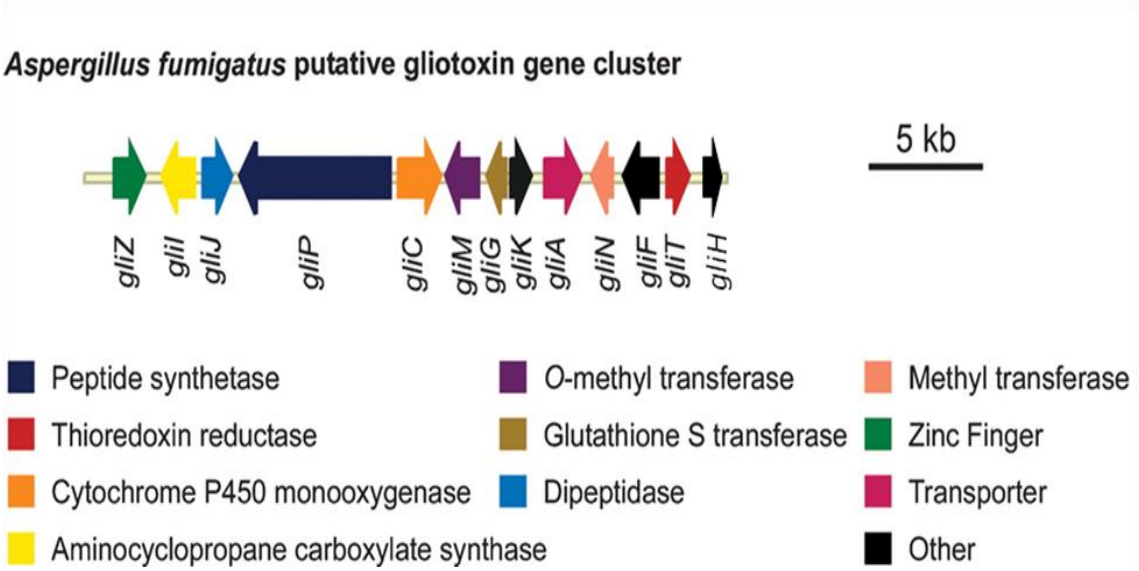

Figure 1.3 Gliotoxin biosynthetic cluster *gli* from *A. fumigatus*. Diagram modified from Gardiner *et al*, (2005) including the recent addition of the thirteenth *gli* cluster gene *gliH* (Schrettl *et al.*, 2010).

A later study which created a Δ*gliT* strain, illustrated that similar to Δ*gliZ* gliotoxin biosynthesis was abolished with no detectable gliotoxin levels found in culture supernatants (Schrettl *et al.*, 2010). Unlike Δ*gliZ*, *A. fumigatus* Δ*gliT* exhibited a hypersensitive phenotype to gliotoxin, demonstrating the role of gliT in self-protection against gliotoxin (Schrettl *et al.*, 2010). This same study also demonstrated that *gliT* was still expressed in Δ*gliZ* in the presence of gliotoxin, depicting *gliT* regulation is

independent of *gliZ* and that gliotoxin presence could induce expression of its own biosynthetic cluster (Schrettl *et al.,* 2010). GliT is an oxido-reductase responsible for the closure of the disulphide bridge of gliotoxin (Scharf *et al.,* 2013)

As mentioned, g*liP* encodes a non-ribosomal peptide synthetase which consists of two condensation, two adenylation and three thiolation domains (Balibar & Walsh 2006). It's responsible for the formation of the diketopiperazine backbone of gliotoxin from the amino acids L-serine and L-phenylalanine (Balibar & Walsh 2006). Loss of *gliP* results in loss of gliotoxin biosynthesis and subsequent attenuation of infection in an immunocompromised murine infection model (Cramer *et al.,* 2006; Kupfahl *et al.,* 2006). g*liG* encodes a glutathione S-transferase and has been shown to catalyse the incorporation of two glutathione molecules in the latter stages of gliotoxin biosynthesis which act as the sulphur sources required for the formation of its disulphide bridge (Davis *et al.,* 2011). In *A. fumigatus* Δ*gliG*, a subsequent loss in gliotoxin biosynthesis was seen as well as the accumulation of 6-benzyl-6-hydroxy-1-methoxy-3-methylenepiperazine-2,5-dione, believed to be a shunt metabolite produced in the absence of GliG enzymatic activity (Davis *et al.,* 2011). *GliK* has been previously shown to be involved in gliotoxin biosynthesis with an *A. fumigatus* Δ*gliK* strain unable to produce gliotoxin and possessed elevated intermediates lacking disulfide or thiol groups (Gallagher *et al.,* 2012). This gliotoxin biosynthetic activity of GliK was later confirmed and identified as a γ-glutamate cyclotransferase (Scharf *et al.,* 2013). Similarly, a homologue in the chaeotocin A ETP cluster of *Chaetomium virescens*, *chaK*, was found to be have γ-glutamylcyclotransferase activity, which may be involved in processing a biosynthetic intermediate diketopiperazine-glutathione adduct (Gerken & Walsh 2013). Creation of a Δ*gliK* strain has illustrated that it may also play a role in the oxidative stress response, with loss of *gliK* eliciting increased sensitivity to the presence of H_2O_2, which was subsequently alleviated upon exogenous gliotoxin addition highlighting an anti-oxidant potential for gliotoxin (Gallagher *et al.,* 2012). g*liI* has been demonstrated to be involved in the cleaving the C-S bond resulting in the formation of the epidithiol moiety of gliotoxin formed via gliKs' putative γ-glutamylcyclotransferase activity. Δ*gliI* strains are unable to produce gliotoxin, highlighting it's essential for gliotoxin biosynthesis (Scharf *et al.,* 2012). A model of gliotoxin biosynthesis is show in Figure 1.4.

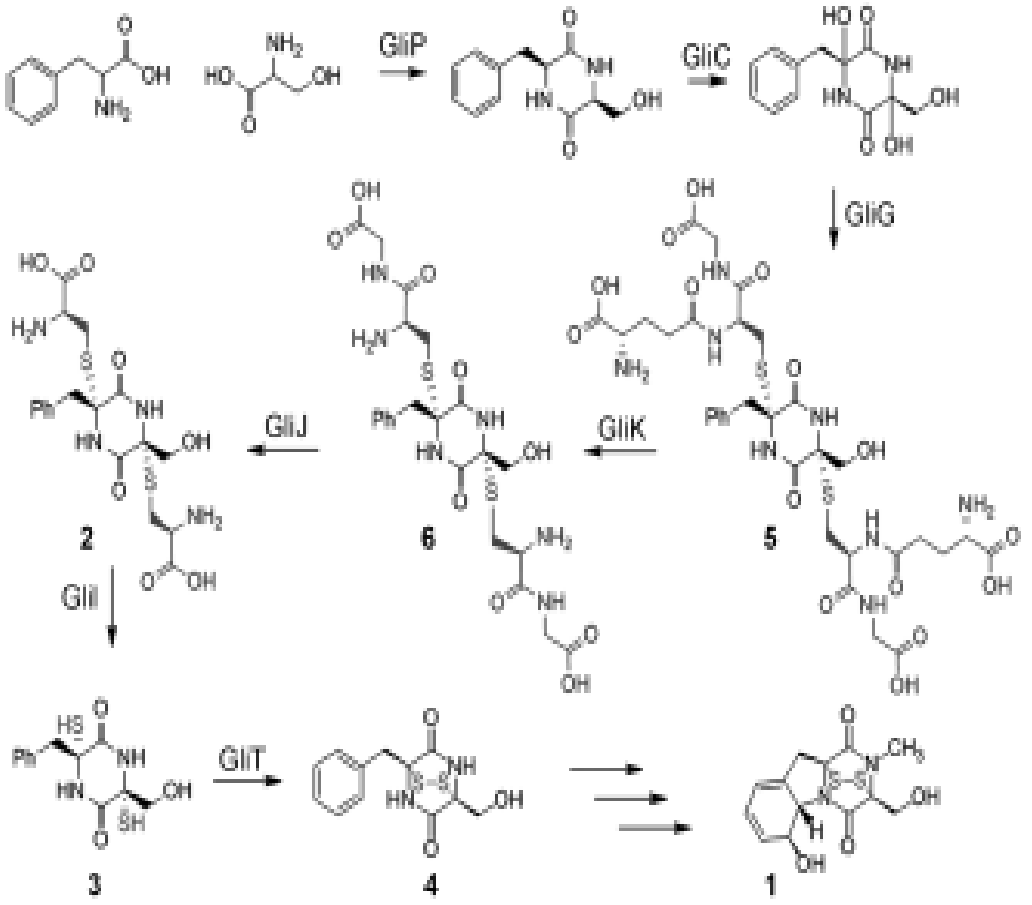

Figure 1.4 Gliotoxin biosynthesis enzymatic pathway. Taken from Scharf *et al.*, 2013. 1= gliotoxin biochemical structure; 2 = biscysteine adduct; 3 = dithiol intermediate; 4 = oxidised disulphide intermediate; 5 = bisglutathione intermediate

Although no functional characterisation of *gliA* has been carried out, a similar transporter, *sirA*, located with the biosynthetic cluster of another ETP molecule, sirodesmin, from *Leptosphaeria maculans* has highlighted its role in gliotoxin detoxification (Gardiner *et al,* 2005). Δ*sirA* sensitivity to exogenous gliotoxin was attenuated upon transformation of *L. maculans* Δ*sirA* with *A. fumigatus gliA,* however no alteration of the phenotype was seen to exogenous sirodesmin, illustrating GliA-mediated attenuation of gliotoxin toxicity to be gliotoxin specific (Gardiner *et al,* 2005).

1.6 Gliotoxins affect on host immune cells

As stated, gliotoxin is an important causative factor in IA. It achieves this through the biological activity of its indispensible disulphide bridge which facilitates potential conjugation to the thiol residues within proteins, subsequently leading to protein inactivation (Mullbacher *et al.,* 1986; Waring *et al.,* 1995; Pahl *et al.,* 1996; Hurne *et al.,* 2000). Gliotoxin has been shown to inhibit the formation of the respiratory burst NADPH oxidase complex, used by polymorphonuclear leukocytes in the superoxide killing of invading pathogens (Tsunawaki *et al.,* 2004). Additionally, a study using the insect model *Galleria mellonella* found that gliotoxin specifically repressed the translocation of $p47^{phox}$ and $p67^{phox}$ homologues which resulted in basal levels of superoxide generation (Renwick *et al.,* 2006).

Through this ability, gliotoxin is also able to undergo redox cycling resulting in the production of reactive oxygen species (ROS), which can cause oxidative stress and damage to the cell (Waring, *et al.,* 2005). The role of gliotoxin as an immunosuppressant was first demonstrated in 1988 where it was found to induce apoptosis in macrophages (Waring *et al.,* 1988). It has also been demonstrated to repress macrophage function as well as target antigen presenting cells (e.g., dendritic cells), thus repressing the antigen-presenting response and maturation of *A. fumigatus* specific T-cells (Stanzani *et al.,* 2005). Furthermore gliotoxin has deleterious affects on other cell types such as hepatic, endothelial, and anthrocyte cells (DeWitte-Orr & Bols 2005; Kweon *et al.,* 2003; Caprariello *et al.,* 2013)

Alongside this, gliotoxin has also been shown to promote inflammation with low levels of the toxin eliciting an induction in the pro-inflammatory cytokine TNF-α, while simultaneously reducing the expression of the anti-inflammatory Il-10 (Johannessen *et al.*, 2005).

1.7 Gliotoxin as an anti- fungal, bacterial and viral agent

Much of the original interest in gliotoxin was focused around its potent anti-fungal properties in which "toxic compounds" from *Trichoderma viride* which were later isolated and named gliotoxin, were noted to inhibit the growth of the soil fungus *Rhizoctonia solani* (Weindling and Emerson 1936). Gliotoxin has been demonstrated to inhibit the growth of an array of different fungal species including *A. nidulans, A. terreus, A. niger* and *Saccharomyces cerevisiae*, and has been utilised as an antifungal antibiotic, most notably in the treatment of soil borne fungi (Chamilos *et al.*, 2008; Carberry *et al.*, 2012; Howell & Stipanovic 1995; Aliaa 2008; Losada *et al.*, 2009) .

Similarly, gliotoxin has been demonstrated to possess anti-bacterial properties inhibiting proteasomal activity in certain bacterial strains and ultimately growth (Paugam *et al.*, 2002; Hatabu *et al.*, 2006) as well as inhibiting viral RNA replication, affecting many types of viruses such as poliovirus types I-III, Nipah, Hendra, and Influenza A viruses (Larin *et al.*, 1965; Aljofan *et al.*, 2009).

1.8 Gliotoxin detoxification

As mentioned previously, gliotoxin is a potent anti-fungal agent and elicits inhibition of growth of other *Aspergilli spp.* (Schrettl *et al.*, 2010). To prevent auto-toxicity, *A. fumigatus* would require the presence of gliotoxin detoxification mechanisms. One such mechanism mentioned earlier is GliT, which can alter the redox state of gliotoxin via enzymatic manipulation of its disulphide bridge from its toxic oxidised form, to its non-toxic reduced form as seen in figure 1.5. Many other

mechanisms have been put forward as being potential detoxification mechanisms. The putative MFS transporter protein GliA has been previously demonstrated to attenuate gliotoxin sensitivity of *L. maculans* exposed to exogenous gliotoxin (Gardiner *et al.,* 2005) and may be involved in detoxification of gliotoxin via its efflux from the cell thereby preventing accumulation and subsequent toxicity. GliG was also hypothesised to be involved in gliotoxin toxicity, however a Δ*gliG* strain educed no sensitivity when exposed to gliotoxin suggesting gliG alone at least, is not involved in gliotoxin detoxification (Davis *et al.,* 2011).

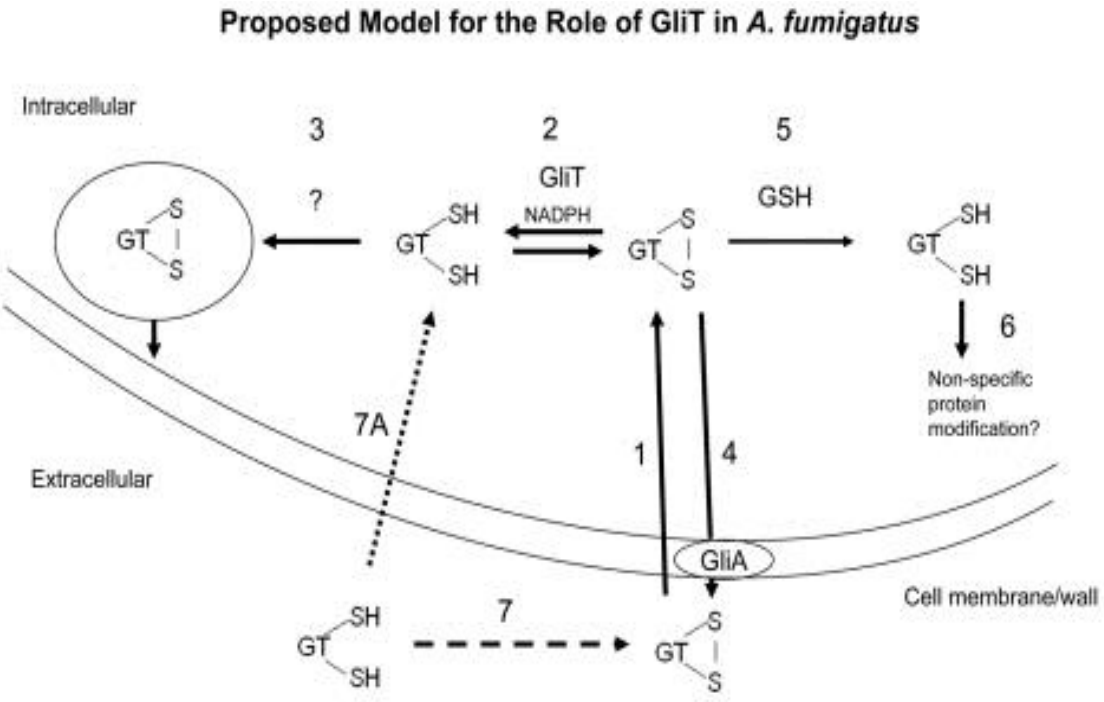

Figure 1.5 Proposed model of GliT mediated protection against gliotoxin GliT protects the cell by acting as an oxido-reductase altering the trans-molecular disulphide bridge from the reduced form of gliotoxin (GT-SH-SH) to the oxidised form (GT-S-S) facilitating its efflux. Image taken from Schrettl *et al.,* (2010)

Gliotoxin can also be found in an alternative form, other than the reduced and oxidised forms discussed earlier. Bis-methylated gliotoxin (Bm-GT), has an m/z of 357 by LC-MS can be found in equimolar and sometimes 100 fold more concentrated in

tissue samples from patients suffering from *A. fumigatus* infection (Amitani *et al.,* 1995; Bernardo *et al.,* 2003). This form of gliotoxin would require the disulphide gliotoxin to be reduced, exposing the two thiol groups, onto which two methyl groups can be transferred in the presence of a methyl donor as seen in figure 1.6. Bm-GT shows no toxic effects to cells, indicating it's unlikely to be an active mycotoxin. Because of this, its relatively stable chemical nature and the fact it was found to not be concentrated in fungal cells, Bm-GT has been hypothesised as being the product of gliotoxin detoxification and is currently being used as a biomarker for *A. fumigatus* infection from patient serum (Bernardo *et al.,* 2003; Domingo *et al.,* 2012).

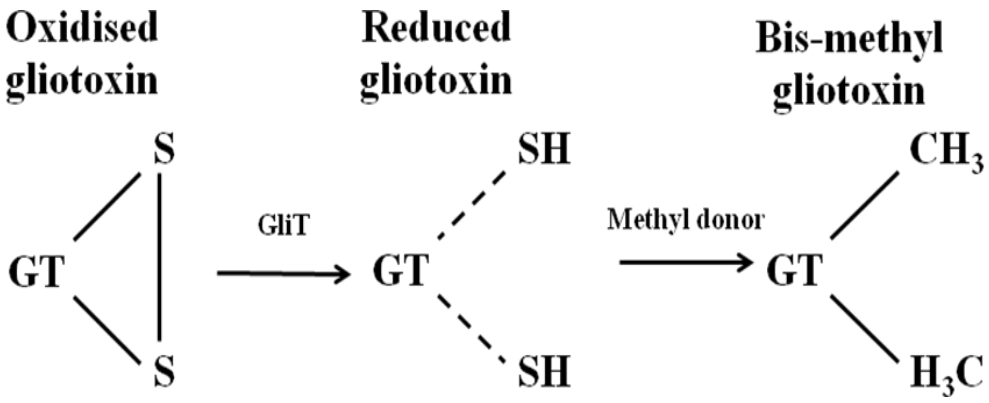

Figure 1.6 Diagram of bismethyl-gliotoxin production in *A. fumigatus*

1.8.1 Oxidative stress response in fungi

Fungal cells are exposed to an environment which is in a constant flux, requiring the fungus to continually adapt to its surroundings in order to survive (Schimel *et al.,* 2007). Many common variables exist which can greatly affect the growth of fungi, as well as other organisms, including pH, temperature, nutrient type and availability and the presence of reactive oxygen species (ROS) (Arst Jr & Penalva 2003; Bellí *et al.,*

2004; Narasimha *et al.,* 2006; Angelova *et al.,* 2005). ROS are reactive molecules such as the super oxide radical, and hydroxyl radical, which are produced both endogenously as by-products of metabolism, oxidative phosphorylation through reduction of molecular oxygen and by external factors in the environment such as the production of secondary metabolites like gliotoxin, or as part of a host immune response such as the superoxide burst seen in human neutrophils (Jamieson 1998; Montibus *et al.,* 2013; Izawa *et al.,* 1995). The fungus employs various enzymatic and non-enzymatic methods to attenuate the levels of the various ROS, in a response known as the oxidative stress (OS) response, preventing intracellular damage of important macromolecules (Sato *et al.,* 2013). ROS are non-specific and can induce oxidation of organic molecules, sulphur containing amino acids and functional iron clusters. The efficiency of the OS response has been attributed to the pathogenicity of certain fungi, allowing for dismantling of host immune systems as mentioned in the case of gliotoxin and IA (Moye-rowley 2003; Montibus *et al.,* 2013). Some of the mechanisms utilised by the OS response include the redox thiol glutathione, superoxide dismutases, and catalases which will be discussed in more detail in the following sections.

1.8.2 Glutathione, role and biosynthesis

Glutathione (γ-glutamyl-cysteinyl-glycine) is a ubiquitous low molecular mass tripeptide which possesses a redox active free thiol group (Meister & Anderson 1983). It acts as a redox buffer and radical scavenger of ROS and xenobiotics which cause oxidative damage to proteins and other macromolecules (Schafer & Buettner 2001; Grant 2001). It achieves this through the interaction of its free thiol moiety, which is essential for its function, with ROS and xenobiotics present in the cell resulting in the oxidation of GSH to its oxidised from GSSG (Alton Meister 1988; Pompella *et al.,* 2003). The GSH:GSSG ratio is maintained in favour of the reduced from, with dysregulation of the GSH:GSSG ratio indicative of a cell under OS due to increased GSH oxidation via peroxide detoxification (Schafer & Buettner 2001; Ostergaard *et al.,* 2004). GSH regeneration requires the FAD-dependant enzyme glutathione reductase (GR) using NADPH as an electron donor to reduce GSSG to GSH and maintain the redox balance of the cell (Grant *et al.,* 1996; Sato *et al.,* 2013).

In addition to its radical scavenging role in the OS response, glutathione has also been demonstrated to possess a role as a cofactor in the reactions of other OS response mediators and as a means of protein modification (Grant 2001). Glutathione presence is necessary for the disulphide reductase activity of certain glutaredoxins, helping to reduce protein disulphide formation created by the presence of ROS (Holmgren 1989). Similarly, GSH acts as an electron donor to glutathione peroxidases in the reduction of H_2O_2 to H_2O (Draculic *et al.,* 2000).

Glutathione s-transferases (GSTs) are cytosolic enzymes which also contain a redox active sulphydral group (Hayes *et al.,* 2005). This group of enzymes mediate the transfer and conjugation of GSH to xenobiotics and other ROS agents. GSH-conjugates are then transported to vesicles in which they are detoxified (Coleman & Randall 1997; Klein *et al.,* 2007). GSTs also possess a role in disulphide reduction via GSH and glutathionylation modification as seen in gliotoxin biosynthesis with the *gli* cluster GST GliG (Davis *et al.,* 2011). Glutathione can also modify proteins via its s-glutathionylation mechanism, interacting with the free thiol groups of proteins (Cotgreave & Gerdes 1998; Jacob *et al.,* 2003; Yang *et al.,* 2010). This helps protect proteins from irreversible oxidative damage induced by ROS thus reducing OS stress.

Information of glutathione biosynthesis in filamentous fungi is sparse, but is well documented in the yeast *S. cerevisiae* (Izawa *et al.,* 1995; Pompella *et al.,* 2003; Schafer & Buettner 2001). Glutathione is made as product of the sulphur amino acid biosynthesis pathway in yeast by the combination of three amino acids L-glutamate, L-glycine and L-cysteine. The latter is a product of the sulphur amino acid pathway produced from L-homocysteine which is catalysed via cystahionine β-synthase (Cys4) and L-cystathionine which is catalysed by cystathionine γ-lyase (Cys3) (Ono *et al.,* 1988). Both are found to be up-regulated under sulphur starvation due to the ability of *S. cerevisiae* to use L-methionine, L-homocysteine, glutathione or L-cysteine as a sulphur source required for nominal growth (Hiraishi & Miyake 2008).

Two key enzymes catalyse the formation of GSH. γ-glutamylcysteine synthetase 1 (Gsh1) and glutathione synthetase (Gsh2) (Lee *et al.,* 2001). Gsh1 catalyses the formation of the dipeptide γ-glutamylcysteine, and has been demonstrated to be the rate limiting step in GSH biosynthesis (Ohtake *et al.,* 1990). Loss of *GSH1* in yeast results

in the abrogation of glutathione biosynthesis and subsequent sensitivity to ROS (Lee *et al.,* 2001). Gsh2 catalyses the final step producing GSH with subsequent loss of *GSH2* resulting in GSH biosynthesis being abolished, yet this does not elicit sensitivity to the ROS agent H_2O_2 due to an accumulation of the Gsh1 intermediate γ-glutamylcysteine (Lee *et al.,* 2001).

Previous work has demonstrated a relationship between GSH and gliotoxin. Gliotoxin was found to be reversibly taken up by cells in a GSH dependant manner, as well as forming gliotoxin-GSH conjugates (Bernardo *et al.,* 2001, 2003). Similarly, addition of gliotoxin to *A. fumigatus* cells was found to reduce the GSH pool and also stimulate the levels of *GSH1* (Carberry *et al.,* 2012; Axelsson *et al.,* 2006) In a study using a human neuroblastoma cell line, artificially reducing the GSH levels attenuated gliotoxin toxicity highlighting the potential of GSH to facilitate gliotoxin toxicity in cells and how these two redox active molecules interact (Axelsson *et al.,* 2006).

1.8.3 Superoxide dismutase

Superoxide dismutases (SOD) are metalloenzymes which act on the dismutation of the superoxide radical O_2^- to molecular oxygen and the less toxic H_2O_2 (Mccord & Fridovich 1969; Bannister *et al.,* 1987). In cells, there is an array of different types of SOD enzymes which vary on the metal cofactor attached. These include the copper-zinc SOD (CuZnSOD), manganese SOD (MnSOD), nickel SOD (NiSOD) and iron SOD (FeSOD) (Mccord & Fridovich 1969; Youn *et al.,* 1996; Yost & Fridovich 1973). In *A. fumigatus* there are four genes encoding putative superoxide dismutases (*SOD1-4*) based on orthologs in other organisms (Lamarre *et al.,* 2001; Hwang *et al.,* 2002). In *S. cerevisiae*, there are two SOD genes, *SOD1* and *SOD2* which encode a CuZnSOD and MnSOD respectively (Bermingham-mcdonogh *et al.,* 1988; Van Loon *et al.,* 1986). These two enzymes have been demonstrated to be homologous to Sod1p and Sod2p in *A. fumigatus*. Sod1p is located in the cytosol of the cell while Sod2p is based in the mitochondrion with loss of either resulting in sensitivity to subsequent ROS. There is some evidence which illustrates a role for different SODs in the pathogenesis of

different fungi, helping to attenuate the superoxide burst of human neutrophils (Lambou *et al.,* 2010)

1.8.4 Catalase

Catalases react with H_2O_2, breaking it down to water and molecular oxygen (Cross & Ruis 1987). H_2O_2 can be produced *in vivo* as a result of redox cycling reactions as described previously, or as a by-product of other OS responses, namely SOD dismutaion of O_2^- (Waring *et al.,* 1995; Jamieson 1998). There are two catalases in yeast, cytoplasmic catalase T (Ctt1) and the peroxisomal catalase A (Cta1). Loss of either elicits increased sensitivity to OS stress (Todorova *et al.,* 2009; Delaney *et al.,* 2013) . In *A. fumigatus* there are a total of three catalases, one conidial catalase (CatA) and two mycelia catalases (Cat1 and Cat2). Interestingly, Cat2 was found to be bi-functional acting as a catalase-peroxidase in the cell (Paris *et al.,* 2003).

Similar to SOD, the presence of certain catalases have been attributed to virulence and the ability to counteract the host immune response. In an *A. fumigatus* Δ*cat1*Δ*cat2* strain, only slight sensitivity is seen to H_2O_2, yet a significant delay in infection time was seen in Δ*cat1*Δ*cat2* infected murine hosts (Paris *et al.,* 2003)

1.9 S-adenosyl-L-methionine cycle

S-adenosyl L-methionine (SAM) is the principle methyl source for a myriad of biological reactions (Chiang *et al.,* 1996). Its structure was first elucidated in 1951 and since then has been demonstrated to be vital in many cellular processes including polyamine biosynthesis, gene expression and as a source of L-cysteine for the production of glutathione (Cantoni 1951; Eloranta & Kajander 1984; Finkelstein & Martin 1990). Altered SAM levels have been attributed to many diseases in humans and it has been employed as a therapeutic, treating liver problems as well as neurological ailments including depression (Friedal *et al.,* 1989; Papakostas *et al.,* 2010). SAM has two main roles in the cell, as an s-methyl donor through its methyl donor activity or as an enzymatic inducer, and is produced via the SAM cycle (Chiang *et al.,* 1996). SAM

biosynthesis occurs in the cytosol in all cells as seen in Figure 1.7. L-homocysteine, which is produced as part of the sulphur amino acid biosynthetic pathway from L-cysteine, is methylated by a methionine synthase to form L-methionine (Mato *et al.*, 1997; Kacprzak *et al.*, 2003). An adenosyl group is attached to this via the s-adenosylmethionine synthases, Sam1 and Sam2, to form s-adenosly-L-methionine. After donating its methyl group as part of some biological reaction, s-adenosyl-L-homocysteine is produced from s-adenosyl-L-methionine, which is later hydrated and converted back to L-homocysteine via s-adenosyl-homocysteinase (i.e., s-adenosyL-homocysteine hydrolase) in yeast (Kredich & Hershfield 1979; Tehlivets *et al.*, 2004).

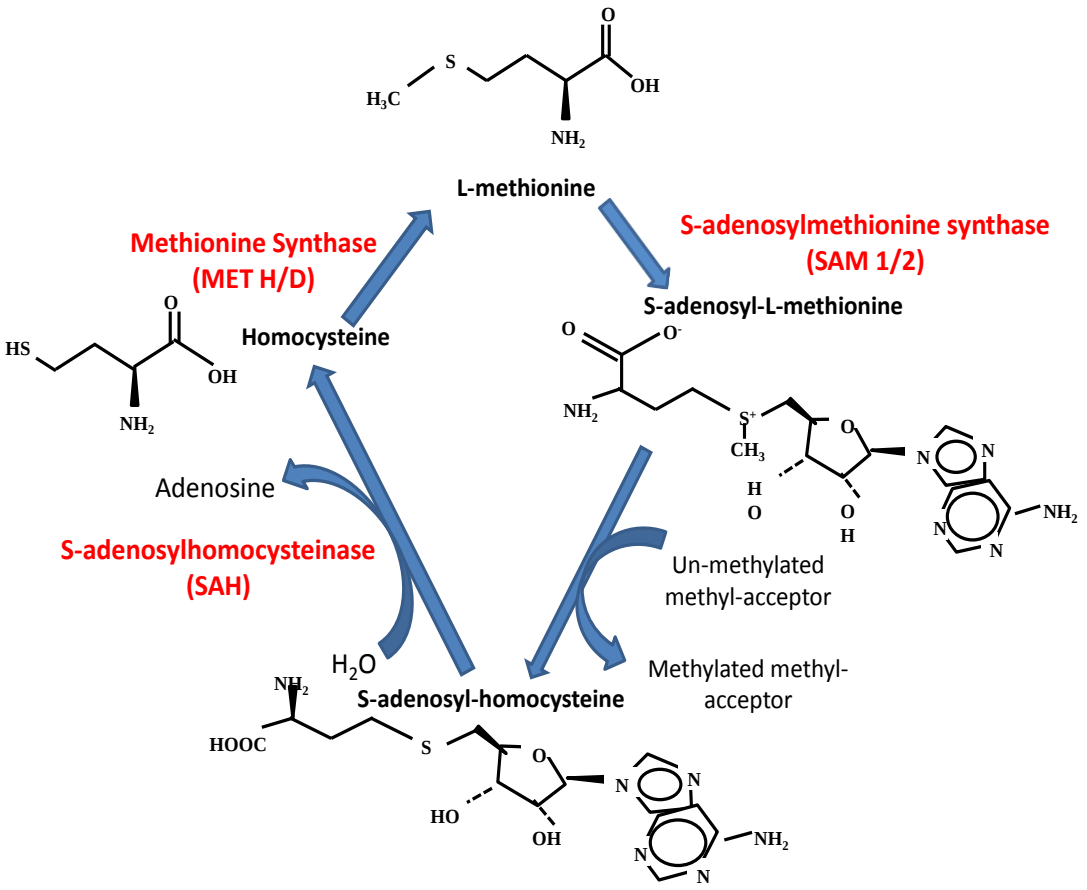

Figure 1.7 S-adeonosyl-L-methionine biosynthesis cycle Enzymes involved in catalysing the biosynthesis of key components of the SAM cycle are depicted in red. The chemical structure of L-homocysteine, L-methionine, S-adenosyl-L-methionine, S-adenosylhomocysteine are given for each.

SAMs methyl donor activity is facilitated by the addition of an ATP molecule during its biosynthesis. ATP is transferred to L-methionine via SAM synthase resulting in the formation of a high energy sulfonium ion which readily donates its methyl groups to suitable methyl acceptors (Chiang *et al.,* 1996; Cosper *et al.,* 2003).

Prior to polyamine biosynthesis, SAM is decarboxylated via SAM decarboxylase and the subsequent aminopropyl group is transferred to putrescine via spermidine synthase to form spermidine (Finkelstein & Martin 1990). Polyamines have a multitude of roles in the cell possessing the ability to interact with nucleic acid due to their highly protonated nature which can affect gene regulation, as well as protecting the cell from oxidative damage and ROS, highlighting a role for SAM in the OS response of cells (Chattopadhyay *et al.,* 2002).

S-adenosyL-homocysteine (SAH) is produced after every SAM reaction (Deguchi & Barchas 1971). SAH has been demonstrated to inhibit certain methyltransferase reactions in the cell including SAM methyl donor reactions via competition of the SAM binding domain. It has also been linked to adenosine toxicity in humans suffering from the immune deficiency disease ADA, with increasing levels of SAH resulting in a simultaneous increase in adenosine through its catabolism by SAH hydrolase (Kredich & Hershfield 1979). Similarly, L-homocysteine accumulation has been linked to adverse affects on the cell causing a subsequent defect in purine biosynthesis, (Fujita *et al.,* 2006) and sterol biosynthesis (Mccammon & Parks 1981). Importantly, an alteration to the levels of either of these two compounds, particularly uncontrolled elevation, would have deleterious effects on the cell.

1.10 Proteomic analysis in *A. fumigatus*

With the increasing number of sequenced genomes and rising availability of next generation sequencing tools, there has been a subsequent rise in the importance for proteome analysis in these organisms (Bhadauria *et al.,* 2007). Proteome analysis allows for the specific location and identification of certain proteins depending on the sample origin, as well as analysis of any post-translational modifications which would not be described in genome or transcriptome studies (Lu *et al.,* 2010; Wartenberg *et al.,* 2011).

Similarly, genomic studies cannot predict the number of proteins a single gene may encode meaning the predicted protein coding sequence number given in these studies may not be a true representative of the total number of proteins which can be expressed (Griffin *et al.,* 2002). Of particular importance, is the analysis of the *A. fumigatus* proteome response.

Previous proteomic studies in *A. fumigatus* have helped further elucidate the cellular response of this fungus under different conditions identifying proteins which are vital to the response to adverse conditions analogous to a human host such as hypoxia (Vodisch *et al.,* 2011), as well as the response of conidia upon initial contact with human cells (Teutschbein *et al.,* 2010). Additionally, these studies can also be used for the identification of diagnostic markers which can be employed for the detection of *A. fumigatus* via a bioassay (Kniemeyer *et al.,* 2009).

This approach has helped identify some of the major intracellular proteins found in *A. fumigatus* as well as key enzymes involved in secondary metabolism, oxidative stress response, cell wall biosynthesis and the enzymes which are secreted as part of the secretome of the fungus which facilitates its saprophytic niche as well as its ability to infect immuno-compromised individuals and evade their immune response (Carberry *et al.,* 2006; Reeves *et al.,* 2006; Bruneau *et al.,* 2001; Wartenberg *et al.,* 2011).

From this, identified proteins can be either isolated from the fungus or expressed via recombinant mechanisms in order to characterise their function *in vitro*. One such example is the characterisation of GliT activity on gliotoxin. In a neat experiment, Schrettl *et al.,* were able to identify thart native GliT catalysed the NADPH dependant reduction of oxidised gliotoxin, confirming its gliotoxin reductase activity (Schrettl *et al.,* 2010).

1.11 Transcriptome analysis in filamentous fungi

Transcriptomics is the global study of gene expression taken at the RNA level (Feder & Walser 2005). The availability of the *A .fumigatus* genome allows for the mapping of gene sequences from a given sample to the reference genome allowing for it

to be identified and most importantly, quantified (Groot *et al.*, 2007). Although the protein and mRNA levels have been shown to not correlate well in previous studies in yeast, it does give a wider look at what is happening in the cell at a given time point and response (Griffin *et al.*, 2002). Figure 1.8 depicts the general process of transcriptomics from sample to data analysis which can be summarised into RNA extraction, library construction, sequencing and data analysis (Barker *et al.*, 2012)

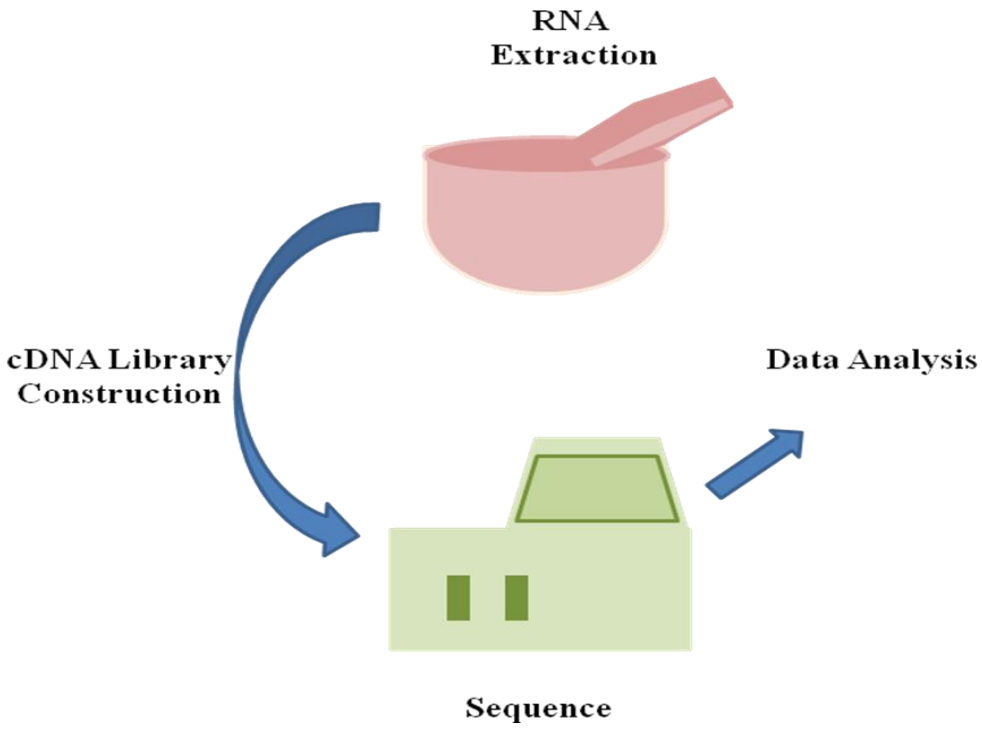

Figure 1.8 Transcriptomic sequencing work flow

There are many different methods which can be utilised to deduce the transcriptome profile of a given sample. Microarrays are a popular method of identification of target cDNA sequences creating from extracted RNA, identified utilising a corresponding unique cDNA probe which is attached to a glass plate (Hegde *et al.*, 2000). Detection is measured by the use of fluorescently labelled RNA probes, whereby the amount of fluorescence is proportional to the amount of that specific transcript present and therefore its expression. This method requires prior amplification of cDNA of target genes either from extracted RNA or from a previously constructed cDNA plasmid library. Due to the limited number of targets it can detect, it's not useful

for whole transcriptome analysis nor will it detect any change in other highly expressed transcripts if there is not a corresponding probe present (Hegde *et al.,* 2000).

Gel based methods like Differential display (DD) and cDNA-amplified fragment length polymorphism (AFLP) involve PCR mediated amplification of different cDNA fragments separated on a poly-acrylamide gel, subsequent excision of the band(s) of interest and sequencing which can be laborious and time consuming (Liang & Pardee 1992; Bachem *et al.,* 1996).

Tag based systems like Sequence Analysis of Gene Expression (SAGE), Cap Analysis of Gene Expression (CAGE) or Massively Parallel Signature Sequencing (MPSS) are a high through-put sequencing method yielding precise gene expression levels with a digital output (Velculescu *et al.,* 1995; Kodzius *et al.,* 2006; Brenner *et al.,* 2000). SAGE relies on the principle that 10-30 bp of a specific cDNA fragment is sufficient to uniquely identify that particular fragment when the relative location is also known (Velculescu *et al.,* 1995). The second principle involves synthesis of cDNA fragments using biotinylated oligo dT primer and cleaving the fragment using restriction enzymes with 4 base pair recognition sites. The biotin located at the 3' ends are then attached to streptavidin allowing for isolation of bound fragments and separated into two fractions which are ligated to two different linkers which contained a 20 bp endonuclease site (Velculescu *et al.,* 1995). These linker sequences serve two purposes, firstly they facilitate release of the linker and a short cDNA fragment and secondly serve as primer sites for the amplification of cDNA-linker fragments after they have been ligated together which can then be cloned and sequenced. Unlike gel based methods, this method allows for quantitative analysis of cDNA fragments.

Similarly, CAGE and MPSS utilise this tag based method of cDNA identification and measurement. Unlike SAGE, CAGE uses tags which target the 5' end or 'cap' of the extracted mRNA prior cDNA synthesis, but is similar to SAGE in the use of linker molecules and restriction endonucleases (Kodzius *et al.,* 2006). MPSS involves the cloning of template cDNA onto individual micro-beads (Brenner *et al.,* 2000). The main principle of MPSS is the serial ligation of target fragments with adaptor fragments which attach onto a micro-bead and can be subsequently measured photometrically.

Although these tag based systems, also known as expressed sequence tags (EST), allow for quantification of gene expression, the generation of cDNA clone libraries is a major drawback as it doesn't allow for the identitification of unique transcripts. Also, the use of short fragment lengths for detection of fragments can become an issue when trying to identify short mRNA molecules (Wang *et al.,* 2009).

The recent breakthrough in being able to map genes and quantify them using RNA sequence technology (RNA Seq), has become the pinnacle of transcriptome profiling in science. This technology uses similar EST principles described earlier, with cDNA libraries being attached to adaptor sequences and the creation of an EST library with adaptors attached to either one or both ends of the cDNA fragment. Sequences undergo high through put sequencing, resulting in short sequences obtained from either one end, known as pair-end sequencing, or both ends, known as pair end sequencing (Wang *et al.,* 2009).

Some of the major RNA Seq systems available for transcriptome analysis include: Sanger automated sequencing Illumina IG, 454 pyro sequencing by Roche; SOLiD by Applied Biosystems and Heliscope by Helicos (Wang *et al.,* 2009). This method does not require a reference genome, allowing for the sequencing of non-model organisms (Vera *et al.,* 2008). It also has low background due to the mapping of genes to unique regions of the genome and the high detection rate of amplification of specific genes (Nagalakshmi *et al.,* 2008). As the costs for this kind of analysis become more affordable the potential in furthering our understanding of the inner workings of an organism and how it responds to specific stimuli will increase dramatically.

1.12 Omics analysis in organisms

Advancement and availability of different scientific techniques involved in global characterisation such as phenomics, transcriptomics, proteomics, secretomics, metabolimics collectively termed as 'omics' research, allow for the quantitative, high through put analysis between different biological molecules at a given state (Kandpal *et al.,* 2009). Although each omics technique has its own advantages with the potential in yielding a plethora of results, one single technique is insufficient in elucidating the

complexity of an organisms' response and so the use of multiple types is becoming more prevalent in the literature (Kniemeyer *et al.,* 2009; Schrettl *et al.,* 2010; Teutschbein *et al.,* 2010; Vodisch *et al.,* 2011). Multi-layer omics approaches have become more popular due to the increasing availability of sequenced genomes, online databases and advancing bioinformatic analytic tools (Nierman *et al.,* 2005; Machida *et al.,* 2005; Arnaud *et al.,* 2011; Goujon *et al.,* 2010).

With the increasing usage of these types of techniques, we begin to see the interaction between certain responses at different levels, gene to protein, and ultimately the molecules produced as the end product, a branch of research aptly named 'Interactomics' (Kandpal *et al.,* 2009). Gautam *et al.,* used this approach investigating the proteomic and transcriptomic response of *A. fumigatus* to the polyene anti-fungal amphotericin B identifying ergosterol biosynthesis, cell stress and cell wall proteins and genes dysregulated in response to this drug (Gautam *et al.,* 2008). Similarly, Teutschbein *et al.,* (2010) coupled their proteomic study of *A. fumigatus* conidia proteome with the conidia transcriptome of Lamarre *et al.,* allowing for the identification of 25 similar hits highlighting a correlation of these results from the transcript to the protein level (Lamarre *et al.,* 2008; Teutschbein *et al.,* 2010).

The use of genomic tools, particularly functional genomics, has highlighted the importance of particular genes and subsequent proteins when used in conjunction with other omic techniques. For example, a number of gene knockout studies, most notably in the opportunistic pathogen *A. fumigatus* have been studied in conjunction with phenomic and metabolomic analysis to help elucidate key components of gliotoxin self protection, gliotoxin biosynthesis and characterisation of previously un-annotated genes (Schrettl *et al.,* 2010; Davis *et al.,* 2011; Gallagher *et al.,* 2012; Scharf *et al.,* 2013).

Combining omic technologies allows for a deeper understanding of the response of an organism to a particular stimulus, and should be employed further when trying to elucidate the mode of action of the many mechanisms which still eludes us in the field of microbiology such as the biosynthesis and response to secondary metabolites of certain fungi.

1.13 *S. cerevisiae*, a model organism

S. cerevisiae is a tractable eukaryotic model organism and since being the first eukaryotic organism to have its genome sequenced, *S. cerevisiae* has been at the forefront of other key areas of eukaryotic research. The ability to use 'simpler' organisms like *S. cerevisiae* has many advantages such as cost, pliable nature and genetic similarity to other higher eukaryotes including filamentous fungi and human cells. For example, Botstein *et al.,* calculated 31 % of yeast genes had homologs in humans, highlighting the comparability of yeast to other eukaryotes (Botstein *et al.*, 2011).

S. cerevisiae has been employed to investigate the anti-fungal activity of various chemicals and secondary metabolites, most notably gliotoxin. In a study by Chamilos *et al.*, a yeast gene deletion library consisting of a total of 4,787 haploid strains were screened for sensitivity to gliotoxin. From this study, 56 strains (44 which were sensitive to gliotoxin and 12 which were resistant) were identified to have an altered phenotype to gliotoxin exposure (Chamilos *et al.*, 2008). This inspired a follow up study by Carberry *et al.*, which helped identify other resistant and sensitive strains which were originally overlooked in the Chamilos study (Carberry *et al.*, 2012). Utilising this model organism, Schrettl *et al.*, further confirmed the protective function of GliT by expressing this fungal protein in yeast eliciting increased resistance to gliotoxin exposure (Schrettl *et al.*, 2010).

With a high proportion of conserved gene regions and homology to certain genes and pathways in *S. cerevisiae* and other filamentous fungi, comparison of yeast to other fungi is possible and may help highlight key cellular pathways which may remain elusive in more complex models. Also, due to the availability of mutant strains in *S. cerevisiae*, the identification of key genes and biological pathways in response to anti-fungal agents like gliotoxin is relatively easier than creating a homologous gene deletion in *A. fumigatus*.

1.14 Transformation and gene replacement in *A. fumigatus*

With the sequencing of the *A. fumigatus* genome, there is a necessity to confirm and characterise the function of the many putative and uncharacterised genes in this organism (Nierman *et al.,* 2005). Advancements in gene targeting systems, gene deletion construct creation and the creation of non-homologous end joining (NHEJ) *A. fumigatus* strains have improved the success rate of gene replacement in this organism (Nielsen *et al.,* 2006; Krappmann *et al.,* 2006). Protoplast transformation is the most commonly used means of gene targeting used in *A. fumigatus* gene deletion studies however there are others such as electroporation, and *Agrobacterium tumefaciens* mediated transformation (Meyer 2008) This method involves the temporary degradation of the cell wall using lytic enzymes. Once this is ready, transforming DNA constructs are taken up by the cell which is facilitated either by heat shock or by the addition of chemicals such as PEG and $CaCl_2$ (Brookman & Denning 2000). Variations to this type of transformation exist, whereby the membrane of the protoplasts is sonicated causing reversible permeabilisation facilitating uptake of the transforming constructs (Ruiz-Díez 2002).

Transforming DNA constructs consist of regions homologous to flanking the gene of interest which are amplified via PCR amplification using specific primers that are subsequently ligated to a selection marker as seen in Figure 1.9 (Brakhage & Langfelder 2002). These are than transformed into the protoplasts of the fungus. There are a range of methods for gene replacement in *A. fumigatus* such as plasmid integration, single construct insertion, double joint method and the bi-partite technique (Kubodera *et al.,* 2000; Kuwayama *et al.,* 2002; Yu *et al.,* 2004; Nielsen *et al.,* 2006). This last method involves the formation of transforming constructs as described before, however it involves a second round of PCR which utilises a nested primer located within each flanking region and another located within the region of the selection marker that amplifies a select part of the selection marker for each construct with a shared region which can homologously recombine (Figure 1.10) (Nielsen *et al.,* 2006).

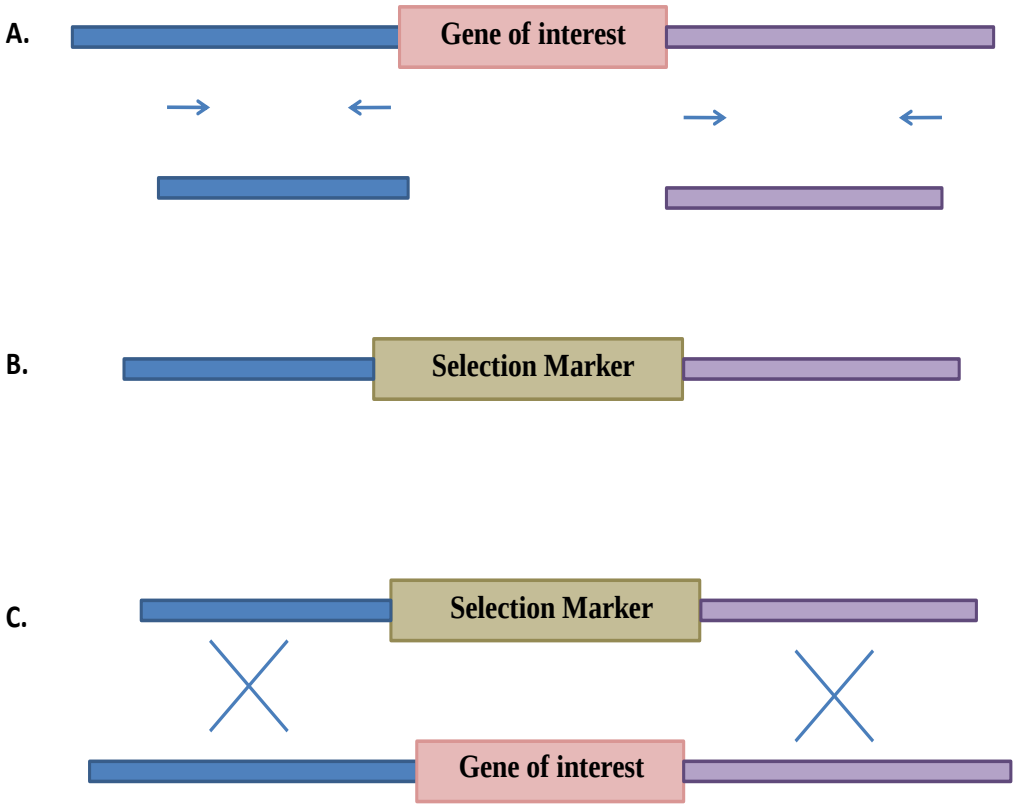

Figure 1.9 Schematic of transformation of *A. fumigatus* (A) Flanking regions are amplified using primers 5' and 3' of each. Each set of primers will have a restriction site included which will allow for ligation to the selection marker. (B) Flanking regions from A and the selection marker are digested with restriction enzymes and subsequently ligated together forming transformation constructs. (C) Transformation constructs from B are transformed into *A. fumigatus* protoplasts and flanking regions will attach to homologous flanking regions via homologous recombination. Arrows represent primer sites used for the amplification of flanking regions. Crosses represent homologous recombination of the nucleotide regions.

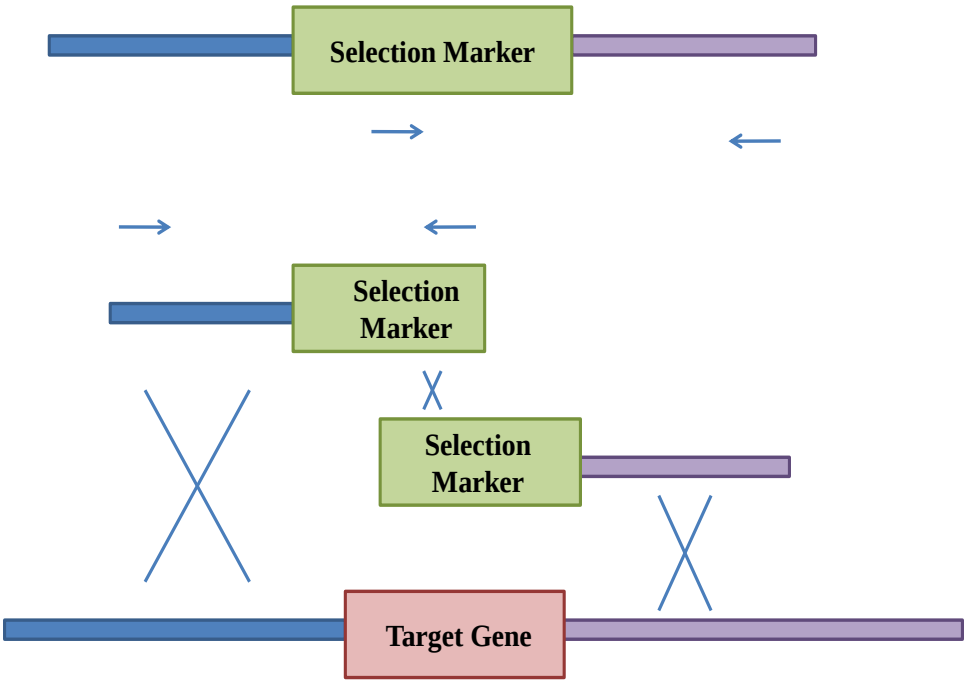

Figure 1.10 Bi-partite transformation of *A. fumigatus*. Image illustrates the two homologous reactions which take place between the two flanking regions and the selection marker fragments which recombine to form the full selection marker cassette. Arrows represent primer sites used to amplify the flanking region and part of the selection marker. Crosses represent sites of recombination.

There are many different types of selection markers which can be used in this process. The most commonly used are anti-fungal resistance cassettes which elicit resistance in transformants to a specific anti-fungal agent, such as pyrathiamine or gliotoxin (Kubodera *et al.,* 2000; Schrettl *et al.,* 2010) This last method involves the use of *gliT* resistance to gliotoxin as a selection marker of potential transformants (Schrettl *et al.,* 2010).

There has also been some success with the use of auxotrophic strains, most notably in the deletion of the uracil/uridine biosynthesis gene orotine 5'-monphosphate (*pyrG)* (De Enfert 1996). Genes in these auxotrophic strains can be deleted using *pyrG* isolated from *A.* niger, with subsequent selection on media lacking uracil or uridine (De Enfert 1996). This particular cassette has a bacterial transposon repeating sequence on either side of the *pyrG* gene, allowing for removal of the *pyrG* gene on FOA media which facilitates recombination of these transposon sequences and *pyrg* removal. (De Enfert 1996)

1.15 Infection models in research of fungal pathogens

The rise in fungal infections in recent years has brought with it a need to broaden our understanding of fungal disease (Zilberberg *et al.,* 2008; Low & Rotstein 2011). This entails the use of infection models, organisms which are purposefully injected with a pathogenic organism in order to study its progression, virulence and the factors which enable its infection. Traditionally mouse models have been used to study filamentous fungal infection due to the similarity of its immune response to humans', as well as analogous organs which can be targeted in a similar fashion (Arvanitis *et al.,* 2013). Many types of mouse models have been used to investigate IA infection including intravenous and, the more reproducible, inhalation models (Fordi & Friedman 1967; Sheppard *et al.,* 2004). In Verweij *et al.,* the susceptibility of an amphotereicin-B resistant *A. fumigatus* strain was assessed using a novel echinocandin, identifying it elicited significantly greater survival rates in IA infected mice (Verweij *et al.,* 1998). Bozza *et al.,* demonstrated that pre-exposure of mice to *A. fumigatus* allergens induced $CD4^+$ Th1 cell activation and subsequent resistance to *A. fumigatus* (Bozza *et al.,* 2002).

Similarly mouse models have been used to examine the importance of particular genes during in *A. fumigatus* infection. This is achieved using gene deletion strains and measuring the survival rate of the infected immuno-compromised mice. For example, loss of gliotoxin biosynthesis due to the deletion of *gliP* reduced virulence of Δ*gliP A. fumigatus* strains in mice (Sugui *et al.,* 2007), while loss of the NRPS *pes3* was found to augment virulence of Δ*pes3 A. fumigatus* strains in mice (O'Hanlon *et al.,* 2011).

Although there are many clear advantages in using mouse models there are also some disadvantages. Firstly, a response found in one organism may not be common to all organisms. This particularly found in clinical trials where a lot of trials rarely pass the *in vitro* to *in vivo* transition (Johnson *et al.,* 2001). Secondly, relative cost and ethical concerns have created a demand for new types of infection models and the use of invertebrate models has been on the rise (Heemskerk *et al.,* 2002). Invertebrate models are a low cost model which addresses other concerns associated with more complex models, with most invertebrates having relatively short life spans and ideal candidates for large scale studies (Arvanitis *et al.,* 2013). Three of the main invertebrate models used are the fruit fly *Drosophila melanogaster* which has been used to identify the importance of the dorso-ventral regulatory cassette 'Toll' in *A. fumigatus* pathogenesis; *Caenorhabditis elegans* which has been shown to express proteins comparable to those of the human innate immune response when exposed to different fungi and *G. mellonella* which will be discussed in more detail in the next section (Lemaitre *et al.,* 1996; Couillault *et al.,* 2012)

1.16 *Galleria mellonella*

The larvae of the greater wax moth (Figure 1.11), *G. mellonella*, has emerged as a popular insect model. *G. mellonella* has been employed to assess new therapeutic agents and as a model for virulence of different bacterial and fungal strains (Rowan *et al.,* 2009). Traditionally used for fishing bait, *G. mellonella* is a low cost model allowing for increased test sample size, and has been previously demonstrated to survive temperatures of 37 ^{0} C making it a prime candidate as a model organism of human pathogens (Cotter *et al.,* 2000).

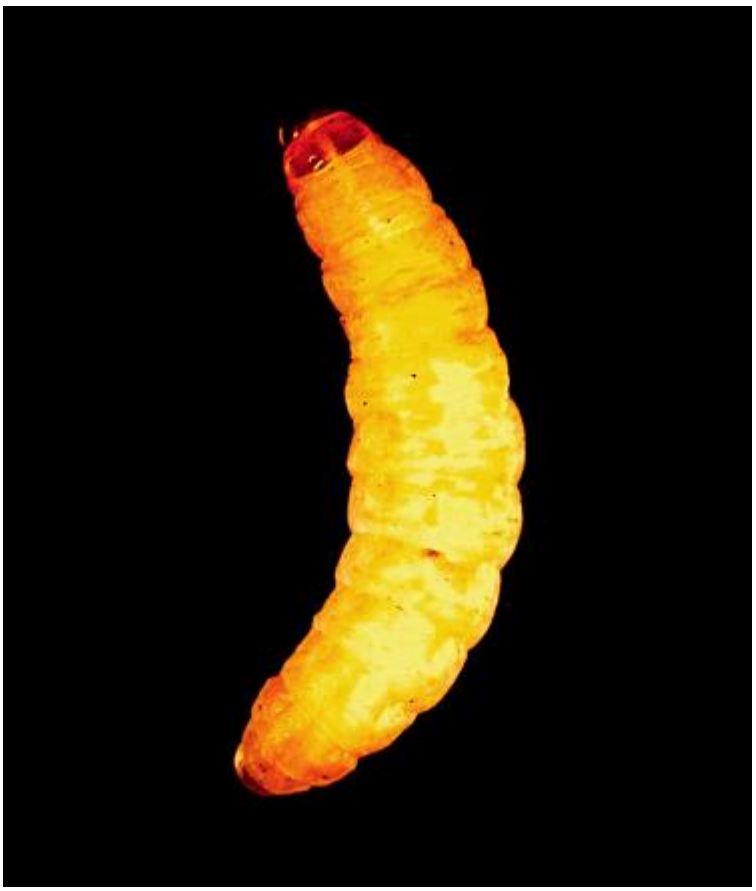

Figure 1.11 Larva of the greater wax moth *G. mellonella* Picture taken from the journal of American Microbiology http://jb.asm.org/content/186/3.cover-expansion

Importantly, *G. mellonella* was found to elicit similar responses when exposed to different pathogens when compared with previous results seen in mammalian models (Cotter *et al.,* 2000; Brennan *et al.,* 2002; Reeves, *et al.,* 2006). The most crucial result was the identification of an immune system present in these larvae closely resembling the innate immune response of mammals. It is an immediate response which consists of both a humoral response and a cellular response (Angrgaeni & Ratcliffe 1991). The humoral response involves two key responses, the first is a signalling cascade known as the propphenoloxiase system which results in melanisation through the activity of serine proteases on zymogenic molecules (Brookman *et al.,* 1989). This helps augment the humoral response of the insect larvae by inducing sequestration of the foreign body and also facilitating different host defence mechanisms such as the production of quinones which help in the ROS killing of foreign cells (Slepneva *et al.,* 1999). The second

involves anti-microbial peptides (AMPs) which are effector molecules produced in the fat body of the larvae which are then secreted into the haemolymph where they will come into contact with invading pathogens (Hoffmann 1995). There are a range of AMPs in insects which respond to particular types of cells and cell markers; lysozyme breaks down the peptidoglycan wall of bacterial cells further enhancing immune response; defensins which have been found to specifically attack the cell walls of gram positive bacteria and apolipophorin 3 which has been demonstrated to bind lipopolysaccharide molecules found on bacterial cell walls (Kavanagh & Reeves 2004). Other responses include the production of transferrins which limit the iron availability of the larvae subsequently limiting bacterial growth *in vivo* (Yoshiga *et al.,* 1999; Mowlds & Kavanagh 2008).

The cellular response is made up of different sub-types of immune cells known as haemocytes. These cells can recognise foreign bodies through specific signalling cascades which in turn increases the production of haemocytes, a trend that can be used as a marker of the infection of a pathogen in a given test sample (Mowlds *et al.,* 2010). The principle roles of haemocytes are the encapsulation, nodulation and phagocytosis of pathogens (Mowlds *et al.,* 2010).

Survival time of *G. mellonella* over a given time period can be measured to assess the pathogenicity of particular strains. This has been used assessing the virulence of different bacterial strains like *Listeria monocytogenes*, *Pseudomonas aeruginosa* and *Staphylococcus aureus* (Mukherjee *et al.,* 2010; Seed & Dennis 2008; Gibreel & Upton 2013). Similarly, this has also been used for the study of fungal infections, most notably *A. fumigatus*. Reeves *et al.,* illustrated the correlation between gliotoxin biosynthesis and virulence, implicating higher gliotoxin levels resulted in an increase in *G. mellonella* death (Reeves *et al.,* 2004). Renwick *et al.,* (2006) showed that *A. fumigatus* infection in this model varied depending on the germination stage of the injected conidia, highlighting the importance of conidia age and size which can result in increased larval death (Daly, *et al.,* 2006). Exposure of *G. mellonella* larvae to *A. fumigatus* gene deletion strains by Slater *et al.,* implicated that loss of genes involved in siderophore biosynthesis resulted in attenuation of *A. fumigatus* virulence, thus highlighting a role of this pathway in *A. fumigatus* pathogenesis (Slater *et al.,* 2011).

The similarities of these responses to components of the mammalian immune response, makes *G. mellonella* a suitable and efficient model for the study of virulence of bacterial and fungal infections *in vivo*.

Aims of study

The characterisation and elucidation of the *A. fumigatus* response to the fungal secondary metabolite gliotoxin has been elusive to date. The components of gliotoxin biosynthesis and their importance in this response have also been equally elusive.

To this end, the aims of this study are:

1) Create a double gene deletion in *A. fumigatus* lacking the two key gliotoxin biosynthetic genes Δ*gliT* and Δ*gliZ*, using a targeted gene deletion approach, and subsequent phenotypic characterisation.

2) Investigate the *A. fumigatus* proteome response to gliotoxin using *gliT* and *gliZ* deletion strains using 2D-PAGE

3) Investigate the *A. fumigatus* transcriptome response to gliotoxin by comparative transcript profiling between wild-type and Δ*gliT* strains.

4) Exploit the yeast based system *S. cerevisiae* to further elucidate the anti-fungal activity of gliotoxin and identify key genes and cellular pathways involved in gliotoxin toxicity applying a gene candidate approach.

Chapter 2

Materials and Methods

2.1.1 Materials

2.1.1.1 Strains in this study

Table 2.1 lists *S. cerevisiae* and bacterial strains used in this study, Table 2.2 lists the *A. fumigatus* strains used in this study..

Table 2.1 *S. cerevisiae* and bacterial strains used

Strain	Genotype	Source
BY4741	MATa *his3*Δ 1, *leu2*Δ, *met15*Δ 0, *ura3*Δ 0	Euroscarf
BY4742	MATα *his3*Δ *1; leu2*Δ *0; lys2*Δ *0; ura3*Δ 0	Euroscarf
BY4741 Δ*gsh1*	MAT a; *his3*Δ1; *leu2*Δ0; *met15*Δ*0*; *ura3*Δ0; *gsh1*::kanMX4	Euroscarf
BY4742 Δ*gsh1*	MATα *his3*Δ *1; leu2*Δ *0; lys2Δ 0; ura3*Δ 0 *gsh1*::kanMX4	Euroscarf
BY4741 Δ*gsh2*	MAT a; *his3*Δ1; *leu2*Δ0; *met15*Δ*0*; *ura3*Δ0; *gsh2*::kanMX4	Euroscarf
BY4741 Δ*cys3*	MAT a; *his3*Δ1; *leu2*Δ0; *met15*Δ*0*; *ura3*Δ0; *cys3*::kanMX4	Euroscarf
BY4742 Δ*cys3*	MATα *his3*Δ *1; leu2*Δ *0; lys2*Δ *0; ura3*Δ 0 *cys3*::kanMX4	Euroscarf
BY4741 Δ*cys4*	MAT a; *his3*Δ1; *leu2*Δ0; *met15*Δ*0*; *ura3*Δ0; *cys4*::kanMX4	Euroscarf
BY4742 Δ*cys4*	MATα *his3*Δ *1; leu2*Δ *0; lys2*Δ *0; ura3*Δ 0 *cys4*::kanMX4	Euroscarf
BY4741 Δ*sod1*	MAT a; *his3*Δ1; *leu2*Δ0; *met15*Δ*0*; *ura3*Δ0; *sod1*::kanMX4	Euroscarf
BY4742 Δ*sod1*	MATα *his3*Δ *1; leu2*Δ *0; lys2Δ 0; ura3*Δ 0 *sod1*::kanMX4	Euroscarf
BY4741 Δ*yap1*	MAT a; *his3*Δ1; *leu2*Δ0; *met15*Δ*0*; *ura3*Δ0; *yap1*::kanMX4	Euroscarf
BY4742 Δ*yap1*	MATα *his3*Δ *1; leu2*Δ *0; lys2Δ 0; ura3*Δ 0 *yap1*::kanMX4	Euroscarf
BY4741 Δ*ctt1*	MAT a; *his3*Δ1; *leu2*Δ0; *met15*Δ*0*; *ura3*Δ0; *ctt1*::kanMX4	Euroscarf
BY4742 Δ*ctt1*	MATα *his3*Δ *1; leu2*Δ *0; lys2Δ 0; ura3*Δ 0 *ctt1*::kanMX4	Euroscarf
BY4741 Δskn7	MAT a; *his3*Δ1; *leu2*Δ0; *met15*Δ*0*; *ura3*Δ0; *skn7*::kanMX4	Euroscarf
BY4741 Δ*ku70*	MAT a; *his3*Δ1; *leu2*Δ0; *met15*Δ*0*; *ura3*Δ0; *ku70*::kanMX4	Euroscarf
BY4741 Δ*ku80*	MAT a; *his3*Δ1; *leu2*Δ0; *met15*Δ*0*; *ura3*Δ0; *ku80*::kanMX4	Euroscarf
BY4741 Δ*apt1*	MAT a; *his3*Δ1; *leu2*Δ0; *met15*Δ*0*;	Euroscarf

	*ura3*Δ0; *apt1*::kanMX4	
BY4741 Δ*str2*	MAT a; *his3*Δ1; *leu2*Δ0; *met15*Δ*0*; *ura3*Δ0; *str2*::kanMX4	Euroscarf
BY4741 Δ*met6*	MAT a; *his3*Δ1; *leu2*Δ0; *met15*Δ*0*; *ura3*Δ0; *met6*::kanMX4	Euroscarf
DH5α *E. coli*	Ampicillin resistance cassette	Life Technologies

Table 2.2 *Aspergillus fumigatus* strains used

Strain	Genoptype	Source
A. fumigatus ATCC46645	Wild-type	ATCC collection
A. fumigatus AF 293	Wild-type	Gift from Dr. Markus Schrettl
ATCC26933	Wild-type	ATCC collection
A. fumigatus Δ*gliT*	ATCC46645 and ATCC26933 with AFUA_6G09740 coding region disrupted with pyrithiamine resistance gene from *A. oryzae*	Dr. Markus Schrettl, NUI Maynooth
A. fumigatus Δ*gliZ*	AF293 with AFUA_6G09630 coding region disrupted with pyrG marker from *A. parasiticus*	Gift from Dr. Nancy Keller
A. fumigatus Δ*gliT*Δ*gliZ*	Δ*gliZ* strain with coding region AFUA_6G09740 disrupted with pyrithiamine resistance gene from *A. oryzae*	This study

2.1.1.2 Plasmids used in this study

Table 2.3 lists the plasmid vectors used in this study for both *S. cerevisiae* and *Aspergillus fumigatus* experimental work.

Table 2.3 Plasmids vectors used

Plasmid Name	Description	Source
pRS315	Centromeric *S. cerevisiae* shuttle vector *LEU2* marker	Sikorski and Hieter 1989
pC210-*gliT*	Vector containg *Aspergillus fumigatus* thioredoxin reductase *gliT* cDNA under the *SSA2* promoter and a *LEU2* marker	Schrettl *et al*., 2010

pSK275	Vector containing the *ptrA* pyrithiamine resistance cassette originating from *A. oryzae*	Kind gift from Dr. S. Krappmann

2.1.1.3 Primers used in this study

Table 2.4 shows primer sequences used in this study.

Primer Name	**Sequence 5'- 3'**
ogliT-4	GGACTAGTTATGCGCGAGAGTAGTGG
ogliT-5	GCGCTTCTTGATCGG
OptrA1	GACCTGGACAAGTAC
OptrA2	CGTGACCAGTGGTAC
GliJ_F	AGACGGATCTCCAGCGTCTA
GliJ_R	CGATCAGTCTGTGGATCACG
AFUA_2G11120_F	TCCAGCGTACTCAACCACAC
AFUA_2G11120_R	CGTCTGGAAAGCTCTGGAAG
LaeA_F	AGGCCGCTCAAGAAACAAC
LaeA_R	TCGTCCGTTCTCCTGATAGC
GliM_F	AAGCTTCAACTGCAGCTCGT
GliM_R	AGACCGAGCGTTGATACAGG
CatB_F	TCAACGACAATGATGCCTTC
CatB_R	AAGAAGCCGCAGTGATGTTC
gliZcomp_F	TGCACTGCGATAGAAGGTTAAA
gliZcomp_R	GTTACATGGTCCATACTGTGAT

2.1.2 Chemicals and reagents used in this study

All chemicals and reagents were ordered from Sigma-Aldrich ltd. unless otherwise stated.

2.1.2.1 Gliotoxin (GT)

Gliotoxin was prepared by the addition of 25 ml methanol (MeOH) to 25 mg neat Gliotoxin. Once fully dissolved, this was aliquoted into 5x5 ml working stocks in glass containers and stored at -20 ℃.

2.1.2.2 Cystathionine

L-cystathionine (4.5 mg) was added to 20 ml sterile distilled dH_2O creating a 1 mM stock. This was filter sterilised and stored at -20℃ until required.

2.1.2.3 Diamide

A 0.0125 M working stock was made by adding 100 mg of diamide to 50 ml sterile distilled water. This was then filter sterilised and kept at – 20℃ until required.

2.1.2.4 1-Chloro-2, 4-dinitrobenzene (CDNB)

CDNB (0.101 g) was dissolved in 10 ml of 100 % (v/v) ethanol and stored at -20℃ C until required.

2.1.2.5 H_2DCFDA

H_2DCFDA dessicate (100 mg) (Invitrogen Molecular Probes Ltd.) was re-suspended in 2 ml DMSO creating a 50 mg/ml stock which was stored at -20℃.

2.1.2.6 Hydrogen Peroxide

A 30 % v/v stock of hydrogen peroxide, 11.8 M, (H_2O_2) was ordered and kept at 4℃. This was diluted in molten agar to the desired molarity.

2.1.2.7 Ampicillin

Ampicillin salt was added to 100 ml dH_20 to create a 50 mg/ml stock, which was filtered sterilised and stored at -20℃ until required.

2.1.2.8 Pyrithiamine

Pyrathiamine stocks of 0.1 mg/ml (w/v) were made using dH_2O and stored at -20℃.

2.1.3 Microbiological Media and Reagents

2.1.3.1 Yeast Peptone Dextrose (YPD)

Bacto-yeast extract (10 g, BD& Co.), bacto-peptone (20 g, BD &Co.) and D-glucose (20 g) were added to 800 ml dH_2O and dissolved. The solution was made up to 1 L with dH_2O subsequently autoclaved and stored at room temperature (RT).

2.1.3.2 YPD Agar

Bacto-agar (20 g, BD & Co.) was added to liquid YPD prior to being made up to 1 L with dH_2O. This was then autoclaved, allowed to cool and poured into sterile petri dishes under sterile conditions till it had solidified. Subsequent agar plates were stored at 4℃ until required.

2.1.3.3 Dropout Mix

Two grams of the following amino acids (Table 2.5) were added to a sterile pestle and mortar where they were ground and mixed and stored at RT:

Table 2.5 Amino acids required for dropout mix

Amino Acid
alanine, arginine, aspartic acid, cysteine, glutamic acid, glutamine, isoleucine, phenylalanine, proline, serine, threonine, tyrosine, valine, inositol, para-aminobenzoic, methionine*, lysine

*= For assays which required the absence of one or more of the marked amino acids, alternative dropout mixes were made lacking the respective amino acid.

2.1.3.4 Amino acid supplemental stocks

Strains used in this study are auxotrophic for particular amino acids depending on their genotypic background (Table 2.1). Working stocks were made as described in Table 2.4, in dH_2O, autoclaved and stored at 4℃ until required. Stock concentrations:

Table 2.6 Amino acid stock concentrations and final concentration when added to SC media

Amino acid	Working Stock Conc.	Volume added to 1 L SC media	Final amino acid conc. (µg/ml)
L-leucine	1 g/100 ml	10 ml	100
L-histidine	1 g/100 ml	2 ml	20
L-uracil	0.2 g/100 ml	10 ml	20
L-methionine	1 g/100 ml	2 ml	20
L-lysine	1 g/100 ml	2 ml	20
L-adenine	0.2 g/100 ml	10 ml	20

2.1.3.5 Synthetic Complete (SC)

Yeast nitrogen base (YNB) without amino acids (6.7 g, BD &Co.), D-glucose (20 g) and dropout mix (1.5 g) were added to 800 ml dH_2O and dissolved. This was supplemented, as required, with the necessary amino acids using stocks as described in section 2.1.3.4. This was topped up to 1 L using dH_2O, autoclaved and stored at room temperature.

2.1.3.6 SC Agar

Bacto-agar (20 g) was added to liquid SC prior to being topped up to 1 L using dH_2O. This was autoclaved and then allowed to cool. SC agar plates were stored at 4℃.

2.1.3.7 SC+Gliotoxin

SC agar was made as described previously (2.1.5.6). 25 ml was added to a sterile 50 ml Falcon tube. To this, gliotoxin stock solution was added to bring it to the desired concentration (Table 2.6). The SC + gliotoxin molten agar was mixed by inversion then

poured into sterile petri-dishes. This was carried out in duplicate for each concentration desired. SC-gliotoxin agar plates were stored at 4℃ for a maximum of one week.

Table 2.7 Volumes of 1 mg/ml gliotoxin stock added to 25 ml molten SC agar

Desired gliotoxin concentration (µM)	Volume added from 1 mg/ml gliotoxin stock (µl)
12.5	100
25	200
37.5	300
50	400

2.1.3.8 SC + L-cystathionine

SC agar was made as described previously (2.1.5.6). Once cool, 25 ml was added to a sterile 50 ml Falcon under sterile conditions. To this, L-cystathionine stock solution was added to bring it to the desired concentration (Table 2.8). The SC+L-cystathionine molten agar was mixed by inversion then poured into sterile petri dishes under sterile conditions. This was carried out in duplicate for each concentration. SC+L-cystathoinine agar plates were stored at 4℃ until required.

Table 2.8 Volumes of 1 mM L-cystathionine stock added to 25 ml molten SC agar

Desired L-cystathionine concentration (µM)	Volume added from 1 mM L-cystathionine stock (ml)
50	2.5
100	5
250	12.5
350	17.5

2.1.3.9 SC + H_2O_2

SC agar was made as described previously (2.1.5.6). Once cool, 25 ml was added to a sterile 50 ml Falcon under sterile conditions. H_2O_2 stock solution was added to the desired concentration (Table 2.9). The SC+H_2O_2 molten agar was mixed by inversion then poured into sterile petri dishes under sterile conditions. This was carried out in duplicate for each concentration. SC+H_2O_2 agar plates were stored at 4℃ until required.

Table 2.9 Volume of 11.8 M H_2O_2 stock added to 25 ml molten SC agar

Desired H_2O_2 concentration (mM)	Volume added from 11 M H_2O_2 stock (µl)
1	2.2
2	4.4
2.5	5.5
3	6.6

2.1.3.10 *Aspergillus* Trace Elements

$Na_2B_4O_7$ (0.04 g), $CuSO_4.5H_20$ (0.5 g), $FeSO_4.7H_20$ (1.2 g), $MnSO_4$ (0.7 g), $Na_2MoO.2H_20$ (0.8 g) and $ZnSO_4.7H_2O$ (10 g) were added to 800 ml dH_20 and once dissolved was made up to 1 L and autoclaved.

2.1.3.11 *Aspergillus* Salt Solution

KCL (26 g), $MgSO_4.7H_20$ (26 g), KH_2PO_4 (76 g) and *Aspergillus* trace elements (2.1.6.1.; 50 ml) were added to 800 ml dH_20 and once dissolved was made up to 1 L and autoclaved. Solution was stored at room temperature.

2.1.3.12 100x Ammonium Tartrate

Ammonium tartrate (92 g) was dissolved in 800 ml dH_2O; subsequently topped up to 1 L and autoclaved. Solution was stored at room temperature.

2.1.3.13 Malt Extract Agar

Malt extract agar (25 g; Difco, Maryland, USA) was added to a total 500 ml dH_2O and subsequently autoclaved. Once cool, 25 ml was poured into petri dishes, under sterile conditions. Once set plates were stored at 4℃ until required.

2.1.3.14 *Aspergillus* Minimal Media (AMM)

Ammonium tartrate (10 ml; section 2.1.3.13), *Aspergillus* salt solution (20 ml; section 2.1.3.12) and D-glucose (20 g) were added to 800 ml dH_20 until they were fully dissolved. Solution was pH adjusted to pH 6.8, made up to 1 L using dH_2O and autoclaved. AMM was stored at 4 ^{0} C until required.

2.1.3.15 *Aspergillus* Minimal Media (AMM) Agar

AMM was made as described previously (section 2.1.3.15). Once pH adjusted agar (20 g; Scharlau Chemie S.A., Barcelona, Spain) was added and then made up to 1 L using dH_2O. AMM agar was autoclaved and allowed to cool before being poured under sterile conditions into petri dishes

2.1.3.16 Sabouraud-Dextrose (SB) Media

Sabouraud-Dextrose media (30.12 g; Oxoid Ltd., Basingstoke, Hampshire, England) was added to 800 ml dH_2O and dissolved. Solution was made up to 1 L and autoclaved. SB media was stored at 4 ^{0} C until required.

2.1.3.17 Sabouraud-Dextrose (SB) Agar

Sabouraud-Dextrose media was made as previously described (section 2.1.3.17). Agar (20 g) was added and the solution was made up to 1 L. SB agar was autoclaved and allowed to cool before being poured, under sterile conditions, into petri dishes.

2.1.3.18 Phosphate Buffered Saline (PBS)

PBS (1 x tablet; Oxoid Ltd., Basingstoke, Hampshire, England) was added to 200 ml dH_2O and autoclaved. PBS was stored at room temperature until required.

2.1.3.19 Phosphate Buffered Saline-Tween-20 (PBST)

Tween-20 (0.1 ml) was added to 200 ml PBS (section 2.1.3.19). This was filtered sterilised through a 45 µm filter to create 50 ml aliquots which were stored at room temperature.

2.1.3.20 Luria-Bertani (LB) Broth

LB broth (25 g Difco, Maryland, USA) was added to 1 L dH_2O and dissolved with the aid of a magnetic stirring rod. LB solution was autoclaved and stored at 4^0 C until required.

2.1.3.21 Luria-Bertani (LB) Agar

LB agar (40 g; Difco, Maryland, USA) was added to 1 L dH_2O and dissolved with the aid of a magnetic stirring rod. LB agar was autoclaved and once cool, was poured (25 ml) under sterile conditions into petri dishes. Solidified LB agar plates were stored at 4^0 C until required.

2.1.3.22 Luria-Bertani (LB) Broth + Ampicillin

LB broth was made as previously described (section 2.1.3.21). Before inoculation, using a 50 mg/ml ampicillin stock, ampicillin (0.1 mg/ml) was added to 5 ml LB broth.

2.1.3.23 Luria-Bertani (LB) Agar + Ampicillin

LB agar was made as previously described (section 2.1.3.21). Using a 50 mg/ml ampicillin stock, ampicillin (0.1 mg/ml) was added and LB-agar-ampicillin was poured (25 ml) under sterile conditions into petri dishes.

2.1.3.24 40 % (v/v) Glycerol

Glycerol (40 ml) was dissolved in 60 ml dH_2O. Solution was autoclaved and stored at room temperature.

2.1.3.25 80 % (v/v) Glycerol

Glycerol (80 ml) was added to 20 ml dH_2O and dissolved by heating and with the aid of a magnetic stirrer. Solution was autoclaved and stored at room temperature.

2.1.4 *S. cerevisiae* Genomic DNA Isolation Reagents

2.1.4.1 1 M Sorbitol/100 mM EDTA

Sorbitol (18.2 g) was dissolved in 20 ml dH_2O by heating on a heat block. Once dissolved, 2.92 g of EDTA was added and the solution was topped up to a total volume of 100 ml with dH_2O. Solution was autoclaved and stored at room temperature

2.1.4.2 5 mg/ml Zymolase

Zymolase (500 mg) was dissolved in a total volume of 100 ml dH_2O creating a 5 mg/ml working stock. This was then filter sterilised, aliquoted into 1 ml fractions in 1.5 ml microfuge tubes and stored at -20 ^{0} C until required.

2.1.4.3 1 M Tris/100 mM EDTA

EDTA (2.92 g) was dissolved in 20 ml dH_2O. Next 12.1 g of Tris was added and once dissolved the solution was topped up to a final volume of 100 ml using dH_2O. Solution was autoclaved and stored at -20 ^{0} C.

2.1.4.4 5 M Potassium Acetate (KAc)

KAc (49 g) was dissolved in 20 ml dH_2O before adjusting the volume to 100 ml using dH_2O. This was then autoclaved and stored at room temperature.

2.1.5 Agarose Gel Electrophoresis Reagents

2.1.5.1 50 X Tris-Acetate (TAE)

Trizma base (342 g) was added to 57.1 ml glacial acetic acid and 100 ml of EDTA (0.5 M). This was pH adjusted to pH 8.0 and made up to 1 L with dH_2O and stored at room temperature.

2.1.5.2 1 X Tris-Acetate (TAE)

50 X TAE (20 ml) (section 2.1.5.1) was added to 980 ml dH_2O. 1 X TAE was mixed and subsequently stored at room temperature until required.

2.1.5.3 0.8 % (w/v) Agarose Gel

Agarose (0.4 g) was dissolved in 50 ml 1 X TAE (section 2.1.5.2). This was brought to boil until all the agarose had been dissolved then allowed to cool until 'hand hot' before being poured into a gel casting tray. Before being allowed to set, 4 µl ethidium bromide was added and mixed into the molten agar by using a gel comb until all the ethidium bromide was dissolved. Gel was then allowed to set for at least 20 min.

2.1.5.4 100 % (v/v) Ice Cold Ethanol

Molecular grade ethanol (100 %, v/v; Merck Ltd.) was aliquoted into 50 ml sterile Falcon tubes and stored at $-20\ ^{0}$ C until required.

2.1.5.5 70 % (v/v) Ice Cold Ethanol

Ice cold ethanol (35 ml 100 % (v/v)) (section 2.1.5.4) was added to 15 ml molecular grade H_2O in a sterile 50 ml Falcon tube and stored at $-20\ ^{0}$ C until required.

2.1.5.6 3 M Sodium Acetate

Sodium acetate (12.3 g) was dissolved in 50 ml molecular grade H_2O in a sterile 50 ml Falcon tube. This was then pH adjusted to pH 5.2 and stored at room temperature.

2.1.5.7 10 mg /ml Ethidium Bromide

1 µl of a 10 mg/ml ethidium bromide stock was added to 50 ml molten agar for DNA visualisation under U.V.

2.1.6 Yeast Transformation Buffers

2.1.6.1 50 % (w/v) Polyethylene Glycol (PEG)

PEG (50 g) was dissolved in 100 ml dH_2O, autoclaved and stored at 4^0 C.

2.1.6.2 1 M Lithium Acetate

Lithium acetate (6.59 g) was dissolved in a 100 ml dH_2O, autoclaved and stored at room temperature.

2.1.6.3 100 mM Lithium Acetate

Lithium acetate (1 M, 10 ml) was added to 90 ml dH_2O, autoclaved and stored at room temperature.

2.1.7 *E. coli* Transformation Buffers

2.1.7.1 RF1 Buffer

Potassium acetate (1.47 g), 0.75 g $CaCl_2.2H_2O$ and 70 g glycerol were dissolved in 450 ml dH_2O. Solution was pH adjusted to pH 5.92 after which 6 g rubidium chloride and 4.95 g manganese chloride were added. Volume was topped up to 500 ml using dH_2O and was filter sterilised and stored at 4^0 C.

2.1.7.2 RF 2

Rubidium chloride (0.6 g), 5.5 g calcium chloride, 1.05 g of 3-(N-morpholinopropaesulfonic acid (MOPS) and 75 g glycerol were dissolved in 450 ml dH_2O. Solution was pH adjusted to pH 6.8 before being topped up to 500 ml using dH_2O. This was filter sterilised and stored at 4^0 C.

2.1.8 *Aspergillus* Transformation Buffers

2.1.8.1 Buffer L1

KH_2PO_4 (1.7 g) was dissolved in 500 ml dH_2O to yield 50 mM KH_2PO_4 stock.

2.1.8.2 Buffer L2

K_2HPO_4 (0.87 g) was dissolved in 200 ml dH_2O to yield a 50 mM K_2HPO_4 stock.

2.1.8.3 Lysis Buffer

A 0.8 M KCL solution was prepared by dissolving 26.1 g of KCL in 350 ml buffer L1 (2.1.8.1). This was pH adjusted to pH 5.8 using buffers L1 and L2 (sections 2.1.8.1 & 2.1.8.2 respectively). This was brought to a final volume of 500 ml using dH_2O, autoclaved and stored at room temperature.

2.1.8.4 Mycelium Lysing Solution

Trichoderma harzianum Lytic enzymes (0.9 g) were dissolved in 30 ml Lysis buffer (section 2.1.8.3) and filtered through a 0.45 µm filter.

2.1.8.5 0.7 M KCl

KCl (26.1 g) was dissolved in 500 ml dH_2O, autoclaved and stored at room temperature.

2.1.8.6 L6 Buffer

1 M sorbitol (72.88 g), 10 mM Tris-HCL (0.484 g) and 10 mM $CaCl_2.6H_2O$ (0.876 g) were dissolved in 300 ml dH_2O. The pH was then adjusted to pH 7.5 and brought to a final volume of 400 ml with dH_2O. L6 buffer was autoclaved and stored at room temperature.

2.1.8.7 L7 Buffer

PEG 6000 (60 g) was dissolved in 40 ml dH_2O. 10 mM Tris-HCL (0.157 g) was added to this and dissolved. The solution was pH adjusted to pH 7.5, autoclaved and stored at room temperature.

2.1.8.8 *Aspergillus* Regeneration Media

Ammonium tartrate (10 ml) (section 2.1.3.13), 20 ml *Aspergillus* salt solution (section 2.1.3.12), 10 g glucose and 342 g sucrose were dissolved in 800 ml dH_2O. The solution was pH adjusted to pH 6.8 and topped up to a total volume of 1 L with dH_2O prior to the addition of 18 g agar (Scharlau Chemie S.A., Barcelona, Spain). Solution was autoclaved and allowed cool before being poured into petri-dishes.

2.1.8.9 *Aspergillus* Transformation Soft Agar

Ammonium tartrate (10 ml, section 2.1.3.13), 20 ml *Aspergillus* salt solution (section 2.1.8.3.12), 10 g glucose and 342 g sucrose were dissolved in 800 ml dH_2O. The solution was pH adjusted to pH 6.8 and topped up to a total volume of 1 L with dH_2O prior to the addition of 7 g agar. Solution was autoclaved and allowed cool before being poured into petri-dishes.

2.1.9 Southern Blotting Reagents

2.1.9.1 Southern Transfer Buffer

NaOH (16 g) and 0.6 M NaCl (35.06 g) were dissolved in 1 L dH_2O. This was made up just before carrying out the Southern blot.

2.1.9.2 20 X SSC Buffer

NaCl (175.3 g) and sodium citrate (88.2 g) were dissolved in 800 ml dH_2O. This was then pH adjusted to pH 7 and brought to a final volume of 1 L with dH_2O. Solution was autoclaved and stored at room temperature.

2.1.9.3 10 X SSC Buffer

500 ml of 20 X SSC buffer (section 2.1.9.2) was to 500 ml dH_2O and stirred to ensure it was homogenous. This was autoclaved and stored at room temperature.

2.1.9.4 2 X SSC Buffer

100 ml of 20 X SSC buffer (section 2.1.9.2) was added to 900 ml dH_2O and stirred to ensure it was homogenous. This was autoclaved and stored at room temperature.

2.1.9.5 10 % (w/v) Sodium Dodecyl Sulphate (SDS)

SDS (100 g) was dissolved in 1 L dH_2O with the aid of a magnetic stirrer and a heat block to help get it into solution. The solution was autoclaved and stored at room temperature.

2.1.9.6 0.1 % (w/v) SDS/1 X SSC Buffer

SDS (10 ml of 10 % (w/v), section 2.1.9.5) and 50 ml of 20 X SSC (section 2.1.9.2) were dissolved in a total volume of 1 L dH_2O. This was made on the day it was required and stored at room temperature before use.

2.1.10 Digoxigenin (DIG) Detection Buffers

2.1.10.1 10 % Blocking reagent

Blocking reagent (20 g) was dissolved in 200 ml dH_2O with the aid of a magnetic stirrer and hot plate. Solution was stored at 4^0 C.

2.1.10.2 Membrane Pre-hybridisation Buffer

SDS (35 g), 250 ml de-ionised formamide, 100 ml 10 % (w/v) blocking reagent (section 2.1.10.1) and 5 ml (w/v) laurylsarcosine were dissolved in a total 500 ml dH_2O with the aid of a magnetic stirrer and hot plate. The solution was stored at 4^0 C.

2.1.10.3 DIG Buffer 1

Maleic acid (1.1.61 g) and NaCl (0.876 g) were dissolved in 80 ml dH_2O. This was then pH adjusted to pH 7.5 and brought to a final volume of 100 ml using dH_2O. This was filter sterilised using a 0.45µm filter and stored at room temperature.

2.1.10.4 DIG Buffer 2/Antibody Blocking Buffer

Blocking reagent (0.4 g) was dissolved at 50^0 C in 40 ml DIG buffer 1 (section 2.1.10.3) just before use.

2.1.10.5 DIG Buffer 3

Tris-HCl (1.57 g), NaCl (0.58 g) and $MgCl_2.6H_2O$ (1.01 g) were dissolved in 80 ml dH_2O. This was pH adjusted to pH 9.5 and brought to a final volume of 100 ml using dH_2O. Solution was filter sterilised using a 0.45 µm filter and stored at room temperature.

2.1.10.6 DIG Wash Buffer

Tween-20 (0.15 g) was dissolved in 50 ml DIG Buffer 1 (section 2.1.10.3) and stored at room temperature.

2.1.10.7 Anti-DIG FaB Fragments-alkaline phosphatase

Anti-DIG FaB fragments (1 µl, Roche), was added to 10 ml antibody blocking buffer (section 2.1.10.4) just before usage in a 50 ml Falcon tube.

2.1.10.8 CSPD Chemi-luminescent substrate

CSPD (50 µl, Roche) was added to 4.95 ml DIG Buffer 3 (section 2.1.10.5) just before use in a 50 ml Falcon tube.

2.1.10.9 DIG-labelled Deoxynucleotide Triphosphates (dNTP's)

Pre-mixed DIG-labelled dNTP's (Roche) were used as per suppliers instructions for the generation of Southern blot probes.

2.1.11 Blot Development Solutions

2.1.11.1 Kodak Developing Solution

Developing solution (200 ml, Kodak) was added to 400 ml dH_2O in a Duran bottle covered in tin foil. Developer was stored in the dark at room temperature.

2.1.11.2 Kodak Fixing Solution

Fixing solution (150 ml, Kodak) was added to 350 ml dH_2O in a Duran bottle covered in tin foil. Fixer was stored in the dark at room temperature.

2.1.12 LC-MS Stocks and Buffer

2.1.12.1 Bovine Serum Albumin (BSA)

BSA (1 g) was added to 10 ml dH_2O to create a 100 mg/ml stock. 100 µl of this was then transferred to 1.5 ml microfuge tubes and stored at -20 ^{0} C until required.

2.1.12.2 Iso-electric Focussing Buffer

Urea (24.02 g), 7.61 g thio-urea, 2 g 3-[(3-Cholamidopropyl)dimethylamoonio]-1-propanesulfonate (CHAPS), 500 µl Triton X-100 and 0.06 g tris-base were dissolved sequentially in dH_2O and brought to a total volume of 50ml using dH_2O. This was stored at -20 ^{0} C until required.

2.1.12.3 Rehydration Buffer

Urea (24.02 g), 0.25 g CHAPS, 0.1 g dithiothreitol (DTT) and 100 µl ampholytes (GE Healthcare) were dissolved sequentially in dH_2O and brought to a total volume of 50 ml using dH_2O.

2.1.12.4 Reduction Buffer

Glycerol (150 ml), 10 g SDS, 180 g urea and 3.03 g tris were dissolved sequentially in 300 ml dH_2O and brought to pH 6.8. This was brought to a total volume of 500 ml using dH_2O. 50 ml fractions were transferred to 50 ml Falcon tubes and stored at -20 ^{0} C until required. Prior to use DTT (0.02g/ml) was added.

2.1.12.5 Alkylation Buffer

Glycerol (150 ml), 10 g SDS, 180 g urea and 3.03 g tris were dissolved sequentially in 300 ml dH_2O and brought to pH 6.8. This was brought to a total volume of 500 ml using dH_2O. 50 ml fractions were transferred to 50 ml Falcon tubes and stored at -20 ^{0} C until required. Prior to use, iodoacetamide (0.025g/ml) was added, along with 100 µl 1% bromophenol blue solution.

2.1.12.6 10 X Running Buffer

Trizma base (30 g), 144 g glycine and 10 g SDS were dissolved in 800 ml dH_2O with the aid of a heat block and magnetic stirrer. Once fully dissolved the solution was brought to a total volume of 1 L using dH_2O and stored at room temperature.

2.1.12.7 1 X Running Buffer

10 X running buffer (100 ml, section 2.1.12.6) was added to 900 ml dH_2O and stored at room temperature.

2.1.12.8 10% Ampholytes

Ampholytes (500 µl, APS) (GE Healthcare) was added to 4.5 ml dH_2O creating a 10 % APS stock. 1 ml aliquots were transferred to fresh 1.5 ml microfuge tubes and stored at -20 ^{0} C until required.

2.1.12.9 Agarose Sealing Solution

Trizma base (1.5 g), 7.2 g glycine, 0.5 g SDS, and 1.5 g agarose (Electran) were added to 80 ml sequentially. A pinch of bromophenol blue was added prior to the solution being topped up to 100 ml with dH_2O and was kept molten in a water bath prior to use.

2.1.13 Coomassie Staining Reagents (Colloidal Method)

2.1.13.1 Fixing Solution

Ethanol (500 ml), 30 ml phosphoric acid were topped up to 1 L with dH_2O, solution was made on day of usage.

2.1.13.2 Incubation Buffer

Methanol (340 ml), 30 ml phosphoric acid and 170 g ammonium sulphate were brought up to 1 L using dH_2O. This was made on day of usage.

2.1.13.3 Stain Solution

Methanol (340 ml), 30 ml phosphoric acid, 170 g ammonium sulphate and 0.35 g Colloidal Coomassie Blue G-250 (Serva) were brought to 1 L using dH_2O.

2.1.13.4 Neutralisation Buffer

Tris base (12.11 g) was dissolved in 900 ml dH_2O. This was pH adjusted to pH 6.5 using phosphoric acid after which it was brought to a total volume of 1 L using dH_2O

2.1.14 Mass Spectrometry Reagents

2.1.14.1 Destaining Buffer

Ammonium bicarbonate (0.79 g) was dissolved in 100 ml HPLC-grade dH_2O and diluted 1:1 HPLC grade aceto-nitrile. This was made fresh on the day.

2.1.14.2 Trypsin Reconstitution Buffer

Ammonium bicarbonate (10 mM) and 10 % (v/v) acetonitrile were brought to a final volume of 10 ml using HPLC-grade dH_2O. This was made fresh on the day

2.1.14.3 Trypsin Digestion Buffer

Trypsin (20 µg) was diluted in 1.5 ml reconstitution buffer giving a 13 ng/µl working stock. Surplus trypsin digestion buffer was stored at -20 ^{0} C.

2.1.14.4 50 mM Ammonium bicarbonate

200 mg ammonium bicarbonate was dissolved in 50 ml HPLC-grade dH_2O, on day of usage.

2.1.14.5 Extraction Buffer

5 % (v/v) formic acid and HPLC-grade acetonitrile were mixed 1:2 (v/v). This was made fresh on day of use.

2.1.14.6 0.1 % Formic Acid

0.1 % (v/v) was added to a total 10 ml HPLC-grade dH_2O, fresh on the day of use.

2.1.15 Glutathione Assay Buffers

2.1.15.1 1 M NaCl

NaCl (5.844 g) was dissolved to in 100 ml dH_2O, autoclaved and stored at room temperature.

2.1.15.2 Pepstatin A 1 mg/ml

Pepstatin A (10 mg) was added to 10 ml dH_2O to give a 1 mg/ml pepstatin A stock. This was filter sterilised using a 0.45 µm filter and 500 µl fractions were aliquoted into 1.5 ml microfuge tubes and stored at -20 ^{0} C.

2.1.15.3 Phenylmethylsulfonyl fluoride (PMSF)

PMSF (0.435 g) was dissolved in 5 ml dH_2O to yield a 500 mM PMSF stock. 1 ml fractions were aliquoted into 1.5 ml microfuge tubes and stored at -20 ^{0} C.

2.1.15.4 Lysis Buffer

Tris-HCl (1.576 g), 5 ml of 1 M NaCl (section 2.1.15.1), EDTA (0.745 g), Glycerol (10 ml) were dissolved in 80 ml dH_2O. Solution was pH adjusted to pH 7.5 and brought to a final volume of 100 ml with dH_2O, autoclaved and stored at 4 ^{0} C. 30 mM DTT (0.4627 g), 100 µl of 1 mg/ml pepstatin A stock (section 2.1.15.2) and 200 µl of 500 mM PMSF stock (section 2.1.15.3) were later added just before use.

2.1.15.5 GSH Assay Buffer

Sodium phosphate (1.5 g) was dissolved in 80 ml dH_2O. Solution was pH adjusted to pH 7.5. EDTA (0.2345 g) was then dissolved and the solution was brought to a final volume of 100 ml using dH_2O.

2.1.15.6 5 % (w/v) Sulfo-salicyclic Acid (5 % SSA)

SSA (0.5 g) was dissolved in 10 ml GSH assay buffer (section 2.1.15.5) fresh and kept on ice until required.

2.1.15.7 Triethanolamine

Triethanolamine was diluted 1:2 (v/v) using GSH assay buffer (section 2.1.15.5), and kept on ice.

2.1.15.8 2-vinylpyridine

2-vinylpyridine was diluted 1:5 (v/v) in GSH assay buffer (section 2.1.15.5) under a fume hood and kept on ice.

2.1.15.9 5,5′-Dithiobis(2-nitrobenzoic acid) (DTNB) + Glutathione Reductase

DTNB (11.89 mg) and 157.1 µl glutathione reductase were added to 3 ml GSH assay buffer in a 15 ml Falcon wrapped in tin foil and stored on ice.

2.1.15.10 NADPH

A 25 mg/ml NADPH stock solution was made by adding 1 ml GSH assay buffer (section 2.1.15.5) to 25 mg NADPH. 200 µl aliquots were added to 1.5 ml microfuge tubes wrapped in tin foil and stored at -20 ^{0} C until required.

2.2 Methods

2.2.1 Microbiological Methods

2.2.1.1 *S. cerevisiae* growth, maintenance and storage

S. cerevisiae strains were grown on YPD agar plates (section 2.1.3.2) at 30 ^{0} C in a static incubator for ~48 h in the dark. For liquid cultures, *S. cerevisiae* strains were inoculated in liquid YPD (section 2.1.3.1) at 200 rpm (Innova 4000 Orbital Shaker, New Brunswick Scietnific, UK) at 30 ^{0} C. Growth and maintenance of those strains which contained plasmids was carried out using SC media (section 2.1.3.5) or SC agar (section 2.1.3.6) lacking an appropriate amino acid to maintain selection for that particular plasmid. Working stocks of strains were kept at 4 ^{0} C for short term use and were re-inoculated every few weeks. Long term stocks were generated using 500 µl of freshly grown cells, mixed with 40 % (v/v) glycerol (section 2.1.3.25) in a 1.5 ml microfuge tube. This was then 'flash-frozen' using liquid Nitrogen and stored at -70 ^{0} C until required.

2.2.1.2 *E. coli* growth, maintenance and storage

E. coli cells were grown on LB-ampicillin agar plates (section 2.1.3.24) and grown at 37 ^{0} C, or in LB-amp broth (section 2.1.3.23) at 37 ^{0} C shaking at 200 rpm. Working stocks were kept at 4 ^{0} C for short term use. Long term stocks were generated using 500 µl of freshly grown cells (in appropriate selective media) and mixed with 40 % (v/v) glycerol (section 2.1.3.25). This was then 'flash-frozen' using liquid Nitrogen and stored at -70 ^{0} C until required.

2.2.1.3 *Aspergillus fumigatus* growth, maintenance and storage

A. fumigatus strains were stored on either AMM (section 2.1.3.16) or MEA (section 2.1.3.14) agar plates at 4 ^{0} C. To culture strains, a loop of spores from a stock spore solution was spread around an appropriate culture plate under sterile conditions and incubated at 37 ^{0} C for 3-4 days depending on growth rate of that particular strain. Conidia were then harvested by adding 10 ml sterile PBST (section 2.1.3.20) to the plate while rubbing the surface with a sterile inoculation loop to get the conidia into solution. The conidial-PBST solution was aliquoted from the plate into a sterile 50 ml Falcon tube using a sterile Pasteur pipette, sealed with parafilm and stored at 4 ^{0} C until required. From this, liquid cultures were inoculated (usually at a concentration of 5 X 10^{6} spores/ml) for relevant experiments. These were then incubated for the appropriate length of time, depending on the experiment, at 37 ^{0} C shaking at 200 rpm.

Resulting mycelia could be harvested by filtering the culture through sterile Mira-cloth and washed using sterile water to remove residual media. Washed mycelia were removed from the Mira-cloth and were either immediately used or wrapped in tin foil and flash frozen in liquid nitrogen. Mycelia could then be used for the relevant experiment or stored at -70 ^{0} C until required. Long term conidial stocks were prepared by aliquoting 800 µl of a conidial-PBST suspension to 200 µl 80 % (v/v) glycerol solution (section 2.1.3.26). Tubes were mixed by vortexing and stored at -70 ^{0} C.

2.2.1.4 Measuring *S. cerevisiae* cell density

Overnight cultures were diluted 1/50 by adding 100 µl of culture to 4.9 ml fresh media. The OD_{600nm} was then measured using a spectrophotometer (Eppendorf). Depending on the OD_{600nm} required, more culture would be added to increase the OD or removed and more media added in its place to lower the OD until at the desired concentration. This was carried out under sterile conditions.

2.2.1.5 Dot assay/Comparative growth analysis

5 ml overnight cultures were diluted the next morning to an OD_{600nm}=0.15 in 5 ml fresh media. Diluted cultures were incubated at 30 ^{0} C at 200 rpm until at a concentration of 3 x 10^{6} cells/ml. Cultures were pelleted by centrifugation at 1677 g

(Centrifuge 5810R, Eppendorf) for 5 min and re-suspended to a concentration of 5 x 10^6 cells/ml. Using a 96 well plate (Sarstedt), 200 µl neat culture was added to wells in column '1'. In the wells of columns 2-6 inclusive, 160 µl fresh media was added. Using a multi-channel pipette, a 1/5 serial dilution was carried out by removing and adding 40 µl from well A1 through to well A6. With a sterilised 96 well replicator (Sigma), cells transferred agar plates under sterile conditions. Cells were allowed to dry before being incubated at 30 ^{0} C static for 48 h.

2.2.1.6 *A. fumigatus* Plate Assays

A. fumigatus strains were spotted onto AMM agar plates (section 2.1.3.16) with or without the added experimental variable. 5 X 10^6 conidia/20 µl spot was incubated at 37 ^{0} C static for 72 h after which mycelia radii were measured as an indicator of growth. Significance was measured by a two way ANOVA using two replicates for each strain.

2.2.1.7 *Galleria mellonella* Virulence Testing

G. mellonella testing was carried out as described by Reeves *et al.,* (2004). Sixth instar *G. mellonella* larvae (Lepitdoptera: Pyralidae, the Greater Wax Moth) (Mealworm company, Sheffield, England) were stored in the dark at 15 ^{0} C in wood shavings. Larvae weighing 0.2 and 0.4 g were used in this study. All *A. fumigatus* conidial suspensions used were prepared in sterile PBS (section 2.1.3.19). 5 X 10^6 conidia per 20 µl inoculum was injected into the last left proleg of *G. mellonella* hosts (n=10). All injections were carried out using sterile syringes (1ml, 27 g). Un-injected *G. mellonella* and injections using 20 µl PBS served as negative controls. Two sets of injections were carried out for each replicate and each data set was repeated in triplicate on three independent occasions. Mortality rates and melanisation rates were measured over a 72 h period with a positive death being confirmed by lack of movement from larvae in response to stimulation and a discolouration of its cuticle.

2.2.2 Molecular Biological Methods

2.2.2.1 Isolation of Genomic DNA from *S. cerevisiae*

S. cerevisiae strain(s) were inoculated in 2 ml YPD (section 2.1.3.1) and incubated overnight at 30 ^{0} C shaking at 200 rpm. Cells were pelleted at 1077 g for 5 min. and resulting pellets were re-suspended in 150 µl 1 M sorbitol/100 mM EDTA (section 2.1.4.1) and aliquoted into a sterile 1.5 ml microfuge tube. 12 µl of 5 mg/ml zymolase (section 2.1.4.2) was added to the cell mixes and incubated for 1 h at 37 ^{0} C static. Samples were spun at 13000 rpm for 5 s and re-suspended in 150 µl 1 M Tris/100 mM EDTA (section 2.1.4.3). 10 µl of 10 % SDS solution (section 2.1.9.5) was added to each sample and mixed. Solutions were then incubated at 65 ^{0} C for 30 min after which 60 µl of 5 M KAc (section 2.1.4.4) was added to each sample and subsequently cooled on ice for 1 h. Samples were centrifuged at 18894 g for 5 min and resulting supernatants were transferred to new microfuge tubes. To this, 195 µl of iso-propanol was added and left to incubate at room temperature for 5 min permitting DNA precipitation. Samples were centrifuged briefly at 18894 g for 10 s to form a DNA pellet. Supernatant was removed and the pellets were air dried and subsequently re-suspended in 30-50 µl dH_2O. DNA samples were stored at -20 ^{0} C until required.

2.2.2.2 Isolation of Genomic DNA from *A. fumigatus*

50 ml SB media (Section 2.1.3.17) were inoculated using an *A. fumigatus* conidial suspension (usually at a concentration of 5 x 10^6 conidia/ml). These cultures were incubated overnight at 37 ^{0} C shaking at 200 rpm after which mycelia was harvested by filtering through sterile Mira cloth. Media were washed from the mycelium using sterile dH_2O and scraped from the Mira cloth using a sterile spatula. This was then wrapped in the Mira cloth and dried using tissue paper ensuring none of the mycelium was exposed to the tissue. Once dry, the mycelium was wrapped in tinfoil and flash frozen in liquid nitrogen. Samples could be stored at this point at -70 ^{0} C until required. Prior to DNA isolation, frozen mycelium was crushed using a sterile pestle and mortar until a powdery consistency was formed. To prevent the mycelium from thawing during this process, more liquid nitrogen would be added. 100 mg of ground mycelia was then added to a ZR BashingBead$^{TM.}$ Using the ZR Fungal/Bacterial DNA Kit^{TM} (Zymo Research U.S.A) DNA was isolated using reagents and materials as

instructed by the manufacturers guidelines. To elute the DNA, 50 µl sterile water was added to the centre of the spin column and centrifuged at 11180 g for 1 min and collected in a sterile 1.5 ml microfuge tube and stored at -20 ^{0} C.

2.2.2.3 Genomic DNA Precipitation in *A. fumigatus*

DNA samples from section 2.2.2.2 were topped up to a total volume of 100 µl using sterile dH_2O. 10 µl 3 M sodium acetate (section 2.1.5.6) and 250 µl ice-cold 100% ethanol (v/v) (section 2.1.5.4) were added and mixed by inversion. Samples were then incubated at -20 ^{0} C for at least an hour and subsequently centrifuged at 18894 g for 10 min at 4 ^{0} C. Supernatants were carefully removed ensuring not to disturb the pellet and 100 µl 70 % (v/v) ethanol was added to the tube. Samples were centrifuged at 18894x g for 10 min at 4 ^{0} C after which the supernatants were removed and samples were centrifuged again at 11180 g for 15 secs. Residual ethanol was removed and the pellet was air dried and re-suspended in 16 µl sterile dH_2O.

2.2.2.4 Polymerase Chain Reaction (PCR)

PCR was employed to amplify fragments of DNA for cloning into plasmids, generation of gene disruption cassettes, DIG-labelled probes, and knockout qualification of transformants. For the production of DIG-labelled probes and gene disruption cassettes, a high fidelity, high proof read *Taq* polymerase was used, either Platinum *Taq*^{TM} (Invitrogen) or Accu*Taq* LA polymerase. All other PCR reactions were carried out using NEB *Taq* polymerase.

PCR using Platinum *Taq* polymerase

10X High fidelity reaction buffer	5 µl
dNTP mix (10 µM)	2 µl
Forward primer (100 pmol/µl)	2 µl
Reverse primer (100 pmol/µl)	2 µl
$MgSO_4$	2 µl
Template DNA	(10-100 ng)

Platinum High Fidelity *Taq*™	0.5 µl
Sterile dH_2O	to a total volume of 20 µl

PCR using Accu*Taq* LA polymerase

10X Reaction buffer	2 µl
dNTP mix (10 µM)	2 µl
Forward primer (100 pmol/µl)	1 µl
Reverse primer (100 pmol/µl)	1 µl
DMSO	0.8 µl
Template DNA	(10-100 ng)
Accu*Taq* LA polymerase™	0.25 µl
Sterile dH_2O	to a total volume of 20 µl

PCR using NEB *Taq* polymerase

10X reaction buffer	2 µl
dNTP mix (10 µM)	1 µl
Forward primer (100 pmol/µl)	1 µl
Reverse primer (100 pmol/µl)	1 µl
$MgCl_2$	1 µl
Template DNA	(50-100 ng)
Taq polymerase	0.5 µl
Steril dH_2O	to a total volume of 20 µl

PCR Reaction Cycle

The following reaction cycle is a typical example of what was used unless otherwise stated: Step 1: 95 ^{0} C (denaturing) 5 min; Step 2: 95 ^{0} C (denaturing) 1 min; Step 3: 55 ^{0} C*(annealing) 1 min 30 secs; Step 4: 72 ^{0} C (extension) 1 min$^+$; repeat X30 cycles from step 2; Step 5: 72 ^{0} C (extending) 10 min.

*Annealing temperatures were calculated by setting them 4 ^{0} C below the lowest melting temperature (T_m) of the primers being used.

Extension times were chosen as 1 min/kb of target DNA to be amplified. When either Accu*Taq* or Platinum *Taq* were being used the extension time was reduced to 68 ^{0} C as per suppliers recommendations.

For difficult to amplify targets Fusion PCR was carried out using a high fidelity *Taq*. Protocol was followed as described in Szewczyk *et al*., (2006).

2.2.3 DNA Gel electrophoresis

2.2.3.1 Preparation of a 0.8 % agarose gel

Gels were cast in a Biorad casting tray by adding 0.4 g electrophoresis agarose (Biorad) into 50 ml (0.8 % w/v) 1X TAE buffer (section 2.1.5.2) and heated to boiling using a microwave set at maximum power for 1 min. This was allowed to cool till hand hot and was poured into the casting mould. To this 1 µl of a 10 mg/ml ethidium bromide solution was added and mixed into the agar solution by stirring gently. A well comb was then secured in place to create wells for the addition of samples, and allowed to set for 30 min.

2.2.3.2 Loading and running of samples

Before loading onto a gel, DNA samples must first be mixed with a 6X loading dye (Promega). To estimate sample size, a molecular weight marker was also added to one lane. Marker VII (DIG-labelled)(Roche), 1 kb DNA ladder (New England Biolabs) and 50 bp DNA ladder (New England Biolabs) were used throughout this study. Each was subsequently loaded into respective wells and run at 90 V for 45 min depending on the size of the expected sample.

2.2.3.3 DNA Gel extraction

For the extraction of sample products separated on an agarose gel, bands were excised using a sterile scalpel and transferred to a sterile, pre-weighed, 1.5 ml microfuge tube. The weight of the gel slice was then weighed and treated using the QIA quick gel extraction kit (Qiagen) and the reagents and columns provided as per the manufacturers guidelines.

DNA was eluted using 30 µl sterile dH_2O added directly to the centre of the spin column, leaving to stand for 2 min. This was centrifuged at 16099 g for 1 min and the eluted DNA was stored at -20 ^{0} C until required.

2.2.3.4 DNA Restriction digest

DNA restriction digest was used for the digestion of genomic DNA used in Southern blotting, release of target regions contained within a plasmid, linearising a plasmid, to enable the subsequent ligation of gene disruption cassettes and insertion of genes of interest into plasmid vectors. Restriction-digest enzymes and buffers were supplied from New England Biolabs and reactions were carried out as per their instructions e.g.: DNA 1-5 µg; enzyme 1 1 µl; enzyme 2 1 µl; 10 X buffer 2.5 µl; 10X BSA 2.5 µl; sterile dH_2O to a total volume of 25 µl. Reactions were usually carried out at 37 ^{0} C for three hours, however due to different requirements this could be altered as per manufacturers' guidelines.

2.2.3.5 DNA ligation

Gene disruption cassettes and genes required to be cloned via vectors were created by restriction digest with specific enzymes and DNA ligation. After the creation of compatible fragments (section 2.2.3.4) digested DNA samples were separated via gel electrophoresis (section 2.2.3.2) and correctly sized bands were excised from the gel (section 2.2.3.3). DNA fragments were ligated using T4 DNA ligase (Promega) as per manufacturers' guidelines. After digestion, double stranded DNA will have a single stranded overhang if they are cohesive ends or none as is the case in blunt ended molecules. All digested DNA samples used in this study possessed cohesive ends. Ligation reactions were carried using this formula:

$$\frac{(\text{ng of vector}) * (\text{kb size of insert})}{\text{kb size of vector}} * \frac{3}{1} = \text{ng of insert}$$

2.2.4 *Aspergillus fumigatus* mutant strain generation

2.2.4.1 Gene disruption cassette generation

A. fumigatus genes were disrupted by employing a bi-partite strategy. This employs PCR (section 2.2.2.4) to amplify the gene cassettes ligated to a selectable marker facilitating relatively quick generation when compared to methods which enlist bacterial sub-cloning practices (Nielson *et al*., 2006). This technique amplifies regions outside the gene of interest (GOI) flanking the gene on its 5' side and 3' side (usually between 1200-1500 bp in size). The primers used to amplify these regions will contain two restriction sites not normally found in this ORF. The incorporation of these restriction sites facilitates the next step of ligating each flanking region to the selectable marker. In this study, the pyrithiamine resistance gene (*ptrA*) from *Aspergillus oryzae* (Kubodera *et al*., 2000; 2002) was used. This was liberated from a plasmid vector pSK275 using the restriction enzymes which correspond to the restriction sites found on the flanking regions. Following subsequent digestion of the flanking regions (section 2.2.3.4) to create combatable ends to *ptrA*, they were then respectively ligated (section 2.2.3.5) to the *ptrA* gene.

Subsequent ligation reactions were then used as DNA template for another round of PCR using a nested primer within the flanking region and an internal *ptrA* (optra) primer amplifying only a portion of the *ptrA* gene. All PCR reactions were carried out using a high fidelity *Taq* to ensure no loss of homology. PCR products were separated by gel electrophoresis (section 2.2.3.2) and purified using a Qiagen gel extraction kit (section 2.2.3.3). Upon transformation the flanking regions should homologously recombine with the corresponding flanking regions within the organism, while the *ptrA* partially amplified regions will homologously recombine along the portion which is common in both (Figure 2.1)

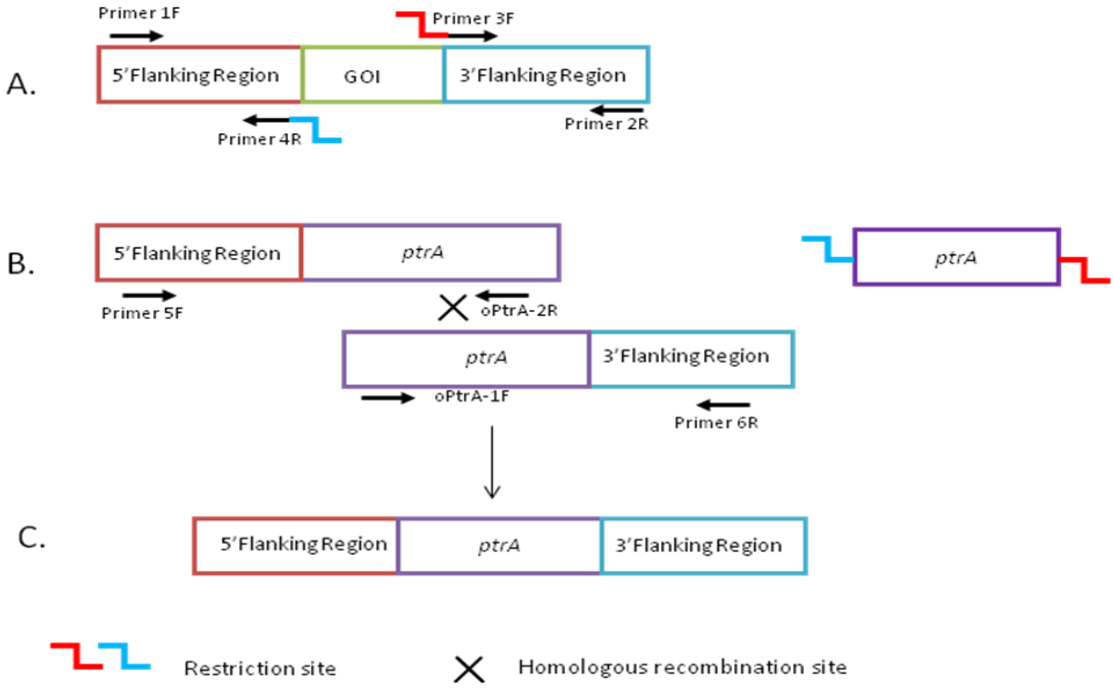

Figure 2.1 Bi-partite strategy for gene disruption in *A. fumigatus* using a *ptrA* selectable marker. Using specific primers (1-4), two regions from the 5' and 3' regions flanking a gene of interest are amplified (A), using suitable restriction enzymes engineered for *ptrA* (B). Using primer 5F-oPtrA-2R and 6R-oPtrA-1F respectively another round of PCR generates two new constructs which consists of only two thirds of the *ptrA* gene. Three sites will then homologously recombine with their corresponding regions: 5'flanking region, 3' flanking region and *ptrA*.

2.2.4.2 *A. fumigatus* Protoplast Production

A. fumigatus conidial suspensions were used to inoculate 2X 200 ml AMM media (section 2.1.3.15) cultures and were incubated at 37 ^{0} C overnight shaking at 11 g. Mycelia were harvested through sterile Mira-cloth and excess media was rinsed off using sterile dH_2O. Harvested mycelia was dried using sterile tissue paper and

subsequently 1.5 g dried mycelia was transferred to a sterile 50 ml Falcon tube in duplicate. To each, 15 ml mycelium lysing solution (section 2.1.8.4) was added and each was incubated for 20 min at 30 ^{0} C shaking at 3 g with each tube set lying down. After this, the tubes were removed and homogenised using a Gilson pipette and a 1000 µl tip. Each sample was aliquoted up and down to break up the cells and remove clumps. Next a 200 µl pipette tip was placed onto the other tip and the samples were once again aliquoted up and down. Once each sample was completely homogenised they were placed back into the incubator at 30 ^{0} C shaking at 3 g for another 2 h and 40 min. Samples were placed on ice for at least 5 min afterwards to stop the lysing reaction. They were centrifuged with the brake off, preventing protoplast disruption, at 1073 g for 18 min to collect cellular debris. Supernatant was filtered through sterile Mira-cloth into fresh 50 ml Falcon tubes and the volume was brought to 40 ml using 0.7 M KCl solution (section 2.1.8.5). Protoplasts solutions were centrifuged at 4293 g for 18 min. Supernatant was removed carefully ensuring not to disturb the pellet. Pellets were re-suspended in 10 ml 0.7 M KCl and centrifuged at 4293 g for 12 min. Again, supernatant was immediately removed and tubes were left to dry upside down over sterile tissue paper for 1 min. Pellets were re-suspended using 70 µl L6 buffer (section 2.1.8.6) by gently swirling. Samples were briefly centrifuged at 604 g and duplicate samples were combined and left on ice for no longer than 20 min prior to use. At this point protoplasts could be checked for integrity and number by aliquoting 5 µl onto an haemocytometer and visualising using a light microscope and a high power lens.

2.2.4.3 *A. fumigatus* Protoplast Transformation

For each strain to be transformed, 10 µg of the DNA to be transformed was used. DNA was placed in a 50 ml Falcon tube and was brought to a total volume of 50 µl using buffer L6 solution (section 2.1.8.6). 150 µl protoplast solution (section 2.2.4.2) was added to the DNA-L6 buffer and mixed by gently swirling. A negative control was made by adding 15 µl protoplast solution to 185 µl buffer L6 in a separate 50 ml Falcon tube and mixed by gently swirling. 50 µl buffer L7 (section 2.1.8.7) was added to both tubes, shaking gently to mix and left to incubate on ice for 20 min. Buffer L7 (1ml) was

added to each tube and samples were left at room temperature for 5 min. Following this, samples were ready to be plated.

2.2.4.4 Transformed *A. Fumigatus* Protoplasts Plating and Selection on pyrithiamine agar plates

A. fumigatus protoplasts were plated onto *Aspergillus* regeneration media (section 2.1.8.8) with or without pyrithiamine where appropriate. Plates were made prior to the transformation typically during the lysing incubation step (section 2.2.4.2). Before being poured into petri dishes, pyrithiamine (section 2.1.2.8) was added to yield a concentration of 0.1 µg/ml and was added to six plates. Two positive control plates were poured containing no pyrithiamine.

For plating the negative controls (section 2.2.4.3) 1.25 ml of the negative control protoplasts was added to a fresh 50 ml Falcon tube and was brought to a final volume of 6 ml with *Aspergillus* transformation soft agar (section 2.1.8.9) and poured onto a plate containing pyrithiamine. For the positive controls/protoplast viability plates, two concentrations were prepared in two separate 50 ml Falcon tubes. 12.5 µl and 1.25 µl of transformed protoplasts were added to a respective tube with the final volume of each brought to 6 ml using *Aspergillus* transformation soft agar before being poured onto agar plates containing no pyrithiamine. Lastly, the remaining transformed protoplasts solution was topped up to a final volume of 30 ml using soft agar and 6 ml was poured onto each of the 5 remaining pyrithiamine plates ensuring the agar spread completely before setting.

Plates were left on the bench overnight to allow for the protoplasts to re-grow their cell wall (removed via the lysing step in section 2.2.4.2). The next day, negative control and transformed experimental plates were overlaid with another 6 ml soft agar containing 0.1 µg/ml pyrithiamine (section 2.1.2.8). Once the agar had set, all plates were incubated at 37^{0} C static for 4-5 days depending on growth rate.

2.2.4.5 Isolation of *A. fumigatus* Transformants

Growth of transformed protoplasts on agar plates containing pyrithiamine identified potential successfully transformed *A. fumigatus* strains. Number of potential transformants can range from 5-30 colonies from each transformation. Using a sterile 1000 µl pipette tip, plugs of potential transformants were taken under sterile conditions and added to a 1.5 ml microfuge tube, to which 1 ml PBS-T (section 2.1.3.20) was added. Potential transformant plugged samples were vortexed to release the conidia into solution and were re-aliquoted onto fresh AMM agar plates (section 2.1.3.16) containing pyrithiamine to ensure resistance to the marker. 500 µl conidial suspension of plugged samples which proved resistant to pyrithaimine were used to inoculate 50 ml SB media (section 2.1.3.17) and were incubated at 37 ^{0} C at 200 rpm. From these, genomic DNA was extracted as described in section 2.2.2.2, for further analysis via Southern Blotting.

2.2.4.6 *A. fumigatus* Single Spore Isolation

Samples were serially diluted, typically 1:10, 1:100, 1:1000 & 1:2000. The resulting single colonies were isolated as described previously (section 2.2.4.5) and analysed by a second round of Southern blotting.

2.2.5 Southern Blotting

2.2.5.1 gDNA Preparation and Subsequent Nucleic Acid Transfer

Southern blotting was used to detect specific gene fragments at desired loci to help identify successful gene loss in transformants. gDNA was isolated from transformants and wild-type strains as described (section 2.2.2.2), and was restriction digested using an appropriate restriction enzyme. The enzyme used should result in differential cutting between wild-type and knockout strain at the region of interest. Restriction digests was carried out as described (section 2.2.3.4) and were subsequently ran on a 0.8 % (w/v) agarose gel (section 2.2.3.2). Once completed gels were visualised using an ultraviolet light and GelDoc Camera to ensure complete digestion had occurred. Gels were then placed in a UV cross-linking machine and subjected to a 800 µJ pulse creating nicks in the DNA aiding transfer onto a nylon membrane.

Following this the Southern transfer tower was set up. Using a large BioRad gel tank, 1 L of transfer buffer (section 2.1.9.1) was added equally to each side. To this, two sheets of Whatman filter paper (about 1 inch wider than the width of the gel on each side and slightly longer than the width of the gel tray) was added to the transfer buffer and laid across the tank. On top of this the gel(s) (two gels are needed to balance the tower but both don't need to contain sample) were placed with the wells facing down and one piece of Hybond nylon membrane (slightly larger than the gel) was added carefully and directly to the gel which contained DNA. To this, three gel sized pieces of Whatmann filter paper was added on top of which three packs of pocket tissues were taken out of their wrappers and added to each side to ensure the tower stayed balanced. Lastly a glass plate was balanced on top of the two resulting stacks of tissue, Whatmann filter paper, H^+ Nylon Membrane and agarose gels; topped off with a weight in the form of a Duran bottle filled with 500 ml H_2O. Southern blotting was carried out at room temperature, overnight.

2.2.5.2 Disassembly of Southern Transfer Tower

After the overnight blot transfer step in section 2.2.5.1, the Duran bottle and glass plate were taken off. The stacks of tissue were then carefully removed and discarded. The agarose gel was turned over carefully with the Hybond nylon membrane and gel sized Whatmann filter paper still attached and now on the underside of the gel with the wells facing up. Using a sharpened pencil, lines were marked using the wells as a guide in order to see the orientation of the membrane. The agarose gel was then taken off and left to one side while the membrane was carefully placed into a clean container where it was washed twice for 5 min using ~ 10 mls 0.1 % (w/v) SDS/ 1 X SSC Buffer (section 2.1.9.6) rocking. During this step the agarose gel was visualised under a U.V. light to ensure all the DNA was transferred and subsequently discarded. Washed blots were placed into a U.V. cross-linking machine and subjected to a 1200 µJ pulse to prevent any DNA to be washed off in the subsequent steps.

2.2.6 Digoxigenin (DIG) Detection of Hybridised DNA fragments

2.2.6.1 Generation of DIG-labelled DNA probes

DIG-labelled probes were amplified using primers specific to the region of interest. Also DIG-labelled dNTP's (section 2.1.10.9) were used in order to DIG-label the probe itself. PCR amplicons were visualised on agarose gels (section 2.2.3.2) and purified using a Qiagen gel extraction kit (section 2.2.3.3). Prior to being used in the DIG-detection step of Southern blotting, the probe was denatured at 95 ^{0} C for 8 min using a dry bath. DIG probe was the placed on ice and quantified using a Nanodrop spectrophotometer. 400 ng was then added to 5 ml membrane pre-hybridisation buffer (section 2.1.10.2) pre-heated to 65 ^{0} C for at least 30 min. The probe could stored at -20 ^{0} C and re-used for subsequent experiments where it was re-heated to 65 ^{0} C for 30 min prior to use.

2.2.6.2 Pre-hybridisation of Southern Blot Membrane

After U.V. crosslinking (section 2.2.5.2), the blot(s) were added to a Hybaid tube, ensuring to only hold the corners of the membrane i.e. not where the DNA would have transferred to, using a sterile forceps. 10 ml pre-hybridisation buffer, which had been pre-heated at 65 ^{0} C, was poured in down the side of the Hybaid tube and not directly onto the membrane. This was then added to a pre-heated (42 ^{0} C) Hybaid oven and left rotating for 4-5 h to block the blots.

2.2.6.3 Addition of DIG-labelled probe

Pre-hybridisation buffer from section 2.2.6.2 was poured from the Hybaid tube. 400 ng of the denatured DIG-labelled probe solution (section 2.2.6.1) was poured down the side of the Hybaid tube and not directly onto the membrane. This was then placed back into the Hybaid oven and incubated at 42 ^{0} C rotating overnight.

2.2.6.4 DIG Detection

Following overnight incubation of the DIG-labelled probe solution in section 2.2.6.3, the solution was poured into a 50 ml Falcon and stored at -20 ^{0} C for re-use. The blot(s) was taken from the Hybaid tube and placed into a clean container and was

washed 2 X 5 min, rocking in 10 ml 0.1% (w/v) SDS/1 X SSC buffer (section 2.1.9.6). The blot(s) were then placed into a clean Hybaid tube, which was pre-heated in a Hybaid oven now set to 65 ^{0} C. The tube(s) were filled halfway with 0.1 % (w/v) SDS/1 X SSC (section 2.1.9.6) buffer and incubated for 15 min rotating at 65 ^{0} C. This was repeated and each time the buffer was poured off and the Hybaid tube was placed upside down on clean tissue paper to remove excess buffer.

10 ml DIG wash buffer (section 2.1.10.6) was next added to the Hybaid tube and left rotating at 25 ^{0} C for 5 min. Subsequently, the buffer was poured off and in its place 10 ml Antibody Blocking buffer (section 2.1.10.4) was added and left rotating at 25 ^{0} C for 30 min. This was poured off and the Anti-DIG Fab Fragments – alkaline phosphatase (10 ml) was added (section 2.1.10.7). This was left rotating at 25 ^{0} C for 30 min after which the blot(s) was washed 2 X in 10 ml DIG wash buffer at 25 ^{0} C rotating for 10 min. 5 ml DIG buffer 3 (section 2.1.10.5) was next added to the blot(s) which were then left rotating at 25 ^{0} C for 5min. Buffer was then poured off and the CSPD chemi-luminescent substrate buffer (5 ml) (section 2.1.10.8) was added. Blot(s) were left for a further 5 min rotating at 25 ^{0} C and subsequently the CSPD buffer was collected into a fresh 50 ml Falcon tube wrapped in tin foil (CSPD buffer if kept in the dark can be re-used within a week) and stored at 4 ^{0} C. The blot(s) was carefully removed from the Hybaid tube and wrapped in clingfilm making sure that there were no air bubbles which might obstruct Southern blot development (section 2.2.7). Blots were incubated at 37 ^{0} C static in the dark for 15 min to help intensify the signal emitted from Anti-DIG fab-alkaline phosphatase processing CSPD.

2.2.7 Southern Blot Development

At the end of section 2.2.6.4, blots were placed into a film exposure cassette. Kodak film was then cut to shape, in the dark, and placed on top of the blot and the cassette was shut. Blots were then left to expose at room temperature, usually for 3 h depending on strength of signal and background noise. After being exposed the Kodak film was developed by submerging it in Kodak developing solution (section 2.1.11.1) until bands begin to appear, then rinsing in water and fixing the image in Kodak fixing

solution (section 2.1.11.2). If the signal was very weak, exposure time could be extended using new Kodak film and exposing overnight.

2.2.8 Generation and Transformation of Competent *Saccharomyces cerevisiae* and *Escherichia coli* cells

2.2.8.1 Competent *S. cerevisiae* cells

S. cerevisiae cells were inoculated in 5 ml YPD (section 2.1.3.1) at 30 ^{0} C shaking at 200 rpm . The next morning the cultures were added to 50 ml fresh media in a 250 ml sterile conical flask at an OD_{600nm}=0.4 and incubated at 30 ^{0} C for 3 h until at a concentration of 1 x 10^{7} cells/ml. The culture was then split into two 25 ml fractions in two 50 ml Falcon tubes. Cells were centrifuged at 1677 g for 5 min, subsequently washed with 25 ml dH_2O then centrifuged again at 1677 g for another 5 min. Supernatants were removed from each respective tube, and the cell pellets were re-suspended in 1 ml 100 mM lithium acetate (section 2.1.6.3). Re-suspended cells were transferred to microfuge tubes and centrifuged at 18894 g for 5 secs (Centrifuge 5415D, Eppendorf AG, Hamburg). Resulting pellets were re-suspended in 500 µl 100 mM lithium acetate and stored at 4 ^{0} C.

2.2.8.2 *S. cerevisiae* transformation of competent yeast

50 µl of competent yeast (section 2.2.8.1) were centrifuged for 5 secs at maximum speed and any residual lithium acetate was aliquoted out. To the cell pellet the following was added in order without mixing: 240 µl 50 % (w/v) PEG (section 2.1.6.1); 36 µl 1 M lithium acetate (section 2.1.6.2); 25 µl single stranded carrier DNA (2 mg/ml stock) and 50 µl DNA/dH_2O mix to be transformed

Once all components were added they were mixed and incubated at 30 ^{0} C for 30 min. This was then treated to a 42 ^{0} C heat-shock (Accublock Digital Dry Bath, Labnet International Inc.) for 20 min. Mixtures were subsequently centrifuged at 18894

g for 15 secs and supernatants were removed. Resulting pellets were re-suspended in 200 µl dH_2O, plated onto selective agar plates and incubated for 48 hrs at 30 ^{0} C static.

2.2.8.3 Competent *E. coli* cells

E. coli DH5α cells were inoculated in 10 ml LB broth (section 2.1.3.21) and incubated at 37 ^{0} C at 250 rpm overnight. This 10 ml culture was then added to 1 L LB broth and incubated again at 37 ^{0} C for 2 h at 200 rpm. This was subsequently split into 4 x 250 ml centrifugation tubes and chilled on ice for 10 min. Cells were pelleted in a GSA rotor at 4293 g at 4 ^{0} C. Cells were re-suspended in RF1 buffer (section 2.1.7.1) and kept on ice for a further 30 min. Cells were next centrifuged at 5000 rpm for 10 min at 4 ^{0} C and each subsequent pellet was re-suspended in 3.2 ml RF2 buffer (section 2.1.7.2). Samples were kept on ice for 15 min, after which 100 µl aliquots were transferred to pre-cooled 1.5 ml microfuge tubes and stored at -70 ^{0} C until required.

2.2.8.4 *E. coli* transformation

Plasmid DNA (~1 µg) was added to 100 µl competent *E. coli* cells (section 2.2.8.3) and incubated on ice for 30 min. Cells underwent a 42 ^{0} C heat shock treatment for 1 min in a digital dry bath followed by a recovery period whereby 1 ml liquid LB (section 2.1.3.21) was added. Transformed cells were incubated for 1 hr at 37 ^{0} C and plated onto LB-Amp-agar plates (section 2.1.3.24) and incubated overnight at 37 ^{0} C.

2.2.8.5 "Lazy Bones" *E. coli* transformation

LB-Amp-agar plates were pre-warmed at 37 ^{0} C for 1 hr prior to transformation. 1-5 µl plasmid DNA was added to 50 µl pre-thawed competent *E. coli* (section 2.2.8.3)**.** These were incubated on ice for 5 min then plated onto the pre-warmed LB-amp-agar plates and incubated overnight at 37 ^{0} C.

2.2.9 Plasmid Isolation in *S. cerevisiae* and *E. coli*

2.2.9.1 Plasmid Isolation and Purification from *S. cerevisiae*

Plasmid isolation and subsequent purification was carried out according to the Qiagen plasmid purification manual using all buffers, reagents and materials provided in the QIA prep miniprep kit as per manufacturers' instructions. 5 ml selective SC medium (section 2.1.3.5) was inoculated with the appropriate *S. cerevisiae* strain and incubated at 30 ^{0} C shaking at 200 rpm overnight. This was centrifuged the following morning at 1073 g for 5 min and treated as described in the QIA prep miniprep kit instructions. To elute the plasmid DNA 30 µl of dH_2O was added directly to the centre of the spin column and let stand for 1 min at room temperature. Plasmid DNA was collected by centrifuged at 18894 g for 1 min and stored at -20 ^{0} C until required.

2.2.9.2 Plasmid Isolation and Purification from *E. coli*

A single colony from a transformed *E. coli* LB-amp-agar plate (section 2.1.3.24) was inoculated in 5 ml LB broth + AMP (section 2.1.3.23) and incubated at 250 rpm at 37 ^{0} C overnight. Cells were pelleted via centrifugation for 5 min at 4000 rpm. To elute the plasmid DNA 30 µl of dH_2O was added directly to the centre of the spin column and let stand for 1 min at room temperature. Plasmid DNA was collected by centrifugation at 18894 g for 1 min and stored at -20 ^{0} C until required.

2.2.10 RNA Methodological Analysis

2.2.10.1 RNA Extraction

RNA was extracted from *A. fumigatus* strains using the QIAGEN RNeasy plant mini kit as per manufacturers' guidelines. All buffers and filter columns were supplied with the kit as well as the constituents of the buffers used. All other materials used were double autoclaved and treated with RNase Zap^{TM} (Invitrogen) prior to use to remove any un-wanted RNases. All workspaces were thoroughly washed with 70 % (v/v) ethanol and RNaseZap for the same reason. 50 ml SB media (section 2.1.3.17) was inoculated with 500 µl conidial suspension and incubated overnight at 37 ^{0} C shaking at 200 rpm. Mycelia were harvested through sterile Mira-cloth and excess medium was washed off using dH_2O. Mycelia were then dried using sterile tissue paper, wrapped in

tin foil and flash frozen in liquid nitrogen. Samples could be stored from this point at -70 ^{0} C until required. Frozen mycelia were placed in respective pestle and grinded till at a powdery consistency. Powdered tissue (100 mg) was added to a sterile 2 ml microfuge tube and kept in an ice bucket containing liquid N_2 until ready to proceed to the next step. To this 450 µl of RLC buffer (containing β-mercaptoethanol which has to be added the first time the buffer is used) and the tube was vortexed vigourously until homogenous. The lysate was then treated as per manufacturers' instructions carrying out any optional steps which are suggested to increase yield and purity.

RNA was eluted by adding 30 µl RNase free water directly to the centre of the column and letting it stand for 1 min. Column was then centrifuged at 11180 g for 1 min and resulting elute was aliquoted back up using a sterile tip and passed through the column again to help concentrate the RNA. RNA was stored at -70 ^{0} C until required.

2.2.10.2 DNase Treatment of RNA Samples

RNA samples extracted from *A. fumigatus* (section 2.2.10.1) were DNase treated using a DNase kit purchased from Sigma-Aldrich Ltd. 500 ng *A. fumigatus* was brought to a final volume of 8 µl using DEPC treated distilled water in a RNase free, sterile 500 µl microfuge tube. To this, 1 µl 10 X reaction buffer and 1 µl DNase were added and were incubated at room temperature for 15 min. Afterwards, 1 µl stop solution (part of kit) was added and subsequently incubated at 70 ^{0} C for 10 min. Samples were placed on ice for at least 1 min, and stored at -70 ^{0} C until required.

2.2.10.3 cDNA Synthesis

cDNA was synthesised using the qScript^{TM} cDNA Supermix (Quanta Biosciences). All reagents and buffers are contained a single reagent supplied in the kit. cDNA was synthesised as per manufacturers' instructions. 500 ng of RNA (section 2.2.10.1) was added to a RNase and DNase free 500 µl microfuge tube. To this 4 µl of the qScript cDNA Supermix 5 X was added and topped up to a final volume of 20 µl using diethyl-pyrocarbonate (DEPC) treated dH_2O.

Samples were vortexed briefly and centrifuged for a few seconds to collect all of the reaction mix. They were then incubated using a PCR cycler using the following incubation protocol: 5 min at 25 ^{0} C; 30 min at 42 ^{0} C; 5 min at 85 ^{0} C; hold at 4 ^{0} C. Once completed the cDNA is now ready for use in RT-PCR reactions or alternatively can be stored at -20 ^{0} C until required.

2.2.10.4 Semi-quantitive RT-PCR

Before carrying out qRT-PCR (section 2.2.10.5), genes of interest were amplified using PCR (section 2.2.2.4) along with the household gene Calmodulin control. As all primer sets used in this study for genes of interest and calmodulin, span an intron any gDNA contamination would be clearly visible when resolved on an agarose gel (section 2.2.3.2) as it would be slightly larger than an amplicon derived from cDNA alone. Once a positive single signal was observed, qRT-PCR could be carried out on that sample.

2.2.10.5 Real-time PCR

A. fumigatus strains were inoculated in 50 ml SB media (2.1.3.17) and incubated for 21 h at 37 ^{0} C shaking at 200 rpm. At the 21 h time point, cultures were exposed to either a solvent control (MeOH) or 5 µg/ml gliotoxin (section 2.1.2.1) for three hours at 37 ^{0} C shaking at 200 rpm. RNA was extracted as described in section 2.2.10.1 and cDNA was synthesised as in section 2.2.10.2. RT-PCR was carried out using the LightCycler® 480 Real-Time PCR System and KAPA Biosystems SybrFast Mix. Relative quantification analysis of differences in gene expression between different growth conditions and between different *A. fumigatus* strains was carried out using the Relative Quantification module allowing for differences in gene expression levels between samples to be calculated. Standard curves for the gene *calm* (internal control) and other genes of interest were created to measure PCR efficiency.

Standard curves were prepared for *calm* and each of the genes of interest by creating 5 orders of 10 fold serial dilutions of control cDNA in DEPC treated molecular H_2O using 5 experimental replicates for each dilution series and for each PCR reaction

with their respective specific primer pairs. Cycling conditions were carried out as per manufacturers' guidelines having 45 cycles per cycle being performed. Standard curves were calculated using the Relative Quantification Module which yielded a specific efficiency figure based on the reaction. An efficiency of 2 +/- 0.2 meant the PCR was successful and was saved for reference during experiments using these same cycling requirements for subsequent RT-PCR.

For this cDNA was diluted 1:2 in order for it to fit within the standard curve, and was done in quintuplicate for each sample and for each gene of interest being amplified. Relative program 2-(Delta Delta C(T)) method (Livak & Schmittgen, 2001) with results being given as a bar chart and table depicting the mean values for all genes and the relative ratio of a particular gene of interest:*calm* expression.

2.2.11 mRNA Isolation and Preparation for Transcriptomic Analysis

2.2.11.1 mRNA Isolation and Purification

A. fumigatus cultures were grown for 21 h at 37 ^{0} C shaking at 200 rpm. At the 21 h mark biological replicates for each strain and each condition, were exposed to a solvent control (MeOH) or 5 µg/ml gliotoxin where appropriate. Samples were then incubated for three hours to bring the total incubation time to 24 hrs at 37 ^{0} C shaking at 200 rpm. RNA was extracted as described in section 2.2.10.1. For mRNA isolation and purification from these RNA samples were treated using Ambion® MicroPoly(A) Purist^{TM} (Life technologies) which enriches mRNA found in a given RNA sample. It achieves this by using an oligo (dT) binding to the poly A tail of mRNA and different wash steps which removes any non-mRNA. Samples were treated as per manufacturers' guidelines using all reagents and buffers contained within the kit as instructed.

A total amount of 10 µg RNA (section 2.2.10.1) was topped up to a volume of 250 µl using RNase free water and treated as per kits protocol. mRNA purification can be carried out twice for increased purity and removal of other unwanted RNA's however this greatly reduced mRNA yield. Samples were dissolved in 50 µl RNA storage solution (provided in kit) and stored at -70 ^{0} C until required.

2.2.11.2 Preparation of mRNA Samples for 2100 Agilent Bioanalyzer Analysis

To check mRNA samples (section 2.2.10.6) for integrity, they were analysed using an Agilent 2100 Bioanalyzer^{TM} and an Agilent RNA 6000 Nano Kit (Agilent). This system analyses both total RNA and mRNA using a chip system consisting of micro-fluidic channels which help separate RNA fragments based on their size as they are moved electrophoretically via an electrode chip insert. The day before use, the electrode chip insert was treated using RNase Zap (Agilent) to remove any un-wanted RNases which may be present, then placed in a petri dish filled with DEPC treated water (Sigma-Aldrich) and left in a dessicator overnight. The following morning this was placed back into the Agilent 2100 Bioanalyzer. Where appropriate, mRNA samples were diluted in RNase free water to a concentration of 250 ng/µl, in order for them to stay within range of the chip system. All reagents were allowed to equilibrate to room temperature for at least 30 min before being used.

550 µL RNA gel matrix was added to a RNase free sterile spin column (supplied in kit) and was centrifuged at 1370 g for 10 min. 65 µl of the filtrate was added to a sterile 0.5 ml microfuge tube. To this 1 µl RNA dye concentrate was added and the tube was vortexed for at least 10 secs to mix properly. RNA gel matrix-dye mix was then centrifuged at 13000 rpm for 10 min and kept at room temperature until use.

Using a cleansing chip, 350 µl of RNase Zap was added and placed into the Bioanalyzer for 1 min to further clean the electrode. After this the cleansing chip was washed using DEPC treated water until clean of residual RNase Zap. Next 350 µl DEPC treated water was added to the cleansing chip and placed into the Bioanalyzer for 1 min to remove any RNase Zap which could degrade any sample loaded later. The entire plate surface was then washed using RNase Zap. All samples and RNA ladder (provided in kit) were heated for 2 min at 70 ^{0} C.

A new RNA 6000 chip was placed in the chip priming station (Agilent). In well D-3, 9 µl of the gel-dye mix was added, ensuring the pipette tip was at the very bottom of the well and not at the side etc. Once aliquoted, the chip was primed using an

attached syringe which was positioned to the 1 ml mark. The syringe plunger was pushed down until held by the priming chip plunger and the syringe was held beneath the clip for 30 secs before being released slowly back to the 1 ml mark. This step allows for the application of defined pressure for chip priming.

To wells D-1&2 another 9 µl of gel-dye mix was added, any remaining gel-dye mix was discarded. To all 13 wells i.e. all wells except for D 1-3 inclusive, 5 µl RNA marker (provided with kit) was added. This RNA marker is a 25 bp marker which aids in standardising all sample wells to the RNA ladder. To lane D-4 1 µl RNA ladder was added while 1 µl of sample was added to each respective sample well, namely any wells apart from wells D 1-4 inclusively. For any sample well which no samples was added, 1 µl RNA marker was added so each well contained the same volume.

The finished chip was then placed in an IKA vortexer for 1 min at 2400 rpm before being placed in the Bioanalyzer.

2.2.11.3 RNA Integrity Number and Bioanalyzer Analysis of Prepared mRNA Samples

After a prepared Agilent Nano chip (section 2.2.11.2) was placed into the 2100 Agilent Bioanlayzer, the chip loading station was closed and the '2100 Agilent Programme File was opened and the 'Instrumental' context was set to mRNA. As the chip was running sample information could then be entered. A chip run was 30-40 min long. Upon completion, RNA ladder was checked for a successful run. A typical run should yield 7 peaks: 1 marker peak and 6 separate RNA peaks each well separated from each other, each representing different sized RNA fragments. Successful mRNA samples should yield one clear marker peak and one 'hump' which represents mRNA. If more than one peak was found, sample was positive for ribosomal contamination and RNA (section 2.2.10.1) was treated again.

To measure RIN of samples, total RNA (section 2.2.10.1) was prepared for Bioanalyzer analysis (section 2.2.11.3) instead of mRNA samples (section 2.2.11.1). Here the ratio of the 18 S and 28 S ribosomal RNAs is measured and given as an

indicator for RNA integrity. Anything below a RIN value of 8 was discounted and new RNA was extracted as decribed in section 2.2.10.1.

2.2.11.4 RNA Seq Analysis

Duplicate samples for each strain and condition were sequenced using the Sanger method in the Wellcome Trust. mRNA fragments were synthesised into cDNA by targeting of the poly(A) tail of the mRNA molecule and aligned to an *Aspergillus fumigatus* reference genome. Similar reads were assembled together using the RNA Seq analysis software Cuffdiff, part of the popular Cufflinks™ analysis software which yielded a table for all reads/genes and their relative expression. This same software also depicts the p- and corrected q-value for all genes mapped, Significantly expressed genes ($p < 0.05$) were subsequently functionally characterised using FunCat™ analysis

2.2.12 Proteomic Techniques

2.2.12.1 Protein Extraction of *A. fumigatus* for 2D-PAGE Analysis

Liquid cultures of *A. fumigatus* were filtered using sterile Mira-cloth and washed using sterile PBS. Washed mycelia was then ground in liquid nitrogen using a sterile pestle and mortar. Crushed mycelium (250 mg) was weighed into a 15 ml Falcon tube and was re-suspended in 1500 µl 10 % TCA which was pre-cooled to 4 ^{0} C. Each sample was then sonicated three times for 10 s at 10 % power, cooling samples on ice in between each sonication. Samples were incubated on ice for 30 min and then centrifuged for 15 min at 1677 g at 4 ^{0} C. Half the supernatant was removed and discarded using a Pasteur pipette while the remaining supernatant was used to re-suspend the pellet. The re-suspended pellet was then transferred to a 2 ml microfuge tube and centrifuged at 11180 g at 4 ^{0} C for 10 min. Supernatant was removed and pellets were re-suspended in 60 µl dH_2O and vortexed. To each sample, 1 ml of ice-cold acetone was added and mix by pipetting and vortexing to get the pellet into solution. Samples were stored at -20 ^{0} C and vortexed every 10 min for a total 1 h after which they were left at -20 ^{0} C overnight.

Samples were centrifuged at 11180 g for 10 min and the supernatant was removed. 500 µl ice-cold acetone was added to each sample and were then centrifuged at 11180 g for 10 min. Supernatant was removed and samples were left to air dry for a maximum of 5 min. Samples were re-suspended in 500 µl IEF buffer (section 2.1.12.2) and left at room temperature for 1 hour. Afterwards, samples were centrifuged at 18894 g for 1 min and the supernatants were removed to a clean microfuge tube.

2.2.12.2 Bradford Protein Assay

Protein samples (section 2.2.12.1) were quantified using the Bradford protein assay. Using a BSA stock (1 mg/ml) (section 2.1.12.1) protein solutions of known protein concentration were created to generate a protein standard curve. Samples were diluted 1:10, 2 µl of which was added to a 96 well plate (Starstedt). 200 µl BioRad protein assay was added to each sample/standard and following a 10 min incubation at room temperature, absorbances were read using a spectrophotometer set at $A595_{nm}$ (Eppendorf Biophotometer). Protein concentration of samples was calculated using a plotted $A595_{nm}$ versus BSA concentration standard curve. All protein samples were analysed in triplicate.

2.2.12.3 Iso-electric Focusing (IEF)

Protein samples (section 2.2.12.1) were diluted to have a final concentration of 300 µg/250 µl using rehydration buffer (section 2.1.12.3). Into each sample, bromophenol blue was added and samples were then centrifuged at 16099 g for 5 min to remove any insoluble material. Samples were then transferred to one end of an IPG strip holder before an IPG strip (GE Healthcare) was placed gently, gel side facing down on top of the protein pushing it along the holder with the strip using a forceps to prevent contamination. Each strip was then overlaid with 1 ml overlay fluid (GE Healthcare) and subjected to iso-electric focusing on an IPGphor II IEF unit using the following programme:

Step	50 Volt	12 hours
Step	250 Volt	0.15 hours
Gradient	5000 Volt	2 hours
Step	5000 Volt	5 hours
Gradient	8000 Volt	2 hours
Step	8000 Volt	1 hour

After IEF, IPG strips were placed in 10 ml reduction buffer (section 2.1.12.4) for 20 min, immediately followed by equilibration in 10 ml alkylation buffer (section 2.1.12.5) for a further 20 min. IPG strips were then rinsed in 1 X running buffer (section 2.1.12.7) before proceeding to 2D separation.

2.2.12.4 12% SDS Gels for 2-D Poly Acrylamide Gel Electrophoresis (PAGE)

12% SDS gels were prepared by adding 280 ml Protogel (National Diagnositics), 182 ml resolving buffer (National Diagnostics), 230.3 ml sterile dH_2O and 2.8 ml 10 % APS (section 2.1.12.8). Gel glass plates were washed with 70 % ethanol and placed in a gel casting system (GE Healthcare) using plastic spacers between each plate pair. Just before being cast, 280 µl TEMED (Sigma-Aldrich) was added and mixed gently. Gel was then immediately poured slowly into the caster and 0.1 % 10X SDS buffer was sprayed on top of each gel to prevent air bubbles being formed. The casting cassette was sealed tightly in clingfilm and left at room temperature overnight to allow complete solidification of the gels.

Equilibrated IPG strips (section 2.2.12.3) were placed horizontally with the gel side facing the user and the positive end at the left hand side of the gel. Molten agarose

sealing solution (section 2.1.12.9) was aliquoted onto each strip sealing the gel. For second dimension separation, the BioRad PROTEAN® Xi-II Plus Dodeca™ Cell System was used. Gels were placed into the vertical electrophoresis cells as per manufacturers' instructions. 3 L 10 X running buffer (section 2.1.12.6) was then poured and topped up if necessary using sterile dH_2O. The Dodeca lid was secured and the gels were run at 1.5 W per plate at a maintained temperature of 6 ^{0} C for 20 h or until the bromophenol blue indication line was at the bottom of the gel.

2.2.12.5 Coomassie Staining- Colloidal Method

Once gels had finished running (section 2.2.12.4) the glass plates were removed and the gels were placed in fixing solution (section 2.1.13.1) rocking for 3 h at room temperature followed by 2 x 30 min washes in dH_2O. Next gels were placed in incubation buffer for 1 hour rocking at room temperature after which they were left to stain in stain solution (section 2.1.13.3) and were left rocking at room temperature overnight in the staining solution. The next day stain solution (section 2.1.13.3) was removed and the gels were placed in neutralisation buffer (section 2.1.13.4) for 3 min after which gels were washed in 25 % methanol rocking for 1 min. After this wash step, gels were placed in fixing solution and incubated overnight, rocking at room temperature. Gels were produced in triplicate for each strain and condition used and were scanned using an HP Scanjet 5400C.

2.2.12.6 Progenesis™

Protein spots were analysed using Progenesis™ same spot software to determine differential expression between different samples. Samples with a significance value ≥0.05 were used later for LC-MS identification.

2.2.13 Mass Spectrometry (LC-MS)

2.2.13.1 Protein Spot Preparation-Shevchenko method (Shevchenko *et al.*, 2006)

2D-PAGE separated spots were chosen as described in section 2.2.12.6. All reagents used were HPLC grade and all 1.5 ml microfuge tubes were treated with aceto-

nitrile prior to use. Each gel was washed once using sterile water before chosen spots were cut out using a sterile scalpel and placed into pre-washed a 1.5 ml tube. Gel pieces were incubated in 100 µl de-staining buffer (section 2.1.14.1) shaking at room temperature for 30 min, or until all the stain was removed. Next, 500 µl acetonitrile was added to each of the gel pieces and was left for 10 min at room temperature causing the gel pieces to shrink and turn white indicating removal of the majority of the coomassie stain.

Samples were then trypsin digested with 50 µl (or enough to cover the gel piece) trypsin buffer (section 2.1.14.3) and incubated on ice for 30 min. More trypsin buffer was added if necessary. Gel pieces were incubated for a further 90 min to saturate gel pieces with trypsin after which 20 µl of 50 mM ammonium bicarbonate solution (section 2.1.14.4) was added to prevent the gel pieces becoming dehydrated during digestion. Gel pieces were then incubated at 37 ^{0} C static overnight to allow for complete trypsin digestion of sample peptides.

Digested peptide products were transferred to a new sterile 1.5 ml microfuge tube. To each digested gel piece tube, 100 µl extraction buffer (section 2.1.14.5) was added and each sample was incubated for 15 min at 37 ^{0} C shaking to help collect any residual peptide fragments. The supernatant from this was added to the trypsin digest supernatant and were dried overnight in a vacuum centrifuge. Dried extracts could be stored at this point at -20 ^{0} C for a few months.

Prior to LC-MS analysis, dried extracts were re-suspended in 20 µl 0.1 % formic acid (v/v) (section 2.1.14.6). Sample were then sonicated in a sonication bath for 5 min and subsequently centrifuged at 5478 g for 2 min. Samples (15 µl) were aliquoted into LC-MS loading vials (Agilent) and analysed using and Agilent 6340 Ion Trap Liquid Chromatography Mass Spectrometer.

2.2.14 Glutathione Assay

2.2.14.1 *A. fumigatus* Lysate Preparation

A. fumigatus mycelia were harvested through sterile Mira-cloth, washed with dH_2O and dried using tissue paper, to remove as much liquid as possible. Dried mycelia

(250 mg) was then weighed into a 2 ml microfuge tube, to which 600 µl ice-cold 5 % SSA (w/v) (section 2.1.15.6) was added along with a tungsten bead. This was repeated using glutathione lysis buffer (section 2.1.15.4). Both sets of samples were bead beated at 30 Hz for 3 min and subsequently centrifuged at 11180 g at 4 ^{0} C for 10 min. Supernatants were removed to a clean microfuge tube wrapped in tin foil, and kept on ice. Glutathione lysis buffer samples were used for protein quantification as described in section 2.2.12.2. 5 % SSA treated samples were neutralised using tri-ethanolamine. For reduced glutathione (GSH) quantification, samples were diluted 1/10 using Glutathione assay buffer (section 2.1.15.5), while for oxidised glutathione (GSSG) samples were diluted 1/5 in Glutathione assay buffer. All samples, GSH & GSSG, were then centrifuged at 11180 g at 4 ^{0} C for 10 min. Supernatant was removed to a clean microfuge tube wrapped in tin foil and kept on ice. Any excess of sample could be stored at -70 ^{0} C for a few months.

2.2.14.2 *S. cerevisiae* Lysate Preparation.

S. cerevisiae samples were incubated in 5 ml appropriate media at 30 ^{0} C shaking at 200 rpm overnight. Cells were harvested via centrifugation at 1677 g. Resulting pellet was re-suspended in 500 µl ice-cold PBS and re-centrifuged at 11180 g at 4 ^{0} C for 10 min. Cells were then re-suspended in either 250 µl lysis buffer (section 2.1.15.4) or 5 % SSA (w/v) (section 2.1.15.6) and transferred to a screw top microfuge tube. To this ~100 µl silica beads were added and the sample were bead beated for 1 min 30 secs at 30 Hz. Samples were then centrifuged at 11180 g at 4 ^{0} C for 10 min and prepared as described in section 2.2.14.2.

2.2.14.3 GSH/GSSG Standard Preparation

Using a 1 mg/ml solution of GSH and a 2.01 mg/ml solution of GSSG, serial dilutions of known glutathione molarity were made: 13.2, 6.6, 3.3, 1.65, 0.825 and 0.4125 nmol/ml for both GSH and GSSG.

2.2.14.4 GSH/GSSG Assay

All samples/standards and reagents were kept on ice and kept from direct exposure from the light (all reagents were wrapped in tin foil, and ice buckets were covered when able. All GSSG samples/standards (100 µl) were treated with 2 µl of a 1/5 dilution of 2-vinyl-pyridine this blocks any free GSH in these samples from giving a false positive result later on. They were left for 1 hour at room temperature after which the reaction was stopped by adding 6 µl of a 1/2 dilution of tri-ethanolamine which neutralises the 2-vinyl-pyridine. This was left at room temperature for at least 10 min prior to being used in the assay.

NADPH (5 mM, section 2.1.15.10) was thawed on ice making sure not to expose it to any unnecessary heating or light exposure. 20 µl of samples/standards and blanks were aliquoted to a 96 well plate. To this, 44.2 µl of 10 mM DTNB + Glutathione reductase mix was added. Next 42 µl of 5 mM NADPH was added to each well and the plate was shaken gently to mix. Reaction was left at room temperature for 1 min and 30 secs before the absorbance was measured at 412_{nm}. GSH levels were given by subtracting the absorbance values of the total GSH samples from the absorbance values of their respective GSSG samples. This gave the true GSH absorbance and both the GSH and GSSG levels could be measured directly from their respective standard curves.

2.2.15 Oxidative Stress Assays

2.2.15.1 Catalase Assay

Protein lysates from either *A. fumigatus* (section 2.2.13.1) or *S. cerevisiae* (section 2.2.13.2) were used to measure the redox state of samples under different conditions. Catalase is an enzyme which breaks down hydrogen peroxide into water and O_2, using known concentrations of hydrogen peroxide (5 mM) and increasing units of catalase (0, 0.1, 0.5, 1 & 3 U/ml) the reduction in absorbance was measured indicating a reduction in hydrogen peroxide concentration due to increasing levels of catalase. 50 µl of sample lysate was added to 5 mM hydrogen peroxide which already had its initial absorbance measured. The reduction in absorbance was recorded over 360 s and the Units of catalase/ml were calculated using the formula:

$$\frac{OD_{240}(360\ s) - OD_{240}(0\ s)}{360\ s} = \text{U/ml catalase}$$

2.2.15.2 Superoxide Dismutase Assay

Protein lysates from either *A. fumigatus* (section 2.2.13.1) or *S. cerevisiae* (section 2.2.13.2) were used to measure the SOD levels under different conditions. In a plastic cuvette, 940 µl of a 6 X 1 mM Xanthine/0.3 mM Nitrotetrazolium Blue Chloride (NBT) was added. To this different U/ml of SOD was added in order to generate a standard curve of % inhibition. Lastly 0.3 U/ml Xanthine oxidase was added to initiate the reaction.

SOD activity was calculated by measuring the $\lambda\ 560_{nm}$/min for each sample/control and calculated by the following formula:

$$\frac{\lambda\ 560_{nm}\ 5min30s - \lambda\ 560_{nm}\ 30s}{5min} = \lambda\ 560_{nm}/min$$

Using this value the % inhibition was calculated by comparing the $\lambda\ 560_{nm}$/min of the negative control (no SOD present) and the respective sample using the following formula:

$$\frac{\lambda\ 560/min\ control - \lambda\ 560/min\ sample}{\lambda\ 560/min\ Control} \times \frac{100}{1}$$

Using the % inhibition results for the standards, a standard curve was generated with % inhibition versus SOD concentration U/ml. From this the U/ml SOD could be calculated for each sample using their respective % inhibition.

2.2.15.3 H_2DCFDA Superoxide Detection in *A. fumigatus*

A six well plate was inoculated with with 1 X 10^6 conidia/ml in a total volume of 4 ml Sabouraud media (section 2.1.3.17). To each well a sterile microscope coverslip was added and cultures were incubated at 37 ^{0} C static overnight. The following

morning any excess mycelia was removed leaving only the supernatant and lower mat of cells. To each well in duplicate, solvent control (MeOH), positive control (Hydrogen peroxide) and/or gliotoxin were added. Samples were incubated at 37 ^{0} C static for 30 min. Afterwards supernatant was removed and cells were washed in 4 mls PBS for 5 min. This was removed and another 3 mls SB media was added to which a 2.5 µg/ml H_2DCFDA was added. Cells were incubated at 37 ^{0} C for 40 min before being placed on a microscope slide and visualised using a fluorescent microscope and a GFP filter.

2.2.16 Organic Extraction of *S. cerevisiae* Culture Supernatant for LC-MS

S. cerevisiae strains were inoculated in triplicate in 5 ml YPD media (section 2.1.3.1) and were incubated overnight at 30 ^{0} C shaking at 200 rpm. The following morning these cultures were used to re-inoculated another 30 ml fresh YPD in a 50 ml Falcon tube and let grow till at mid exponential phase. At this point cells were exposed to either solvent control or 5 µg/ml gliotoxin (section 2.1.2.1) for 3hours. Afterwards samples were centrifuged at 4293 g for 10 min transferring the supernatant to a new Falcon tube. To this equal volume of chloroform was added and mixed by inversion. To further separate the organic phase from the inorganic phase, samples were centrifuged at 3000 rpm for 3 min. Using a sterile Pasteur pipette, the organic phase was removed to a fresh 50 ml Falcon tube and left in an extraction hood overnight to allow the chloroform to evaporate and only the organic pellet to remain. Pellet was re-suspended in 1/100th its original volume and transferred to a glass LC-MS sampling tube (Agilent) whereby it was now ready to be run on the LC-MS for organic metabolite detection.

Chapter 3

Phenotypic and biochemical characterisation of *A. fumigatus gliT*, *gliZ* mutants

3.1 Introduction

The fungal secondary metabolite gliotoxin, was first identified in 1936 in the culture filtrate of *Trichoderma spp*, (Weindling & Emerson 1936). It wasn't until Johnson *et al.,* (1943) isolated gliotoxin from *Gliocladium fibriatum*, that gliotoxin was named and a corrected mass of 326 Da was identified. The structure of gliotoxin, Figure 3.1, was elucidated by Bell *et al.,* (1958) and later confirmed by the isolation of the crystal structure of gliotoxin using X-ray crystallography and later, Nuclear Magnetic Resonance (NMR) (Beecham *et al.,*1966; Kauadji 1990). Gliotoxin is classed as an epipolythiodioxopiperazine (ETP) based on the presence on the indispensible trans-molecular di-sulphide bridge and piperazine ring (Gross *et al.,* 2010).

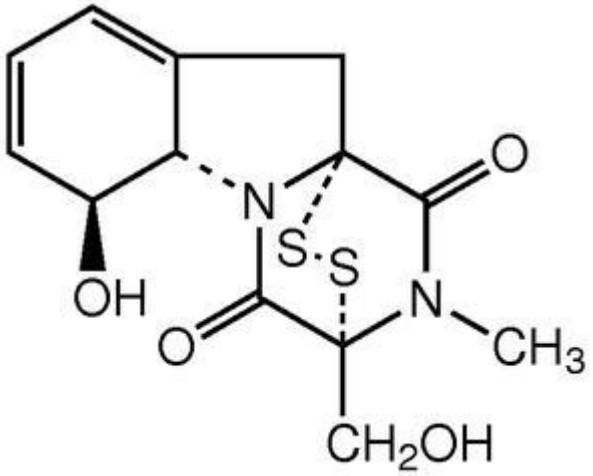

Figure 3.1 Chemical structure of the non-ribosomal peptide gliotoxin. Note the trans-molecular disulphide bridge shown here in its closed oxidised form. Source: http://www.abcam.com/ps/datasheet/images/142/ab142437/Gliotoxin-ab142437-ChemicalStructure-1.jpg

The key precursors utilised in the formation of gliotoxin were found via radio-labelled amino acid studies identifying L-phenylalanine and L-serine as the main components utilised in the formation of the diketopiperazine structural scaffold required for gliotoxin biosynthesis (Suhadolnik & Chenoweth 1958). As neither, L-

phenylalanine nor L-serine possess a sulphur moiety, labelled L-cysteine, L-methionine and sodium sulphate were used in order to identify the precursors of disulphide bridge formation in gliotoxin. These were found to act as donors of their sulphur atoms but did not reflect actual *in vivo* gliotoxin biosynthesis (Suhadolnik & Chenoweth 1958; Gardiner *et al.*,2005). The key components involved in this *in vivo* biosynthesis of gliotoxin were later identified following the discovery of the genes responsible for gliotoxin biosynthesis.

Following the full genome sequencing of *A. fumigatus*, a 12 gene cluster was identified which closely resembled a similar ETP secondary metabolite cluster, the sirodesmin biosynthetic cluster, found in *Leptosphaera maculans* and was identified as the putative gliotoxin biosynthetic cluster, *gli* Figure 4.2 (Gardiner & Howlett 2005). This *gli* cluster was later updated to include another gene, *gliH* which encodes a hypothetical protein, bringing the total number to 13 (Schrettl *et al.,* 2010).

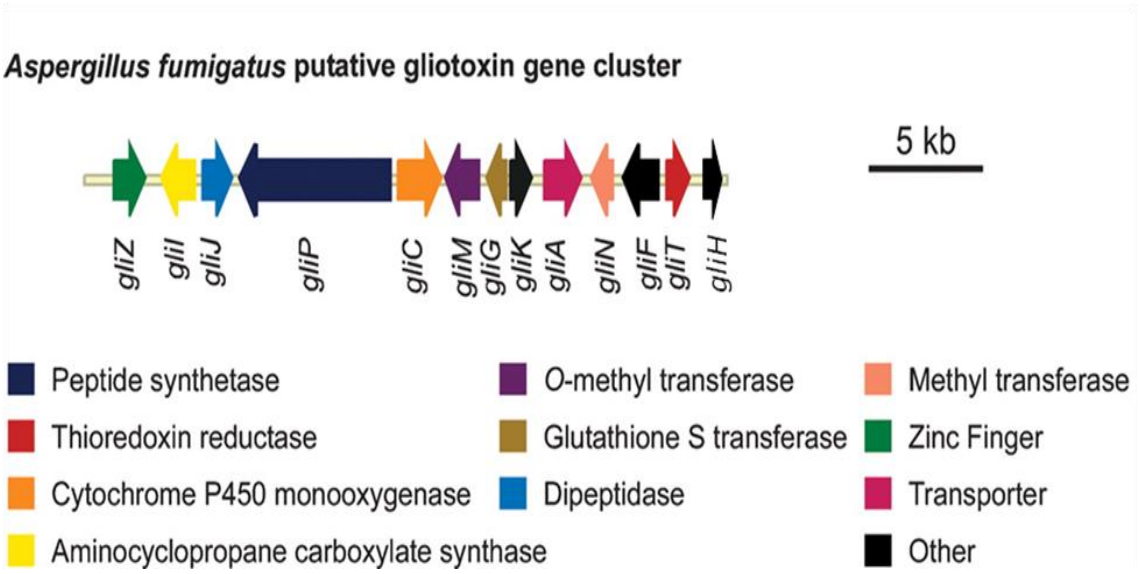

Figure 3.2 Gliotoxin biosynthetic cluster *gli* from *A. fumigatus*. Diagram modified from Gardiner *et al*, (2005) including the recent addition of the thirteenth *gli* cluster gene *gliH* (Schrettl *et al.,* 2010).

The functions of certain *gli* genes have been characterised using a functional genomics approach. g*liZ* has been annotated as the transcriptional regulator of the *gli* cluster, with loss of *gliZ* resulting in the complete abolishment of gliotoxin biosynthesis, and believed to silence the entirety of this cluster (Gardiner & Howlett 2005; Bok *et al.*,2006; Forseth *et al.*,2011). g*liZ* encodes a Zn_2Cys_6 binuclear finger transcription factor responsible for the transcriptional regulation of the *gli* cluster (Bok *et al.,* 2006). In *A. fumigatus* Δ*gliZ,* expression of *gliI* and gliotoxin biosynthesis was found to be abolished (Bok *et al.,* 2006). Over-expression of *A. fumigatus gliZ* induces a corresponding increase in gliotoxin production (Bok *et al.,* 2006). Additionally, Forseth *et al.,* (2011) identified 9 *gliZ* dependent metabolites absent in Δ*gliZ* organic extracts using 2D NMR spectroscopy and are believed to be involved in gliotoxin metabolism in a *gliZ* dependant manner.

Interestingly *A. fumigatus gliT*, annotated as a thioredoxin oxidoreductase, was found to be independent of *gliZ* regulation and could be induced upon exogenous gliotoxin addition (Schrettl *et al.,* 2010). Furthermore, *A.fumigatus* Δ*gliT* was unable to produce any detectable gliotoxin and elicited a hypersensitive phenotype to exogenous gliotoxin highlighting its role in self-protection against gliotoxin exposure (Schrettl *et al.,* 2010). GliT is involved in the oxidation of reduced gliotoxin closing the disulphide bridge (Figure 3.3). Only oxidised gliotoxin is actively effluxed from the cell, presumably facilitated by GliA, with the loss of GliT mediated oxidation and subsequent efflux has attributed to Δ*gliT* sensitivity to exogenous gliotoxin (Bernardo *et al.,* 2003; Schrettl *et al.,* 2010).

The presence of a disulphide bridge is indispensible for gliotoxin toxicity (Scharf *et al.,* 2010; Scharf *et al.,* 2011). Up until recently, no concurrent proof of the mechanism for the incorporation of the necessary sulphur moieties was to be found. *GliG* is annotated as a glutathione-S-transferase, an enzyme involved in the incorporation of glutathione molecules into different chemical structures, however what role it may play in gliotoxin biosynthesis was unclear (Gardiner & Howlett 2005). When disrupted in *A. fumigatus,* gliotoxin biosynthesis is abolished, indicating *GliG* is fundamental in some part of the gliotoxin biosynthesis pathway (Davis *et al.,* 2011).

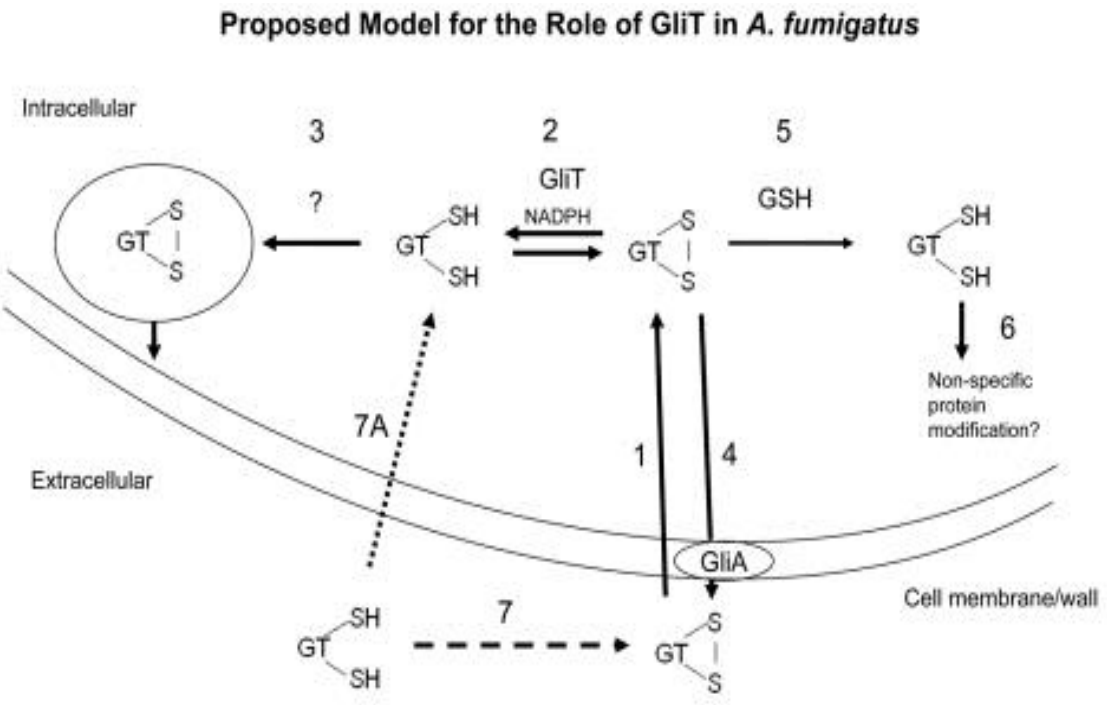

Figure 3.3 Proposed model of GliT mediated protection against gliotoxin GliT protects the cell by acting as an oxido-reductase altering the trans-molecular disulphide bridge from the reduced form of gliotoxin (GT-SH-SH) to the oxidised form (GT-S-S) facilitating its efflux. Image taken from Schrettl *et al.,* (2010)

Comparative LC-MS ToF analysis identified an accumulation of a metabolite specifically in *A. fumigatus ΔgliG* supernatant extracts which was absent form *A. fumigatus* wild-type (Davis *et al.,* 2011). NMR spectroscopy later identified this as 6-benzyl-6-hydroxy-1-methoxy-3-methylenepiperazine 2,5-dione, a shunt metabolite involved in the latter stages of gliotoxin biosynthesis (Davis *et al.,* 2011). Based on the presence of a hydroxyl group found on its C-6, this work proposed that GliG was involved in the incorporation of two glutathione molecules at these C-6 and C-3 positions after hydroxylation at these sites and subsequent elimination of water creating a reactive acyl-imine (Davis *et al.,* 2011). This was the first work which demonstrated GliG glutathione S-transferase activity, and due to *A. fumigatus* Δ*gliG* ability to grow equally well as *A. fumigatus* wild-type in the presence of exogenous gliotoxin, confirmed it was not involved in gliotoxin auto-protection (Davis *et al.,* 2011).

GliP encodes a non-ribosomal peptide synthetase, enabling gliotoxin to be produced outside of the ribosomal dependent pathway and is instead produced via modification of L-phenylalanine and L-serine (Gardiner & Howlett 2005; Cramer *et al.*,2006) . Loss of *gliP* leads to abolition of gliotoxin production, highlighting its role in gliotoxin biosynthesis (Cramer *et al.,* 2006). Interestingly, mice infected with *A. fumigatus* Δ*gliP* conidia showed that loss of *gliP* attenuates *Aspergillus* infection when compared to wild-type (Sugui *et al.,* 2007). Similarly, larvae of the greater wax moth, *Galleria mellonella,* show reduced infection when injected with conidial suspensions of *A. fumigatus* Δ*gliT* when compared to *A. fumigatus* wild-type (Schrettl *et al.,* 2010). Both these results highlight gliotoxin as an important virulence factor.

GliK function was not characterised until relatively recently. In an *A. fumigatus* Δ*gliK* strain, gliotoxin biosynthesis was abolished indicating GliK was involved in gliotoxin biosynthesis (Gallagher *et al.,* 2012). This biosynthetic function was later confirmed *in vitro* as γ-glutamate cyclotransferase activity (Scharf *et al.,* 2013). Contrary to other *gli* genes, H_2O_2 (1 mM) was found to significantly increase expression of *A. fumigatus gliK* not gliotoxin (Gallagher *et al.,* 2012). *A. fumigauts* Δ*gliK* also showed increased sensitivity to exogenous gliotoxin exposure, however it was not as sensitive as Δ*gliT* (Gallagher *et al.,* 2012; Schrettl *et al.,* 2010). Increased expression of *gliK* upon addition of H_2O_2 in *A. fumigatus* and corresponding sensitivity of *A. fumigatus* Δ*gliK* to exogenous H_2O_2, suggests a role in tackling with H_2O_2 mediated O S.

Reverse phase HPLC and liquid chromatography mass spectrometry identified unique metabolites extracted from *A. fumigatus* Δ*gliK* culture supernatants which were absent in the wild-type, as well as significantly elevated levels of ergothioneine in Δ*gliK* compared to wild-type (Gallagher *et al.,* 2012). Interestingly exogenously added gliotoxin efflux of *A. fumigatus* Δ*gliK* was significantly reduced compared with *A. fumigatus* wild-type, suggesting GliK facilitates gliotoxin efflux by some currently undefined mechanism (Gallagher *et al.,* 2012).

GliA is annotated as a Major Facilitator Superfamily (MFS) transporter with the putative function of gliotoxin efflux from the cell (Gardiner & Howlett 2005). In *L. maculans* Δ*sirA* lacking the sirodesmin putative ABC transporter, sensitivity to both gliotoxin and sirodesmin was seen (Gardiner *et al.,* 2005). When transformed with *A. fumigatus gliA*, this sensitivity was reduced towards gliotoxin only and not sirodesmin, showing GliA attenuation of gliotoxin toxicity presumably through facilitating gliotoxin efflux (Gardiner *et al.,* 2005; Gallagher *et al.,* 2012). Interestingly, loss of *L. maculans sirA* elicited increased secretion of sirodesmin which may suggest that *sirA* is involved in control of secretion of sirodesmin rather than as an efflux pump (Gardiner *et al.,* 2005).

Although there has been much progress into the functional characterisation of these genes in recent years, there are a lot of questions which remain unanswered. The fact that *gliT* is still expressed in *A. fumigatus* Δ*gliZ* means that the cluster is not actually silent in this mutant. This means there is a need to create a strain in which the *gli* cluster is completely silenced. To this end, an *A. fumigatus* double knockout was created lacking the cluster transcriptional activator *gliZ* and the independently regulated oxido-reductase *gliT* with the aim of characterising the response of this strain to gliotoxin.

3.2 Generation of Δ*gliT*Δ*gliZ*[293]

Bok *et al.,* (2006) created an *A. fumigatus* Δ*gliZ* strain in a uracil/uridine auxotroph *A. fumigatus* wild-type, replacing the *gliZ* gene with a *pyrG* cassette creating a uracil/uridine prototroph. Using this strain, a bipartite gene disruption technique (Nielsen *et al.,* 2006) was employed to knockout *A. fumigatus gliT* (AFUA_6G09740) replacing the gene with a pyrithiamine (*ptrA*) resistance marker. This was achieved by amplifying two separate genomic regions from a Δ*gliT* strain which was originally created in Schrettl *et al.,* (2010). Constructs used for the disruption of *A. fumigatus gliT* in *A. fumigatus* Δ*gliZ* were amplified using genomic DNA isolated from *A. fumigatus* Δ*gliT* strain. Each construct contained sequences of homology flanking *gliT* (1.3 and

1.2 kb respectively) and two part regions coding the pyrithiamine resistance marker with a region of 560 bp in common (Figure. 3.4) (Schrettl *et al.*, 2010) giving total construct sizes of 2.6 kb and 2.2 kb respectively.

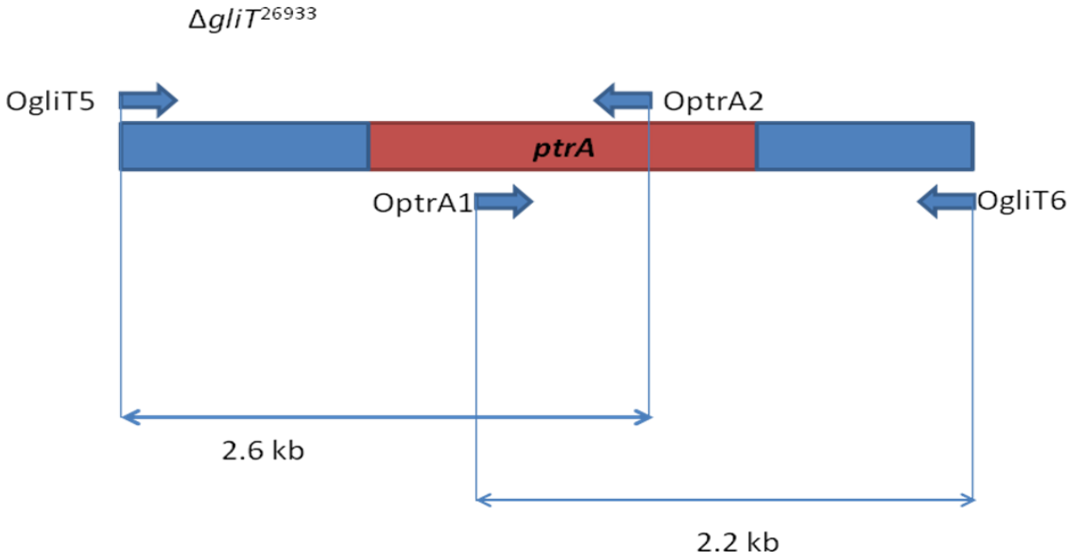

Figure 3.4 Illustration of gene disruption cassettes used to disrupt Δ*gliT*: 5' and 3' gene disruption cassettes were amplified using primers OgliT + OptrA2 & OptrA1 + OgliT6 respectively to yield constructs of 2.6 and 2.2 kb in length.

Constructs were amplified using a high fidelity taq with a high proof read ability to ensure sequence integrity. Resulting PCR amplified constructs were separated via gel electrophoresis to check for single bands and correct size (Figure. 3.5).

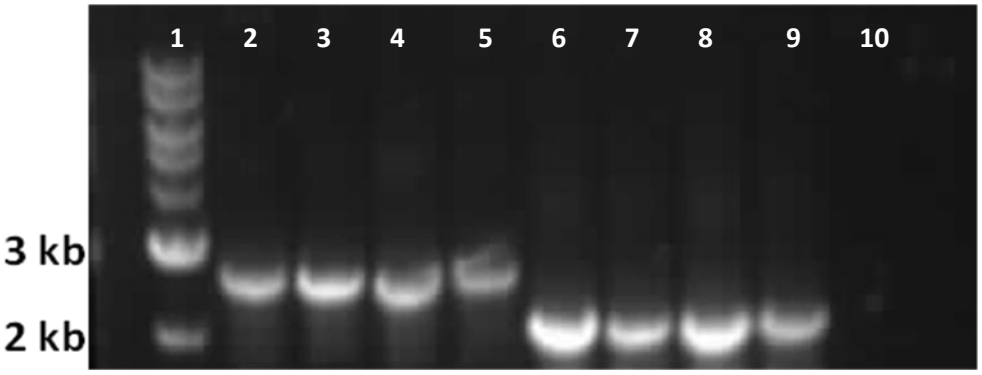

Figure 3.5 PCR amplification of transformation constructs from Δ*gliT* genomic DNA Lane 1= 1 kb NEB ladder, lanes 2-5= 5' construct, lanes 6-9= 3' construct, lane 10= negative control

PCR products from Figure 3.5 were excised and purified prior to transformation. Transformants were identified by resistance to pyrithiamine on agarose plates. A total number of 25 transformants elicited resistance to pyrithiamine. These were isolated and their gDNA extracted. Potential transformants were checked by PCR qualification amplifying the resistance marker via an internal pyrithiamine primer and an external primer which was located outside the constructs used in the original transforming procedure for both 5' and 3' ends of *gliT* to yield an expected band size of 3.3 kb and 2.5 kb respectively in strains lacking *gliT* (Figure. 3.6 A & B).

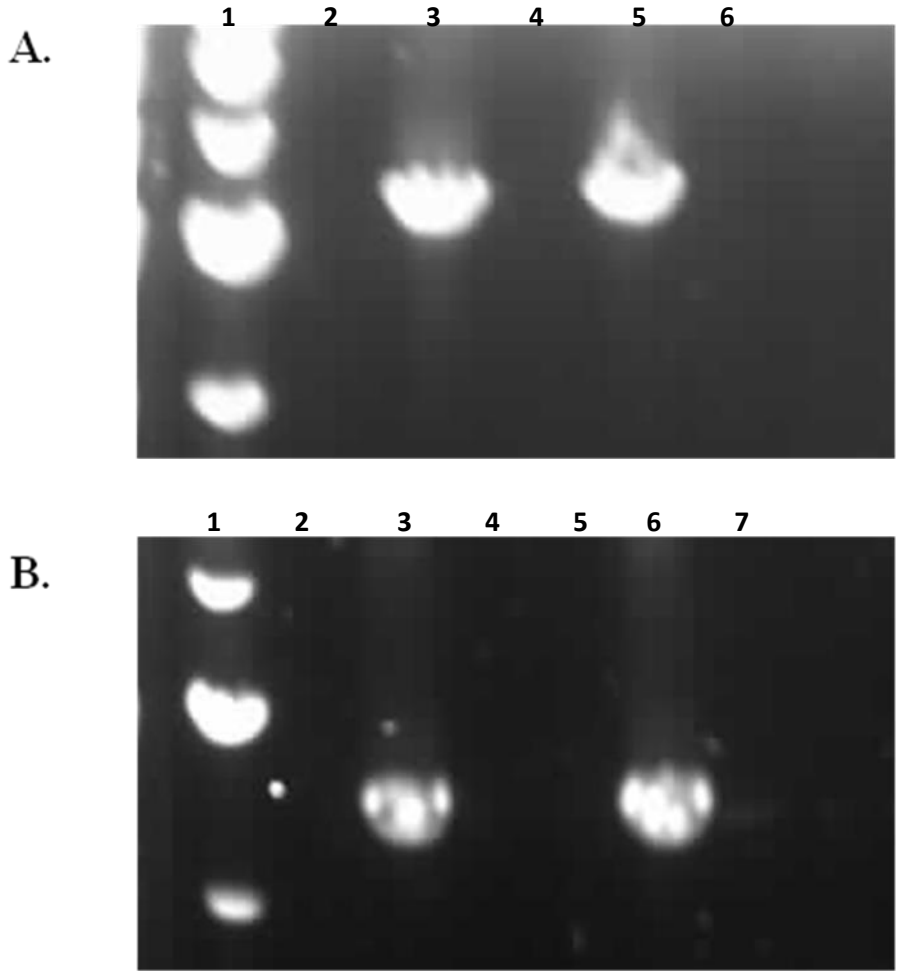

Figure 3.6 A-B PCR qualification of pyrithiamine resistance cassette insertion in place of *A. fumigatus gliT* A= 5' *gliT* region; lane 1 = 1 kb NEB ladder, lane 2= AF293, lane 3= Δ*gliT*^{26933}, lane 4= Δ*gliZ*^{293}, lane 5= sample 11, lane 6= negative control. B = 3' *gliT* region; lane 1- 1 kb NEB ladder, lane 2 = AF293, lane 3= Δ*gliT*^{26933}, lane 4= Δ*gliZ*^{293}, lane 5= sample 10, lane 6= sample 11, lane 7= negative control.

Out of all the transformants screened, only one yielded the correctly sized bands for an *A. fumigatus* Δ*gliT*Δ*gliZ*^{293} strain. This PCR qualification allowed for quick selection of possible candidates and meant instead of a total 25 possible transformants to be checked by Southern blotting, only two transformants were checked. A total amount of 10 µg of gDNA from AF293, Δ*gliT*^{26933}, Δ*gliZ*^{293} and transformants were restriction digested using XbaI for 3 hours at 37 ^{0} C and separated by gel electrophoresis.

The 5' end of the *A. fumigatus gliT* region was probed using a DIG-labelled oligo probe**.** The expected hybridisation pattern of *A. fumigatus* wild-type and Δ*gliT* were 6.4 kb and 3 kb respectively as seen in Figure 3.7 which represents the expected hybridisation pattern in *A. fumigatus* wild-type of the *gliT* probe (Figure. 3.7 A) and Δ*gliT* (Figure. 3.7 B).

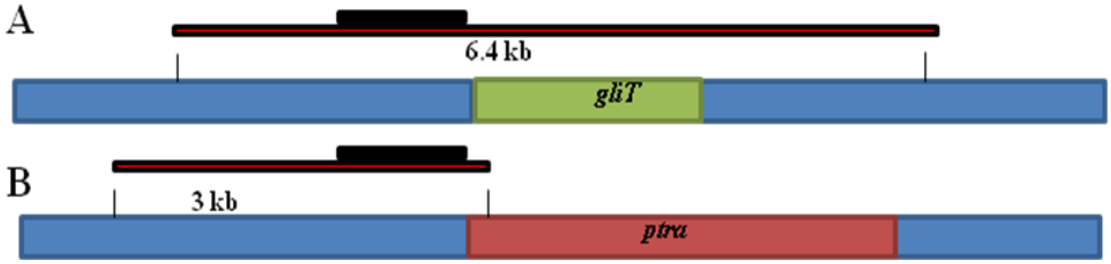

Figure 3.7 A-B Hybridisation of 5' *gliT* probe during Southern Blotting in wild-type (A) and Δ*gliT*Δ*gliZ*. This represents the probing strategy used in the confirmation of disruption of *gliT* in Δ*gliZ* showing the flanking regions in blue, *gliT* gene in green, pyrithiamine resistance cassette in red (*ptrA*), the 5', 1 kb DIG-labelled probe in black and the length of fragment after restriction digestion with XbaI

The resulting southern blot was exposed and developed as seen in Figure 3.8**.** From Figure 3.8 below, one transformant had the correct sized fragment for *gliT* replacement with *ptrA* which was also identical to the Δ*gliT* fragmentation pattern used

as a positive control. The *A. fumigatus* wild type signal identifying *gliT* presence, was still present and could be seen in AF293 (wild-type) and Δ*gliZ*^{293}. The multiple fragments seen for the sample 10 suggest multiple integrations of the resistance cassette, one of which is positive for *gliT* presence and none of which are positive for *gliT* loss. The presence of a single KO band for sample 11 confirmed the creation of an *A. fumigatus* Δ*gliT*Δ*gliZ*^{293}.

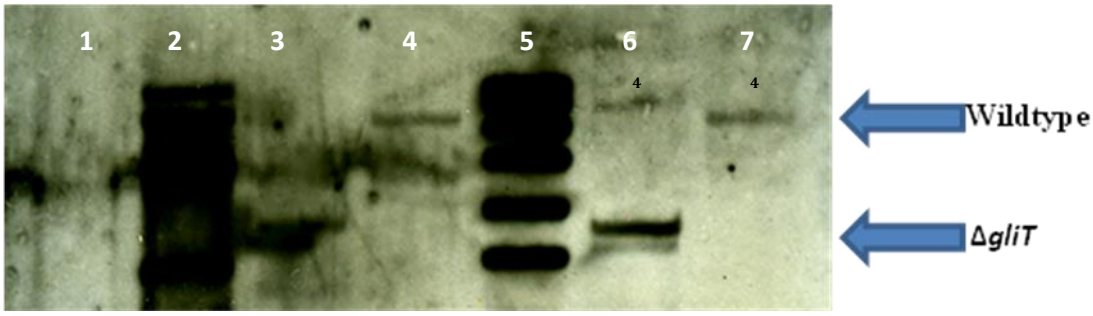

Figure 3.8 Southern blot confirmation of Δ*gliT*Δ*gliZ*^{293} strain: Successful *gliT* replacement with the pyrithiamine resistance cassette confirmed using a 1 kb DIG-labelled probe of the 5' *gliT* region after previously being restriction digested with XbaI. *A. fumigatus* wild-type and Δ*gliT* band sizes are shown with arrows of 6.4 kb and 3 kb respectively. Lane 1= negative control, lane 2= sample 10 , lane 3= sample 11/ Δ*gliT*Δ*gliZ*, lane 4 = Δ*gliZ*^{293}, lane 5= DIG-labelled ladder VII, lane 6= Δ*gliT*^{26933} lane 7= AF293 wild-type

3.3 Growth response of *gliT, gliZ* mutants in the presence of gliotoxin

A. fumigatus can grow in the presence of exogenous gliotoxin (< 20 µg/ml) showing no reduction in its growth response. Deletion of *gliT* elicits a highly sensitive response to relatively low gliotoxin concentrations (5 µg/ml) (Schrettl *et al.,* 2010). Deletion of *gliZ,* elicits some sensitivity but nothing as dramatic as Δ*gliT*, presumably due to *gliT* still being expressed in this strain (Gardiner & Howlett 2005; Schrettl *et al.,* 2010). In an *A. fumigatus* Δ*gliT*Δ*gliZ* strain, the cluster should now be completely silent and may be expected to elicit a sensitive response to gliotoxin exposure.

In Figure 3.9 A, *A. fumigatus* Δ*gliT*Δ*gliZ*^{293} grows like AF293 wild type and Δ*gliZ*^{293} indicating no loss in fitness on AMM once the both genes are absent, however

Δ*gliT*^{26933} growth is slightly altered perhaps due to a difference in its strain background i.e. AF293 vs. ATCC26933. When challenged with gliotoxin, the growth response of each strain changes dramatically (Figures. 3.9 B and C).

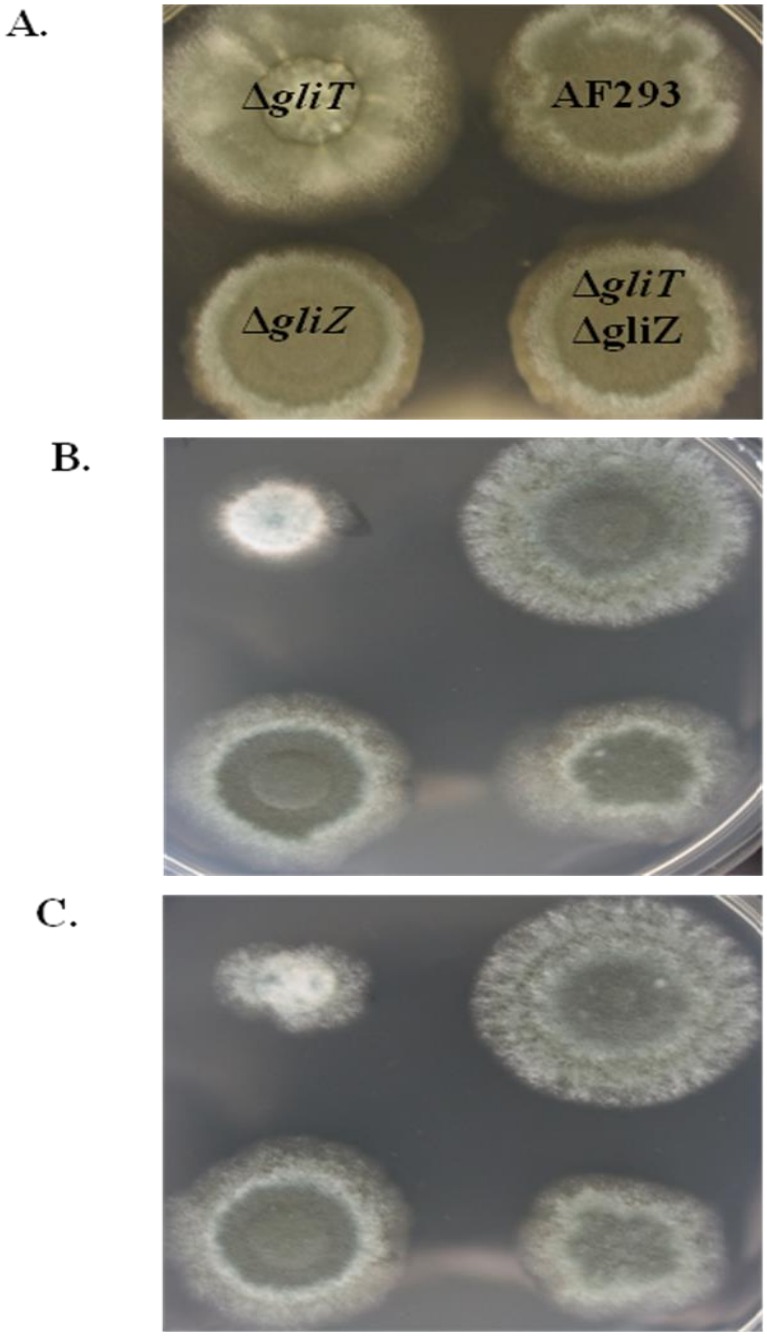

Figure 3.9 A-C Phenotypic growth analysis of *A. fumigatus gliT*, *gliZ* mutants in the absence and presence of gliotoxin Representative images of comparative growth analysis of *A. fumigatus* strains Δ*gliT*^{26933} (top left), AF293 (top right), Δ*gliZ*^{293} (bottom left) and Δ*gliT*Δ*gliZ*^{293} (bottom right) on AMM media (A), 5 µg/ml gliotoxin (B) and 10 µg/ml gliotoxin (C) repeated on three independent occassions

5 µg/ml gliotoxin elicits a sensitive phenotypic response in *A. fumigatus* Δ*gliT*Δ*gliZ*^{293} when compared to *A. fumigatus* wild-type, which is greater than Δ*gliZ* sensitivity yet not as dramatic as Δ*gliT*^{26933}. This suggests that the absence of *gliT* and *gliZ* is less deleterious than loss of *gliT* alone but more than loss of *gliZ* alone.

These results may suggest the existence of some gliotoxin biosynthesis in Δ*gliT* which augments exogenous gliotoxin toxicity. In Δ*gliT*, gliotoxin can still potentially be produced, however without GliT it can no longer be oxidised and subsequently effluxed from the cell. This could lead to an accumulation of gliotoxin *de novo* thus potentiating cell stress explaining Δ*gliT*s sensitivity to gliotoxin.

Δ*gliT*Δ*gliZ*^{293} is sensitive to gliotoxin, but more resistant than Δ*gliT*^{26933}. This relative resistance could be attributed to the inability of this strain to produce gliotoxin unlike Δ*gliT*^{26933}, due to complete inactivation of the *gli* cluster.

3.4 Phenotypic response of *gliT*, *gliZ* mutants to diamide, and hydrogen peroxide

Comparative analysis of the phenotypic growth response of *gliT* and *gliZ* mutants to oxidative stress was carried using the thiol oxidising agent diamide and the ROS producer H_2O_2. The growth response of three *A. fumigatus gli* mutants: Δ*gliT*, Δ*gliZ* and Δ*gliT*Δ*gliZ*, were compared to each other and the *A. fumigatus* AF293 wild type strain AF293 to a range of concentrations of diamide (1 & 2 mM) and H_2O_2 (0.5-2 mM).

Previously exposure to H_2O_2 was demonstrated to elicit a sensitive phenotype in *A. fumigatus* Δ*gliK* indicating its role in OS response (Gallagher *et al.,* 2012). With this in mind, it was questioned whether sensitivity would be seen in other *gli* mutants which no longer expresse *gliK*. Figure 3.10 A-C illustrates the growth response of AF293, Δ*gliT*, Δ*gliZ* and Δ*gliT*Δ*gliZ* when exposed to diamide. 2mM diamide elicited significant differences in the growth response of strains. *A. fumigaus* Δ*gliT* is significantly different from all strains i.e. AF293 ($P = 0.012$), Δ*gliZ* ($P = 0.01$) and Δ*gliT*Δ*gliZ* ($P = 0.015$).

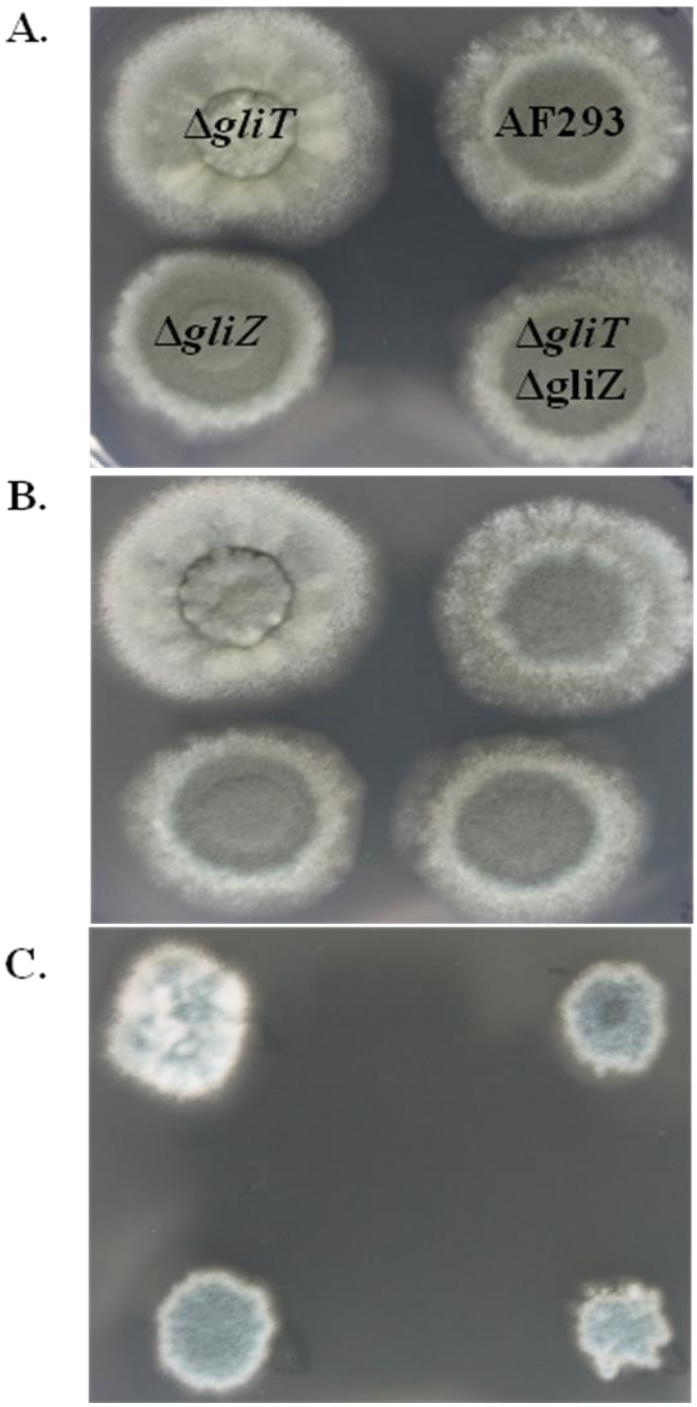

Figure 3.10 A-C Phenotypic growth analysis of *A. fumigatus gliT, gliZ* mutants in the absence and presence of diamide Representative images of comparative growth analysis of *A. fumigatus* strains Δ*gliT*^{26933} (top left), AF293 (top right), Δ*gliZ*^{293} (bottom left) and Δ*gliT*Δ*gliZ*^{293} (bottom right) on AMM media (A), 1 mM diamide (B) and 2 mM diamide (C) repeated on three independent occassions.

Exposure to 2 mM diamide elicits a significant decrease (P = 0.017) in the radial growth Δ*gliT*Δ*gliZ* when compared to AF293 wild-type. Interestingly, there is also a significant decrease (P= 0.019) in radial growth response between Δ*gliZ* and Δ*gliT*Δ*gliZ*. AF293 is not significantly different than Δ*gliZ* indicating it has a wild-type growth response to diamide exposure and the significant decrease seen in Δ*gliT*Δ*gliZ* compared to AF293 and Δ*gliZ* is due to complete silencing of the *gli* cluster. Diamide induces stress via the oxidation of glutathione to its oxidised GSSG form, with strains having naturally higher levels of GSH being increasingly sensitive to diamide, and cells with low levels of GSH being naturally resistant (Kosower *et al.,* 1969). These results could suggest that Δ*gliT*Δ*gliZ* may have naturally altered levels of GSH/GSSG *in vivo.*

Exposure to a range of H_2O_2 (0.5-2 mM) does not result in any significant sensitivity in any of the strains Figure 3.11 A-C. This implies that loss of the gliotoxin self protection mechanism (GliT) and/or gliotoxin biosynthesis are not crucial in OS induced by exposure to H_2O_2.

The sensitivity of Δ*gliT*Δ*gliZ* to diamide but not H_2O_2 implies the glutathione levels may be altered when the *gli* cluster has been silenced. This implied alteration to GSH levels could be directly linked to the absence of *gliT* creating a subsequent greater demand for GSH to replace GliT activity in the cell. The reason the same phenotype is not seen in Δ*gliT* could be due to gliotoxin presence which could be redox cycling in the presence of diamide i.e. GliT activity is being chemically substituted by the presence of diamide. Δ*gliZ* on the other hand still has *gliT* expression and is thus un-perturbed to diamide toxicity.

A. fumigatus Δ*gliK* sensitivity to H_2O_2 appears to be unique to this strain as H_2O_2 exposure in Δ*gliZ* and Δ*gliT*Δ*gliZ*, which have no *gliK* expression, does not have a deleterious effect. Δ*gliK*s sensitivity to H_2O_2 could be caused by some component of gliotoxin biosynthesis which, in the absence of GliK, potentiates H_2O_2 stress e.g. a reactive intermediate which requires GliK to be active to prevent auto-toxicity.

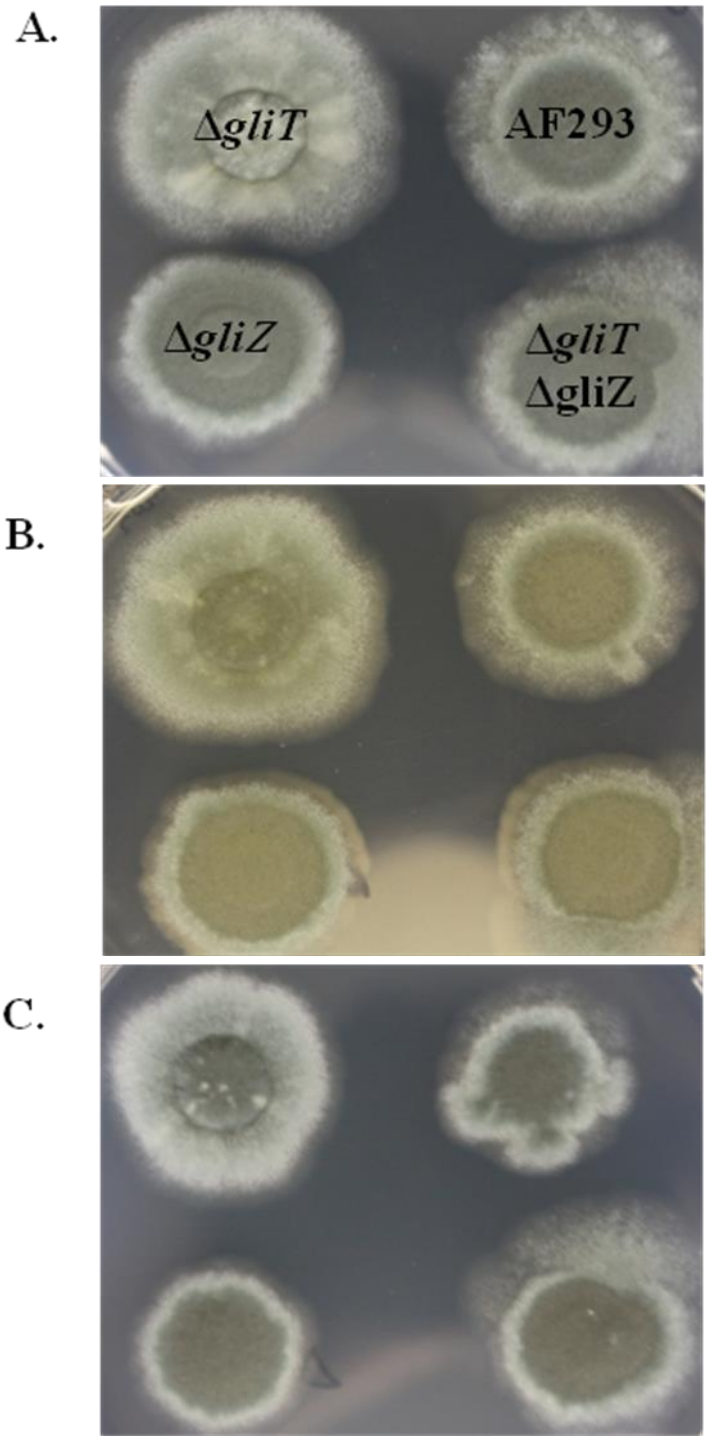

Figure 3.11 A-C Phenotypic growth analysis of *A. fumigatus gliT, gliZ* mutants in the absence and presence of H_2O_2 Representative images of comparative growth analysis of *A. fumigatus* strains Δ*gliT*^{26933} (top left), AF293 (top right), Δ*gliZ*^{293} (bottom left) and Δ*gliT*Δ*gliZ*^{293} (bottom right) on AMM media (A), 1 mM H_2O_2 (B) and 2 mM H_2O_2 (C) repeated on three independent occassions.

3.5 Gliotoxin induction of oxidative stress

Previously in section 3.4, H_2O_2 exposure was found not to elicit any sensitivity in *A. fumigatus gliT* and *gliZ* deletion strains. However each of them possess varying degrees of sensitivity when challenged with gliotoxin (Figure 3.9 A-C). Gliotoxin has been previously demonstrated to induce OS via redox cycling between its oxidised and reduced form (Sutton & Waring 1996). Gliotoxin can directly interact with elements of the OS response, particularly the glutathione and the thioredoxin system, each key in maintaining redox balance inside the cell and preventing OS (Bernardo *et al.,* 2001; Choi *et al.,* 2007). To biochemically analyse the effect gliotoxin exposure had on enzymes involved in the OS response, two biochemical assays were set up using protein lysates from *A. fumigatus* mycelia exposed and un-exposed to 5 µg/ml gliotoxin.

3.5.1 Gliotoxin induces superoxide dismutase expression

Superoxide dismutases (SOD) are key enzymes in the OS response, involved in dismutating the superoxide anion to H_2O_2 and oxygen (Mccord & Fridovich 1969). An increase in superoxide dismutase activity marks an increase in the presence of super oxide radicals and is a good indicator of OS. SOD activity can be measured spectrophotmetrically at Δ_{560nm} by measuring SODs ability to inhibit the formation of the anion Nitroblue tetrazolium-formazan (NBT-formazan) from nitroblue tetrazolium (NBT) resulting in a lower absorbance Figure 3.12.

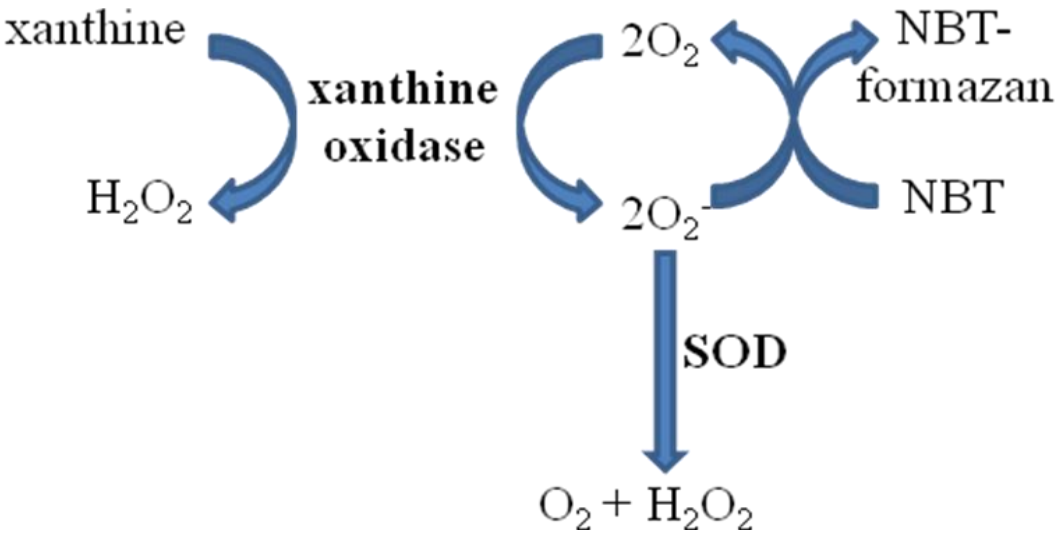

Figure 3.12 SOD inhibition assay. Xanthine is broken down into hydrogen peroxide and the superoxide radical via xanthine oxidase. In the absence of SOD, these superoxide radicals are then utilised to form the anion NBT-formazan from NBT creating a purple precipitate.

From Figure 3.12, the presence of SOD can inhibit the formation of NBT-formazan which subsequently reduces the amount of precipitate that is formed and thus the absorbance of the sample. Approximately 1 U/ml SOD results in 50 % inhibition of this reaction once all components are present. Using a standard curve based on different U/ml of SOD, it is possible to calculate the concentration of SOD in a given sample based on the total % inhibition. *A. fumigatus* samples were treated with either 5 µg/ml gliotoxin or methanol (solvent control) to see if gliotoxin induces SOD expression and thus OS.

Figure 3.13 illustrates the mean SOD concentration (U/ml/mg of protein) in ATCC26933 +/- 5 µg/ml gliotoxin. In the absence of gliotoxin, no induction of SOD can be detected. However, once challenged with 5 µg/ml gliotoxin, this changes significantly.

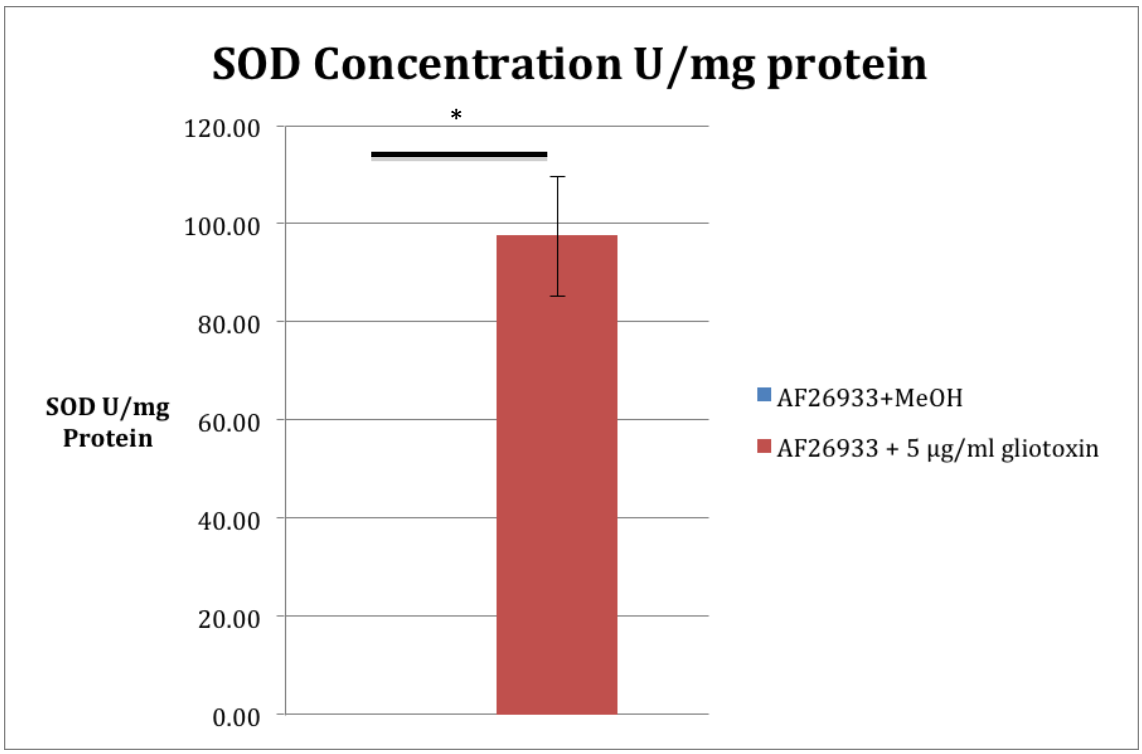

Figure 3.13 SOD concentration in *A. fumigatus* protein lysates in the presence and absence of 5 µg/ml gliotoxin The above graph represents the mean concentration of SOD in U/ml per mg protein from samples carried out in triplicate for each condition respectively. This was determined by calculating the % inhibition of the formation of NBT-formazan which corresponds to the concentration of SOD in that sample.

Although the levels of SOD in the control samples were too low to be quantified, the concentration found in samples treated with gliotoxin yielded significantly higher (P =0.02) levels of SOD in these samples. This highlights gliotoxin presence increases SOD expression in *A. fumigatus* cells due to the increased production of superoxide radicals which would augment toxicity to *A. fumigatus* cells.

3.5.2 Gliotoxin induces catalase expression

Gliotoxin has previously been shown to alter the levels of a mycelial catalase (AFUA_3G02270) (Carberry *et al.*, 2012). Catalase catalyses the breakdown of H_2O_2 to water and oxygen, and is an important part of the OS response against endogenous stress. Catalase activity can be quantified by measuring the breakdown of H_2O_2 at ΔA_{240nm}. Using known amounts of catalase, a standard curve can be created to calculate the respective catalase levels in a given sample. Figure 3.14 illustrates the mean concentration of catalase (U/ml/mg protein) in *A. fumigatus* protein lysates treated with either methanol (solvent control) or 5 µg/ml gliotoxin.

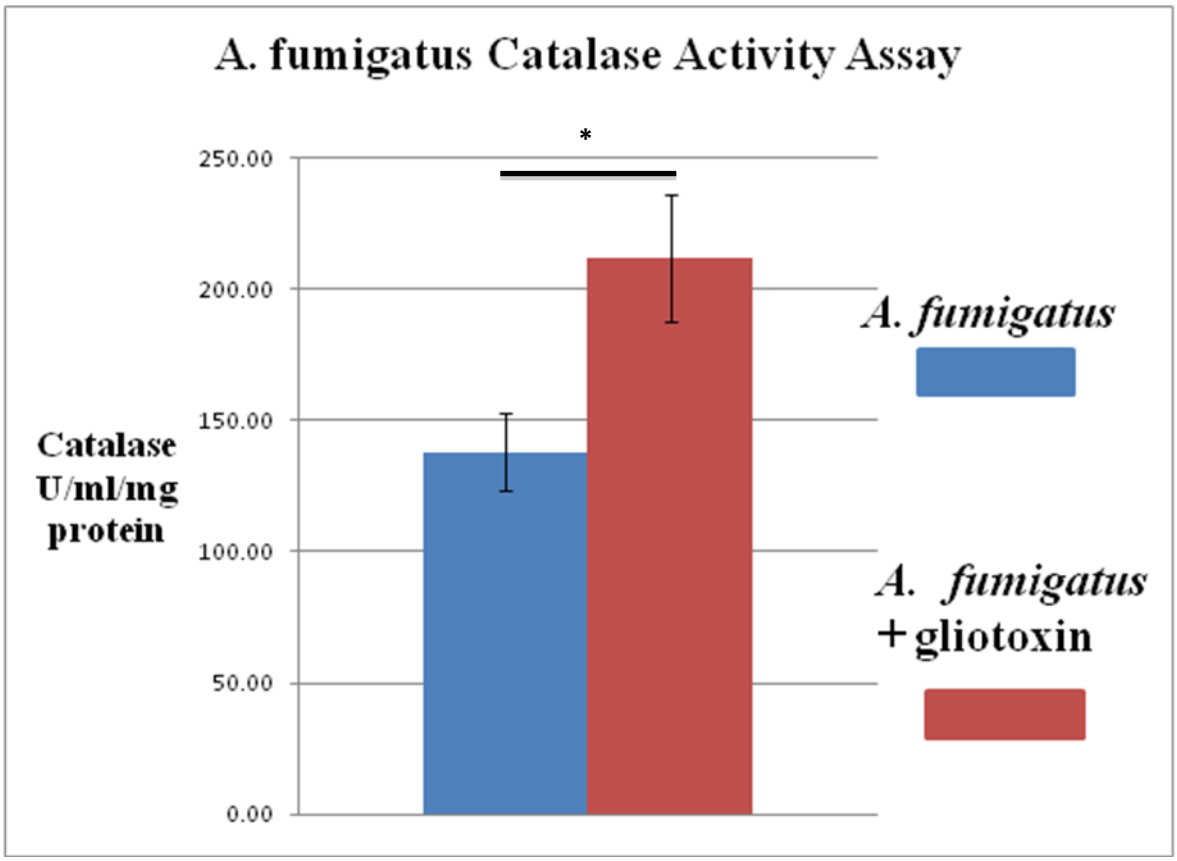

Figure 3.14 Catalase concentration in *A. fumigatus* protein lysates in the presence and absence of 5 µg/ml gliotoxin The above graph represents the mean concentration of catalase in U/ml per mg protein from samples carried out in triplicate for each condition respectively. This was determined by calculating the ΔA_{240}/min for each sample and plotting these values on a standard curve which was created using known amounts of catalase.

Gliotoxin exposure induces a significant increase (P = 0.03) in the expression of catalase in *A. fumigatus*. Expression of a mycelia catalase (AFUA_3G02270) was found to decrease over 40 fold upon gliotoxin exposure (Carberry *et al.,* 2012). Increase in catalase seen here could be due to an increase in other catalases found within the cell which weren't detected in the 2D PAGE work carried out by Carberry *et al.,* (2012).

3.5.3 Gliotoxin induces ROS production in *A. fumigatus*

The use of biochemical assays like those described above give a picture of what is occurring inside the cell once challenged with a particular chemical, in this case gliotoxin. Being able to visualise the effects of gliotoxin *in vivo* holds even more advantages as it allows for a snap shot of any stress and location of said stress after the addition of the toxin. H_2DCFDA is a fluorogenic dye that measures hydroxyl, peroxyl and other reactive oxygen species, notably the superoxide radical. It readily diffuses into the cell and at this point is not fluorescent. Once inside the cell it becomes de-acetylated via cellular esterases and later becomes oxidised by ROS to form the highly fluorescent 7'-dichlorofluorescein. Figure 3.15 shows *A. fumigatus* cells treated with either methanol, 5 mM H_2O_2 or 15 µg/ml gliotoxin. All treated cells showed some degree of fluorescence, indicating the presence of ROS in those cells. 5 mM H_2O_2 yielded the greatest production of fluorescence. As a known OS inducer and producer of ROS this is not too surprising. The small fluorescence seen in methanol treated samples could be endogenous ROS, ROS production induced by methanol exposure or a combination of the two. The fact that the fluorescence seen in the 15 µg/ml gliotoxin treated samples is greater than the methanol treated samples, shows that this increase in fluorescence is gliotoxin specific and demonstrates gliotoxin induction of ROS. Although this induction is clear in the gliotoxin treated samples, its fluorescence is far less than that of those treated with 5 mM H_2O_2.

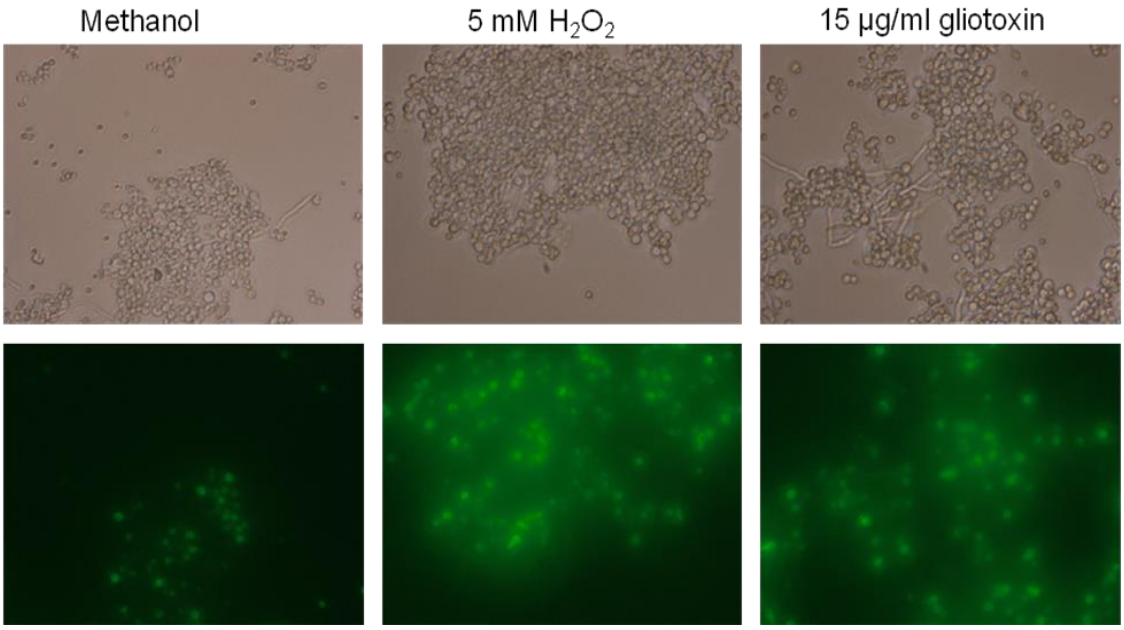

Figure 3.15 *A. fumigatus* cells treated with methanol, 5 mM H_2O_2 or 15 µg/ml gliotoxin as viewed under both white light and GFP at X 40 magnification: The top row shows treated cells under normal light, while the bottom row shows those same cells under a GFP filter. A bright green fluorescence is a positive result for the presence of ROS.

3.6 Anti-oxidant potential of gliotoxin

Gliotoxin is a redox active molecule, cycling between an oxidised and reduced form, facilitated by the presence of its trans-annular di-sulphide bridge (Waring & Beaver 1996). Co-addition of gliotoxin to agarose plates containing H_2O_2 has been previously demonstrated to alleviate H_2O_2 stress in a gliotoxin dependant manner (0-10 µg/ml) (Gallagher *et al.,* 2012). Gliotoxin attenuation of H_2O_2 toxicity indicates an anti-oxidant activity in gliotoxin through its redox cycling ability perhaps through gliotoxin oxidation mediated by H_2O_2 resulting in the formation of oxidised gliotoxin which can effluxed from the cell, and the degradation of H_2O_2 to water (Figure 3.16).

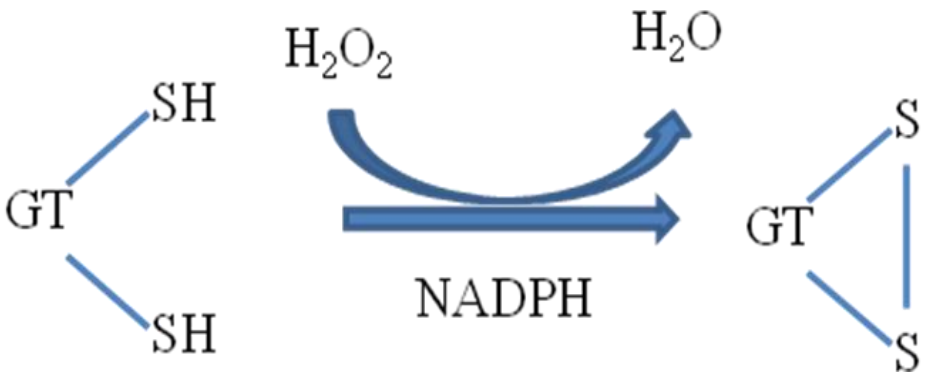

Figure 3.16 Proposed gliotoxin anti-oxidant mechanism in *A. fumigatus*: in the presence of excess H_2O_2 gliotoxin is oxidised ultimately resulting in the breakdown of hydrogen peroxide to water, and efflux of gliotoxin

.

This model indicates that increasing levels of gliotoxin should result in increasing attenuation of H_2O_2 induced toxicity, as seen in Gallagher *et al.*, (2012).

Employing the flourogenic dye H_2DCFDA, *A. fumigatus* cells were exposed to a combination of 5 mM H_2O_2 and 15 µg/ml gliotoxin, (Figure 3.17) and compared to cells exposed to just 5 mM H_2O_2 or 15 µg/ml to examine if this anti-oxidant mechanism could be visualised *in vivo*.

A.

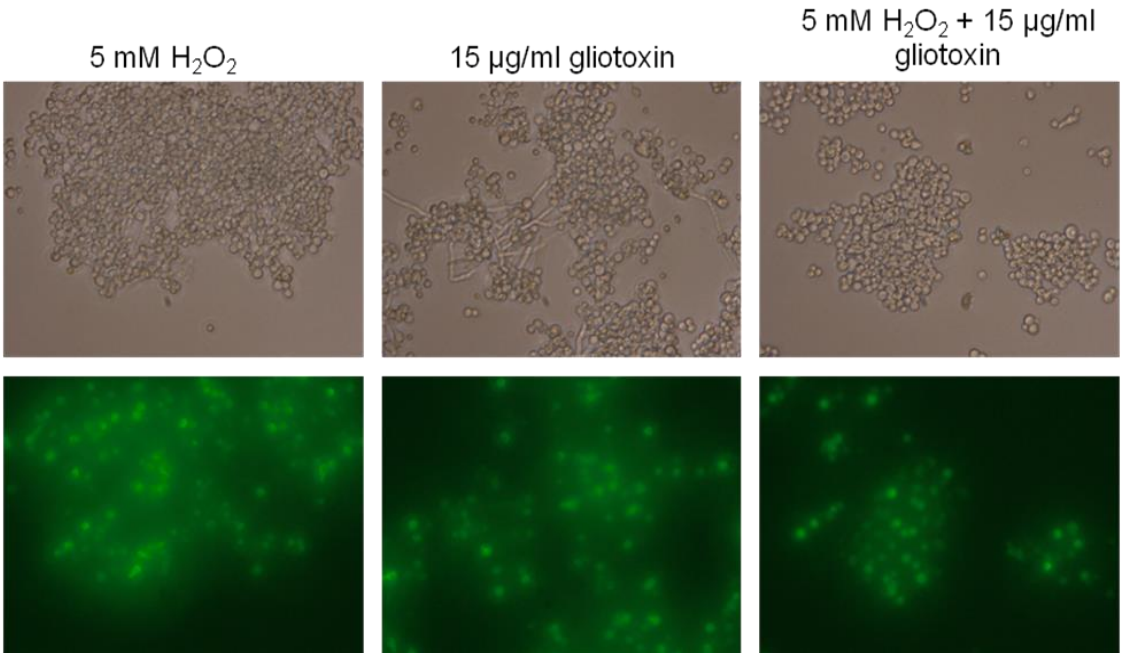

B.

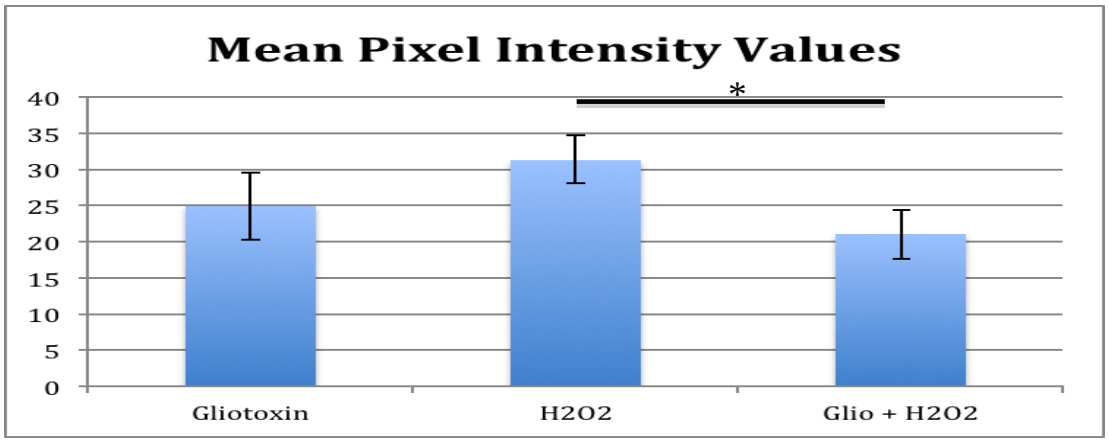

Figure 3.17 *A. fumigatus* cells treated with 5 mM H_2O_2, 15 µg/ml gliotoxin or 5 mM H_2O_2 + 15 µg/ml gliotoxin, as viewed under both white light and GFP at X 40 magnification (A) and respective mean pixel intensity: (A) The top row shows representative images of treated cells under normal light, while the bottom row shows those same cells under a GFP filter. A bright green fluorescence is a positive result for the presence of ROS. Assays were repeated on three independent occassions. (B). Designated areas of biological replicate sample were measured for pixel intensity at three different locations for each strain, condition and replicate and the mean was plotted.

From Figure 3.17 A and B, a reduction in fluorescence in the 5 mM H_2O_2 + 15 µg/ml gliotoxin when compared to 5 mM H_2O_2 or 15 µg/ml gliotoxin only treated cells, with a significant reduction (P = 0.004) in pixel intensity seen in gliotoxin and H_2O_2 combinaiton assay compared with H_2O_2 only treated cells, indicating co-addition of gliotoxin alleviates H_2O_2 stress in the cell perhaps through some gliotoxin cycling mechanism.

3.7 Gliotoxin and H_2O_2 plate assays

In section 3.6, gliotoxin was demonstrated to attenuate H_2O_2 induction of ROS indicating gliotoxin anti-oxidant activity. This led to the hypothesis that cycling of reduced gliotoxin to oxidised gliotoxin utilising H_2O_2 in the process as an electron donor could be occurring. This would corroborate the theory that gliotoxin is actually an accidental toxin and is primarily an anti-oxidant molecule in *A. fumigatus* (Schrettl *et al.,* 2010). This can also be seen in Gallagher *et al,* where H_2O_2 sensitivity in *A. fumigatus* can be reduced by the addition of gliotoxin in a dose dependant manner (Gallagher *et al.,* 2012). From this result it was hypothesised that under some conditions some if not all the *gli* mutants used in this study would show similar improvement in growth when grown on agarose plates with H_2O_2 (0.5-2 mM) and gliotoxin (1-10 µg/ml).

Previously, exposure to H_2O_2 elicited no sensitivity in *A. fumigatus gliT* and *gliZ* mutants, yet exposure to gliotoxin induced a range of sensitivity in all *A. fumigatus* strains. When exposed to a combination of both H_2O_2 and gliotoxin, growth of all strains is significantly altered (Figure 3.18).

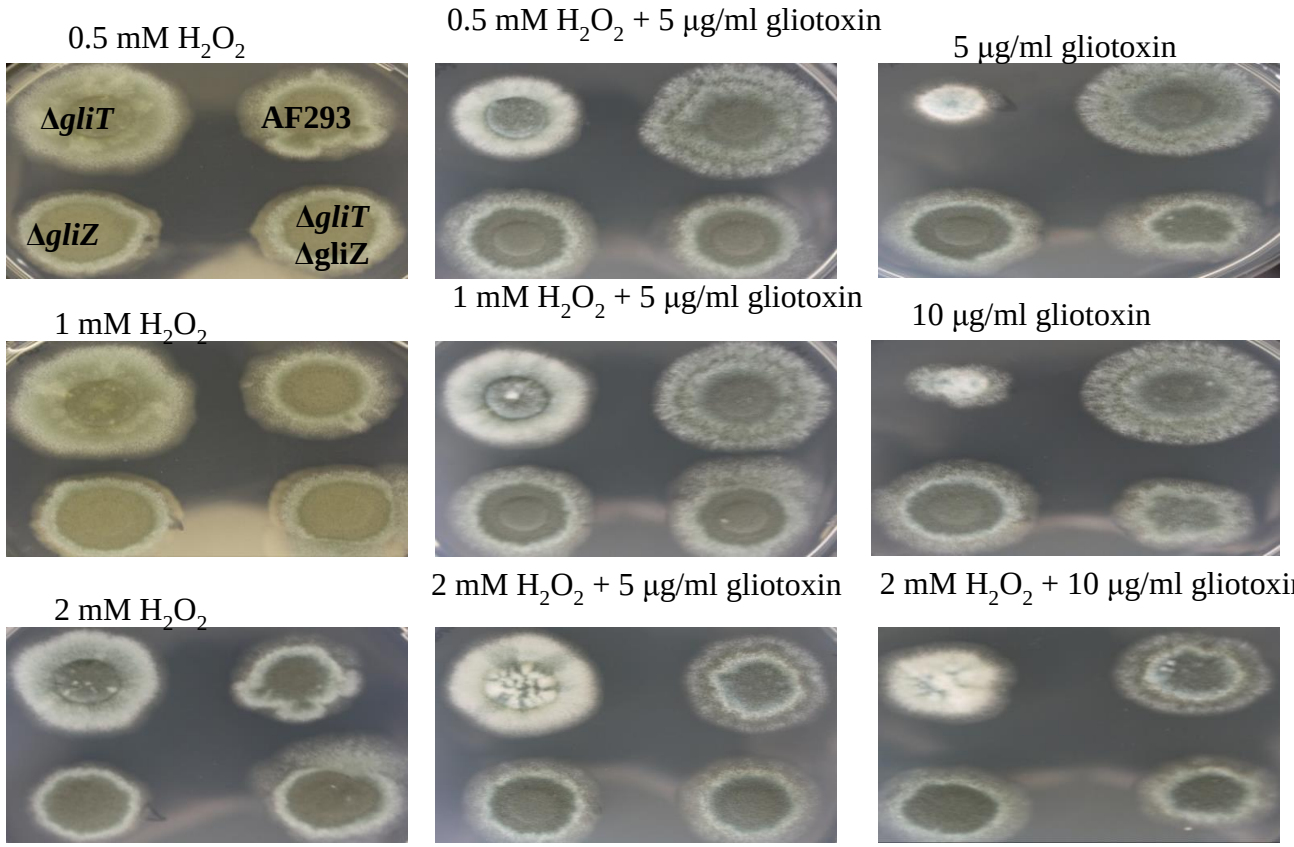

Figure 3.18 Comparative growth analysis of *A. fumigatus gliT* and *gliZ* mutants exposed to H_2O_2 0.5-2 mM, gliotoxin 5 μg/ml and a combination of both AF293 (top right), Δ*gliT*^{26933} (top right), Δ*gliZ*^{293} (bottom left) and Δ*gliT*Δ*gliZ*^{293} (bottom right).

In Figure 3.18, gliotoxin appears to not improve growth on H_2O_2. Interestingly the opposite is happening, with addition of H_2O_2 alleviating gliotoxin toxicity in a dose dependant manner, most notably for Δ*gliT* and to a lesser extent Δ*gliT*Δ*gliZ*. *A. fumigatus* Δ*gliT* has been previously shown to be unable to produce gliotoxin, with no detectable gliotoxin from organic extracts from culture supernatant (Schrettl *et al.*, 2010). However, there could still potentially be some intracellular gliotoxin biosynthesis in this mutant, with gliotoxin efflux inhibited. Schrettl *et al.*, (2010) identified a predicted monothiol form of gliotoxin in *A. fumigatus* Δ*gliT*, which was not present in the wild-type; with a mass of 279 *m*/*z* and could be an indication of some type of gliotoxin biosynthesis occurring *de novo*. GliT has been demonstrated to be involved in closing the disulphide bridge of gliotoxin which is required for gliotoxin transport from the cell, meaning that there is still the potential for gliotoxin to produced in Δ*gliT*, albeit only in the reduced form.

Without GliT mediating oxidation of reduced gliotoxin, efflux of gliotoxin could be halted as only the oxidised form of gliotoxin has been seen to be readily effluxed from the cell (Bernardo *et al.*, 2003; Schrettl *et al.*, 2010). *A. fumigatus* Δ*gliT* sensitivity to gliotoxin could in fact, be due to accumulation of both exogenous gliotoxin and endogenous gliotoxin toxicity.

From Figure 3.18, the presence of H_2O_2 inside the cell could be chemically substituting for GliT absence, aiding in gliotoxin oxidation and subsequent efflux from the cell. This could explain how addition of 1 and 2 mM H_2O_2 respectively restores Δ*gliT* growth on 5 µg/ml gliotoxin to wild-type; with Δ*gliT* radial growth on 2 mM H_2O_2 + 5 g/ml gliotoxin significantly improves ($P = 0.047$) when compared with Δ*gliT* grown on 5 µg/ml gliotoxin alone. No significant difference was seen between AF293 wild-type and Δ*gliT* on 2 mM H_2O_2 + 5 µg/ml gliotoxin highlighting addition of H_2O_2 restores Δ*gliT* growth to wild-type levels.

A. fumigatus Δ*gliT*Δ*gliZ*[293] radial growth, significantly improves ($P = 0.038$) on the 2 mM H_2O_2 + 5 µg/ml gliotoxin compared to Δ*gliT*Δ*gliZ* on 5 µg/ml gliotoxin alone plates. Δ*gliZ* shows no significant difference between either treatment. Exposure to both H_2O_2 and gliotoxin, elicits a significant increase ($P = 0.015$) in the sensitivity of *A. fumigatus* AF293 when compared to AF293 radial growth on 5 µg/ml gliotoxin alone.

This suggests that the combination of 2 mM H_2O_2 and 5 µg/ml gliotoxin induces a synergistic affect augmenting each others toxic affect on *A. fumigatus* AF293. However, addition of gliotoxin significantly increases (P = 0.04) AF293 radial growth on 2 mM H_2O_2 and 5 µg/ml gliotoxin when compared with AF293 radial growth on 2 mM alone. This highlights that gliotoxin alleviates H_2O_2 stress in *A. fumigatus* AF293, while in the mutant strains the opposite is occurring.

A similar result can also be seen at higher gliotoxin concentrations (10 µg/ml), Figure 3.18. Radial growth of Δ*gliT* is significantly improved (P = 0.007) on 2 mM H_2O_2 + 10 µg/ml when compared to Δ*gliT* radial growth on 10 µg/ml gliotoxin alone

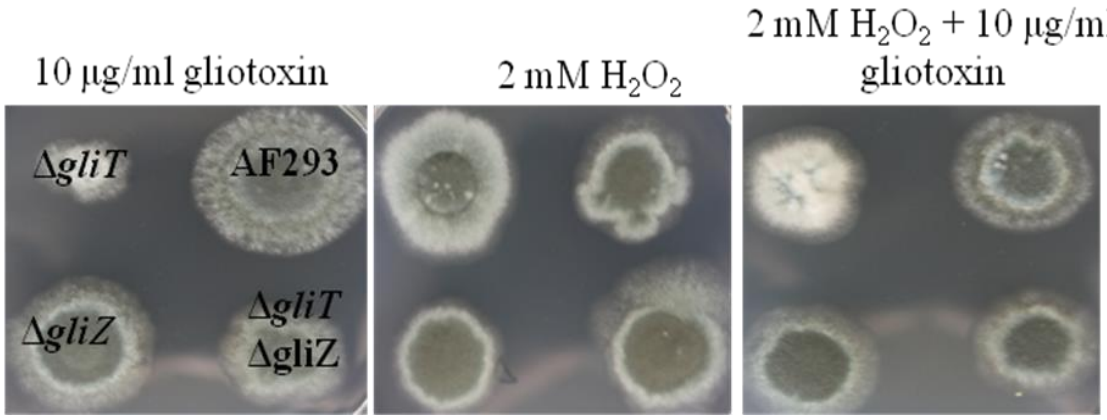

At 10 µg/ml gliotoxin, H_2O_2 attenuation of gliotoxin toxicity is lost in AF293 and Δ*gliT*Δ*gliZ* suggesting this higher gliotoxin concentration is overwhelming the cell and any benefit H_2O_2 presence may have is too little to compensate for increase gliotoxin toxicity.

3.8 Quantification of GSH and GSSG in *A. fumigatus* strains

Glutathione has been seen to be dysregulated in Δ*gliT*^{26933} when compared to *A. fumigatus* ATCC26933 (Carberry *et al.*, 2012). Upon gliotoxin addition these GSH levels decrease significantly (P = < 0.05) when compared to basal levels (Carberry *et al.*, 2012).

Gliotoxin has been shown to directly interact and deplete the *de novo* pool of the intracellular thiol glutathione forming gliotoxin-glutathione conjugates *in vitro* (Bernardo *et al.,* 2001). Disrupting the intracellular levels of this thiol has grave consequences on the cell resulting in a reduced ability to tackle OS and tackling the presence of xenobiotics may be one of many factors which affect Δ*gliT* sensitivity to exogenous gliotoxin (Grant *et al.,* 1996).

Interestingly, addition of reduced glutathione (20 mM) was found to abolish gliotoxin toxicity in both *A. fumigatus* ATCC26933 and Δ$gliT^{26933}$. Addition of reduced gliotoxin only (10 μg/ml), still resulted in Δ*gliT* being sensitive, however not to the same extent as non-reduced gliotoxin, suggesting that the status of the disulphide bridge can influence the growth response of Δ*gliT* to gliotoxin (Carberry *et al.,* 2012).

Gliotoxin transport has been previously shown to occur in a glutathione dependent manner (Bernardo *et al.,* 2003). Bernardo *et al.,* (2003) demonstrated only the oxidised form of gliotoxin was found to actively enter the cell. Higher than normal levels of this thiol could have the potential for a proportional increase in gliotoxin influx into the cell. This hypothesis would predict that strains with higher levels of GSH would have some form of sensitivity to gliotoxin due to GSH mediated influx of gliotoxin, as seen in Carberry *et al,* (2012).

The total GSH and GSSG levels were quantified in strains AF293, Δ*gliT*^{26933}, Δ*gliZ*^{293} and Δ*gliT*Δ*gliZ*^{293}, with the hypothesis that strains which show sensitivity when grown in the presence of gliotoxin may have altered levels of glutathione (Figure 3.21).

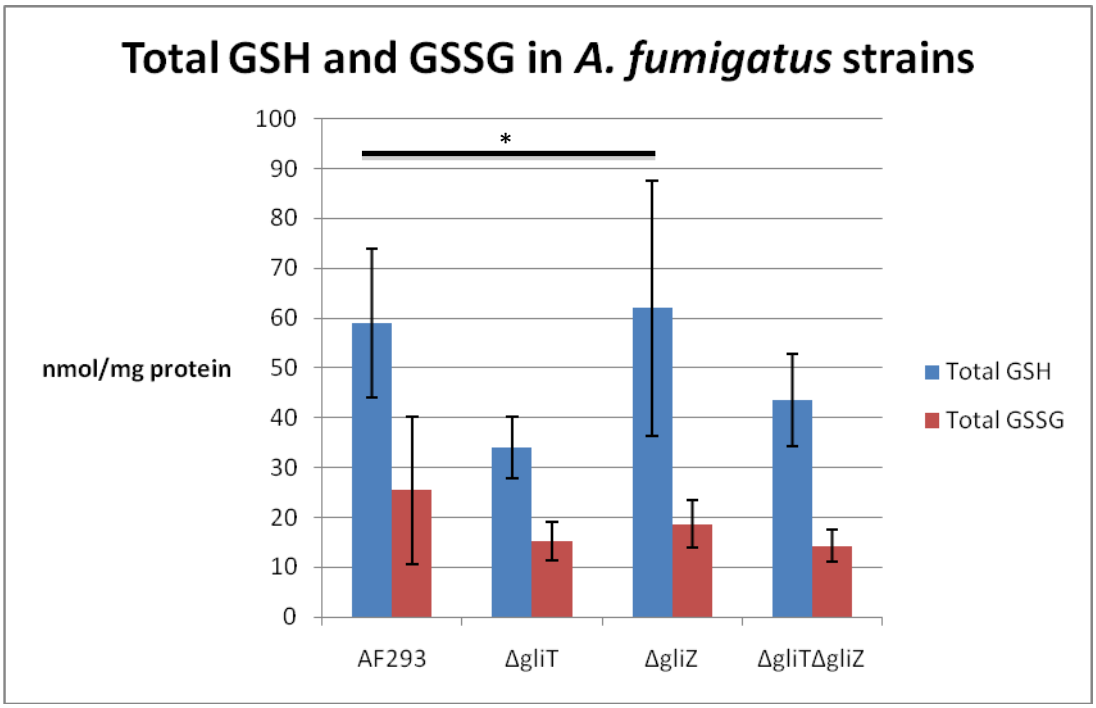

Figure 3.20 Total GSH and GSSG levels in *A. fumigatus*: Total GSH and GSSG content of strains AF293, Δ*gliT*^{26933}, Δ*gliZ*^{293} and Δ*gliT*Δ*gliZ*^{293} was quantified from mycelia grown in Sabouraud liquid media.

In Figure 3.20 there are clear differences in the GSH/GSSG levels amongst the strains. Interestingly Δ*gliT* has significantly lower levels of GSH than AF293 and Δ*gliZ* (P = 0.02 & 0.03, respectively). This contradicts what was seen previously in Carberry *et al.*, (2012) in which Δ*gliT* was found to have significantly higher levels of GSH than ATCC26933 (Carberry *et al.*, 2012). This could be due to a difference in the media which were used, Sabouraud media was used as opposed to AMM as the latter did not produce a high amount of mycelia. A difference in GSH content could be due to a higher availability of nutrients in Sabouraud and decreased stress response compared to AMM grown cultures. This is further supported when the growth response of these

same strains is compared on AMM and Sabouraud media in the absence and presence of exogenous gliotoxin Figure 3.21.

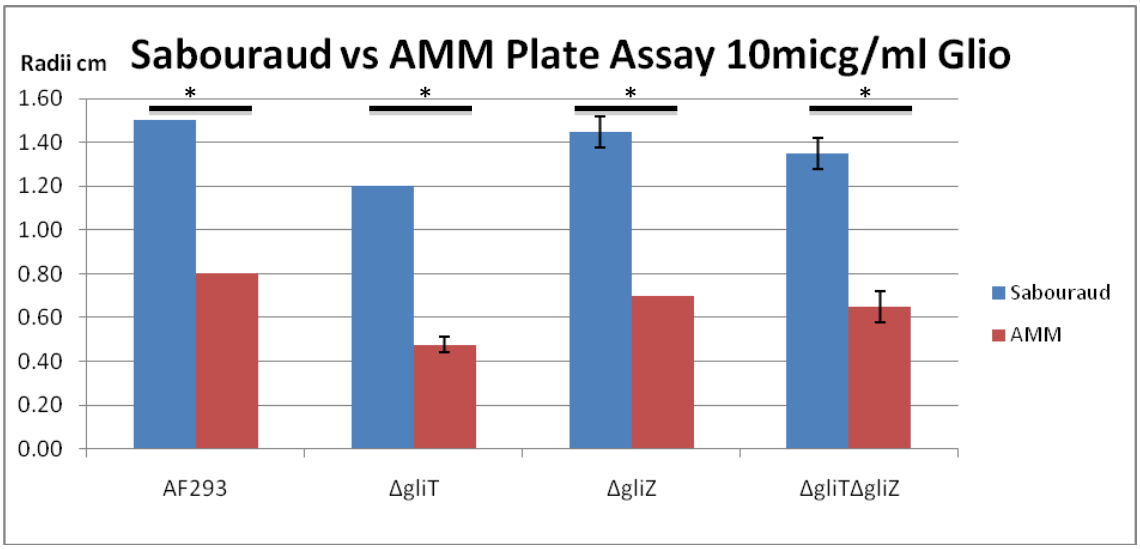

Figure 3.21 Radial growth response of *A. fumigatus* strains on Sabouraud and AMM agarose plates containing 10 µg/ml gliotoxin.

The growth of all strains on Sabouraud media was significantly different then their respective growth on AMM ($P = <0.05$), suggesting Sabouraud may artificially manipulate the GSH levels in cells. Importantly, it does not alter the trend in gliotoxin response in these mutants. The greater growth response on Sabouraud media is presumably due to greater availability of nutrients facilitating improved growth.

When the radial growth response of these strains on gliotoxin plates, seen in Section 3.3, Figure 3.9, is compared to their respective GSH content, there is a similar trend. For example, both Δ*gliZ*[293] and AF293 show a similar growth response to gliotoxin with no significant difference found between them. They also have similar levels of GSH and GSSG suggesting a possible link between GSH levels and growth response to gliotoxin. This is further supported when the three *gli* mutants are compared. *A. fumigatus* Δ*gliT* has the lowest concentration of GSH, with Δ*gliT*Δ*gliZ* having slightly higher and Δ*gliZ* having the highest amongst the three. This is similar to their growth response to gliotoxin i.e. Δ*gliT* is the most sensitive, with Δ*gliT*Δ*gliZ* being more resistant than Δ*gliT* and Δ*gliZ* being the most resistant amongst the three mutants.

These results further show the importance of GliT in the response to gliotoxin toxicity. It was hypothesised that high levels of GSH may pre-dispose cells to being increasingly sensitive to gliotoxin toxicity, yet Δ*gliT* has been shown to possess both significantly higher and lower levels of glutathione on different media types, but is still highly sensitive when challenged with exogenous gliotoxin regardless of the media. This suggests that any benefit which may be seen in cells with low GSH levels of glutathione is insufficient to compensate for the loss of GliT.

3.9 Metformin plate assay

Metformin is a drug which acts as an hypoglycaemic agent in treating type-2 diabetes and polycystic ovary syndrome and in some early cancer treatments (Li *et al.,* 1999; Dowling *et al.,* 2011; Anisimov *et al.,* 2011). Recently it has been shown to influence the methionine biosynthesis cycle, by increasing the levels of S-adenosyl L-homocysteine and S-adenosyl-L-methionine, two key components which are utilised in the methylation of various important components, oxidative stress response and methionine biosynthesis (Mato *et al.,* 1997; Onken & Driscoll 2010; Cabreiro *et al.,* 2013).

From RNA Seq. data retrieved from *S. cerevisiae* cells exposed to gliotoxin, the methionine and GSH biosynthetic pathways were significantly altered (O'Brien 2011). Metformin was employed to examine the phenotypic response to this compound and if it could alter the response to gliotoxin in *gliT*, *gliZ* strains through manipulation of the L-methionine biosynthesis pathway Figure 3.22 A-C.

In Figure 3.22 A, addition of metformin has no adverse affect on cell growth. The combination of both 5 µg/ml gliotoxin and 100 mM metformin, Figure 3.22 B, significantly improves the radial growth of *A. fumigatus* Δ*gliT* ($P = < 0.05$) when compared to its respective radial growth on 8 µg/ml gliotoxin only plates Figure 3.22 C. This metformin meditated improvement is not seen in *A. fumigatus* wild-type strains AF293 or ATCC26933, nor Δ*gliZ* and Δ*gliT*Δ*gliZ*, indicating that metformin is only advantageous in the absence of GliT, and presence of GliZ.

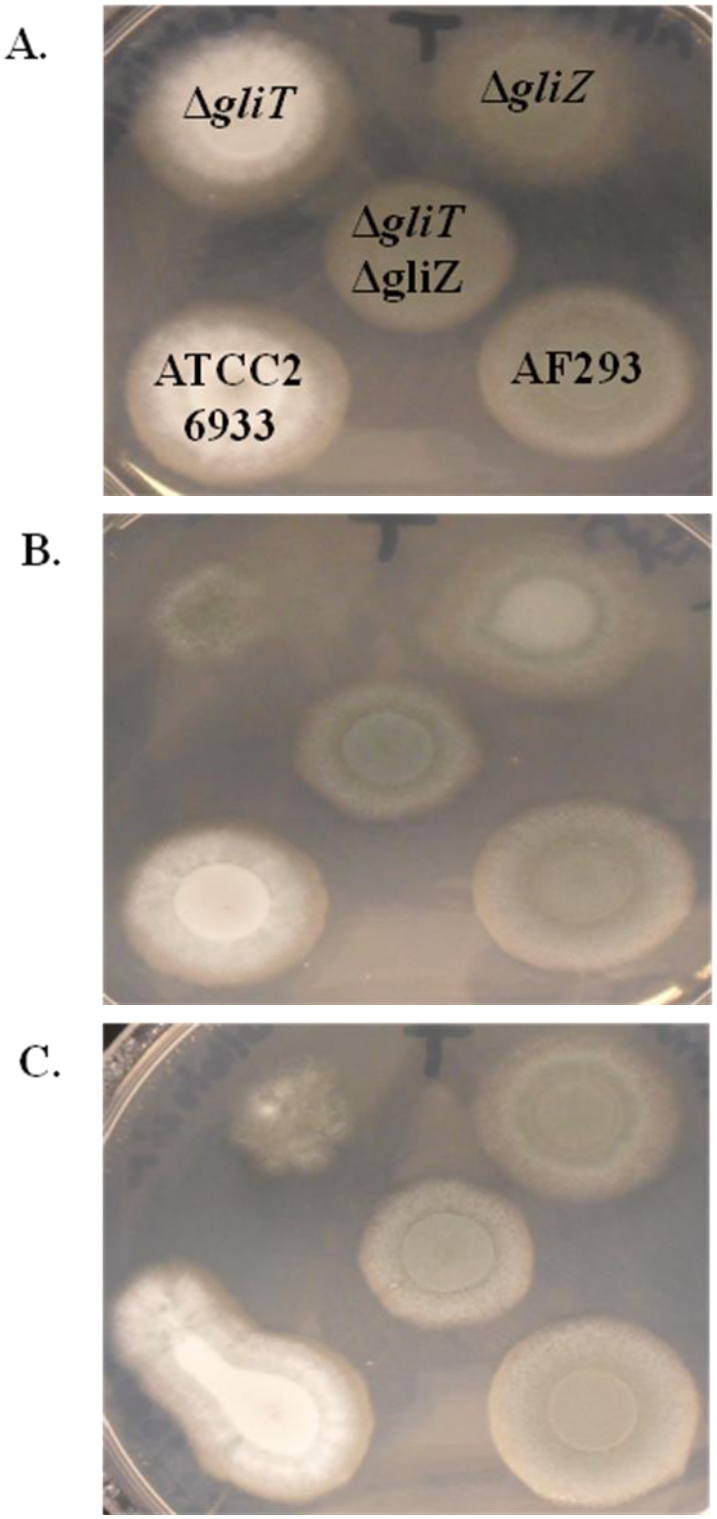

Figure 3.22 Comparative growth analysis of *A. fumigatus gliT* and *gliZ* mutants in the presence of metformin and/or gliotoxin Representative growth analysis of strains exposed to A= 100 mM metformin, B= 8 µg/ml gliotoxin, C= 100 mM metformin + 8 µg/ml gliotoxin repeated on three independent occassions.

In a recent study, Cabreiro *et al.,* (2013) demonstrated that *E. coli* grown on plates containing a range of metformin concentrations which were subsequently consumed by *C. elegans*, could influence the longevity of the *C. elegans* strains. They also found that presence of metformin induced methionine restriction in *E. coli* based on its ability to inhibit expression of methionine synthase and increase the levels of S-adenosyl-L-methionine (SAM) and S-adenosyl-L-homocysteine (SAH) (Cabreiro *et al.,* 2013). An increase in the levels of 5-tetrahydrofolate and simultaneous decrease in tetrahydrofolate levels were also found, indicating metformin induced alteration of both methionine metabolism and folate biosynthesis (Cabreiro *et al.,* 2013). The inhibition of methionine synthase would have a number of consequences in the cell such as reduced re-methylation of L-homocysteine to form L-methionine; increased 5-methyltetrahydrofolate (THF) and reduced levels of tetrahydrofolate (Suliman *et al.,* 2005; Cabreiro *et al.,* 2013).

SAM is an important methyl donor in the cell involved in the methylation of proteins, purine biosynthesis and acting as a co-repressor of genes inside the cell (Chiang *et al.,* 1996). An example of this co-repression activity can be seen in the repression of the folate cycle and inhibition of methylene-THF reductase which reduces 5,10-methylene-THF to 5-methyl-THF resulting in an increase in 5,10-methylene-THF in the cell (Cabreiro *et al.,* 2013). Accumulation of SAM, SAH, 5,10-methylene-THF and 5-methyl-THF results in methionine restriction in *E. coli* cells which further induces methionine restriction in their host (*C. elegans*) increasing life-span (Cabreiro *et al.,* 2013).

This increase in SAM may be responsible for the improved growth of Δ*gliT* seen in Figure 3.22 C. Bis-methylated gliotoxin (Bm-GT) is a methylated form of gliotoxin which has been hypothesised as a product of gliotoxin detoxification (Domingo *et al.,* 2012). Bm-GT would require the presence of a methyl donor i.e. SAM to donate the two methyl groups required for its biosynthesis.

Addition of metformin results in a significant improvement in Δ*gliT* radial growth on 8 µg/ml gliotoxin, presumably due to an alteration in SAM levels and

perhaps, Bm-GT biosynthesis. However no Bm-GT was detected in Δ*gliT* by Schrettl *et al.*, (2010) which suggests metformin may in fact help regulate the SAM cycle.

Dysregulation of the SAM cycle can result in the accumulation of L-homocysteine and SAH, both of which are deleterious to the cell (Kredich & Hershfield 1979; Fujita *et al.*, 2006). This may suggest that in the presence of exogenous gliotoxin, the SAM cycle is dysregulated in *A. fumigatus* Δ*gliT* resulting in L-homocysteine/SAH associated cytotoxicity. However, addition of metformin helps reduce this toxicity through L-methionine restriction.

In *A. fumigatus* AF293, ATCC26933, Δ*gliZ* and Δ*gliT*Δ*gliZ,* metformin is not advantageous, showing no improvement of radial growth on metformin and gliotoxin plates. This may suggest that the SAM cycle is un-perturbed in these cells in the presence of gliotoxin and that dysregulation of this pathway only occurs in the absence of *gliT*.

3.10 *Galleria mellonella* virulence study

Virulence of *A. fumigatus gli* mutant strains Δ*gliT*^{26933,} Δ*gliZ*^{293} and Δ*glitT*Δ*gliZ*^{293} were examined utilising the insect *G. mellonella*. Conidial inocula were injected into the left lowest proleg of a *G. mellonella* larvae weighing between 0.1 - 0.2 g using PBS injections of the same volume and non-injected larvae (n = 10/treatment) as negative controls. The larvae were monitored over a 72 hour period and checked for the onset of melanisation which is indicative of an immune response, and death.

. Figure 3.23 depicts the % survival of *G. mellonella* injected with *A. fumigatus* strains over a period of 72 hours at 37 ^{0} C.

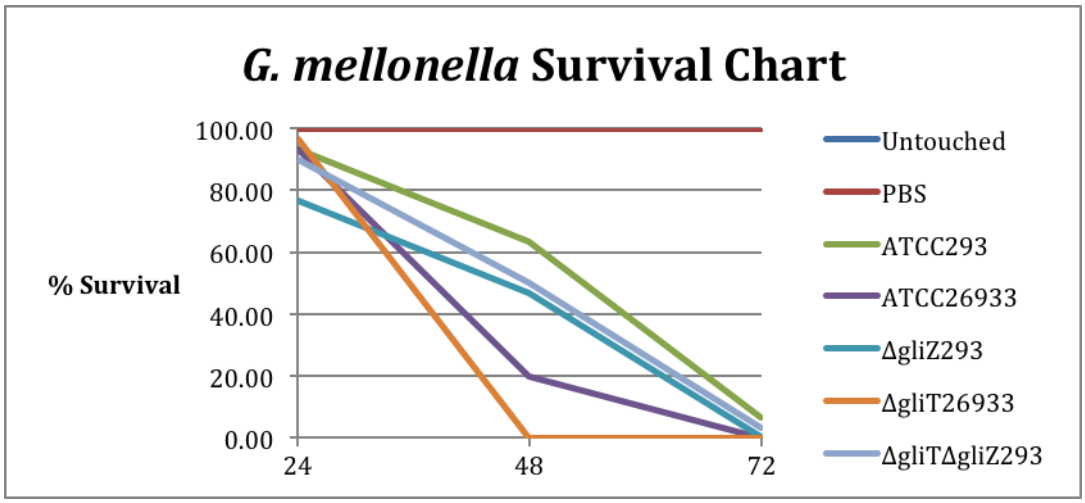

Figure 3.23 % Survival of *G. mellonella* infected with *A. fumigatus gliT, gliZ* mutants *G. mellonella* were infected with 1 x 10^{6} conidial inoculums of *A. fumigatus* strain AF293, ATCC26933, Δ*gliZ* (gliZ), Δ*gliT* (gliT) and Δ*gliT*Δ*gliZ* (gliTgliZ) respectively. Survival counts were taken at three separate time points (24, 48 and 72 hours) and the mean results of three separate infection studies were plotted.

Post 24 hours of infection there is little difference in the virulence of the *A. fumigatus* strains. Infection with *A. fumigatus* Δ$gliZ^{293}$ conidia results in significantly more (P= 0.018) death at 24 hours when compared to *A. fumigatus* AF293 wild type, and when compared with *A. fumigatus* Δ$gliT^{26933}$ (P = 0.037) at this time point. This could be due to the loss of certain *gli* cluster related proteins which are also recognition markers used by the immune response of the insect larvae, allowing for Δ*gliZ* to propagate relatively un-perturbed causing increased mortality.

After 48 hours there is a clear change in the virulence of the *A. fumigatus* strains used. *A. fumigatus* ATCC26933 infection results in a significant increase in mortality when compared with *A. fumigatus* AF293 (P = 0.011); Δ*gliZ* (P= 0.028) and Δ*gliT*Δ*gliZ*. This illustrates that ATCC26933 wild-type is more virulent than the second wild-type strain AF293, as well as the mutant strains created in this background (i.e., Δ$gliZ^{293}$ and Δ*gliT*Δ$gliZ^{293}$). Interestingly Δ*gliT* infection results in significantly more

deaths (P= 0.037) when compared with ATCC26933; Δ*gliZ* (P= 0.009) and Δ*gliT*Δ*gliZ* (P= 0.0025) indicating loss of *gliT* may be advantageous in *A. fumigatus* at this time point. Additionally it has been previously demonstrated that after 48 hours gliotoxin biosynthesis occurs *in vivo* and may explain Δ*gliZ* and Δ*gliT*Δ*gliZ* are not as virulent as other strains, especially when their wild type background (i.e. AF293) is already not very virulent when compared to ATCC26933 wild-type (Gardiner & Howlett 2005).

3.11 Discussion

Gliotoxin has been shown previously to be a highly toxic secondary metabolite (Kamei & Watanabe 2005; Carberry *et al.,* 2012). In this body of work it has been shown that alterations to the biosynthetic cluster responsible in gliotoxin biosynthesis, can significantly alter the growth response of *A. fumigatus* to exogenous gliotoxin. Inability to produce gliotoxin or encode the majority of the cluster, as is the case for Δ*gliZ* which lacks the transcriptional activator of the *gli* cluster, shows no significant increase in sensitivity when challenged with exogenous gliotoxin. This has been attributed to the fact that *gliT*, an important oxido-reductase involved in gliotoxin modification and subsequent detoxification, is independently regulated in this cluster and has been shown to still be highly up-regulated in the presence of gliotoxin (Schrettl *et al.,* 2010).

In *A. fumigatus ΔgliT* growth exposure to exogenous gliotoxin elicits hypersensitivity to concentrations as low as 5 µg/ml. This highlights GliT detoxification of gliotoxin and in the prevention of auto-toxicity. Interestingly, in *A. fumigatus* Δ*gliT*Δ*gliZ* exposure to gliotoxin elicits a sensitive growth response which is significantly greater than Δ*gliZ*, yet significantly less than Δ*gliT* respective growth response to gliotoxin. It has been hypothesised that *A. fumigatus* Δ*gliT* still may have the potential for gliotoxin biosynthesis (Schrettl *et al.,* 2010). Combined with the presence of exogenous gliotoxin, an accumulation of gliotoxin could be occurring which cannot be detoxified on account of *gliT* absence. Although Δ*gliT*Δ*gliZ,* also lacks the self protection mechanism of GliT, gliotoxin biosynthesis should be abolished Δ*gliT*Δ*gliZ* like Δ*gliZ*, suggesting why it's not as sensitive as Δ*gliT* (Bok *et al.,* 2006).

This sensitivity appears to be limited to gliotoxin and does not pre-dispose any of the *A. fumigatus gli* mutants to being sensitive to other oxidative stress inducers such as H_2O_2 or diamide. Neither of these chemicals resulted in any significant difference in the growth response for any of the *A. fumigatus* strains with the different concentrations used. This could suggest that loss of *gliT* and *gliZ* is dispensable and are not vital in the OS response to these to compounds. When *A. fumigatus* cells are exposed to gliotoxin, there is a significant rise in the presence of OS response enzymes i.e. SOD and catalase.. This increase is indicative to an increase in OS inside the cell displaying gliotoxin induction of ROS and OS. This was further visualised *in vivo* using a fluorogenic dye for the detection of ROS and found that gliotoxin did induce greater production of ROS when compared to control samples, however these were significantly less than the H_2O_2 (5 mM) treated samples, exhibiting gliotoxin induced ROS is not as great as other known ROS inducing chemicals. This further suggests that gliotoxin sensitivity observed in these strains is not due to a build up of ROS but by some other form of toxicity e.g. gliotoxin cycling and accumulation *in vivo* which results in the formation of ROS as a by-product but not a primary means of toxicity.

Previous work using other *gli* mutants, namely Δ*gliK*, illustrated a protective role for gliotoxin, depicting a dose dependent alleviation of H_2O_2 induced stress on mycelia when grown in the presence of both H_2O_2 and increasing concentration of gliotoxin (0-10 µg/ml) on agarose plates. This was corroborated in this study whereby the addition of gliotoxin (5 & 10 µg/ml) alleviated H_2O_2 induced stress (1-2 mM) in *A. fumigatus* wild-type cells only.

This anti-oxidant potential of gliotoxin was further investigated *in vivo* measuring the fluorescence of H_2DCFDA in cells exposed to gliotoxin, H_2O_2 and a combination of both in *A. fumigatus*. Here it was found that the presence of gliotoxin and H_2O_2 resulted in significantly lower fluorescence than H_2O_2 only treated mycelia confirming gliotoxin can act as an anti-oxidant in the presence of OS inducing chemicals such as H_2O_2.

In contrast to this, Δ*gliT* did not show this trend. Instead, the combination of both H_2O_2 and gliotoxin (0.5 – 2 mM + 5/10 µg/ml respectively) in agarose plates alleviated gliotoxin induced stress in this strain resulting in wild-type like growth.

Unlike the previous result which showed gliotoxin as an anti-oxidant molecule, here the opposite is happening with H_2O_2 attenuating gliotoxin toxicity in this strain by some unknown mechanism. Interestingly this same result isn't seen in either Δ*gliZ*^{293} or Δ*gliT*Δ*gliZ*^{293}which implies this H_2O_2 alleviation of gliotoxin toxicity is due to the unique phenotype of this mutant to gliotoxin exposure.

As mentioned earlier, gliotoxin may still be produced in Δ*gliT*, however its secretion is abolished, resulting in an accumulation of reduced gliotoxin *de novo*. The main reason for this is that GliT can act as both a reducing agent and oxidizing agent on gliotoxin. As only the oxidized form has been shown to readily secreted from the cell, loss of GliT mediated oxidation of reduced gliotoxin would reduce this secretion. With this in mind, it is proposed that H_2O_2 may substitute for GliT by acting as an oxidising agent. Inside the cell H_2O_2 is readily dismutated to water and oxygen, in this model this dismutation could be utilized in the presence of NADPH to form oxidized gliotoxin which can then be secreted from the cell reducing toxicity. This would predict that as the concentration of H_2O_2 increases within the cell, so would the formation of oxidized gliotoxin and thus a proportional decrease in gliotoxin induced toxicity resulting in an improved growth response which is what is seen here.

The GSH/GSSG levels were found to be altered in *A. fumigatus* Δ*gliT* which possessed significantly lower basal levels of GSH when compared with GSH measurements for *A. fumigatus* AF293 and Δ*gliZ* respectively. *A. fumigatus* Δ*gliT*Δ*gliZ* possessed intermediate levels of GSH greater than Δ*gliT* but which were still similar to *A. fumigatus* AF293 wild type and Δ*gliZ*. The altered GSH levels in Δ*gliT* and Δ*gliT*Δ*gliZ* may explain their respective sensitivity to gliotoxin exposure. This is supported by Δ*gliZ* having similar levels of GSH as AF293 as well as having a similar growth response to exogenous gliotoxin on agarose plates presumably due to the presence of GliT.

The attenuation of gliotoxin toxicity of *A.fumigatus* Δ*gliT* growth upon addition of meformin, suggests alteration of the SAM and L-methionine biosynthesis pathways is advantageous in the presence of gliotoxin for this strain. This may be due to an increase in SAM biosynthesis which could in turn result in an increase in Bm-GT formation, a putative gliotoxin detoxification by-product. This would result in a

decrease in gliotoxin toxicity by modifying available gliotoxin. However, as Schrettl *et al.*, (2010) detected no Bm-GT in culture supernatants, this may not be the case.

Instead, the presence of gliotoxin may dysregulate the SAM cycle which would result in altered levels of L-homocysteine and SAH, both which are toxic to the cell. Addition of metformin could induce L-methionine restriction, as seen in Cabreiro *et al.*, (2013) preventing accumulation of toxic SAM cycle intermediates and improving growth. As addition of metformin resulted in no significant improvement in any other *A. fumigatus* strains, it appears that this gliotoxin dysregulation is unique to Δ*gliT* implying GliT may have some role in regulating the SAM cycle, when the rest of the *gli* cluster is active, as Δ*gliT*Δ*gliZ* showed no significant improvement upon metformin addition in the presence of gliotoxin.

This body of work highlights that gliotoxin may have an alternative role in the cell, adding weight to the theory put forward of it being an accidental toxin. It is more likely gliotoxin was originally an antioxidant utilised in protecting fungus during competition with other organisms which employ the use of superoxides to kill off competitors in soil environments e.g., *Pseudomonas aeruginosa*. This is achieved by gliotoxin redox cycling which also facilitates its potent anti-fungal effects. The mechanisms of gliotoxin anti-oxidant activity, anti-fungal toxicity and the complex response of the *gli* cluster mutants examined here identify gliotoxin as a diverse multi-functional secondary metabolite which requires further investigation into its biosynthesis and how *A. fumigatus* responds to it.

Chapter 4

Proteomic analysis of *Aspergillus fumigatus gliT* and *gliZ* mutants response to gliotoxin

4.1 Introduction

Aspergillus fumigatus has been shown to be a very adaptable organism possessing the ability to occupy several different niches including the human body, utilising an array of secondary metabolites such as gliotoxin to achieve this. Since the release of the *Aspergillus* genome sequence (Mabey *et al.*, 2004; Nierman *et al.*, 2005), much study has gone into elucidating its role in pathogenesis, and as a potential anti-fungal agent (Sutton & Waring 1996; Mullbacher *et al.*, 1984).

Subsequent to the release of efficient protein extraction techniques in *Aspergillus spp.* (Scwienbacher *et al.*, 2005), proteomic studies have identified key allergens and pathogenic mechanisms involved in invasive aspergillosis which may prove to be potential drug targets (Asif *et al.*, 2006). Large scale proteomic studies have yielded large quantities of data identifying new interesting areas such as cell growth and development and response to the environment, which are important for the many *Aspergilli* which are used in the biotechnology sector (Lu *et al.*, 2010; Cagas *et al.*, 2011).

With the emergence of more accurate protein identification equipment and the availability of categorised peptide sequences on online databases, proteins are being identified under different conditions yielding a more complete picture of the proteome of this fungus.

Proteomic analysis was employed here to further assess the response to gliotoxin in wild-type *A. fumigatus*, *gliT* and *gliZ* mutants. This study also identifies the different responses to gliotoxin between *gliT* and *gliZ* mutants and highlight key components in gliotoxin tolerance which may be the cause of their respective sensitivity.

4.2 *A. fumigatus* proteomic response to exogenous gliotoxin

4.2.1 Proteomic response of AF293 to exogenous gliotoxin

AF293 mycelia were exposed to either methanol or 5 µg/ml gliotoxin for three hours. This concentration was chosen as it was sufficient to induce a transcriptome and proteome response in *A. fumigatus,* and is far closer to clinical levels than higher concentrations of gliotoxin used in other studies. Proteins extracts were separated using 2D SDS PAGE. Both sets of samples (n=3 / treatment) were compared using PROGENESIS^{TM} software package tool to identify proteins significantly differentially expressed between each condition and were later excised from the gel, treated for LC-MS identification and ran on an AGILENT Orbi Trap LC-MS to identify the resulting peptides. A total of 36 proteins were found to be significantly expressed ($P = < 0.05$) in response to exogenous gliotoxin ranging from 19 kDa to 118.5 kDa (Figure 4.1).

The presence of gliotoxin induces a complex global proteomic response with a significant decrease in expression of proteins involved in metabolism, transcription, translation and protein modification. Interestingly, expression of specific structural component associated proteins are modified in the presence of gliotoxin with a reduction (1.9 fold) in expression of the actin cytoskeleton protein Vip1p (AFUA_2G10030) and an increase (1.3 fold) in an un-characterised ORF (AFUA_6G10060) which has a putative ortholog in yeast with F-actin capping activity (Teutschbein *et al.,* 2010; Kim *et al.,* 2004). There is also reduction (1.7 fold) in AFUA_7G02180 an un-characterised ORF with orthologs in *A. nidulans* with amino acid and nucleotide sugar metabolism as well as UDP-N-acetylglucosamine pyrophosphoryase activity that catalyses the formation of UDP-N-acetyl-alpha-D-glucosamine, an important precursor utilised in the formation of the structural polysaccharide chitin (Kanehisa *et al.,* 2004; Groot *et al.,* 2009).

Three enzymes were identified to be involved in gluconeogenesis: glyceraldehyde 3-phosphate dehydrogenase GpdA (AFUA_5G01970), phosphoglycerate mutase, 2,3- bisphosphateglycerate-independant (AFUA_3G09290) and a putative enolase (AFUA_6G06770) (Sugui *et al.,* 2008; Teutschbein *et al.,* 2010). All three show a significant increase in expression (3, 1.7 and 1.2 fold respectively) in

the presence of gliotoxin. Each are also very close together in the gluconeogenesis pathway with GpdA catalysing the formation of 3-phospho-D-glycerol phosphate from glyceraldehydes 3-phosphate; phosphoglycerate mutase catalysing the formation of glycerate 2-phosphate from glycerate-3 phosphate and the putative enolase catalysing the formation of phosphoenol-pyruvate from glycerate 2-phosphate. This indicates an increase in demand of these products, which feed into L-lactate and acetyl CoA biosynthesis, during gliotoxin exposure.

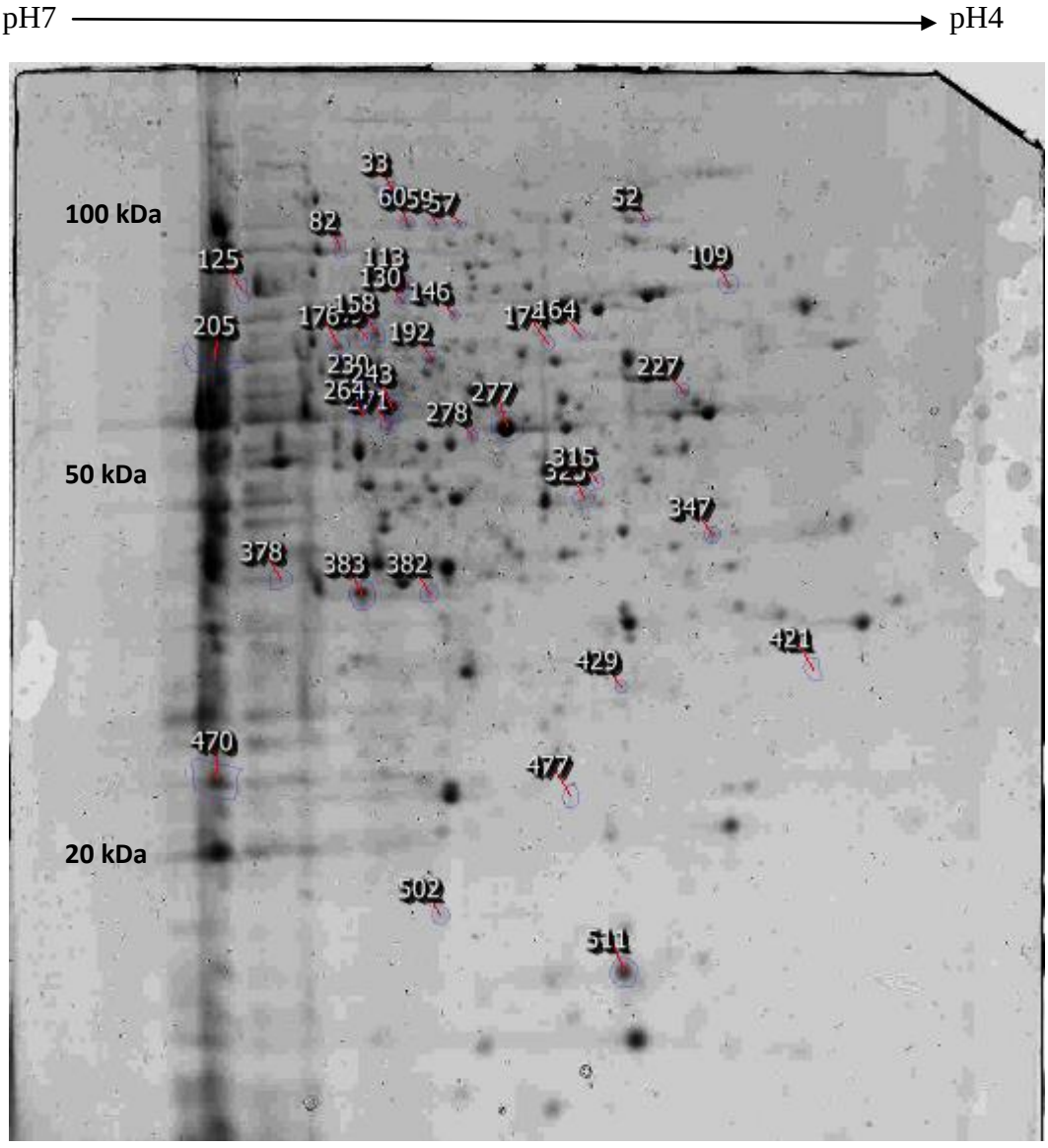

Figure 4.1 2D PAGE analysis of AF293 *A. fumigatus* + 5 µg/ml gliotoxin vs. AF293 *A. fumigatus* + MeOH, separated on pH *4-7* IPG strips on 12 % SDS-PAGE gel**.**

The function of each protein was categorised using the online software package FungiFun (https://www.omnifung.hki-jena.de/FungiFun/) which groups each protein under different categories giving the total number of proteins involved in each individual category (Figure 4.2). The five most abundant categories which can be seen include protein with binding function, metabolism, energy, cellular transport and protein fate. All 36 proteins identified can be seen in Table 4.1.

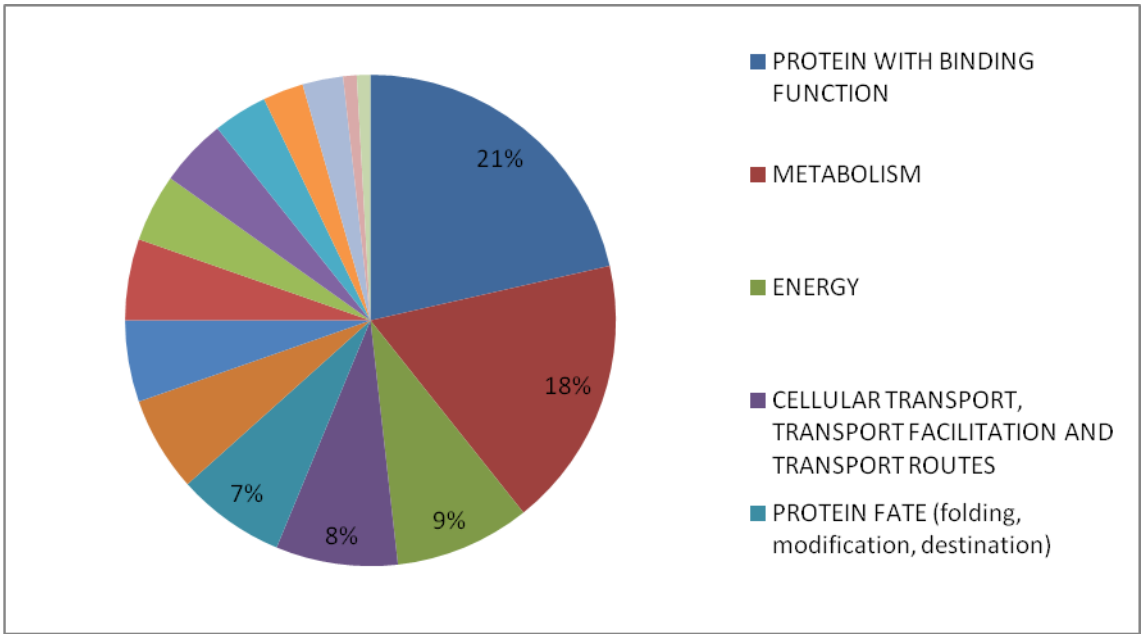

Figure 4.2 Functional categorisation of proteins differentially expressed in AF293 *A. fumigatus* +/- 5 µg/ml gliotoxin

Table 4.1 AF293 *A. fumigatus* proteins (n=36) identified differentially expressed under 5 µg/ml gliotoxin exposure

Protein Name	Fold Difference AF293	Sequence Coverage (%)	Mascot Score	Molecular Mass Da	CADRE I.D.	Spot No#
Proteins Up-regulated						
Molecular chaperone and allergen mod-e/hsp90/hsp1	↑6.6	12	284	80468	AFUA_5G04170	421
Putative transketolase	↑3.2	4	83	56773	AFUA_2G13240	125
Translation elongation factor EF-2 subunit	↑3.1	10	376	93603	AFUA_2G13530	315
Glyceraldehyde 3-phosphate dehydrogenase GpdA	↑3	19	309	36466	AFUA_5G01970	378
Xanthine-guanine phosphoribosyl transferase Xpt1	↑1.9	38	252	19551	AFUA_4G04550	477
Mitochondrial aconitate hydratase	↑1.8	18	508	85997	AFUA_6G12930	82
Phosphoglycerate mutase, 2,3 - bisphosphoglycerate-independent	↑1.7	7	141	57534	AFUA_3G09290	174
Woronin body protein HexA	↑1.5	23	415	61485	AFUA_5G08830	470

Protein Name	Fold Difference AF293	Sequence Coverage (%)	Mascot Score	Molecular Mass Da	CADRE ID	Spot No#
78 kDa glucose-regulated protein homolog	↑1.5	9	129	73414	AFUA_2G04620	109
Putative choline oxidase	↑1.4	42	767	60727	AFUA_8G04090	176
Pyruvate kinase	↑1.2	32	525	58812	AFUA_6G07430	205
Putative enolase	↑1.2	58	1028		AFUA_6G06770	277
Proteins Down-regulated						
40S ribosomal protein s0	↓5.3	30	271	32276	AFUA_3G13320	347
Polyadenylate-binding protein	↓4.6	9	296	81626	AFUA_1G04190	57
Cell division control protein 48	↓4.6	21	672	90845	AFUA_2G17110	52
Transferase Elongation Factor 3	↓3.6	15	739	118506	AFUA_7G05660	33
Polyadenylate-binding protein	↓3	18	565	81378	AFUA_1G04190	60
Ortholog of A. niger CBS 513.88	↓2.9	4	110	69482	AFUA_4G08030	130
Hydroxymethylglutaryl-CoA synthase	↓2.5	21	547	52299	AFUA_8G07210	271
Dipeptidyl peptidase	↓2.5	9	322	87569	AFUA_4G06140	113
Polyadenylate-binding protein	↓2.4	23	758	81378	AFUA_1G04190	59
Hsp70 chaperone (HscA)	↓2	5	128	66046	AFUA_8G03930	227

Protein Name	Fold Difference AF293	Sequence Coverage (%)	Mascot Score	Molecular Mass Da	CADRE ID	Spot No#
Phosphatidylinositol transporter	↓1.9	31	456	37765	AFUA_3G09910	325
Alanine amino transferase	↓1.9	19	405	55622	AFUA_6G07770	230
Translation elongation factor EF-1 alpha subunit	↓1.9	24	430	54273	AFUA_1G06390	264
Actin cytoskeleton protein (VIP1)	↓1.9	36	385	28306	AFUA_2G10030	383
Ubiquitin c-terminal hydrolase	↓1.8	4	63	63414	AFUA_6G02380	146
Eukaryotic translation initiation factor eIF-5A	↓1.8	34	348	21498	AFUA_1G04070	511
UDP-N-acetylglucosamine pyrophosphorylase	↓1.7	11	328	57048	AFUA_7G02180	192
Gamma-glutamyl phosphate reductase	↓1.6	18	341	49016	AFUA_2G07350	278
Asparagine synthetase Asn2	↓1.6	13	280	72467	AFUA_4G06900	158
Putative translation elongation factor EF-2 subunit	↓1.6	7	314	93603	AFUA_2G13530	382
Hypothetical protein	↓1.5	34	367	20344	AFUA_8G05650	502
T-complex protein 1	↓1.5	21	358	59053	AFUA_6G07540	164

Protein Name	Fold Difference AF293	Sequence Coverage (%)	Mascot Score	Molecular Mass Da	CADRE ID	Spot No#
F-actin capping protein alpha subunit	↓1.3	28	348	30519	AFUA_6G10060	429
Succinate dehydrogenase	↓1.3	2	65	70422	AFUA_3G07810	243

4.2.2 Proteomic response of Δ*gliT*^{26933} to 5 µg/ml gliotoxin

Δ*gliT*^{26933} mycelia were treated as described previously (section 4.2.1). A total of 28 proteins were identified to be significantly (P= <0.05), differentially expressed between the two treatments, ranging from 18.7 kDa to 129 kDa (figure 4.3). A full list of proteins identified can be found in Table 4.2.

Similar to AF293, the presence of exogenous gliotoxin induces the expression of proteins involved in many different functions of the cell such as cell division control, amino acid degradation and biosynthesis and RNA degradation. A number of the proteins identified are associated with Hsp70. These included mitochondrial Hsp70 chaperone (AFUA_2G09960), molecular chaperone Hsp70 (AFUA_1G07440), Hsp70 chaperone Hsp88 (AFUA_1G12610) and the Hsp70 chaperone HscA (AFUA_8G03930), all of which had reduced protein expression of 1.9, 1.5, 1.3 and 1.2 fold respectively (Asif *et al.,* 2010; Teutschbein *et al.,* 2010; Lessing *et al.,* 2007).

Two proteins, 3-isopropylmalate dehydrogenase (AFUA_1G15780) and a putative branched chain amino acid transferase (AFUA_2G10420), showed increased expression of 3.2 fold and 1.3 fold respectively in the presence of gliotoxin (Teutschbein *et al.,* 2010; Shimizu *et al.,* 2010). Both these proteins deal with amino acid biosynthesis and degradation, namely with valine, iso-leucine and leucine. 3-isopropylmalate catalyses the formation of 3-isopropylmalate to 2-isopropylmalate, this then spontaneously converts to 4-methyl-2-oxopentanoate which is acted upon by the branched chain amino acid transferase (AFUA_2G10420) and two other enzymes (AFUA_1G101680 and AFUA_4G06160) to from L-leucine (KEGG http://www.genome.jp/kegg/; Kanehisa *et al.,* 2004). These enzymes also catalyse the formation of L-isoleucine from (S)-3-methyl-2-oxopentanoate, and L-valine from 2 oxoisovalerate. All three amino acids, L-valine, L-isoleucine and L-leucine, proceed to their degradation pathway where they are degraded and converted back to 2-oxoisovalerate, (S)-3-methyl-2-oxopentanoate and 4-methyl-2-oxopentanoate respectively by AFUA_2G10420 (Kenehisa *et al.,* 2004).

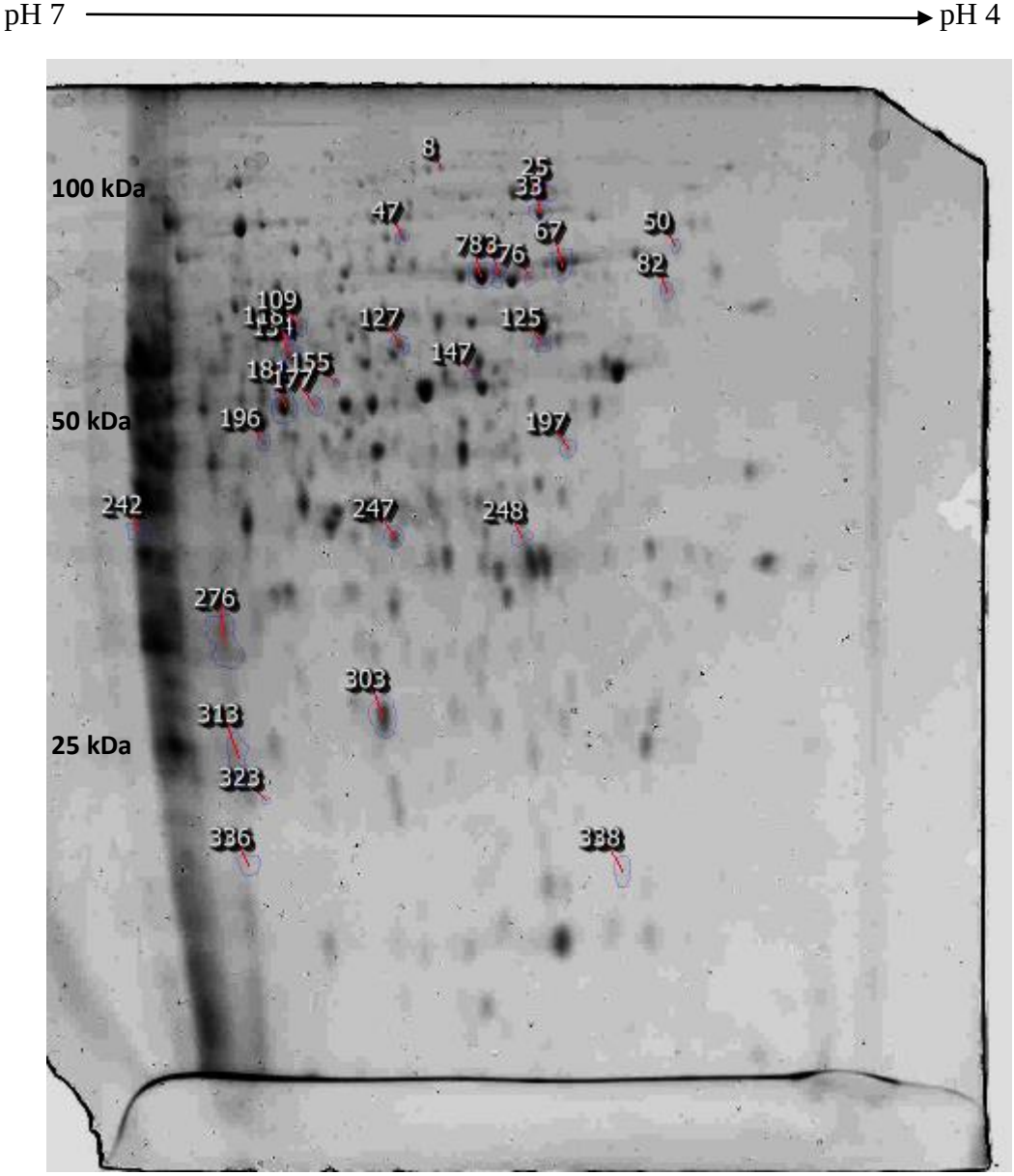

Figure 4.3 PAGE analysis of Δ*gliT*^{26933} *A. fumigatus* + 5 µg/ml gliotoxin vs. Δ*gliT*26933 *A. fumigatus* + MeOH, separated on pH *4-7* IPG strips on 12 % SDS-PAGE gel

Table 4.2 Proteins differentially expressed in the presence of 5 μg/ml gliotoxin in Δ*gliT*[26933] (n=28)

Proposed Name	Fold Difference AF293	Sequence Coverage (%)	Mascot Score	Molecular Mass Da	CADRE ID	Spot No#
Proteins Up-regulated						
40S ribosomal protein s4	↑3.7	31	325	29647	AFUA_3G06840	276
60S ribosomal protein L10	↑3.3	20	132	25860	AFUA_2G09210	313
3-isopropylmalate dehydrogenase	↑3.2	1	35	39048	AFUA_1G15780	336
Glycolipid transfer protein HET-C2	↑3	19	178	22257	AFUA_3G13820	323
Tropomyosin, putative	↑2.5	16	117	18758	AFUA_7G04210	338
Myo-inositol-phosphate synthase	↑1.8	18	381	58809	AFUA_2G01010	118
Adenosylhomocysteinase	↑1.7	26	615	49039	AFUA_1G10130	177
GPI-anchored cell wall organisation protein	↑1.5	17	261	41770	AFUA_4G06820	82
Branched chain amino acid transferase, cytosolic	↑1.3	29	600	44212	AFUA_2G10420	197
Proteins Downregulated						
Carbomyl-phosphate synthase	↓Infinite	8	308	129714	AFUA_2G10070	8

Protein Name	Fold Difference AF293	Sequence Coverage (%)	Mascot Score	Molecular Mass Da	CADRE ID	Spot No#
FAD dependant oxidoreductase	↓3.4	30	685	51468	AFUA_7G05070	155
60S ribosomal protein P0	↓2.4	16	185	33532	AFUA_1G05080	248
Cell division control protein Cdc48	↓2.2	14	538	90510	AFUA_2G17110	25
Aldehyde reductase (GliO)	↓2.1	63	893	35467	AFUA_5G02020	247
Mitochondrial Hsp70 chaperone (Ssc70), putative	↓1.9	25	760	71932	AFUA_2G09960	73
Glutamine amidotransferase:cyclamen	↓1.8	43	847	60558	AFUA_2G06230	127
Argininosuccinate synthase	↓1.7	22	498	46684	AFUA_2G04310	147
Phenylalanyl-tRNA synthetase, beta subunit	↓1.6	2	71	68016	AFUA_1G05620	47
GMP synthase	↓1.6	27	598	61799	AFUA_3G01110	109
Mitochondrial Hsp70 chaperone (Ssc70), putative	↓1.6	50	1562	71932	AFUA_2G09960	78
Triosephosphate isomerise	↓1.6	52	736	28283	AFUA_5G13450	303

Protein Name	Fold Difference AF293	Sequence Coverage (%)	Mascot Score	Molecular Mass Da	CADRE ID	Spot No#
NADH:flavin oxidoreductase/NADH oxidase family protein	↓1.5	24	420	41262	AFUA_2G04060	196
GABA Permease	↓1.5	2	16	55639	AFUA_1G12310	125
Molecular chaperone Hsp70	↓1.5	16	331	69792	AFUA_1G07440	67
Adenosylhomocysteinase	↓1.4	49	1207	49039	AFUA_1G10130	181
C6 finger domain protein	↓1.4	2	19	80854	AFUA_2G05830	134
Hsp70 chaperone Hsp88	↓1.3	35	1011	80313	AFUA_1G12610	33
Hsp70 chaperone (HscA)	↓1.2	19	347	67106	AFUA_8G03930	76

In addition, two different proteins, AFUA_2G10070 which encodes a putative carbomyl-phosphate synthase and AFUA_2G04310 which encodes argininosuccinate synthase; are both down regulated with expression of the carbomyl phosphate synthase expression being completely absent in Δ*gliT* in the presence of gliotoxin and the argininosuccinate with a 1.7 fold reduction in expression (Grosse *et al.,* 2008; Vodisch *et al.,* 2011). Both these proteins are involved in the alanine, aspartate and glutamine biosynthesis pathway with the former utilising L-aspartate for the biosynthesis of L-argininosuccinate and the latter utilising L-glutamine for the biosynthesis of carbomyl-phosphate (Kenehisa *et al.,* 2004). In keeping with this, another protein involved in the early stages of L-histidine biosynthesis was found to have reduced expression in the presence of gliotoxin (1.8 fold) and later identified as glutamine amidotransferase-cyclase (AFUA_2G04310) (Vodisch *et al.,* 2011). This enzyme is involved in a biochemical crossroads whereby it catalyses the formation of two end products: AICAR and imidazole-glycerol-3P. The former is utilised in purine metabolism while the latter continues on the L-histidine biosynthesis pathway (Meister & Buchanan, 1978). Together, these results highlight a complex response to gliotoxin affecting key amino acid biosynthesis and degradation pathways.

As seen previously in AF293 (section 4.2.1), proteins with roles in structural components of the cell are differentially expressed. Two proteins, a GPI-anchored cell wall organisation protein (AFUA_4G06820) and tropomyosin (AFUA_7G04210) showed increased expression of 1.5 fold and 2.5 fold respectively (Chabane *et al.,* 2006; Asif *et al.,* 2006). Both play a role in cell wall maintenance with the former directly involved in cell wall integrity and the latter involved in actin binding and required for actin related a key component in the fungal cell wall.

Of particular interest, adenosylhomocysteinase (AFUA_1G10130) was found to show a 1.7 fold increase in expression. An ortholog of this enzyme in yeast is involved in the cysteine and methionine biosynthetic pathway in which it hydrolyses S-adenosyl homocysteine to form L-homocysteine which can then be used as a cysteine donor in the formation of the radical scavenger glutathione or in the S-adenosyl methionine biosynthesis cycle where it is converted to form L-methionine by methionine synthase and ultimately s-adenosyl methionine (Kenhisa *et al.,*, 2004; Tehlivets *et al.,* 2004).

Dysregulated proteins were categorised according to their respective functions as described previously in section 4.2. The top five functional categories can be seen in Figure 4.4.

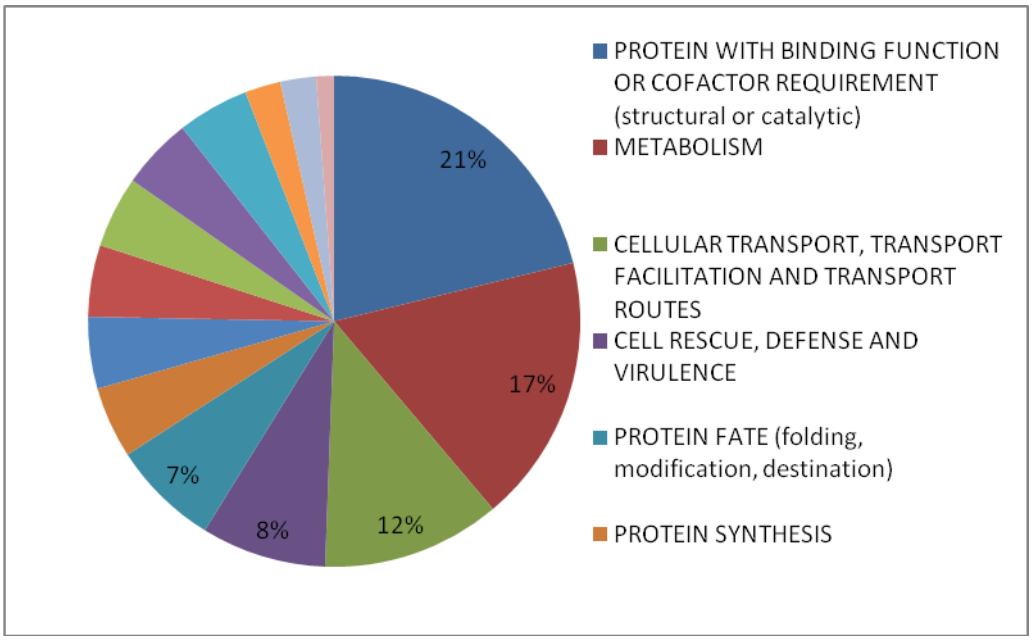

Figure 4.4 Functional categorisation of proteins differentially expressed in Δ*gliT*^{26933} *A. fumigatus* +/- 5 µg/ml gliotoxin

4.2.3 Proteomic response of Δ*gliZ*^{293} to 5 µg/ml gliotoxin

Δ*gliZ*^{293} mycelia were treated as described previously (section 4.2.1) for 2D PAGE and subsequent LC-MS analysis. In contrast a smaller number of proteins (n= 4) were found to be differentially expressed upon gliotoxin addition (Figure 4.5). These are listed in Table 4.4 below. Similarly to wild-type and Δ*gliT*, a heat shock protein was found to be differentially expressed in the presence of gliotoxin. Heat shock protein Hsp30-like (AFUA_6G06470) had a 3.7 fold increase in expression upon gliotoxin addition (Do *et al.,* 2009). Hsp30 is highly up-regulated in the cellular stress response to many types of stressors including heat shock and ethanol stress in yeast as well as being induced in the presence of hydrogen peroxide in a Yap1 dependant fashion (Seymourt & Piper 1999; Piper *et al.,* 1994; Lessing *et al.,* 2007) . Interestingly there was also an increase in expression of a putative transketolase (AFUA_1G13500, 2 fold) which has been shown to be up-regulated during heat shock and hydrogen peroxide suggesting the cell is under stress (Lessing *et al.,* 2007; Albrecht *et al.,* 2010) .

There was also increased expression of a translation elongation factor EF-2 subunit (AFUA_1G13500, 2 fold) and a conserved hypothetical protein (AFUA_1G11480, 1.5 fold) which is as yet, not characterised.

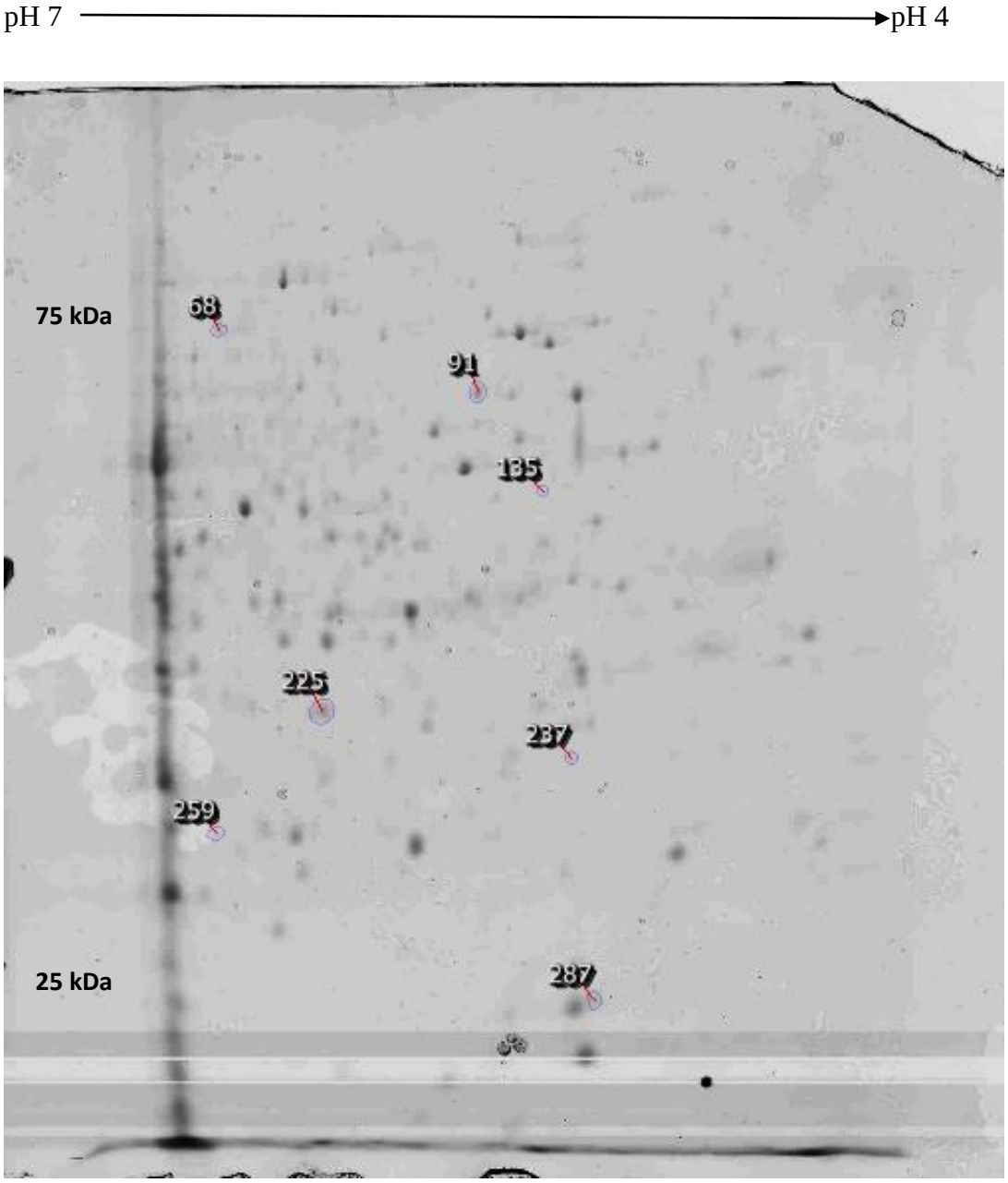

Figure 4.5 2D PAGE analysis of Δ*gliZ*^{293} *A. fumigatus* + 5 µg/ml gliotoxin vs. Δ*gliZ*^{293} *A. fumigatus* + MeOH, separated on pH *4-7* IPG strips on 12 % SDS-PAGE gel

Table 4.3 Proteins differentially expressed in the presence of 5 µg/ml gliotoxin in Δ*gliZ*^{293}

Protein Name	Fold Difference AF293	Sequence Coverage (%)	Mascot Score	Molecular Mass Da	CADRE I.D.	Spot No#
Heat shock protein Hsp30-like	↑3.7	29	185	21678	AFUA_6G06470	237
Transketolase, putative	↑2	25	475	75816	AFUA_1G13500	68
Translation elongation factor EF - 2 subunit	↑1.5	18	607	93603	AFUA_2G13530	225
Conserved hypothetical protein	↑1.5	11	111	20765	AFUA_1G11480	287

Proteins from Table 4.3 were functionally categorised as described previously (section 4.2.1). This can be seen in Figure 4.6 below. As there are only four proteins inputted, the percentage is the same amongst all categories for each protein listed..

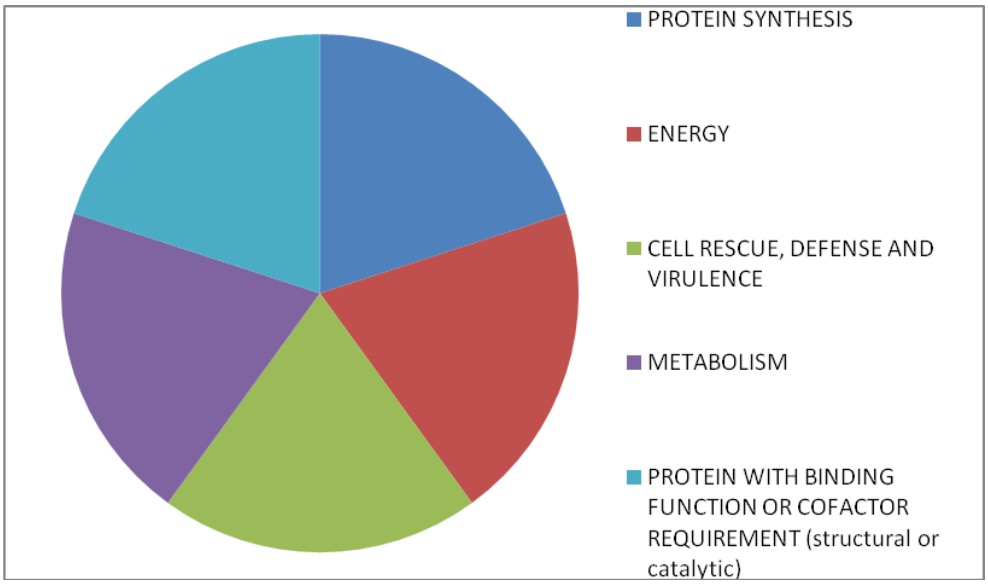

Figure 4.6 Functional categorisation of proteins differentially expressed in Δ*gliZ*^{293}*A. fumigatus* +/- 5 µg/ml gliotoxin

4.2.4 Proteomic response of Δ*gliT*Δ*gliZ*^{293} to 5 µg/ml gliotoxin

Δ*gliT*Δ*gliZ*^{293} mycelia were treated as described previously (section 4.2) for 2D PAGE and subsequent LC-MS analysis. Similar to Δ*gliZ*, a total of only five proteins were found to be differentially expressed upon gliotoxin addition (Figure 4.7). These ranged from30 kDa to 101 kDa and are listed in Table 4.5. Like the last section all the proteins identified were shown to have increased expression when challenged with gliotoxin exposure with no proteins found to have significant reduced expression in this strain in the presence of gliotoxin.

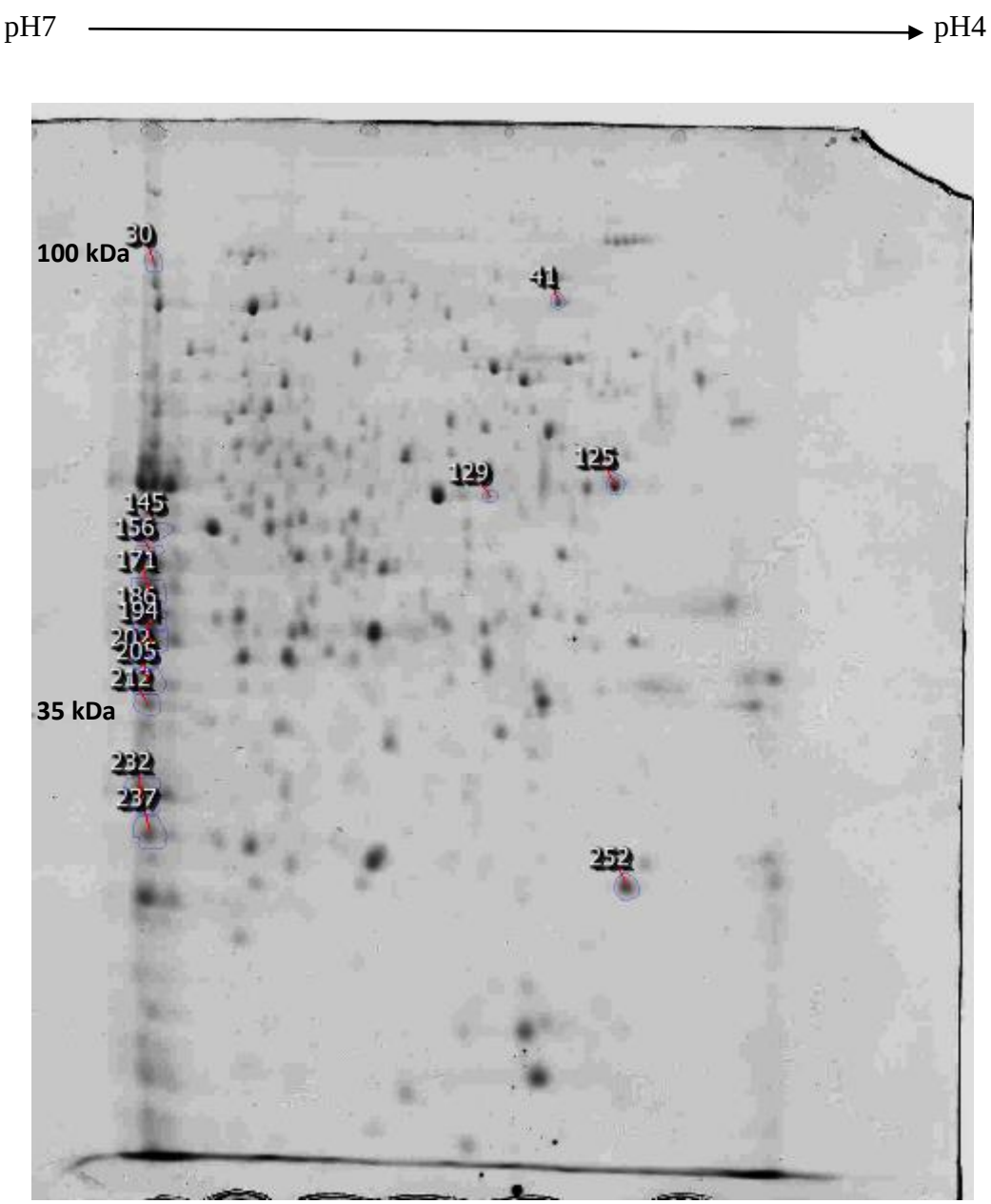

Figure 4.7 2D PAGE analysis of *ΔgliTΔgliZ*^{293} *A. fumigatus* + 5 µg/ml gliotoxin vs. Δ*gliT*Δ*gliZ*^{293} *A. fumigatus* + MeOH, separated on pH *4-7* IPG strips on 12 % SDS-PAGE gel

Two enzymes involved in TCA cycle, malate dehydrogenase (AFUA_7G05740) and malate dehydrogenase, NAD-dependant (AFUA_6G05210), had a 1.7 fold increase in expression in the presence of gliotoxin (Teutschbein *et al.,* 2010; Sugui *et al.,* 2008). Both these enzymes are involved in the same process acting on (S)-malate to form oxaloacetate or vice versa. Each of these steps lead into some form of carbohydrate biosynthesis e.g., malate is later oxidised to form fumarate which is an intermediate of the TCA cycle or citrate; while oxaloacetate is hydrated to form citrate (Kanehisa *et al.*,2004).

In contrast to previous results, this comparison shows no differential expression of any Hsp related proteins, nor any change in proteins associated with cell structure and cell wall integrity. However, similar to AF293, one protein was identified which does play a role in septum damage preventing cytoplasm leakage. Woronin body protein HexA (AFUA_5G08830) showed a 2.3 fold increase in expression when cells were challenged with gliotoxin. As discussed previously, this protein accumulates when the septum is damaged acting like a protein plug preventing cytoplasm leakage and subsequent damage to the cell (Maruyama *et al.,* 2005).

Two other proteins were identified: an outer mitochondrial membrane protein porin (AFUA_4G06910) which showed an increase in expression of 1.7 fold, and the enzyme C1 tetrahydrofolate (THF) synthase (AFUA_3G08650) which was up-regulated 1.5 fold (Grosse *et al.,* 2008). The THF synthase catalyses the formation of 5,10 methylene THF and 5,10 methenyl THF in the folate one carbon pool (Kanehisa *et al.*, 2004)

Proteins and their respective functions are listed in Table 4.4. Their functional categories can be seen in Figure 4.8.

Table 4.4 Proteins differentially expressed in the presence of 5 µg/ml gliotoxin in Δ*gliT*Δ*gliZ*[293]

Protein Name	Fold Difference AF293	Sequence Coverage (%)	Mascot Score	Molecular Mass Da	CADRE I.D.	Spot No#
C1 tetrahydrofolate synthase	↑1.5	24	778	101040	AFUA_3G08650	30
Malate dehydrogenase	↑1.7	47	753	35876	AFUA_7G05740	205
Malate dehydrogenase, NAD-dependent	↑1.7	73	955	34963	AFUA_6G05210	212
Outer mitochondrial membrane protein porin	↑1.7	32	348	30007	AFUA_4G06910	232
Woronin body protein HexA	↑2.3	25	494	61485	AFUA_5G08830	237

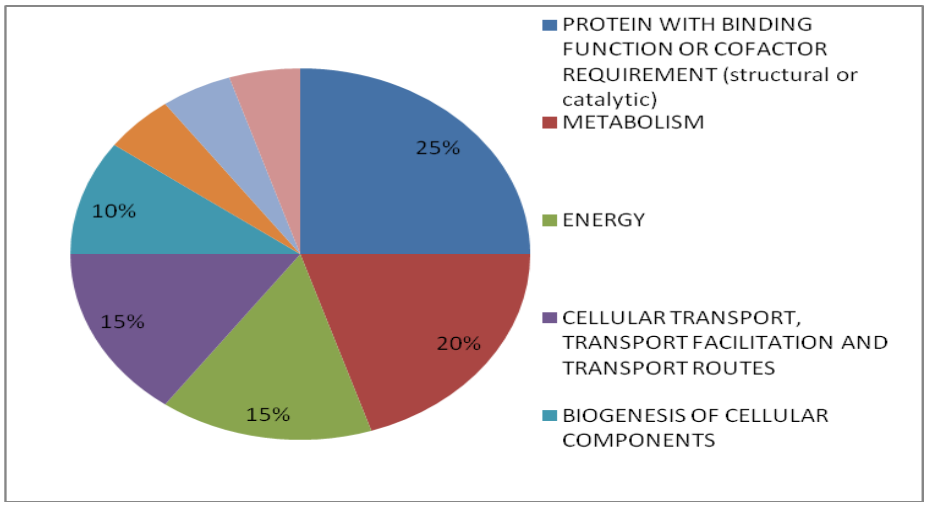

Figure 4.8 Functional categorisation of proteins differentially expressed in Δ*gliT*Δ*gliZ*^{293}*A. fumigatus* +/- 5 µg/ml gliotoxin

4.3 Discussion

This proteomic study reveals that *A. fumigatus* exposed to gliotoxin induces a plethora of effects on the cell response. Structural components of the cell, metabolic pathways and the cellular response to stress, show similar differential expression amongst all *A. fumigatus* strains exposed to gliotoxin. Further, many dysregulated proteins were found to belong to similar functional categories, suggesting similar categories in the cell being affected in each strain.

Although there are many similarities in the general aspects of the cell affected by gliotoxin exposure amongst each strain, only a number of proteins were identified in multiple strains. Cdc48 (AFUA_2G17110), is down regulated in both AF293 +/- gliotoxin and Δ*gliT*^{26933}+/- gliotoxin. (4.6 fold and 2.2 fold respectively). In *S. cerevisiae*, this protein has been shown to be involved in targeting mis-folded proteins of the endoplasmic reticulum for ubiquitination and degradation via the proteosome (Raasi & Wolf 2007). Interestingly, it has also been found to induce disassembly of the sulphur and methionine transcriptional inhibitor Met30 preventing its affect on the methionine biosynthesis pathway (Yen *et al.*, 2012). Met30 responds to s-adenosyl methionine levels in the cell, inhibiting the transcriptional regulator Met4 (Blaiseau &

Thomas 1998; Yen *et al.,* 2012) . In this model, reduced expression of Cdc 48 could result in reduced Met30 disassembly and a subsequent increase in Met30 mediated inhibition of the methionine biosynthesis pathway in the presence of elevated levels of s-adenosyl methionine.

As mentioned previously, gliotoxin can be found in a bis-methylated form (Bm-GT) where it acts as a methyl acceptor for two methyl groups to attach onto its two free thiol groups (Amitani *et al.,* 1995). For this to occur it requires a methyl donor, like SAM. With the addition of exogenous gliotoxin, there could be a corresponding increase in the SAM levels to allow for Bm-GT creation. This suggests that in Δ*gliZ* and Δ*gliT*Δ*gliZ,* loss of the *gli* cluster results in an inability to induce this increase in s-adenosyl methionine, implying some component of the *gli* cluster mediates Bm-GT formation or some step in SAM biosynthesis, and thus no reduction in Cdc48 is seen in these strains.

HscA (AFUA_8G03930) is also down regulated in AF293 +/- gliotoxin and Δ*gliT*+/- gliotoxin (2 fold and 1.2 fold respectively). As mentioned previously, this is an Hsp70 chaperone molecule with proteins orthologous in *E. coli* involved in iron-sulphur cluster assembly (Teutschbein *et al.,* 2010; Silberg *et al.,* 2013). These clusters have a myriad of roles including interacting with SAM where they transfer an electron to SAM causing reductive cleavage of the S-C (5') bond resulting in the formation of L-methionine, 5'deoxyadenosyl radical intermediate and an oxidised protein (Cosper *et al.,* 2003). This further strengthens the above point of the s-adenosyl methionine levels being altered in the presence of gliotoxin. With reduced expression of HscA and subsequent reduction of the Fe-S cluster assembly, there would be a corresponding decrease in SAM reduction. In the presence of gliotoxin, this could be a natural response to regulate levels of SAM to allow for Bm-GT formation.

A translation elongation factor EF-2 subunit (AFUA_2G13530) was identified in both AF293 +/- gliotoxin and Δ*gliZ*^{293} +/- gliotoxin. Multiple identities of this protein were found in the wild type showing both an increase and decrease in expression (3.1 fold and 1.6 fold respectively) while its expression is increased 1.5 fold in Δ*gliZ*^{293}. This protein has previously been shown to be significantly up-regulated in response to heat

stress in *A. fumigatus* and may imply gliotoxin induction of stress related proteins (Albrecht *et al.,* 2010).

Woronin body protein Hex A (AFUA_5G08830) is up-regulated (1.5 fold and 2.3 fold respectively) in both AF293 +/- gliotoxin and Δ*gliT*Δ*gliZ* +/- gliotoxin. As mentioned previously (Section 4.4) this protein acts as a protein plug preventing cytoplasmic leakage after septa cross wall damage (Maruyama *et al.,* 2005). This suggests gliotoxin presence is increasing septum damage in these two strains resulting in the HscA mediated protection. The fact that this protein was not identified in the other two mutants i.e. Δ*gliT* and Δ*gliZ* implies that either having a completely operational *gli* cluster (AF293) and a completely de-activated *gli* cluster (Δ*gliT*Δ*gliZ*) potentiates septum damage by gliotoxin presence, or these conditions allow for a septum damage response which no longer operates in the other two mutants. This is supported in Δ*gliT* where an increase in tropomyosin (AFUA_7G04210, 2.5 fold) involved in actin binding, a crucial component in cell wall and septum formation; and the increase of a GPI anchored cell wall organisation protein (AFUA_4G06820, 1.5 fold) which has been seen to be important in cell wall biogenesis and repair in yeast (Terashima *et al.,* 2000), could prove to be an alternate, less efficient, response to this type of damage induced by gliotoxin exposure.

Of the many differences seen in different proteins being differentially expressed, the clearest difference is the number of proteins identified. In both Δ*gliZ* and Δ*gliT*Δ*gliZ* only a handful of proteins were identified (n= 4 and 5 respectively) to significantly differentially expressed. This suggests that the proteomic response to gliotoxin exposure is greatly dependent on the presence of a functional *gli* cluster and that the many proteins identified in AF293 and Δ*gliT* are *gli* mediated.

Contrary to what is seen in the other three strains, AF293 shows an increase in gluconeogenesis with the identification of three gluconeogenesis related enzymes: glyceraldehyde 3-phosphate dehydrogenase GpdA (AFUA_5G01970), phosphoglycerate mutase, 2,3- bisphosphateglycerate-independant (AFUA_3G09290) and a putative enolase (AFUA_6G06770). There is also an increase in expression of a transketolase (AFUA_2G13240, 3.2 fold), an enzyme involved in the non-oxidative pentose phosphate pathway. An increase in expression of both these pathways is

indicative of cells grown in an hypoxic environment. Other hypoxic related proteins: AFUA_8G07210, AFUA_3G07810, AFUA_6G12930 and AFUA_6G06770, were also found to be differentially expressed in a similar fashion as previously seen in other hypoxic studies, implying gliotoxin maybe inducing a hypoxic environment (Blatzer *et al.,* 2011; Barker *et al.,* 2012; Vodisch *et al.,* 2011).

Δ*gliT* on the other hand does not show any correlation in the expression of the proteins identified with those differentially expressed under hypoxic environments. Nor does it have any increased expression of gluconeogenesis or any component of the pentose phosphate pathway. Instead it shows decreased expression of proteins involved in different types of metabolism e.g. AFUA_2G04310 which encodes argininosuccinate synthase an enzyme involved in the citric acid cycle, and AFUA_5G13450 which encodes triosephosphate isomerise an enzyme involved in glycolysis; are both down regulated (1.7 fold and 1.6 fold respectively). Interestingly, similar to AF293 wild-type, there appears to be an alteration in the regulation of the SAM cycle. In Δ*gliT* +/- gliotoxin, s-adenosyl homocysteinase a.k.a s-adenosyl homocysteine hydrolase (AFUA_1G10130) is both up-regulated 1.7 fold and down regulated 1.4 fold in response to gliotoxin. This enzyme catalyses the formation of L-homocysteine from SAH, which can then feed back into the SAM cycle to produce more SAM (Tehlivets *et al.,* 2004; Kenhisa *et al.,* 2004). An increase in the expression of this protein would mean a corresponding increase in L-homocysteine. This amino acid has been shown previously to be toxic to cells if it's allowed to accumulate in the cells, requiring the cell to regulate L-homocysteine levels via the formation of L-methionine (McCammon & Parks 1981; Fujita *et al.,* 2006). The presence of another s-adenosyl homocysteinase isolated from a different spot implies another isoform of this enzyme. As both appear to be the same mass, as can be seen on the gel, this suggests some form of post-translational modification which has been noted for bacterial orthologs for this enzyme which explains a difference in their respective iso-electric points (Singhal *et al.,* 2013). In the presence of gliotoxin, Δ*gliT* appears to up-regulate the SAM cycle, most likely to form Bm-GT, a process which is hypothesised to be a secondary detoxification pathway utilised by *A. fumigatus* (Li *et al.,* 2012). As this strain no longer possesses the GliT mediated detoxification mechanism, one could presume it would rely heavily on this Bm-GT alternative to compensate. Due to the hypersensitivity of this mutant to

exogenous gliotoxin, this process evidently cannot be used to fully compensate for the loss of GliT.

Δ*gliT*Δ*gliZ*^{293} +/- gliotoxin shows an increase in expression (1.5 fold) of AFUA_3G08650 which encodes C1 tetrahydrofolate synthase (THFS) an enzyme involved in the folate biosynthesis pathway which catalyses the formation of 10-formyl-THF, 5,10-methylene-THF and 5,10-methenyl-THF. The 5,10-methenyl-THF is later changed to 10-formyl-THF by THFS which can then be utilised in purine biosynthesis (Kanehisa *et al.,* 2004). 5,10-methylene-THF is irreversibly converted to 5-methyl THF which feeds into the methionine biosynthesis pathway to form methionine along with l-homocysteine. This could hint at a similar change in the SAM cycle in this strain, requiring increased L-methionine production from intermediates derived from the folate biosynthesis pathway for Bm-GT production.

Contrary to a previous study carried out in ATCC26933 *A. fumigatus* + gliotoxin, AFUA_2G10030 is down regulated in AF293 (1.9 fold). Also, many of the proteins identified in that study were not identified here (Carberry *et al.,* 2012). A possible explanation for this difference is the concentration of gliotoxin used was far greater in the Carberry *et al.,* study (14 µg/ml) compared to 5 µg/ml used in this study, suggesting greater gliotoxin concentrations are required to induce differential expression of particular proteins (Carberry *et al.,* 2012).

The major finding from this study is the up-regulation of components of the methionine/SAM biosynthetic pathways in the presence of gliotoxin. This suggests gliotoxin influences the SAM and methionine cycle by influencing the levels of SAM for its own Bm-GT modification.

4.4 *gliZ, gliT* mutant proteomic response to gliotoxin compared to AF293

In the previous section, the protein response to gliotoxin in cells treated with gliotoxin was compared with cells treated with a solvent control. This gives an insight into the individual response that a particular strain has when challenged with gliotoxin compared with a control condition and how this may differ in other strains. In this

section, mutant control strains and gliotoxin biosynthesis mutant strains are compared to AF293 to see how the proteome differs further between wild-type and mutant, something which has not been done before for these *gli* gene deletions. This allows the assessment of key differences at the protein level in wild-type versus mutant and allows common trends to emerge which may further elucidate the range in sensitivity seen in *gliT* and *gliZ* mutants when compared to AF293 to gliotoxin.

4.4.1.1 Δ*gliT* vs. AF293

As described in section 4.2.1, mycelia of AF293 and Δ*gliT*^{26933} were exposed to either MeOH or 5 µg/ml gliotoxin and proteins were extracted. Protein gels were analysed using Progenesis^{TM} software package and AF293 + MeOH gels (n=3) and Δ*gliT* + MeOH gels (n=3) were compared. Differentially spots were identified and excised from the gel. Spots were trypsin digested and resulting peptides identified using LC-MS peptide identification.

A total of 62 spots were identified between the two treatments (Figure 4.9 A & B). 39 spots were isolated from MeOH treated cells (Figure 4.9 A), 23 from gliotoxin treated cells (Figure 4.9 B) of which 6 were found to be in both, ranging in size from 24 kDa to 129.5 kDa. A list of all proteins identified in MeOH treated cells can be found in table 4.5. In the MeOH treated cells, four enzymes involved in carbohydrate metabolism/biosynthesis were identified. Aldehyde reductase (AFUA_5G02020) had an increase of 6.2 fold in Δ*gliT* + MeOH when compared to AF293 + MeOH. Fructose-biphosphate aldolase (AFUA_3G11690) was identified twice from two different spots indicating two different isoforms also showed increased expression in Δ*gliT* + MeOH compared to AF293 + MeOH of 1.6 and 1.5 fold respectively. Both these enzymes are involved in fructose and mannose metabolism. Similarly, glycerol dehydrogenase (AFUA_5G02020), which is involved in carbohydrate metabolism and transaldolase (AFUA_5G09230), which is involved in the pentose phosphate pathway, showed an increase in protein expression in Δ*gliT* vs. AF293 of 5.8 fold and 1.4 fold respectively.

There is also a decrease in expression in two enzymes involved in amino sugar and nucleotide sugar metabolism. N-acetylglucosamine-phsophate mutase

(AFUA_1G06210) and UDP-N-acetylglucosamine (AFUA_7G02180) showed 3 fold and 1.7 fold decrease in expression respectively in Δ*gliT* vs AF293 + MeOH cells, and orthologs of these enzymes have been seen to be involved in chitin formation (Groot *et al.*, 2009).

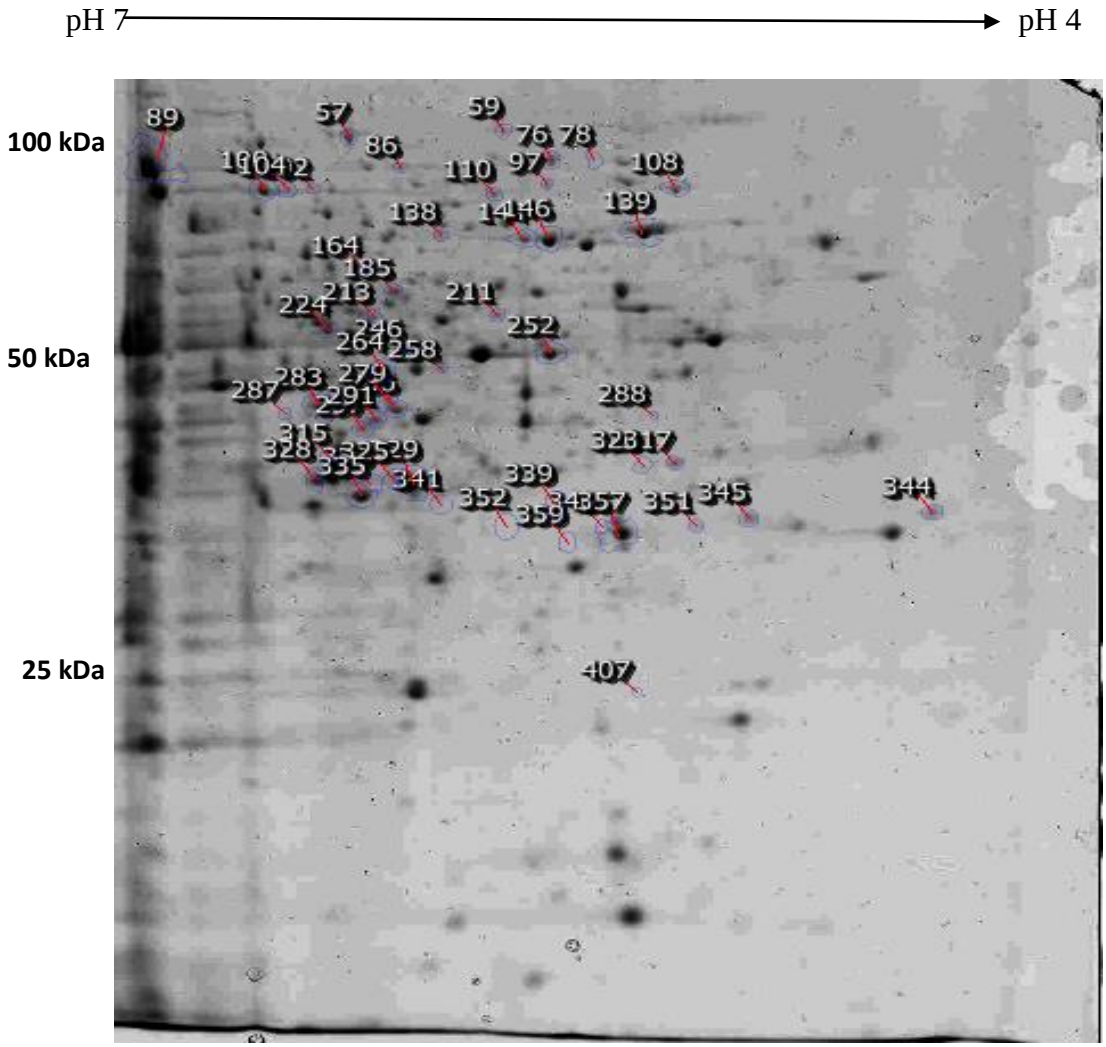

Figure 4.9 A 2D SDS PAGE analysis of Δ*gliT*^{26933} *A. fumigatus* + MeOH vs. AF293 *A. fumigatus* + MeOH, separated on pH 4-7 IPG strips on 12 % SDS-PAGE gel

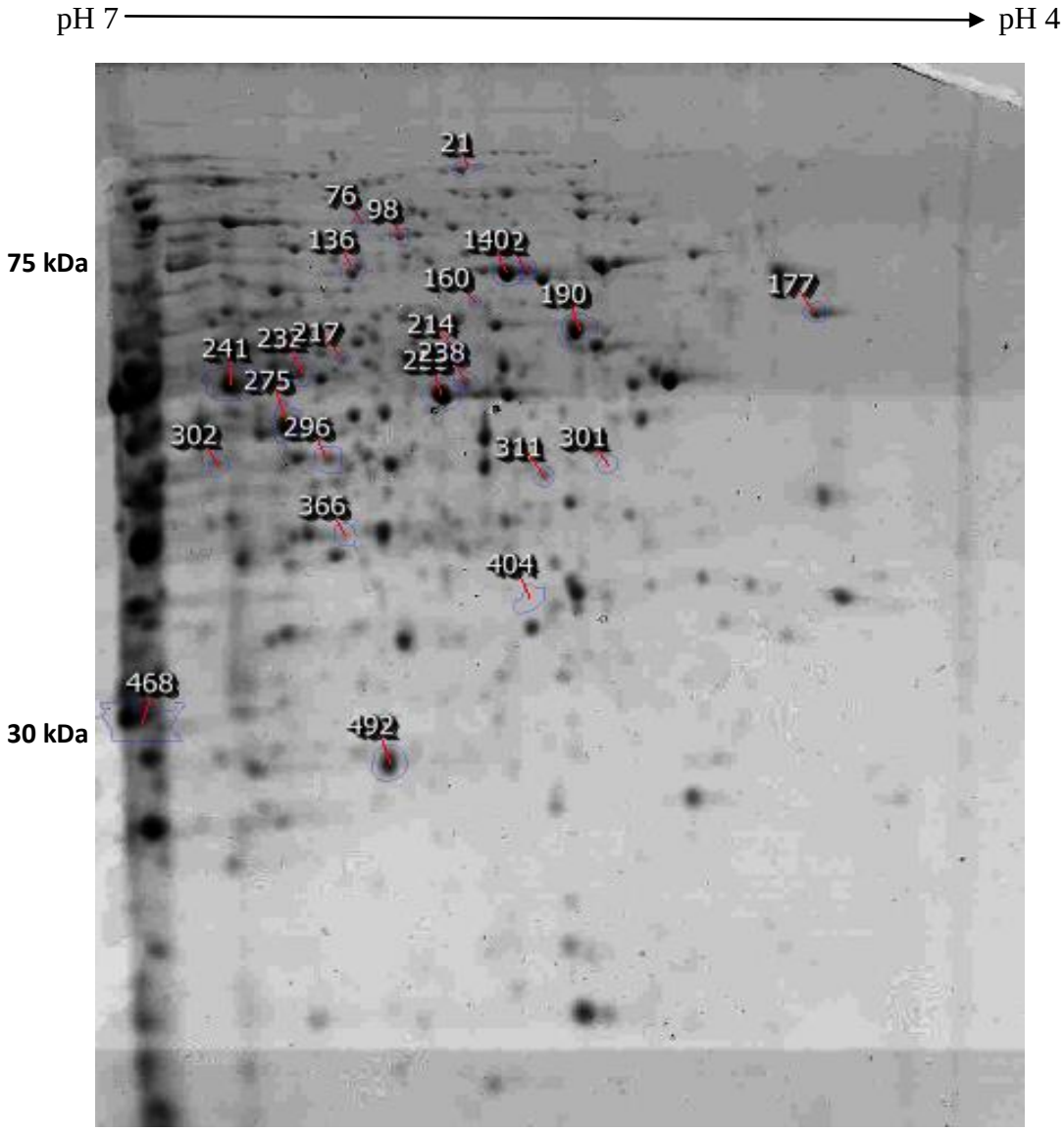

Figure 4.9 B 2D SDS PAGE analysis of Δ*gliT*^{26933} *A. fumigatus* + 5 µg/ml gliotoxin vs. AF293 *A. fumigatus* + 5 µg/ml gltioxin, separated on pH 4-7 IPG strips on 12 % SDS-PAGE gel

Table 4.5 Proteins differentially expressed in the presence in Δ*gliT*^{26933} vs AF293 in the presence of MeOH

Protein Name	MeOH	Sequence Coverage (%)	Mascot Score	Molecular Mass Da	CADRE I.D.	Spot No#
Proteins Up-regulated						
Pyrathiamine resistance gene, thiA	↑16.6	24	351	35309	AO090003000090	352
Pyrathiamine resistance gene, thiA	↑14.3	17	338	35309	AO090003000090	359
Aldehyde Reductase (GliO)	↑6.2	40	833	35467	AFUA_5G02020	341
Pyrathiamine resistance gene, thiA	↑6	18	283	35309	AO090003000090	346
Pyrathiamine resistance gene, thiA	↑5.9	24	394	35309	AO090003000090	339
Glycerol dehydrogenase	↑5.8	31	660	37037	AFUA_4G11730	330
RAS small monomeric GTPase RasA	↑4.5	5	69	24292	AFUA_5G11230	407
12-oxophytodienate Reductase	↑4.1	22	399	46359	AFUA_5G14330	287
NADH:flavin oxidoreductase	↑3.5	19	280	41262	AFUA_2G04060	288
Kelch Repeat Domain	↑3.3	12	130	35955	AFUA_5G12780	320
Inorganic diphosphatase	↑1.7	9	96	43886	AFUA_3G08380	357

Protein Name	MeOH	Sequence Coverage (%)	Mascot Score	Molecular Mass Da	CADRE I.D.	Spot No#
Mitochondrial Processing Peptidase Beta Subunit	↑1.6	10	336	53295	AFUA_1G14200	252
Fructose-biphosphate Aldolase	↑1.6	15	461	39952	AFUA_3G11690	329
Glutamate/Leucine/Valine/Phenylalanine dehydrogenase	↑1.5	35	634	49627	AFUA_4G06620	264
Fructose-biphosphate Aldolase	↑1.5	7	163	39952	AFUA_3G11690	325
14-3-3 Family protein	↑1.5	38	430	30201	AFUA_6G06750	345
Hsp 70	↑1.4	16	331	69792	AFUA_1G07440	139
Transaldolase	↑1.4	42	830	35601	AFUA_5G09230	335
Proteins Down-regulated						
Mycelial catalase, Cat1	↓9.7	4	106	79925	AFUA_3G02270	110
Transferase elongation Factor eEF-3	↓4.8	15	739	118506	AFUA_7G05660	57
Kelch repeat domain	↓4.5	26	490	35955	AFUA_5G12780	317
N-acetylglucosamine-phosphate mutase	↓3	18	411	61825	AFUA_1G06210	164
WW domain protein	↓2.9	23	261	35467	AFUA_5G03750	344
FAD dependant oxidoreductase	↓2.7	19	462	51468	AFUA_7G05070	246

Protein Name	MeOH	Sequence Coverage (%)	Mascot Score	Molecular Mass Da	CADRE I.D.	Spot No#
Lysophospholipase Plb3	↓2.6	10	226	67839	AFUA_3G14680	76
Mannitol-l-phosphate dehydrogenase	↓2.5	12	193	43093	AFUA_2G10660	286
Hsp90	↓2	14	259	50550	AFUA_5G04170	108
Glycerol dehydrogenase	↓1.9	38	660	37037	AFUA_4G11730	328
Peptidyl-prolyl cis-trans Isomerase Cpr7	↓1.8	27	374	41956	AFUA_2G02050	291
UDP-N-acetylglucosamine pyrophosphorylase	↓1.7	11	328	57048	AFUA_7G02180	185
NADH ubiquinone oxidoreductase	↓1.6	25	193	27525	AFUA_2G10600	351
Translation elongation factor Ef-2 subunit	↓1.4	39	1372	93603	AFUA_2G13530	89
Translation elongation factor EF-Tu	↓1.2	21	451	46430	AFUA_1G12170	283

Three proteins involved in translation were identified: translation elongation factor EF-3 (AFUA_7G05660), translation elongation factor EF-2 subunit (AFUA_2G13530) and translation elongation factor EF-Tu (AFUA_1G12170) all had decreased protein expression compared to AF293 (4.8, 1.4 & 1.2 fold respectively). Each of these subunits and elongation factors are involved in some part of protein synthesis, EF-Tu is involved in protein elongations where it binds GTP and aminoacyl-tRNA; EF-2 and 3 subuints are involved in ribosomal translocation during protein synthesis. A list of all proteins identified and their respective fold differences in Δ*gliT* compared to AF293 + MeOH can be seen in Table 4.5. There are also four spots isolated as the same protein, the pyrathiamine resistance gene from *A. oryzae* which was used in Schrettl *et al.,* to knock out the *gliT* gene, which explains why it is so highly up-regulated. The fact it was isolated numerous times suggests different isoforms of the resistance marker being produced in this strain.

From Table 4.6, gliotoxin treated cells show a decrease in the expression of proteins involved in glycolysis and gluconeogensis; SAM cycle and amino acid biosynthesis. Aldehyde dehydrogenase (AFUA_4G08600), enolase Asp F22 (AFUA_6G06770) and triosephosphate isomerase (AFUA_5G13450) are all involved in the glycolysis/gluconeogenesis pathway and have reduced expression in Δ*gliT* gliotoxin challenged cells 1.8, 1.8 and 1.5 fold respectively. In addition to this, there is a corresponding decrease in expression (4.3 fold) of β-D-glucoside glucohydrolase (AFUA_7G06140), an enzyme involved in the biosynthesis of β-D-glucose and α-D-glucose from starch, suggesting a reduction in the production of simple carbon sugars such as glucose from complex carbohydrates in Δ*gliT*, when compared to AF293.

Certain amino acid biosynthesis enzymes are also down regulated, with the predicted branched chain amino acid amino-transferase (AFUA_2G10420), previously described in section 4.2.2, involved in valine/leucine and isoleucine biosynthesis, showing a 2.1 fold decrease in expression in Δ*gliT* + gliotoxin cells (Kispal *et al.,* 1996). Additionally, there is a corresponding 1.4 fold decrease in iso-valeryl-CoA dehydrogenase (AFUA_5G08930) which is involved in valine/leucine and isoleucine.

Table 4.6 Proteins differentially expressed in the presence in Δ*gliT*^{26933} vs. AF293 in the presence of 5 µg/ml gliotoxin

Protein Name	Gliotoxin	Sequence Coverage (%)	Mascot Score	Molecular Mass Da	CADRE I.D.	Spot No#
Proteins Up-regulated						
Thiazole synthase	↑4.4	16	287	35309	AFUA_6G08360	404
Class V Chitinase	↑2.6	11	146	49440	AFUA_3G11280	301
Argininosuccinate Synthase	↑1.6	32	763	46684	AFUA_2G04310	238
Outer Mitochondrial Membrane Protein Porin	↑1.5	73	758	30007	AFUA_4G06910	468
Proteins Down-regulated						
β-D-Glucoside Glucohydrolase	↓4.3	9	202	78738	AFUA_7G06140	76
Translation Elongation Factor Ef-1 Alpha	↓3.6	16	312	54273	AFUA_1G06390	241
Protein Disulfide Isomerase PdiI	↓2.9	35	709	56500	AFUA_2G06150	177
Acyl Co-A Dehydrogenase	↓2.8	18	293	47540	AFUA_1G14850	311
Branched Chain Amino Acid Amino-Transferase	↓2.1	29	600	44212	AFUA_2G10420	302
Enolase Asp F22	↓1.8	53	1662	47392	AFUA_6G06770	53

Protein Name	Gliotoxin	Sequence Coverage (%)	Mascot Score	Molecular Mass Da	CADRE I.D.	Spot No#
Vacular ATP Synthase Catalytic Subunit A	↓1.8	42	1043	75329	AFUA_5G02370	136
Aldehyde Dehydrogenase	↓1.8	34	573	60254	AFUA_4G08600	214
Adenosylhomocysteine	↓1.7	49	1207	49039	AFUA_1G10130	275
Metallopeptidase, MepB	↓1.6	25	564	82046	AFUA_7G05930	98
Triosephosphate Isomerase	↓1.5	52	736	28283	AFUA_5G13450	492
Isovaleryl-CoA Dehydrogenase lvdA	↓1.4	38	936	50784	AFUA_5G08930	296
Antigenic Mitochondrial Protein Hsp60	↓1.3	51	1511	62086	AFUA_2G09290	190

The thiazole synthase enzyme, (AFUA_6G08360) was seen to have a 4.4 increase in expression in Δ*gliT* cells after addition of gliotoxin when compared to AF293. This enzyme is involved in the biosynthesis of the B_1 vitamin, thiamine, and has been demonstrated to have roles in carbohydrate and amino acid catabolism in yeast (Praekalt *et al.*, 1992 & 1994)

S-adenosyl homocysteinase (AFUA_1G10130) is down regulated in Δ*gliT* cells exposed to gliotoxin 1.7 fold. Previously in section 4.3 table 4.2, this enzyme was shown to be dysregulated in *ΔgliT* + gliotoxin when compared to Δ*gliT* + MeOH This result further illustrates that in Δ*gliT*, this enzyme is significantly dysregulated in response to gliotoxin exposure when compared to Δ*gliT* + MeOH or wild type + gliotoxin cells.

A total of six differentially expressed proteins were found to be shared between the two treatments (Table 4.6). Ssc 70 was identified twice in each treatment, isolated from different spots indicating multiple isoforms being differentially expressed. Multiple isoforms has been described previously in *S.cerevisiae* for this Hsp70 chaperone located in the mitochondrion, whereby the functional redundancy among such molecules has resulted in single isoforms of this class of chaperone proteins to be generalised as the function of others (Sharma & Masison 2008). This protein is up-regulated in Δ*gliT* + MeOH vs. AF293 +MeOH 2 and 1.9 fold, yet it's down-regulated in Δ*gliT* + gliotoxin vs. AF293 + gliotoxin 1.3 and 1.9 fold. Ssc 70 is a mitochondrial Hsp 70 chaperone, which is involved in many housekeeping roles in the cell including protein folding or proof reading of newly synthesised proteins (Mayer & Bukau 2005).

In both conditions, there is increased expression of Nmt1, a thiamine biosynthesis protein, 1.7 fold in MeOH treated cells and 3.6 fold in gliotoxin treated cells. As mentioned, thiamine is a B_1 vitamin with a role in sugar and amino acid catabolism. Added to the thiazole synthesis protein (AFUA_6G08360) which is only found to be up-regulated in Δ*gliT* + gliotoxin vs. AF293 + gliotoxin cells, suggests a

greater demand in the biosynthesis of this cofactor in gliotoxin treated cells lacking *gliT*.

Table 4.6 Proteins differentially expressed in Δ*gliT*^{26933} vs. AF293 in the presence of MeOH and 5 µg/ml gliotoxin

Protein Name	MeOH	Gliotoxin	Sequence Coverage (%)	Mascot Score	Molecular Mass Da	CADRE I.D.	Spot No#
Ssc 70	↑2	↓1.3	14/50	478/1562	74478	AFUA_2G09960	144/140
Ssc 70	↑1.9	↓1.9	18/43	666/1049	74478	AFUA_2G09960	146/142
Nmt1	↑1.7	↑3.6	16/30	130/455	38588	AFUA_5G02470	315/366
ATP Citrate Lyase Subunit (ACL)	↑1.2	↓1.6	37/43	723/952	53001	AFUA_6G10660	224/232
Carbomyl phosphate synthase, large subunit	↓3.1	↓7.7	05/11	201/366	129714	AFUA_2G10070	59/21
Succinyl-CoA:3ketocoid-coenzyme A transferase	↓2	↓1.7	26/37	488/666	55815	AFUA_6G12250	213/217

There is also a corresponding decrease in the expression of carbomyl phosphate synthase (AFUA_2G10070) 3.1 fold in MeOH treated cells and 7.7 fold in gliotoxin treated cells and succinyl CoA (AFUA_6G12250) 2 fold in MeOH treated cells and 1.7 fold in gliotoxin treated cells. The former is involved in pyrimidine metabolism, notably in the utilisation of l-glutamine to form carbomyl-phosphate, while the latter is involved in valine/leucine and isoleucine degradation.

The top five functional categories can be seen in Figure 4.10 A (MeOH) and B (gliotoxin) in Δ*gliT* vs. AF293 +/- gliotoxin treated cells.

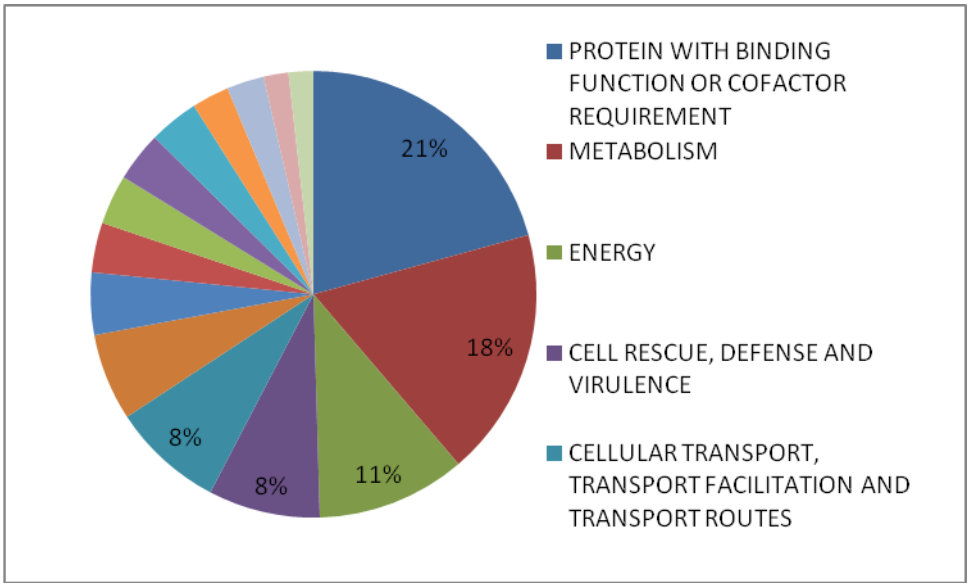

Figure 4.10 (A) Functional categorisation of proteins differentially expressed in Δ*gliT*[26933] *A. fumigatus* vs. AF293 *A. fumigatus* + MeOH.

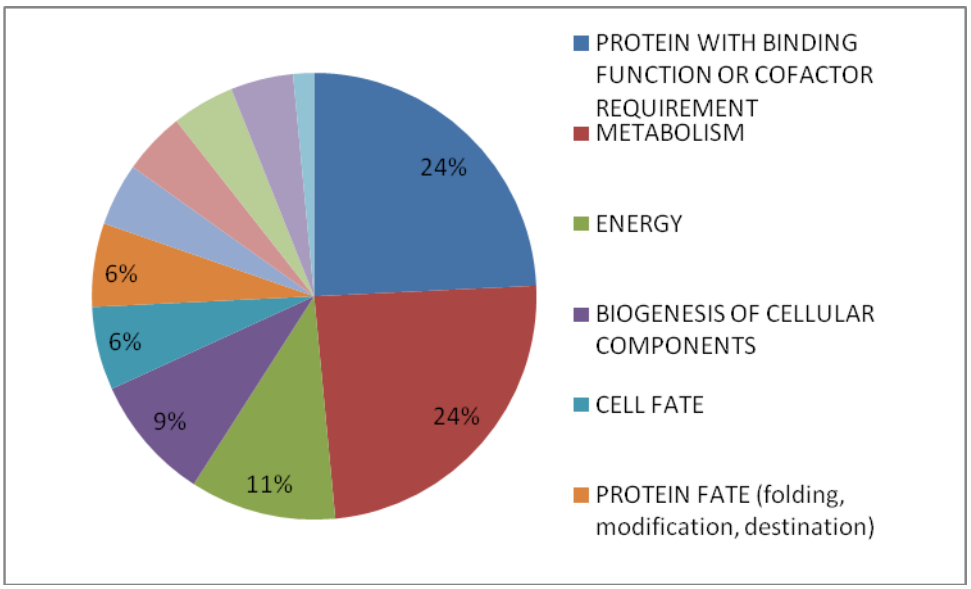

Figure 4.10 (B) Functional categorisation of proteins differentially expressed in Δ*gliT*^{26933}*A. fumigatus* vs. AF293 *A. fumigatus* + 5 µg/ml gliotoxin.

4.4.1.2 Discussion

When comparing the proteome of Δ*gliT* + MeOH and AF293 + MeOH, there are many differences highlighting some of the many consequences of *gliT* loss. Some of the most prominent differences seen in this comparison are the changes in the expression of metabolic related proteins such as an increase in fructose and carbohydrate metabolism with two isoforms of fructose-biphosphate (AFUA_3G11690), aldehyde reductase (AFUA_5G02020) and glycerol dehydrogenase (AFUA_4G11730). Coupled with an increase in proteins which have orthologs with roles in filamentous growth and putative association with actin a major component of cell structure; RasA (AFUA_5G11230) and a kelch repeat protein (AFUA_5G12780), there may be a change in the growth rate between these two strains, or at least in their response to growth thus a need for increased energy creation from certain carbohydrate (Som & Kolaparthit 1994; Arellano *et al.*, 2002) .

Proteins typically associated with the cellular response to stress, most notably mycelial catalase Cat1 (AFUA_3G02270) which had a 9.7 fold decrease in expression and also Hsp90 (AFUA_5G04170). Both these proteins play a role in the cellular response to stress, with the former being directly involved in the cellular oxidative stress response and the latter involved in cell wall integrity and shown previously to be induced in response to H_2O_2 presence (Calera *et al.,* 1997; Lamoth *et al.,* 2012; Fraczek *et al.,* 2010). This suggests that loss of *gliT* induces represses this particular catalase and perhaps Hsp 90. One explanation for this could be due to some reactive intermediates being produced in the *gli* cluster which could be having some form of anti-oxidant function. Interestingly, Cat1 was previously shown to have a significant reduction in expression (> 40 fold) in *A. fumigatus* upon gliotoxin challenge, due to gliotoxin anti-oxidant capability making expression of this catalase redundant (Carberry *et al.,* 2012). However in this body of work, this protein is only found to be differentially expressed when Δ*gliT* is compared to AF293 in the absence of gliotoxin. This suggests that the levels of this enzyme are un-altered in Δ*gliT* compared to AF293 in the presence of gliotoxin which could imply that in the absence of gliotoxin the need for Cat1 is reduced in this strain, perhaps due to some form of redundancy.

When exposed to gliotoxin, there is a decrease in the expression of enzymes involved in glycolysis/gluconeogenesis (AFUA_5G13450, AFUA_4G08600, AFUA_6G06770), as well as proteins involved in translation and protein processing (AFUA_1G06390, AFUA_2G06150) and amino acid biosynthesis/degradation (AFUA_5G08930, AFUA_2G10420), which is indicative of cell undergoing stress (Sha *et al.,* 2013; Harding *et al.,* 2003). The decrease in expression of S-adenosyl homocysteinase in the presence of gliotoxin further highlights the relationship of gliotoxin and the SAM cycle and suggests a putative role of L-homocysteine accumulation and gliotoxin toxicity.

4.4.2.1 Δ*gliZ*^{293} vs. AF293

Cells from AF293 and Δ*gliZ*^{293} were treated as described previously (section 4.4.1.1). A total of 60 protein spots were identified as being significantly (P = < 0.05)

altered in expression between the two comparisons (Δ*gliZ* + MeOH vs. AF293 + MeOH and Δ*gliZ* + 5 µg/ml gliotoxin vs. AF293 + 5 µg/ml gliotoxin. Of these 61 proteins, 32 were identified from MeOH treated cells (Figure 4.11 A), 29 from gliotoxin treated cells (Figure 4.11 B) with 11 identified to be in common. These ranged from 18 kDa to 106.6 kDa in size. A list of all identified proteins found in MeOH treated cells can be found in Table 4.7.

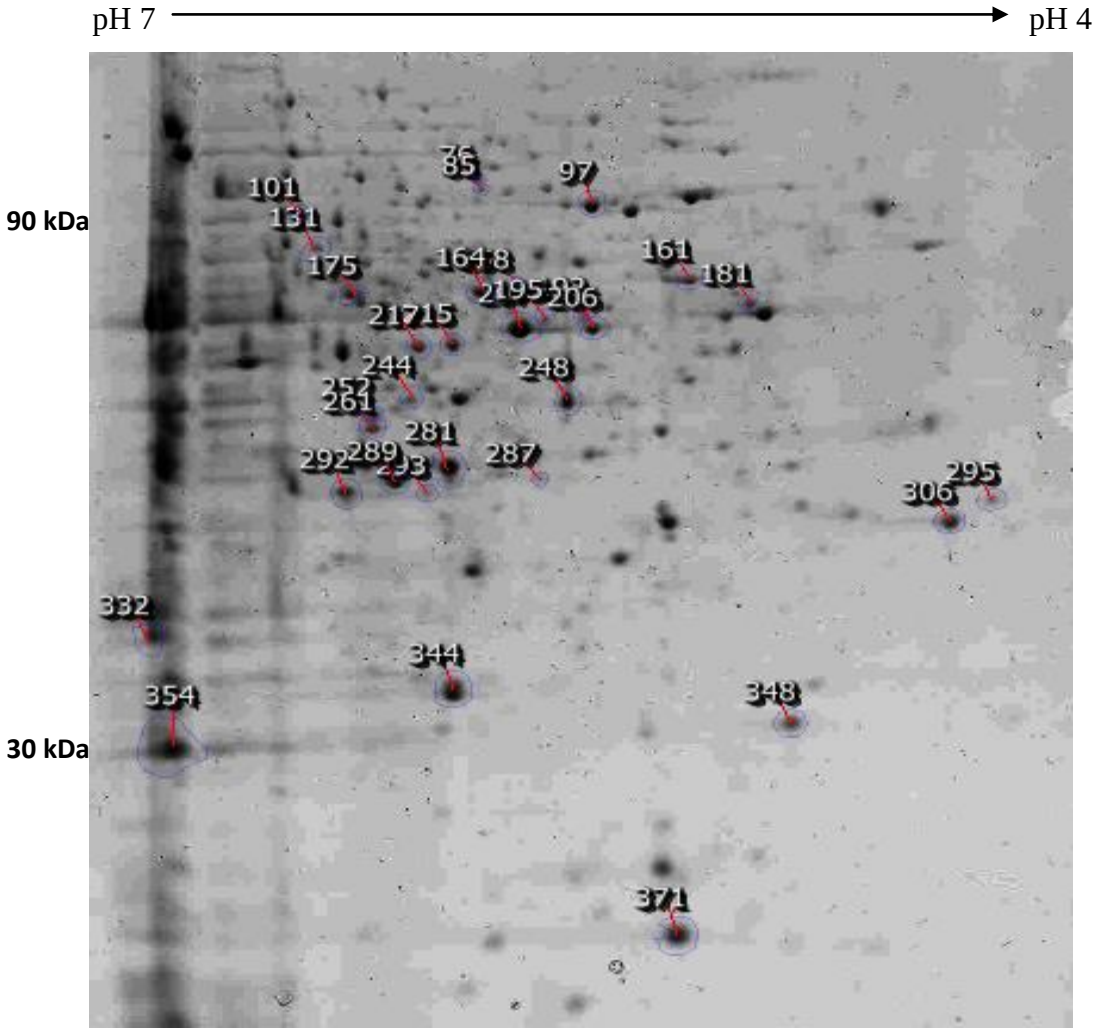

Figure 4.11 A 2D PAGE analysis of Δ*gliZ*[293]A. *fumigatus* + MeOH vs. AF293 *A. fumigatus* + MeOH, separated on pH 4-7 IPG strips on a 12 % SDS-PAGE gel

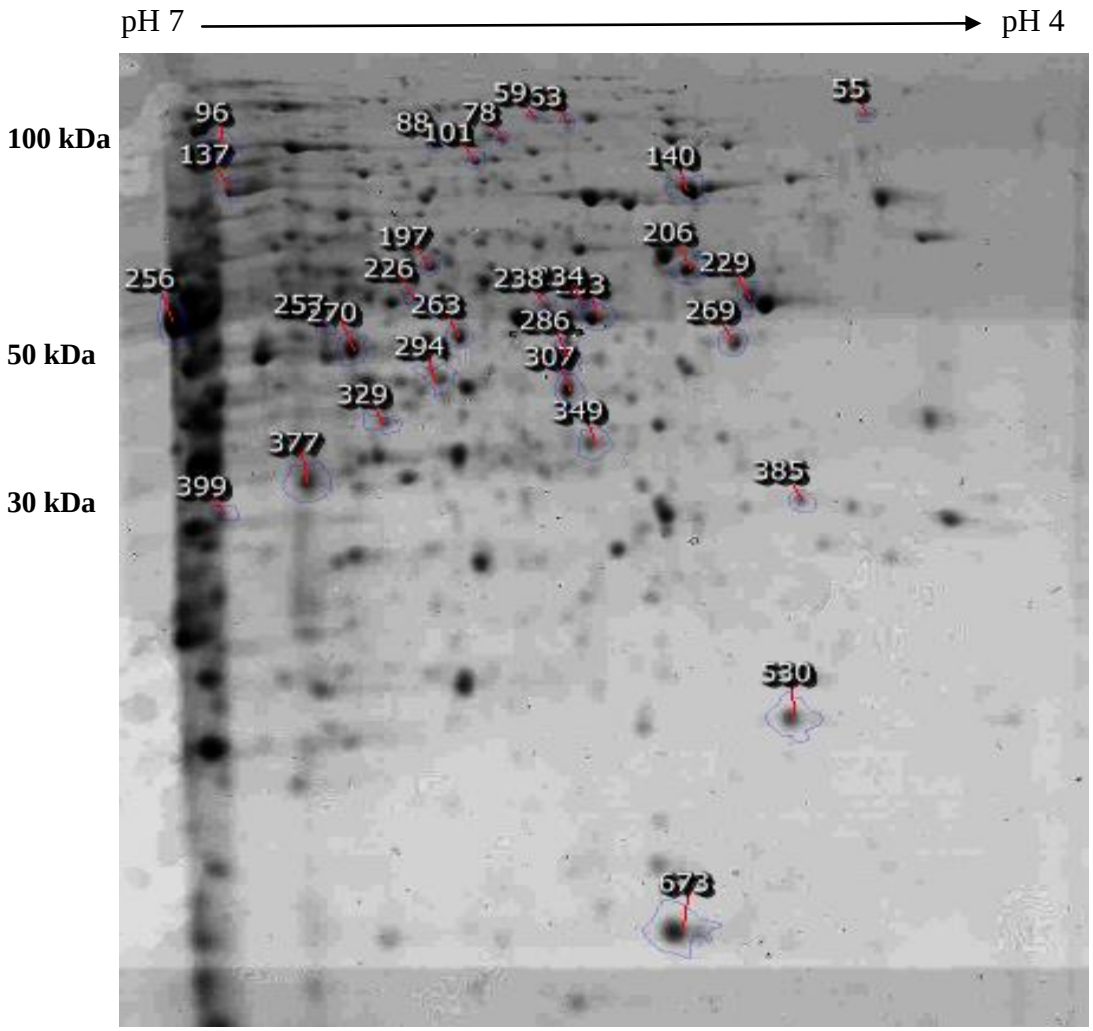

Figure 4.11 B 2D PAGE analysis of Δ*gliZ*[293]A. *fumigatus* + 5 µg/ml gliotoxin vs. AF293 *A. fumigatus* + 5 µg/ml gliotoxin, separated on pH 4-7 IPG strips on a 12 % SDS-PAGE gel

Table 4.7 Proteins differentially expressed in Δ*gliZ*[293] vs. AF293 in the presence of MeOH

Protein Name	MeOH	Sequence Coverage %	Mascot Score	Molecular Mass Da	CADRE I.D.	Spot No.
Proteins Up-regulated						
Putative translation elongation factor EF-2 subunit	↑2.5	7	315	93603	AFUA_2G13530	293
Putative WW domain protein	↑2.4	30	235	28374	AFUA_5G03750	295
Putative outer mitochondrial membrane protein porin	↑2.4	30	372	30007	AFUA_4G06910	332
Putative triosephosphate isomerase	↑1.9	38	483	28283	AFUA_5G13450	344
actin cytoskeleton protein (VIP1)	↑1.8	36	385	28306	AFUA_2G10030	292
Putative class II fructose-bisphosphate aldolase	↑1.7	40	779	39940	AFUA_3G11690	281
Putative peptidyl-prolyl cis-trans isomerase	↑1.7	29	430	41956	AFUA_2G02050	244
Putative manganese superoxide dismutase	↑1.6	43	603	23376	AFUA_1G14550	354

Protein Name	MeOH	Sequence Coverage %	Mascot Score	Molecular Mass Da	CADRE I.D.	Spot No.
Putative mitochondrial Hsp70 chaperone	↑1.6	38	1161	71932	AFUA_2G09960	97
Putative choline oxidase	↑1.6	42	767	60727	AFUA_8G04090	131
Putative glutamate carboxypeptidase	↑1.4	51	794	53272	AFUA_3G05450	164
Putative enolase	↑1.3	58	1028	43705	AFUA_6G06770	207
Proteins Down-regulated						
Putative bifunctional tryptophan synthase	↓3.9	34	1104	77777	AFUA_2G13250	76
Proteasome regulatory particle subunit	↓2.9	27	496	57862	AFUA_5G07050	158
Putative transaldolase	↓2.3	53	1110	35601	AFUA_5G09230	289
Putative aminopeptidase P	↓2.3	11	373	72924	AFUA_5G08050	85
Glutamate/Leucine/Phenylalanine/Valine dehydrogenase	↓1.8	57	1102	49627	AFUA_4G06620	217
Aspartyl-tRNA synthetase	↓1.8	42	1089	61763	AFUA_2G02590	101
Ortholog(s) have protein channel activity, role in protein import	↓1.6	30	436	38366	AFUA_6G05110	287

Protein Name	MeOH	Sequence Coverage %	Mascot Score	Molecular Mass Da	CADRE I.D.	Spot No.
Putative eukaryotic translation elongation factor 1 subunit eEF1-beta	↓1.6	56	397	25230	AFUA_1G11190	306
UDP-glucose 4-epimerase	↓1.6	45	605	40816	AFUA_5G10780	261

4.4.2.2 Δ*gliZ*^{293} vs. AF293 + MeOH

Similar to what was described in Section 4.4.1, there is differential expression of proteins involved in different metabolic pathways, with an increase in the metabolism of simple sugars such as fructose and a corresponding increase in glycolysis and gluconeogenesis. This is supported by a 1.9 fold increase in triosephosphate isomerase (AFUA_5G13450), 1.8 fold increase in class II fructose-bisphosphate aldolase (AFUA_3G11690), both of which are involved in the latter stages of the fructose and mannose biosynthetic pathway catalysing the formation of glyceraldehyde-3P; and a 1.3 fold increase of a putative enolase (AFUA_6G06770) which has a role in glycolysis. A full list of proteins identified in Δ*gliZ* vs AF293 + MeOH can be found in Table 4.7.

Interestingly, there is also increased expression of proteins involved in different aspects of the cell stress response in Δ*gliZ*. Manganese superoxide dismutase Sod3 (AFUA_1G14550) has a 1.6 fold increase in expression. This enzyme is involved in super oxide dismutation, which is natural by-product of aerobic respiration, indicating that there could be higher amounts of this harmful radical in Δ*gliZ* cells when compared to AF293. An increase in ROS in Δ*gliZ* cells is further supported by the 1.4 fold increase in the expression of a putative glutamate decarboxypeptidase (Dug1; AFUA_3G05450), an enzyme involved in the degradation of L-cysteinyl-glycine to L-glycine and L-cysteine in yeast, which can then used again for the formation of GSH, a major component in the ROS response (Ganguli *et al.*, 2007).

A 1.7 fold increase in expression of a peptidyl-prolyl cis-trans isomerase (AFUA_2G02050) and a 1.6 fold increase of choline oxidase (AFUA_8G04090) may support the above point that the cell is undergoing some type of stress as both have been demonstrated to be induced under different kinds of stresses, DNA replication stress and menadione stress respectively (Sims *et al.*, 2005; Pusztahelyi *et al.*, 2011).

Certain amino acid biosynthesis is down-regulated in Δ*gliZ* showing a 1.8 fold decrease in glutamate/leucine/phenylalanine/valine dehyrdogenase (AFUA_4G06620) as well as other amino acid associated enzymes being down-regulated such as a putative aminopeptidase P (AFUA_5G08050) which had a 2.3 fold decrease in expression, and

UDP-glucose- 4-epimerase (AFUA_5G10780) which was down regulated 1.6 fold in Δ*gliZ* vs. AF293.

4.4.2.3 Δ*gliZ*^{293} vs. AF293 + 5 µg/ml gliotoxin

Upon gliotoxin addition, there is further evidence which implicates gliotoxin dysregulating the SAM cycle. As seen previously in Δ*gliT*, s-adenosyl homocysteinase (AFUA_1G10130) was found to have a 1.7 fold decrease in expression when cells were challenged with gliotoxin. Interestingly, another enzyme involved in this pathway was seen to be down-regulated. Cobalamin-independant methionine synthase (AFUA_4G07360) had a 3.3 fold decrease in its expression in Δ*gliZ* cells when compared to AF293 in the presence of gliotoxin. Orthologs of this enzyme catalyse the methylation of L-homocysteine to form L-methionine which can then feed back into the SAM cycle (Kacprzak *et al.,* 2003; Suliman *et al.,* 2005) . A full list of all proteins identified can be found in Table 4.8.

A 4.1 fold decrease in the expression of the putative actin protein (AFUA_6G04740) may suggest a reduction in cell growth of Δ*gliZ* compared to AF293 due to reduced expression of this structural component (Marui *et al.,* 2010). Additionally, there is a decrease in the expression of enzymes involved in complex carbohydrate metabolism e.g. a decrease of 2.8 fold of 1,4 β-glucan hydrolase (AFUA_7G06140), 3 fold decrease of NAD-dependent malate dehydrogenase (AFUA_7G05740) and a 2.3 fold decrease of a transketolase (AFUA_1G13500), all of which are involved in different types of carbohydrate metabolism suggest a cell undergoing energy conservation, and presumably, stress (Kim *et al.,* 2007; Lu *et al.,* 2010; Sørensen *et al.,* 2009) .

As in MeOH treated cells, there is a decrease in amino acid biosynthesis. Sacchropine dehydrogenase (AFUA_4G11340) which has a 2.4 decrease in its expression, is involved in lysine biosynthesis; while AFUA_6G12580 which has orthologs in *S. cerevisiae* (Trp2) involved in tryptophan biosynthesis, is down regulated 2.5 fold. Similarly phosphoribosyl-AMP (AFUA_1G14570) was infinitely decreased in Δ*gliZ* (Vodisch *et al.,* 2011; Zalkinz *et al.,* 1984; Keesey *et al.,* 1979). Orthologs of this

last enzyme are involved in the histidine biosynthesis pathway where it's involved in two key steps in the pathway (Keesey *et al.,* 1979). The first is in catalysing the creation of phosphoribosyl-formimo-AICAR-P, and the second being in the biosynthesis of L-histidine itself (Keesey *et al.,* 1979). Alongside this, a putative amino-peptidase (AFUA_4G09030), whose orthologs have been demonstrated to catalyse the cleavage of amino acids from proteins and peptide chains, is completely absent from Δ*gliZ* showing an infinite decrease in expression compared to AF293 indicating a reduction in protein/amino acid modification in these cells (Basten *et al.,* 2001; Marui & Sawaki 2012) .

Table 4.8 Proteins differentially expressed in Δ*gliZ*[293] vs. AF293 in the presence of 5 µg/ml gliotoxin

Protein Name	Gliotoxin	Sequence Coverage %	Mascot Score	Molecular Mass Da	CADRE I.D.	Spot No.
Proteins Up-regulated						
Thiamine biosynthesis protein	↑1.7	10	129	38588	AFUA_5G02470	349
Putative mannitol-1-phosphate dehydrogenase	↑1.4	19	336	43093	AFUA_2G10660	294
Proteins Down-regulated						
Putative aminopeptidase	↓Infinity	15	533	106624	AFUA_4G09030	63
Putative phosphoribosyl-AMP cyclohydrolase	↓Infinity	4	59	93404	AFUA_1G14570	59
Putative translation elongation factor EF-1 alpha subunit	↓5.4	28	493	54273	AFUA_1G06390	256
Putative metallopeptidase with similarity to mammalian thimet oligopeptidases	↓4.2	3	109	82046	AFUA_7G05930	101
Actin	↓4.1	28	311	41914	AFUA_6G04740	286
Putative cobalamin-independent methionine synthase	↓3.3	33	917	87073	AFUA_4G07360	96
Putative NAD-dependent malate dehydrogenase	↓3	28	360	35876	AFUA_7G05740	399

Protein Name	Gliotoxin	Sequence Coverage %	Mascot Score	Molecular Mass Da	CADRE I.D.	Spot No.
Putative secreted 1,4-beta-D-glucan glucanhydrolase	↓2.8	9	341	78738	AFUA_7G06140	88
Eukaryotic translation initiation factor eIF4A; ATP-dependent RNA helicase	↓2.6	26	454	45981	AFUA_3G08160	269
Ortholog(s) have anthranilate synthase activity, role in cleistothecium development, tryptophan biosynthetic process and anthranilate synthase complex localization	↓2.5	18	286	57389	AFUA_6G12580	197
Saccharopine dehydrogenase	↓2.4	26	446	49940	AFUA_4G11340	257
14-3-3 family protein	↓2.3	21	166	30201	AFUA_6G06750	385
Putative transketolase	↓2.3	31	679	75816	AFUA_1G13500	137
Ortholog(s) have proteasome regulatory particle, lid subcomplex, proteasome storage granule localization	↓2.2	31	446	38971	AFUA_1G07540	329
Putative glutamine synthetase	↓2	25	398	38862	AFUA_4G13120	307
Putative adenosylhomocysteinase	↓1.7	35	649	49039	AFUA_1G10130	270

4.4.2.4 Proteins in common Δ*gliZ*^{293} vs. AF293 +/- gliotoxin

A total of 11 proteins identified were found to be shared between the two comparatives i.e. Δ*gliZ*^{293} vs. AF293 + MeOH and Δ*gliZ*^{293} vs. AF293+ gliotoxin. A full list of proteins identified in common between Δ*gliZ* and AF293 +/- gliotoxin can be found in Table 4.9. Of these eleven, only one showed a difference in its expression from one treatment compared to the next. Allergen Asp F3 (AFUA_6G02280) was found to have increased expression of 2.3 fold in MeOH treated cells but reduced expression of 1.9 fold in gliotoxin treated cells. This enzyme is a putative thioredoxin peroxidase identical to Pmp20, a peroxisomal membrane protein which is involved in tackling ROS via the degradation of lipid hydroperoxides within the peroxisomal membrane (Mabey *et al.,* 2004). As gliotoxin biosynthesis is abolished in this strain, the addition of exogenous gliotoxin does not increase the expression of the entire *gli* cluster, only *gliT*. This may imply that the lower gliotoxin levels in Δ*gliZ*, due to the silencing of the gliotoxin biosynthetic cluster, may be having an anti-oxidant role resulting in the reduced expression of AspF3.

In both Δ*gliZ* and AF293 + gliotoxin comparisons, there is a decrease in the expression of 6-phosphogluconate dehydrogenase (AFUA_6G08050); 4.5 fold in MeOH and 6.6 in gliotoxin treated cells. This protein is involved in the pentose phosphate and glutathione biosynthesis pathways whereby it is one of the controlling factors that mediates GSSG reduction to GSH (Teutschbein *et al.,* 2010; Kaneshira *et al.,* 2004). The addition of gliotoxin results in an increase in the reduction of this protein which suggests that the presence of reduced glutathione is not advantageous to the cell. This result further strengthens the hypothesis made throughout this study of the relationship between glutathione levels and gliotoxin toxicity whereby low glutathione levels are believed to be advantageous to the cell when challenged with gliotoxin (Chapter 3).

As seen in Section 4.4.2.3 and 4.4.2.4, there is a decrease in the expression of different metabolic pathways. Two protein sub-units involved in the pentose phosphate pathway; Tublin α-1 subunit (AFUA_1G02550) and tubulin-β subunit (AFUA_1G10910) have a decrease in expression of 4.2 and 3.6 fold respectively in MeOH treated cells and 2.5 and 2.2 fold respectively in gliotoxin treated cells.

Table 4.9 Proteins differentially expressed in Δ*gliZ*[293] vs. AF293 in the presence of MeOH and 5 µg/ml gliotoxin

Protein Name	MeOH	Gliotoxin	Sequence Coverage %	Mascot Score	Molecular Mass Da	CADRE I.D.	Spot No.
Proteins Up-regulated							
TCTP family protein	↑2.1	↑2.3	21/29	209/312	20350	AFUA_1G16840	348/530
Allergen Asp f 3; peroxiredoxin family reductase;	↑2.3	↓1.9	50/51	369/382	18557	AFUA_6G02280	371/673
Proteins Down-regulated							
6-phosphogluconate dehydrogenase	↓4.5	↓6.6	44/39	849	56228	AFUA_6G08050	215/263
Tubulin alpha-1 subunit	↓4.2	↓2.5	47/12	133	50805	AFUA_1G02550	161/206
Beta-tubulin	↓3.6	↓2	27/37	/454	52283	AFUA_1G10910	181/229
Putative glutamine synthetase	↓3.2	↓2	49/25	/398	38862	AFUA_4G13120	248/307
Molecular chaperone	↓2.1	↓1.8	25/30	641/748	67303	AFUA_1G07440	252/140
Argininosuccinate synthase	↓2	↓1.7	22/13	498/184	46684	AFUA_2G04310	192/234
Putative mitochondrial processing peptidase beta subunit	↓2	↓3.3	33/34	744/767	54981	AFUA_1G14200	206/253

Protein Name	MeOH	Gliotoxin	Sequence Coverage %	Mascot Score	Molecular Mass Da	CADRE I.D.	Spot No.
Putative alanine aminotransferase	↓1.8	↓2.8	50/16	888/321	55622	AFUA_6G07770	175/226
Argininosuccinate synthase	↓1.7	↓1.5	39/37	816/512	46684	AFUA_2G04310	195/238

Three enzymes identified from four spots, were found to be involved in the alanine, aspartate and glutamate metabolic pathway. Argininosuccinate synthase (AFUA_2G04310) was identified from two different spot locations under both conditions and was found to have reduced expression of 2 and 1.7 fold in MeOH treated cells, and 1.7 and 1.5 fold in gliotoxin treated Δ*gliZ* cells when compared to AF293. Glutamine synthetase (AFUA_4G13120) which is involved in the condensation of l-glutamate and ammonia to form l-glutamine, had a 3.2 fold reduction in expression in MeOH treated cells and 2 fold reduction in gliotoxin treated cells. Lastly, alanine transferase (AFUA_6G07770) which reversibly converts L-alanine to pyruvate, was reduced 1.8 fold in MeOH treated cells and 2.8 fold in gliotoxin treated cells.

Dysregulated proteins were categorised according to their respective function as described previously in section 4.2.1. The top five categories are given for Δ*gliZ* vs. AF293 + MeOH (Figure 4.12 A) and Δ*gliZ* vs. AF293 + 5 µg/ml gliotoxin (Figure 4.12 B). Complete list of all proteins identified and their respective functions can be found in Table 4.9.

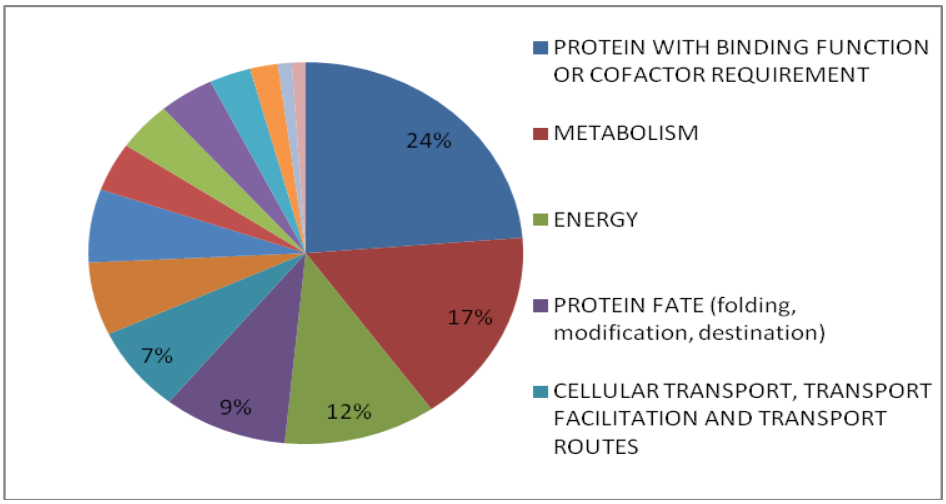

Figure 4.12 (A) Functional categorisation of proteins differentially expressed in Δ*gliZ*[293] *A. fumigatus* vs. AF293 *A. fumigatus* + MeOH

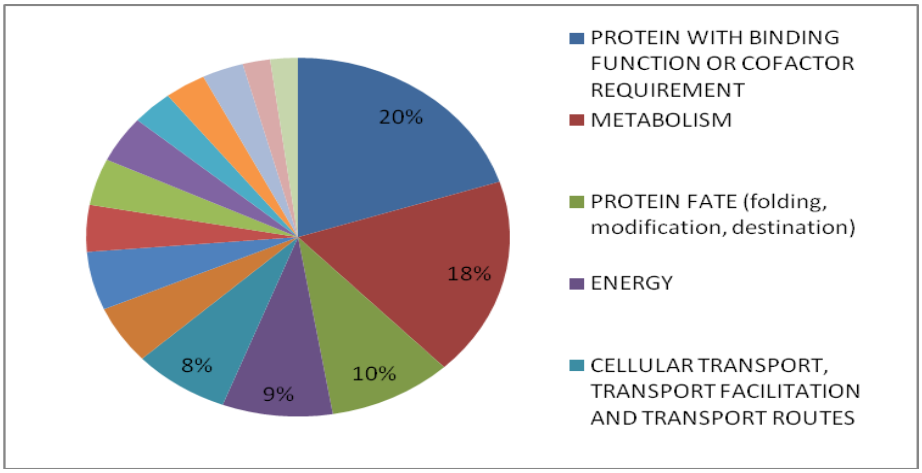

Figure 4.12 (B) Functional categorisation of proteins differentially expressed in Δ*gliZ*[293] *A. fumigatus* vs. AF293 *A. fumigatus* + 5 µg/ml gliotoxin

4.4.2.5 Discussion

In the absence of *gliZ* in *A. fumigatus* there is a shift in the ROS state of the cell. This is supported by the reduced expression of enzymes involved in the OS response, most notably the manganese super oxide dismutase (AFUA_1G14550). This enzyme is located in the mitochondrion and is involved in dismutating O_2^- into H_2O and H_2O_2. A decrease in this enzyme suggests that when gliotoxin biosynthesis is abolished, it is importance is reduced. This could be due to the absence of reactive intermediate steps involved in gliotoxin biosynthesis (Forseth *et al.*, 2011). The increased expression of Dug1 (AFUA_3G05450), an enzyme involved in the alternate glutamyl cycle which degrades L-cysteinyl glycine into L-cysteine and L-glycine, is presumably for glutathione biosynthesis. Once challenged with gliotoxin this changes, with no altered expression for either of these two enzymes seen, indicating the redundancy of Sod3 is no longer present as gliotoxin enters the cell giving way a return to basal levels of this enzyme in. AFUA_6G08050 is down regulated in both MeOH treated cells and shows a further decrease in gliotoxin treated cells. This enzyme is one component of GSSG

reduction to GSH and along with the return to basal levels of Dug1 in gliotoxin treated cells, implies glutathione levels are being carefully regulated in this strain, more so than AF293 re-iterating the point made in the previous chapter about the relationship seen between glutathione levels and gliotoxin toxicity.

As in previous sections, there is further evidence which supports gliotoxin mediated dysregulation of the SAM cycle. This can be seen in the 1.7 fold reduction in the expression of s-adenosyl homocysteinase (AFUA_1G10130) and the 3.3 fold reduced expression of the cobalamin-independant methionine synthase (Met H/D; AFUA_4G07360). As hypothesised earlier, the decrease in s-adenosyl homocysteinase could suggest elevated levels of L-homocysteine, which are toxic to the cell, due to an increase in SAM mediated S-methylation, presumably due to the formation of Bm-GT. The Met H/D is involved in the methylation of L-homocysteine to form L-methionine, a key step in maintaining methionine availability for the SAM cycle. A reduction of the methionine synthase implies that the cell is trying to further control the production of L-homocysteine by down-regulating the SAM cycle. Compared to what was seen in section 4.4.2 with Δ*gliT* vs. AF293, no differential expression was found for Met H/D, indicating in response to gliotoxin, the SAM cycle is further dysregulated in Δ*gliZ* than in Δ*gliT*. Met H/D differential expression in Δ*gliZ*, may suggest that silencing of the *gli* cluster induces repression of this enzyme in gliotoxin exposed.

The altered expression of the Asp F 3 peroxiredoxin protein, highlights gliotoxin's potential as an anti-oxidant molecule resulting in its reduced expression. This same enzyme was found previously by Carberry *et al.,* (2006) to be significantly induced in the presence of 14 µg/ml gliotoxin. One reason for this could be the difference in gliotoxin concentration. At 5 µg/ml gliotoxin the anti-oxidant potential of gliotoxin is sufficient in preventing major hydrogen peroxide stress from being produced. The greater 14 µg/ml gliotoxin appears to overwhelm any benefit seen using the lower 5 µg/ml gliotoxin concentrations, inducing OS and a subsequent up-regulation of OS proteins.

4.4.3.1 Δ*gliT*Δ*gliZ*^{293} vs. AF293

Cells from AF293 and Δ*gliT*Δ*gliZ*^{293} were treated as described previously (Section 4.4.1.1). A total of 71 protein spots were identified as being significantly (P = < 0.05) expressed between the two comparisons (Δ*gliT*Δ*gliZ*^{293} + MeOH vs. AF293 + MeOH and Δ*gliT*Δ*gliZ*^{293} + 5 µg/ml gliotoxin vs. AF293 + 5 µg/ml gliotoxin. Of a total of 68 identified proteins, 27 were identified from MeOH treated cells (Figure 4.13 A), 34 from gliotoxin treated cells (Figure 4.13 B) with 7 identified to be in common, ranging from 18 kDa to 108.7 kDa in size. A full list of proteins identified in Δ*gliT*Δ*gliZ* vs. AF293 + MeOH can be foun in table 4.10.

4.4.3.2 Δ*gliT*Δ*gliZ*^{293} vs. AF293 + MeOH

As seen in earlier sections, there is an increase in the expression of proteins involved in fructose metabolism and glycolysis with a 2.2 fold increase of a protein with predicted oxidoreductase properties, a 2.1 fold increase in mannitol-l-phosphate dehydrogenase (AFUA_2G10660), a 1.7 fold increase in triosephosphate isomerise (AFUA_5G13450), 1.7 fold increase in an aldehyde dehydrogenase (AFUA_4G08600), 1.5 fold increase in a class II fructose bis-phosphate aldolase (AFUA_3G11690) and a 1.3 fold increase in enolase (AFUA_6G06770), indicating an increased demand in the energy held within these carbohydrates. Opposed to this is the decrease in the expression of other carbohydrate metabolic pathways such as the TCA cycle where AFUA_4G04520 has a 2.3 fold decrease in its expression.

A 1.4 fold increase in glutamate carboxypeptidase Dug 1 (AFUA_3G05450), a peptidase involved in the cleavage of L-cysteinyl-glycine to release L-cysteine and L-glycine, key amino acids required in the formation of the tri-peptide thiol glutathione, and a 5.8 fold decrease in the expression of 6-phosphogluconate dehydrogenase (AFUA_6G08050), a component responsible for GSSG reduction to GSH, suggest altered regulation of the glutathione biosynthesis pathway, and glutathione levels in Δ*gliT*Δ*gliZ*.

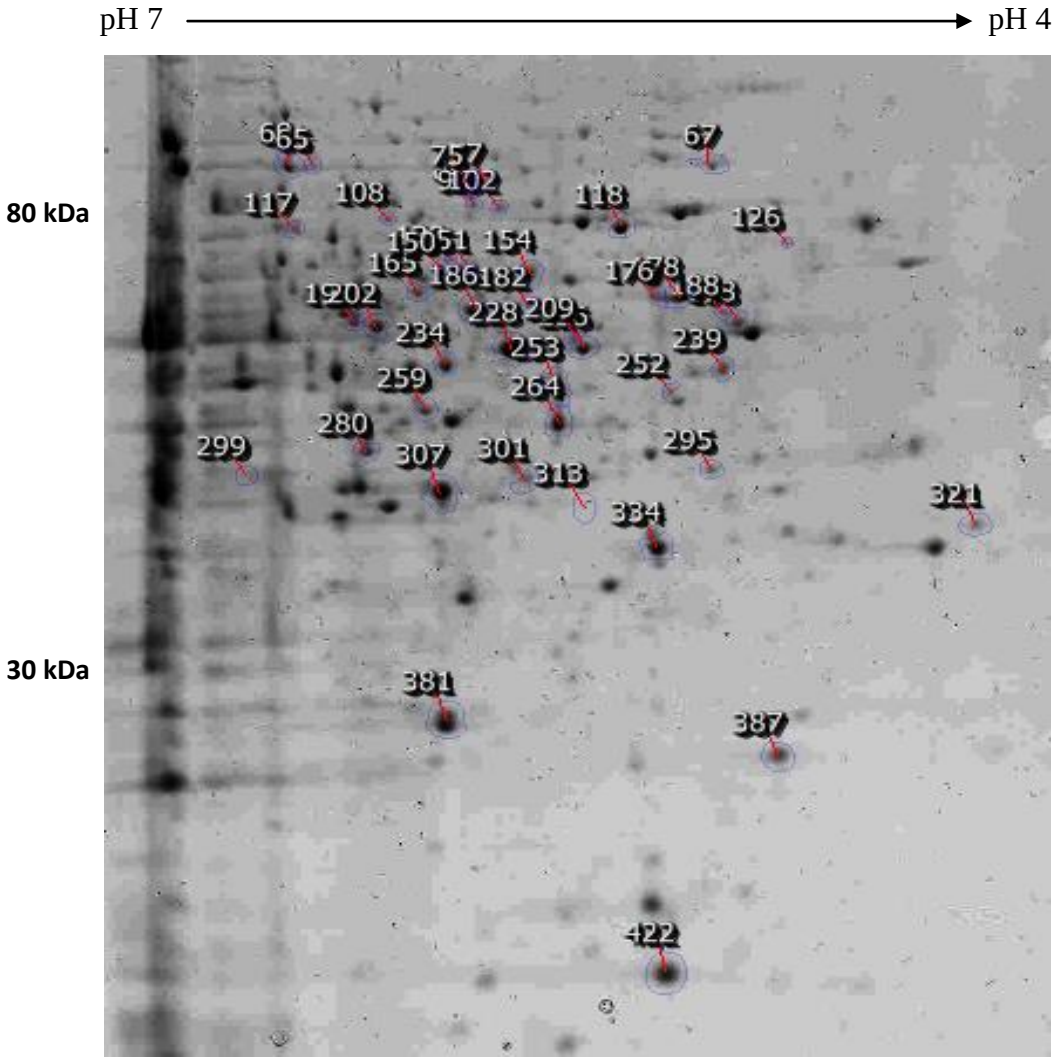

Figure 4.13 A 2D PAGE analysis of Δ*gliT*Δ*gliZ*[293] *A. fumigatus* + MeOH vs. AF293 *A. fumigatus* + MeOH, separated on pH 4-7 IPG strips on 12 % SDS-PAGE gel

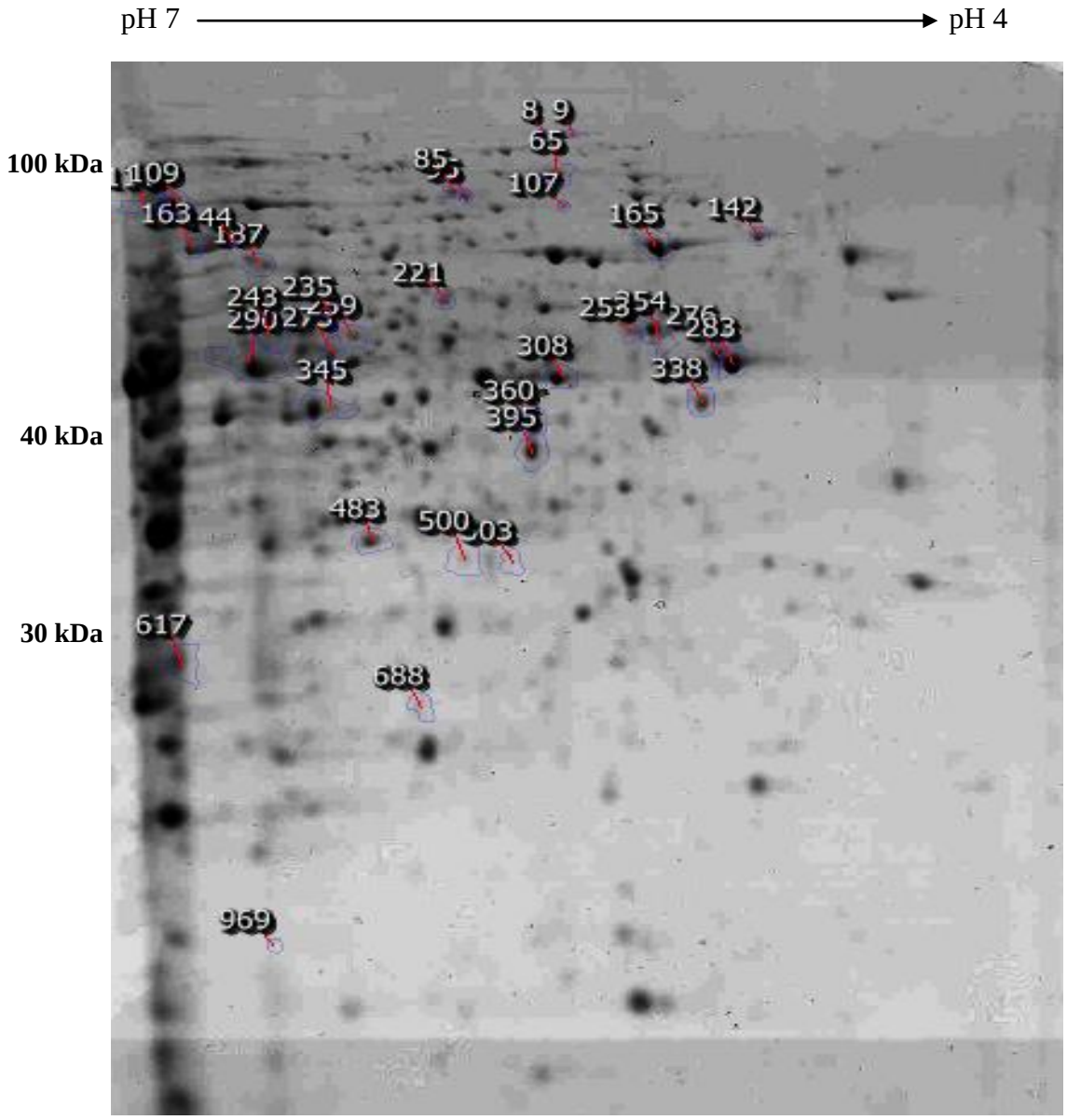

Figure 4.13 B 2D PAGE analysis of Δ*gliT*Δ*gliZ*^{293}*A. fumigatus* + 5 µg/ml gliotoxin vs. AF293 *A. fumigatus* + 5 µg/ml gliotoxin, separated on pH 4-7 IPG strips on a 12 % SDS-PAGE gel

Table 4.10 Proteins differentially expressed in Δ*gliT*Δ*gliZ*^{293} vs. AF293 in the presence of MeOH

Protein Name	MeOH	Sequence Coverage %	Mascot Score	Molecular Mass Da	CADRE I.D.	Spot ID
Proteins Up-regulated						
Allergen Asp f 3	↑2.5	27	112	18453	AFUA_6G02280	422
Has domain(s) with predicted oxidoreductase activity and role in oxidation-reduction process	↑2.2	4	13	32753	AFUA_1G07650	321
Ortholog(s) have phenylalanine-tRNA ligase activity and phenylalanine-tRNA ligase complex localization	↑1.8	18	338	68325	AFUA_1G05620	65
Putative triosephosphate isomerase	↑1.7	13	108	28068	AFUA_5G13450	381
Putative aldehyde dehydrogenase (NAD(P)+)	↑1.7	24	345	60254	AFUA_4G08600	182
Putative class II fructose-bisphosphate aldolase	↑1.5	3	72	39971	AFUA_3G11690	307
Thiamine biosynthesis protein, phoB-regulated	↑1.5	4	39	38323	AFUA_5G02470	301
Putative glutamate carboxypeptidase	↑1.4	58	961	53272	AFUA_3G05450	186
Putative Hsp70 chaperone	↑1.3	5	128	66973	AFUA_8G03930	118
Putative enolase	↑1.3	31	465	47305	AFUA_6G06770	228

Protein Name	MeOH	Sequence Coverage %	Mascot Score	Molecular Mass Da	CADRE I.D.	Spot ID
Putative inorganic diphosphatase	↑1.3	13	97	43624	AFUA_3G08380	334
Proteins Down-regulated						
6-phosphogluconate dehydrogenase	↓5.8	57	1379	56228	AFUA_6G08050	234
Tubulin beta-2 subunit	↓4.4	2	59	49892	AFUA_7G00250	188
Heat shock protein	↓3.9	15	198	80640	AFUA_5G04170	67
Putative V-type ATPase, B subunit	↓2.7	4	83	56418	AFUA_2G13240	165
Ortholog of *A. niger CBS 513.88*	↓2.5	19	275	61344	AFUA_3G02430	126
Putative metallopeptidase with similarity to mammalian thimet oligopeptidases	↓2.4	11	339	82046	AFUA_7G05930	75
Has domain(s) with predicted ATP binding, ligase activity and role in metabolic process	↓2.3	5	83	48017	AFUA_4G04520	252
Putative G1/S-specific cyclin	↓2.1	4	16	47021	AFUA_2G03920	108
Putative mannitol-1-phosphate dehydrogenase	↑2.1	20	93	43004	AFUA_2G10660	259
Protein of unknown function identified by mass spectrometry	↓1.9	4	110	69525	AFUA_4G08030	102

Protein Name	MeOH	Sequence Coverage %	Mascot Score	Molecular Mass Da	CADRE I.D.	Spot ID
Putative glutamine synthetase	↓1.8	6	63/53	39900	AFUA_4G13120	264/395
Argininosuccinate synthase	↓1.8	21	408	46684	AFUA_2G04310	209
Mitochondrial processing peptidase beta-subunit	↓1.6	35	899	54981	AFUA_1G14200	226
Ortholog(s) have proteasome regulatory particle, lid subcomplex, proteasome storage granule localization	↓1.4	7	86	38995	AFUA_1G07540	280
Putative aminopeptidase P	↓1.4	3	73	72680	AFUA_5G08050	97

Similar to a previous result seen in Δ*gliZ* +MeOH, allergen Asp F3 (AFUA_6G02280) was found to have a 2.5 fold increase in expression in Δ*gliT*Δ*gliZ*. As mentioned earlier, this belongs to the peroxiredoxin family of proteins, and has a putative anti-oxidant function in the liposomal membrane. Unlike Δ*gliZ* however, this same enzyme showed no differential expression in the presence of gliotoxin, implying that in Δ*gliT*Δ*gliZ* this enzyme returns to wild-type levels upon gliotoxin addition.

There is also some evidence to suggest an increase in proteins involved in protein biosynthesis, as seen in the 1.8 fold increase in a TCTP family protein (AFUA_1G16840) with orthologs possessing a role in ribosome interaction and apoptosis, and a 1.8 fold increase in the expression of a putative phenylalanine-tRNA ligase (AFUA_1G05620) with orthologs involved in phenylalanine, tryptophan and tyrosine amino acid biosynthesis (Rinnerthaler *et al.,* 2006; Oh *et al.,* 2013; Roy *et al.,* 2005).

4.4.3.3 Δ*gliT*Δ*gliZ*^{293} vs. AF293 + 5 µg/ml gliotoxin

Gliotoxin exposure of Δ*gliT*Δ*gliZ* strains results in a significant decrease in the expression of two proteins involved in protein processing of the endoplasmic reticulum. Hsp70 chaperone (AFUA_2G04620), which has a 4.9 fold decrease in expression, and a different Hsp70 chaperone Lhs1 (AFUA_1G15050), which is completely absent in Δ*gliT*Δ*gliZ*, have orthologs involved in protein import into the endoplasmic reticulum, nucleotide folding and recognition via luminal chaperone (Nishikawa *et al.,* 2001; Sims *et al.,* 2005). A full list of proteins identified in Δ*gliT*Δ*gliZ* vs. AF293 + 5 µg/ml gliotoxin can be found in Table 4.11.

Differential expression was seen in enzymes involved in valine/leucine and isoleucine biosynthesis pathway. A 5.9 fold increase in the expression of 3 isopropylmalate (AFUA_1G15780) and a 3.4 fold increase in a mitochondrial acetolactate synthase (AFUA_4G07210) which catalyse the formation of 2-oxobutanoate and (S)-2-Aceto-2-hydroxybutanoate sequentially, which leads to isoleucine synthesis. There is also a 4.4 fold decrease in the expression of a mitochondrial dihydroxy acid dehydratase (AFUA_1G03550) which is involved in the

later stages of iosleucine synthesis in the condensation of (R)-2,3-dihydroxy-3-methylpentanoate to (S)-3-methyl-2-oxopentanoate.

Table 4.11 Proteins differentially expressed in Δ*gliT*Δ*gliZ*[293] vs. AF293 + 5 µg/ml gliotoxin

Protein Name	Gliotoxin	Sequence Coverage %	Mascot Score	Molecular Mass Da	CADRE I.D.	Spot ID
Proteins Up-regulated						
3-isopropylmalate dehydrogenase with a predicted role in leucine biosynthesis	↑5.9	12	228	39049	AFUA_1G15780	969
Mitochondrial acetolactate synthase small subunit	↑3.4	5	36	35574	AFUA_4G07210	500
Proteins Down-regulated						
Has domain(s) with predicted ATP binding activity	↓Infinity	7	306	108767	AFUA_1G15050	9
Putative aminopeptidase; conidia-enriched protein	↓8.7	29	1251	108707	AFUA_5G04330	95
Putative cobalamin-independent methionine synthase	↓6.7	2	43	86895	AFUA_4G07360	109
ATP synthase F1, beta subunit	↓5.6	20	214	55620	AFUA_5G10550	283
Hsp70 chaperone	↓4.9	9	129	73385	AFUA_2G04620	142
Putative transketolase	↓4.4	42	1176	74828	AFUA_1G13500	163
Putative mitochondrial dihydroxy acid dehydratase	↓4.4	7	180	57877	AFUA_1G03550	163
Ortholog of *A. nidulans FGSC A4*	↓4.3	5	28	43201	AFUA_4G03722	308

Protein Name	Gliotoxin	Sequence Coverage %	Mascot Score	Molecular Mass Da	CADRE I.D.	Spot ID
Molecular chaperone	↓4.2	9	154	69660	AFUA_1G07440	165
Putative hexokinase	↓3.3	15	229	54209	AFUA_2G05910	253
Putative translation elongation factor EF-2 subunit	↓2.5	16	795	93198	AFUA_2G13530	617
Secreted dipeptidyl-peptidase	↓2.3	4	111	70745	AFUA_2G09030	85
Putative adenosylhomocysteinase	↓2.3	4	54	48490	AFUA_1G10130	345
Putative secreted lysophospholipase B	↓2.3	5	79	67417	AFUA_3G14680	65
Putative hydroxymethyl glutaryl-coenzyme A synthase with a predicted role in ergosterol biosynthesis	↓2.1	16	211	50797	AFUA_3G10660	290
Putative transaldolase	↓2.1	4	36	35449	AFUA_5G09230	483
Putative GMP synthase ([glutamine-hydrolyzing)	↓1.8	5	42	61432	AFUA_3G01110	235
Putative GABA permease	↓1.7	19	86	56640	AFUA_1G12310	688
Putative proteasome component	↓1.7	13	233	28206	AFUA_6G08960	688

Hydroxymethyl glutaryl co-enzyme A synthase (AFUA_3G10660) has a 2.1 fold decrease in expression in Δ*gliT*Δ*gliZ* cells in the presence of gliotoxin. This enzyme is involved in the leucine/valine and isoleucine degradation pathway. Here it catalyses the formation of (S)-3-hydroxy-3-methylglutaryl-CoA from acetoacetyl-CoA (Kaneshira *et al.,* 2004). Indicating an increase in certain components involved in the early stages of iso-leucine biosynthesis, however with the later stages being decreased suggesting isoleucine is not the end target.

Similar to Δ*gliZ*, Δ*gliT*Δ*gliZ* has 2.3 fold decrease in the expression of s-adenosyl homocysteinase (AFUA_1G10130) and a 6.7 fold decrease in the cobalamin-independant methionine synthase (AFUA_4G07360). Again, this suggests gliotoxin dysregulation of the SAM cycle has become deleterious to the cell thus the need to alter its regulation via decreasing the expression of key enzymes. A full list of proteins can be seen in Table 4.10. A full list of proteins identified can be seen in Table 4.11.

4.4.3.4 Proteins in common in Δ*gliT*Δ*gliZ*[293] vs. AF293 +/- gliotoxin

As seen in Table 4.12, both MeOH and gliotoxin treated Δ*gliT*Δ*gliZ* cells, display increased expression of 7.9 fold in MeOH treated cells and 3.6 in gliotoxin treated cells of the pyrithiamine resistance gene (AO090003000090) from *A. oryzae*. As described earlier, this gene was used to knock out *gliT* in a Δ*gliZ* background acting as a positive selection marker on pyrithiamine containing plates, and as it is absent from AF293, it would be expected to have increased expression.

Interestingly, two components of microtubule formation were found to have decreased expression in both MeOH and gliotoxin treated cells. β-tubulin (AFUA_1G10910) had a 3.8 fold decrease in expression in MeOH treated cells and 4.8 fold decrease in gliotoxin treated cells. Tubulin α-1 subunit (AFUA_1G02550) was identified twice from two different protein spots in gliotoxin treated cells having a 5.8 and 3.3 respective fold decrease as well as a 2.1 fold decrease in expression in MeOH treated cells.

Table 4.12 Proteins differentially expressed in Δ*gliT*Δ*gliZ*[293] vs. AF293 in the presence of MeOH and 5 µg/ml gliotoxin

Protein Name	MeOH	Gliotoxin	Sequence Coverage %	Mascot Score	Molecular Mass Da	CADRE I.D.	Spot ID
Pyrathiamine resistance gene, thiA	↑7.9	↑3.6	4/16	36/241	35492	AO090003000090	313/503
Eukaryotic translation initiation factor eIF4A	↓5.3	↓6.2	15/8	110/73	45779	AFUA_3G08160	239/338
Beta-tubulin	↓3.8	↓4.8	11/29	190/312	50024	AFUA_1G10910	198/276
Putative prolidase	↓3.1	↓6.1	6/19	122/410	51944	AFUA_2G07500	151/221
Putative ATP citrate lyase subunit	↓2.3	↓3	50/48	958/958	53001	AFUA_6G10660	197/275
Actin	↓2.2	↓4.8	18/10	90/52	43893	AFUA_6G04740	253/360
Tubulin alpha-1 subunit	↓2.1	↓5.8 + ↓3.3	5/33/33	41/448/448	50025	AFUA_1G02550	178/254/253

As seen in Section 4.4.3.2, there is a 4.4 fold decrease in the expression of a different microtubule associated protein, tublin β-2 subunit (AFUA_7G00250). Together they form repeating dimers which constitute the structure of microtubules in the cell. What is clear, is that once gliotoxin is added there is an increase in the fold decrease of these proteins in Δ*gliT*Δ*gliZ*. With this, there is a decrease in the expression of F-actin (AFUA_6G04740) with a 2.2 fold decrease in MeOH treated cells and 4.8 fold decrease in gliotoxin treated cells. It has been demonstrated that both microtubules and F-actin interact for a range of cellular functions.

Dysregulated proteins were categorised according to their respective function as described previously in Section 4.2.1. The top five categories are given for Δ*gliT*Δ*gliZ* vs. AF293 + MeOH (Figure 4.14 A) and Δ*gliT*Δ*gliZ* vs. AF293 + 5 µg/ml gliotoxin (Figure 4.14 B).

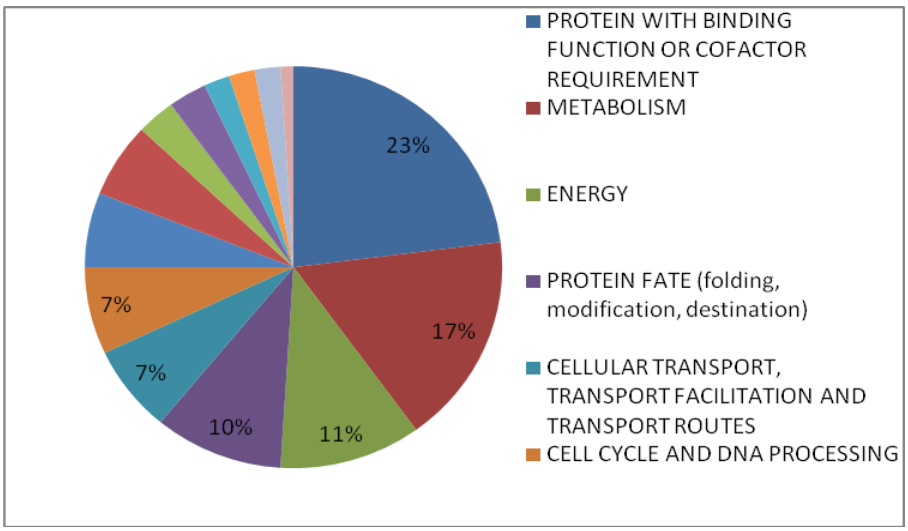

Figure 4.14 (A) Functional categorisation of proteins differentially expressed in Δ*gliT*Δ*gliZ*[293] *A. fumigatus* vs. AF293 *A. fumigatus* + MeOH

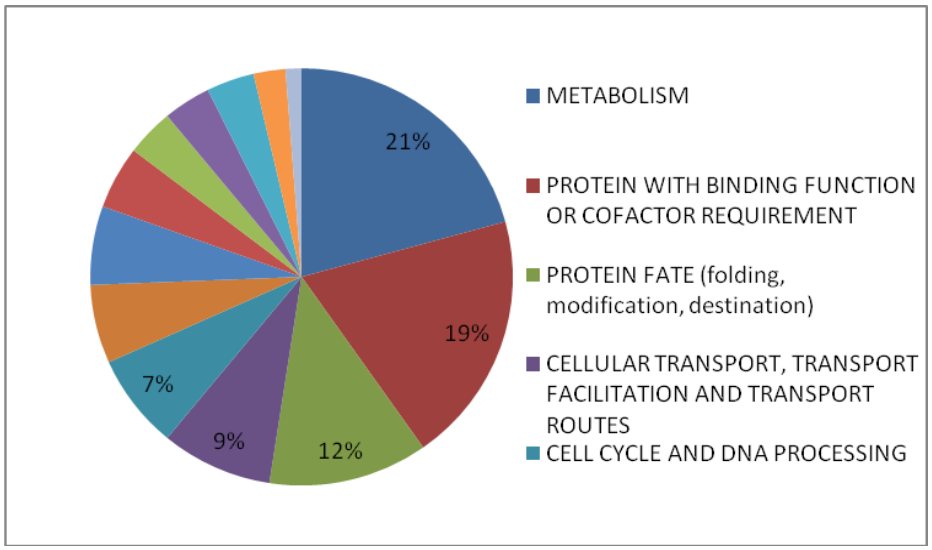

Figure 4.14 (B) Functional categorisation of proteins differentially expressed in Δ*gliT*Δ*gliZ*[293] *A. fumigatus* vs. AF293 *A. fumigatus* + 5 µg/ml gliotoxin

4.4.3.5 Discussion

Proteomic analysis of Δ*gliT*Δ*gliZ* depicts a very similar response to gliotoxin as each of the single mutants. The SAM cycle appears dysregulated via the decrease in the expression of S-adenosyl homocysteinase and cobalmin-independant methionine synthase upon gliotoxin addition, suggesting that absence of *gliZ* is necessary for the altered expression of cobalmin-independant methionine synthase, as it's not dysregulated in Δ*gliT*. This dysregulation could help maintain L-homocysteine levels below a toxic level

Dysregulation of microtubule formation and endoplasmic reticulum components, in gliotoxin exposed cells, could suggest a reduction in protein synthesis in Δ*gliT*Δ*gliZ* upon gliotoxin challenge, and a subsequent decrease in the expression of certain proteins involved in the endoplasmic reticulum and structures which facilitate protein transport such as microtubules (Egan *et al.*, 2012).

Microtubules also have a structural role in the cell (Akashi *et al.*, 1994; Horio & Oakley 2005). The combined decrease in expression of microtubule components and actin may imply reduced cell growth/expansion in Δ*gliT*Δ*gliZ* when challenged with

gliotoxin which may be an attempt to conserve energy to mount a response to gliotoxin. Additionally, like Δ*gliT* and Δ*gliZ*, there is a down regulation of enzymes involved in the TCA cycle (AFUA_6G10660) and pentose phosphate pathway (AFUA_1G13500 and AFUA_5G09230) which also supports the hypothesis that the cell is conserving energy.

Similar to Δ*gliZ*, Δ*gliT*Δ*gliZ* shows altered expression in enzymes involved in glutathione biosynthesis 6-phosphogluconate dehydrogenase (AFUA_6G08050) and glutamate carboxypeptidase (AFUA_3G05450) in the absence of gliotoxin, which could result in the levels of glutathione to be altered. This suggests that silencing of the *gli* cluster causes dysregulation of glutathione biosynthesis, presumably due to glutathione being required in some part of the gliotoxin biosynthetic process which in the absence of *gliZ* is no longer present (Davis *et al.,* 2011).

4.5 Summary of the proteomic response to gliotoxin in *A. fumigatus, gliT* and *gliZ* strains

Proteomic results throughout this Chapter depict a very complex cellular response to gliotoxin exposure in *A. fumigatus*. Differentially expressed proteins identified in different strains were found to belong to similar functional categories suggesting a generic gliotoxin response present in each strain.

This study has highlighted the relationship seen between gliotoxin exposure and the dysregulation of the SAM cycle, most notably the altered expression of s-adenosyl homocysteine. Interestingly this protein was down regulated in all mutant strains in the presence of gliotoxin when compared to AF293 wild-type. It was also found to be both up-regulated and down-regulated in Δ*gliT* +/- gliotoxin indicating multiple isoforms of this enzyme being present which has some precedence in other organisms (Singhal *et al.,* 2013). All spots identified for s-adenosyl homocysteine which showed a decrease in protein expression were isolated from the same location on their respective gels. The form of S-adenosyl homocysteine which was found to up-regulated was isolated only once, with a different, more acidic pI unique to Δ*gliT* +/- gliotoxin. Demonstrating loss of *gliT* results in further altered expression of this enzyme which is not seen in any of the other strains. The altered expression of this enzyme in all mutant strains compared to AF293 wild-type in the presence of gliotoxin reveals that gliotoxin dysregulates the SAM cycle in these strains.

As mentioned previously, L-homocysteine accumulation can be toxic to cells (Fujita *et al.,* 2006). Dysregulation of the SAM cycle could result in altered levels of l-homocysteine as a by-product. The formation of Bm-GT via s-adenosyl methionine mediated methylation could induce such a dysregulation and may potentiate gliotoxin toxicity. A decrease in the expression of S-adenosyl homocysteinase would result in a corresponding reduction in l-homocysteine and prevent its accumulation. Interestingly, altered expression of this enzyme is not seen in Δ*gliZ* and Δ*gliT*Δ*gliZ* +/- gliotoxin indicating there is no change in the levels of this enzyme upon gliotoxin addition. Only Δ*gliT* +/- gliotoxin shows altered expression of S-adenosyl homocysteinase which suggests that dysregulation of the SAM cycle in this strain requires components of the *gli* cluster to be active as well as gliotoxin to be present.

Additionally, both Δ*gliZ* and Δ*gliT*Δ*gliZ* had altered expression of cobalamin-independant methionine synthase, another enzyme involved in the SAM cycle, in the presence of gliotoxin compared to AF293. This enzyme methylates L-homocysteine to form L-methionine which is required for the SAM cycle. Altered expression of both this and the S-adenosyl homocysteinase could help regulate L-homocysteine production via alteration of the SAM cycle. In contrast, Δ*gliT* does not show any altered expression of this enzyme which could suggest silencing of the *gli* cluster could be responsible for its altered expression in Δ*gliZ* and Δ*gliT*Δ*gliZ* in the presence of gliotoxin compared to AF293.

These results indicate that loss of *gliT* and *gliZ* leaves the strain unable to cope with gliotoxin exposure with increased sensitivity seen in these strains on gliotoxin plates which appears to result in the alteration of the SAM cycle causing these strains to dysregulate SAM cycle enzymes in an attempt to reduce gliotoxin toxicity, presumably influencing L-homocysteine levels. They also depict gliotoxin toxicity inducing a global response resulting in differential expression of proteins involved in metabolism, glutathione biosynthesis and the cellular response to stress, further highlighting its effects on the cell.

Chapter 5:

A. fumigatus transcriptomic response to gliotoxin

5.1 Introduction

Transcriptomics was used to gain a further insight into the global cellular response of *A. fumigatus* to the fungal secondary metabolite gliotoxin. ATCC46645 *A. fumigatus* and Δ*gliT*^{46645} were compared to elucidate the subsequent response exogenous gliotoxin presence has in these strains and highlight key areas affected by gliotoxin toxicity. These strains were utilised as ATCC46645 is a low gliotoxin producer, meaning the results seen here are due to the addition of exogenous gliotoxin and not endogenous biosynthesis.

5.2 *A. fumigatus* response to gliotoxin

ATCC46645 and Δ*gliT*^{46645} *A. fumigatus* mycelia were treated with either MeOH (solvent control) or 5 µg/ml gliotoxin for 3 h. A total concentration of 2 µg/µl of extracted total RNA was sequenced employing paired-end sequencing. The mean expression values for each gene were calculated from the resulting transcriptome data for each strain and treatment and employed to compare the difference in the transcriptomic response to gliotoxin for both ATCC46445 and Δ*gliT*^{46645}. These were then compared to each other to calculate the difference in expression levels of particular genes between the two strains.

Genes with ≥ 2 fold expression were deemed to show significant up-regulation while genes with ≤ 0.5 fold expression were significantly down-regulated. Table 5.1 illustrates the total number of genes found to be significantly up and down-regulated in response to gliotoxin in both strains. Between each strain comparison there is a major difference in the total number of genes differentially expressed suggesting different responses between ATCC46645 wild-type and Δ*gliT*^{46645}, presumably due to the loss of *gliT*. Figure 5.1 illustrates the number of genes shared between ATCC46645 +/- gliotoxin and Δ*gliT*^{46645} + gliotoxin which are either significantly up (A) or down (B) - regulated.

Table 5.1 Total number of genes significantly up and down regulated in ATCC46645 and Δ*gliT* +/- gliotoxin

Strain	WT[1] glio[2] / WT MeOH[3]	Δ*gliT* glio / Δ*gliT* MeOH	Δ*gliT* glio / WT glio
Total number of genes up-regulated[4]	636	1022	437
Total number of genes down-regulated[5]	828	2812	2410

1= ATCC46645 *A. fumigatus*. 2= represents strains treated with 5 µg/ml gliotoxin (glio). 3 = strains treated with methanol (MeOH) which served as a solvent control. 4 = genes were deemed significantly up-regulated if they had ≥ 2 fold expression 5 = genes were deemed significantly down-regulated if they had ≤ 0.5 fold expression.

A. Genes with ≥ 2 fold expression

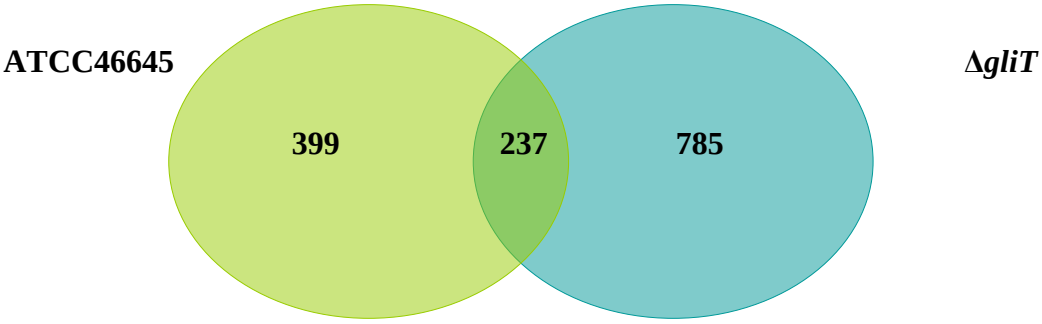

B. Genes with ≤ 0.5 fold expression

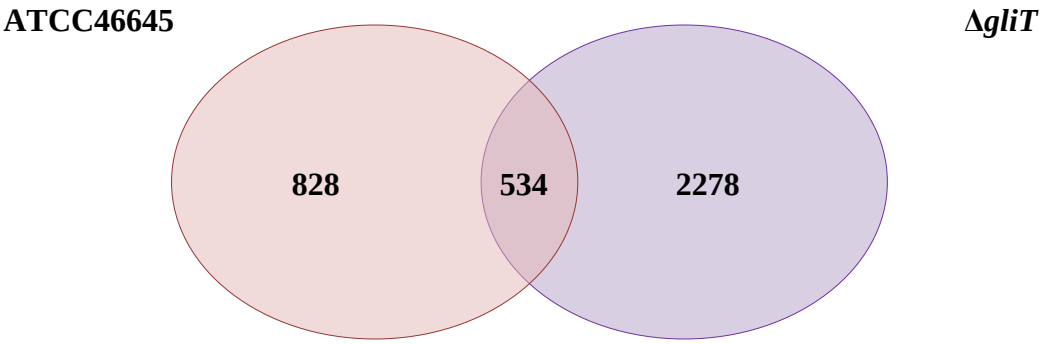

Figure 5.1 Number of significantly expressed genes which overlap in ATCC46645 and Δ*gliT* in the presence of gliotoxin. A- represents the number of genes which are significantly up-regulated in ATCC46645 and Δ*gliT* + gliotoxin. B- represents the number of genes which are significantly down-regulated in ATCC46645 and Δ*gliT* + gliotoxin

5.3 Pathways up- and down-regulated in response to gliotoxin in ATCC46645 and Δ*gliT*^{46645}

Table 5.2 shows the differential expression of genes involved in selected pathways which have been previously shown to be involved in gliotoxin toxicity and other forms of stress. It also shows various secondary metabolite clusters which are differentially regulated in response to gliotoxin in ATCC46645 and Δ*gliT*^{46645}.

Table 5.2 Mean expression values of genes differentially expressed in the presence of 5 µg/ml gliotoxin in ATCC46645 and Δ*gliT*^{46645} *A. fumigatus* strains

Gene ID	Putative function	Fold change WT + glio/ WT + MeOH	Fold change Δ*gliT*+ glio/ Δ*gliT* + MeOH	Fold change Δ*gliT* + glio/ WT + glio
Cysteine and methionine metabolism				
AFUA_1G04160	Has domain(s) with predicted pyridoxal phosphate binding, transaminase activity	0.261	0.060	0.257
AFUA_1G05570	Cysteine dioxygenase	0.611	0.452	0.576
AFUA_1G10130	Putative adenosylhomocysteinase	1.287	3.530	1.682
AFUA_1G10630	Putative S-adenosylmethionine synthetase	1.011	2.480	1.880
AFUA_1G15350	Has domain(s) with predicted O-acetyltransferase activity	0.703	0.093	0.159
AFUA_3G05480	Ortholog(s) have cystathionine gamma-synthase activity	1.003	2.415	2.358
AFUA_3G06830	Aspartate-semialdehyde dehydrogenase	0.983	2.233	2.313
AFUA_3G11640	Homoserine dehydrogenase	0.801	3.067	2.568
AFUA_4G03930	Putative cysteine synthase B	0.892	0.095	0.020
AFUA_4G03950	Ortholog(s) have cystathionine beta-lyase activity	1.273	2.134	1.675
AFUA_4G07360	Putative cobalamin-independent methionine synthase	0.903	4.112	4.138
AFUA_5G01500	Homocysteine S-methyltransferase activity	1.082	2.460	1.807

AFUA_5G02180	Cysteine synthase	0.771	2.914	2.957
AFUA_5G04250	Homocysteine synthase	0.490	0.888	1.880
AFUA_5G07210	Homoserine O-acetyltransferase	1.341	6.805	2.548
AFUA_5G08600	Ortholog(s) have serine O-acetyltransferase activity	2.734	2.384	0.783
AFUA_5G14410	Putative cysteine dioxygenase	1.246	0.205	0.142
AFUA_6G02490	Has domain(s) with predicted pyridoxal phosphate binding, transaminase activity	0.963	2.774	2.128
AFUA_6G03740	Ortholog(s) have role in ascospore formation	0.711	0.281	0.580
AFUA_6G04430	Ortholog(s) have oxidoreductase activity	0.834	0.492	0.567
AFUA_7G01370	Ortholog(s) have thiosulfate sulfurtransferase activity	0.452	0.473	0.841
AFUA_7G01590	Has domain(s) with predicted catalytic activity, pyridoxal phosphate binding activity	0.824	3.450	3.889
AFUA_8G04340	Putative cystathionine gamma-lyase	0.756	0.285	0.270

Sulphur metabolism

AFUA_1G10820	Ortholog(s) have role in methionine metabolic process, sulfate assimilation and intracellular localization	1.734	2.859	1.343
AFUA_2G15590	Putative sulphite reductase	2.126	4.836	2.378
AFUA_3G05480	Ortholog(s) have cystathionine gamma-synthase activity	1.003	2.415	2.358
AFUA_3G07960	Alpha-ketoglutarate-dependent taurine dioxygenase	3.445	1.852	0.966
AFUA_4G03930	Putative cysteine synthase B	0.892	0.095	0.020
AFUA_5G02180	Cysteine synthase (o-acetylserine (thiol)-lyase	0.771	2.914	2.957
AFUA_5G02190	Has domain(s) with predicted electron carrier activity,	2.354	1.217	0.561

	molybdenum ion binding, oxidoreductase activity			
AFUA_5G04250	Homocysteine synthase	0.490	0.888	1.880
AFUA_6G08920	Assimilatory sulfite reductase	0.624	3.474	2.537
AFUA_7G00350	Putative NAD-dependent dehydrogenase	1.934	3.371	1.483
AFUA_7G01370	Ortholog(s) have thiosulfate sulfurtransferase activity	0.452	0.473	0.841
AFUA_7G06030	Alpha-ketoglutarate-dependent taurine dioxygenase;	0.571	0.409	0.331
AFUA_8G02210	Alpha-ketoglutarate-dependent taurine dioxygenase	2.817	5.496	1.964

Glutathione metabolism				
AFUA_1G01370	Predicted glutathione S transferase	0.624	0.371	0.617
AFUA_2G00590	Predicted glutathione S transferase	0.447	0.424	0.198
AFUA_2G08370	Predicted glutathione S transferase	1.646	0.482	0.704
AFUA_3G05450	Putative glutamate carboxypeptidase	0.755	0.280	0.361
AFUA_3G08660	Ortholog of A. nidulans FGSC A4 : AN3028, A. niger CBS 513.88	1.824	2.057	0.955
AFUA_3G10830	Putative glutathione transferase	0.502	0.462	0.640
AFUA_4G08010	Putative ornithine decarboxylase	0.582	0.499	0.655
AFUA_4G13580	Gamma-glutamyltranspeptidase	0.453	0.065	0.109
AFUA_4G14530	Putative theta class glutathione S-transferase	0.921	0.028	0.055
AFUA_5G06610	Ortholog(s) have glutathione synthase activity	0.465	0.441	0.659
AFUA_6G00760	Predicted glutathione S transferase	0.598	0.288	0.571
AFUA_6G09690	Glutathione S-transferase encoded in the gliotoxin biosynthetic gene cluster	205.727	151.605	0.183
AFUA_7G04760	Gamma-glutamyltranspeptidase	0.866	0.292	0.339
AFUA_7G05500	Putative theta class glutathione transferase	3.849	0.412	0.119
AFUA_7G08450	Ornithine decarboxylase	0.585	6.754	8.468

AFUA_8G06540	Has domain(s) with predicted catalytic activity and role in polyamine biosynthetic process	2.272	3.544	0.530

Oxidative stress related proteins				
AFUA_1G02170	Ortholog(s) have role in protein refolding and mitochondrial matrix localization	0.640	0.306	0.387
AFUA_1G14550	Putative manganese superoxide dismutase	0.789	0.037	0.022
AFUA_2G02050	Putative peptidyL-prolyl ciS-trans isomerase	2.316	2.834	1.035
AFUA_2G04320	Has domain(s) with predicted FMN binding, oxidoreductase activity and role in oxidation-reduction process	1.439	0.161	0.168
AFUA_2G09290	Putative antigenic mitochondrial protein	2.469	2.768	1.043
AFUA_2G18030	Putative catalase	0.212	0.836	3.125
AFUA_3G02270	Mycelial catalase	1.647	0.067	0.439
AFUA_3G06540	Ortholog(s) have phosphoadenylyL-sulfate reductase (thioredoxin) activity	0.771	6.841	2.966
AFUA_3G14970	Putative thioredoxin	0.634	0.443	0.839
AFUA_4G05950	Ortholog(s) have disulfide oxidoreductase activity, role in cellular response to oxidative stress, response to osmotic stress	1.018	2.034	1.972
AFUA_4G12990	Putative thioredoxin reductase	2.427	5.076	1.543
AFUA_5G01440	Ortholog(s) have thioredoxin peroxidase activity, role in cell redox homeostasis, cellular response to oxidative stress	0.580	0.264	0.360

AFUA_5G09910	Putative p-nitroreductase family protein	0.583	0.356	0.722
AFUA_5G10270	Ortholog(s) have mRNA binding	0.375	0.835	1.467
AFUA_6G07210	Putative copper-zinc superoxide dismutase	1.232	2.206	1.813
AFUA_7G06420	Ortholog(s) have intracellular localization	1.162	0.406	0.244
AFUA_8G01090	Putative thioredoxin	0.843	0.033	0.073
AFUA_8G01670	Putative bifunctional catalase-peroxidase	3.096	1.095	0.215

Translation and Ribosomal Biogenesis				
AFUA_1G05080	Putative 60S ribosomal protein P0	2.265	5.292	2.113
AFUA_1G05500	40S ribosomal protein S12	2.481	6.270	2.174
AFUA_1G12890	Putative 60S Ribosomal protein L5	2.181	6.717	2.475
AFUA_1G15730	40S ribosomal protein S22	2.495	5.754	2.327
AFUA_2G02150	Putative ribosomal protein S10	2.492	5.421	2.205
AFUA_2G09200	60S ribosomal protein L30	2.036	5.310	2.364
AFUA_2G10100	Allergen Asp f 8; putative ribosomal protein P2	2.326	7.066	2.448
AFUA_2G10300	40S ribosomal protein S17	2.404	5.068	2.415
AFUA_3G05600	60S ribosomal protein L27a	2.065	5.677	2.569
AFUA_3G06760	Ribosomal protein L37	2.231	5.823	2.831
AFUA_3G12300	60S ribosomal protein L22	2.637	6.149	2.126
AFUA_4G07730	60S ribosomal protein L11	2.156	5.449	2.500
AFUA_5G03020	60S ribosomal protein L4	2.291	5.402	2.013
AFUA_5G05630	60S ribosomal protein L23	2.209	5.340	2.606
AFUA_5G06360	60S ribosomal protein L8	2.232	5.715	2.242
AFUA_6G02440	60s ribosomal protein L24	1.895	5.251	2.594

AFUA_6G05200	60S ribosomal protein L28	1.994	5.573	2.476
AFUA_6G11260	Ribosomal protein L26	2.026	5.199	2.386
AFUA_6G12660	40S ribosomal protein S10b	2.554	5.563	2.137
AFUA_6G13250	60S ribosomal protein L31e	2.164	5.294	2.523

Leucine/Valine and Isoleucine degradation				
AFUA_2G10920	Putative enoyL-CoA hydratase/isomerase family protein	0.603	0.282	0.490
AFUA_2G12450	Putative hydroxymethylglutaryL-CoA lyase	0.559	0.231	0.335
AFUA_3G01450	Putative 3-methyL-2-oxobutanoate dehydrogenase	0.314	0.036	0.089
AFUA_3G09470	Has domain(s) with predicted coenzyme binding, nucleotide binding, phosphogluconate dehydrogenase (decarboxylating) activity	0.709	3.609	1.687
AFUA_4G12010	Putative 2-oxo acid dehydrogenases acyltransferase	0.267	0.027	0.106
AFUA_4G12870	Putative methylmalonate-semialdehyde dehydrogenase; transcript up-regulated in conidia exposed to neutrophils	0.636	0.256	0.339
AFUA_5G01250	Has domain(s) with predicted coenzyme binding, nucleotide binding, phosphogluconate dehydrogenase (decarboxylating) activity	0.283	0.058	0.159
AFUA_5G08910	Putative 3-methylcrotonyL-CoA carboxylase subunit alpha	0.419	0.090	0.251
AFUA_5G08930	Putative isovaleryL-CoA dehydrogenase	0.440	0.076	0.208
AFUA_5G08940	Ortholog(s) have methylcrotonoyL-CoA carboxylase activity	0.510	0.150	0.305
AFUA_5G10280	Has domain(s) with predicted 3-hydroxyisobutyrate	0.359	0.489	0.816

	dehydrogenase activity			
AFUA_6G08830	2-oxoisovalerate dehydrogenase complex alpha subunit	0.493	0.068	0.151
AFUA_6G11020	Has domain(s) with predicted 3-hydroxyisobutyrate dehydrogenase activity	0.512	0.025	0.072
AFUA_6G11430	Putative aldehyde dehydrogenase	0.753	0.134	0.135
AFUA_6G12250	Has domain(s) with predicted CoA-transferase activity	0.249	0.025	0.336
AFUA_6G14200	Putative acetyL-CoA acetyltransferase	0.451	0.101	0.197
AFUA_7G01000	Putative alcohol dehydrogenase involved in ethanol metabolism	0.024	0.399	1.196
AFUA_7G01720	Has domain(s) with predicted catalytic activity and role in metabolic process	3.311	2.241	0.578
AFUA_7G04080	3-ketoacyL-CoA thiolase	0.441	0.587	0.950
AFUA_8G07210	HydroxymethylglutaryL-CoA synthase	0.731	0.764	2.068

Gliotoxin biosynthetic cluster				
AFUA_6G09630	Zn2Cys6 binuclear transcription factor	7.553	1.722	0.158
AFUA_6G09640	Predicted 1-aminocyclopropane-1-carboxylic acid synthase	3.266	0.847	0.296
AFUA_6G09650	Predicted membrane dipeptidase	4.622	0.119	0.097
AFUA_6G09660	Non-ribosomal peptide synthetase	69.962	10.582	0.231
AFUA_6G09670	Predicted cytochrome P450 monooxygenase	29.113	25.645	0.482
AFUA_6G09680	Predicted O-methyltransferase	3102.029	108.138	0.238
AFUA_6G09690	Glutathione S-transferase	205.727	151.605	0.183
AFUA_6G09700	Predicted protein	147.280	84.972	0.248
AFUA_6G09710	Predicted major facilitator type glioxin transporter	914.854	374.901	0.483

AFUA_6G09720	Predicted methyltransferase	25.973	10.363	0.261
AFUA_6G09730	Predicted cytochrome P450 monooxygenase	103.947	21.798	0.214
AFUA_6G09740	Gliotoxin sulfhydryl oxidase	534.993	0.159	0.001
AFUA_6G09745	Ortholog of N. fischeri NRRL 181 : NFIA_055440, NFIA_112700	33.129	3.294	0.130

L-tyrosine degradation				
AFUA_2G04190	Ortholog of A. nidulans FGSC A4 : AN1900	0.401	0.415	0.402
AFUA_2G04200	4-hydroxyphenylpyruvate dioxygenase	0.351	0.014	0.041
AFUA_2G04210	Protein with no conserved domains and no similarities to any proteins with known function	0.476	0.025	0.056
AFUA_2G04220	Homogentisate 1,2-dioxygenase involved	0.120	0.012	0.095
AFUA_2G04230	Putative fumarylacetoacetate hydrolase	0.087	0.005	0.044
AFUA_2G04240	Maleylacetoacetate isomerase	0.127	0.016	0.120
AFUA_2G04262	Ortholog(s) have nucleic acid binding transcription factor activity	0.292	0.199	0.506

Pigment biosynthesis				
AFUA_2G17530	Laccase involved in conidial pigment biosynthesis	1.986	0.379	0.230

AFUA_2G17540	Multicopper oxidase involved in conidial pigment biosynthesis	7.984	0.000	0.000
AFUA_2G17550	Conidial pigment biosynthesis protein with a role in polyketide shortening	5.936	0.346	0.244
AFUA_2G17560	1,3,6,8-tetrahydroxynaphthalene reductase involved in conidial pigment biosynthesis	1.209	0.512	0.264
AFUA_2G17580	Scytalone dehydratase involved in conidial pigment biosynthesis	0.935	0.423	0.319
AFUA_2G17600	Polyketide synthase involved in biosynthesis of the conidial pigment	1.063	0.863	0.395

Fumitremorgin B Biosynthesis				
AFUA_8G00170	Putative non-ribosomal peptide synthetase (NRPS)	0.133	0.031	0.157
AFUA_8G00190	Putative cytochrome P450	0.376	0.065	0.321
AFUA_8G00200	Putative O-methyltransferase	0.385	0.047	0.275
AFUA_8G00210	Putative brevianamide F prenyltransferase	0.363	0.009	0.139
AFUA_8G00220	Cytochrome P450	0.642	0.000	0.000
AFUA_8G00230	Non-heme Fe(II) and alpha-ketoglutarate-dependent dioxygenase	0.708	0.005	0.026
AFUA_8G00240	Putative cytochrome P450	1.402	0.051	0.097
AFUA_8G00250	Putative prenyltransferase	1.410	0.033	0.065
AFUA_8G00260	Putative ankyrin repeat protein	0.963	0.466	0.561

5.3.1 Gliotoxin alters cysteine and methionine biosynthesis

Previously, proteomic results indicated that the L-cysteine and L-methionine metabolic pathway was dysregulated when challenged with gliotoxin. Transcriptomic results were identified within this pathway to help corroborate what was seen at the protein level, and further elucidate gliotoxins' affect on this pathway. Gliotoxin presence induces differential expression of genes involved in the L-cysteine and L-methionine biosynthetic pathway. Interestingly in ATCC46445, only four genes show significantly altered expression after gliotoxin challenge. These include genes which encode an L-homocysteine synthase (AFUA_5G04250), a putative transaminase (AFUA_1G04160), a putative thiosulfate sulfurtransferase (AFUA_7G01370) and a putative serine O-acetyltransferase (AFUA_5G08600) (Sugui *et al.,* 2008; Noma *et al.,* 2009). Interestingly in Δ*gliT* +/- gliotoxin, a significant number of genes differentially expressed. Gliotoxin induces significant altered expression of genes involved in L-cysteine and L-methionine biosynthesis, 14 of which showed a > 2.2 fold increase in expression. All genes which have increased expression encode enzymes involved in L-cysteine, L-cystathionine, L-methionine, L-homocysteine and S-adenosyl methionine biosynthesis (Kanehisa *et al.,* 2004). This suggests exogenous gliotoxin increases the need for increased expression of components which feed into the SAM cycle and the SAM cycle itself. The S-adenosyl homocysteinase gene (AFUA_1G10130) shows a 3.5 fold increase in expression, which is similar to what was seen in the proteomics results for the same condition used here whereby S-adenosyl homocysteinase was seen to be differentially expressed (both up and down-regulated), indicating dysregulation of this gene induced by gliotoxin, is continuing on to the protein level.

Genes with decreased expression encode enzymes involved in the methionine salvage pathway and in SAM de-methylation and subsequent S-adenosyl-L-homocysteine production, which could result in a corresponding decrease in S-adenosyl-L-homocysteine being produced in the cell.

5.3.2 Sulphur metabolism

Section 5.3.1 depicts gliotoxin mediated dysregulation of the cysteine and methionine metabolic pathway. Enzymes involved in L-homocysteine biosynthesis were significantly up-regulated in Δ*gliT* +/- gliotoxin. This amino acid can also be produced via the sulphur metabolic pathway acting as another source of L-homocysteine for the cell. In wild-type cells challenged with gliotoxin, five genes which encode enzymes involved in sulphite, sulphate and sulphide biosynthesis showed a significant increase in expression. Interestingly, only two genes showed a decrease in their expression, a putative thiosulfate sulphur-transferase (AFUA_7G01370) and homocysteine synthase (AFUA_5G04250).

In Δ*gliT* +/- gliotoxin, three genes have a decrease in their expression. Similar to wild-type, one of these genes encodes an enzyme involved in thiosulfate to sulphite conversion. A total of 8 genes with increased gene expression were found to encode enzymes involved in sulphite, sulphide, L-cysteine and L-homocysteine biosynthesis. This is at odds with the wild-type which shows reduced expression in homocysteine synthase, highlighting two very different responses in these two *A. fumigatus* strains to gliotoxin.

5.3.3 Glutathione metabolism

Previous results have illustrated how glutathione levels play an important role in gliotoxin toxicity. The aforementioned pathways are also linked to the glutathione metabolic pathway with L-homocysteine, L-cysteine and L-cystathionine being utilised to form glutathione. In ATCC46645 +/- gliotoxin, a total of three genes have a significant increase in their expression, two of which are glutathione transferases (AFUA_6G09690 and AFUA_7G05500). The former is *gliG*, a component of the *gli* biosynthetic cluster. Prior work by Schrettl *et al.,*, has shown that gliotoxin induces expression of certain components of the *gli* cluster, and the increase in expression seen here could be due to this self regulatory effect (Schrettl *et al.,* 2010). Also, there are a total of ten putative glutathione transferases involved in the same function in this pathway indicating some redundancy.

Interestingly, genes involved in glutathione biosynthesis, and glutathione processing, have a significant decrease in expression upon gliotoxin addition in these cells. This could suggest glutathione biosynthesis is not advantageous during gliotoxin exposure thus genes such as glutathione synthase (AFUA_5G06610) and γ-glutamyl trans-peptidase (AFUA_4G13580) show reduced expression. Similar to previous results, Δ*gliT* shows a dramatic change in its response to gliotoxin. As in wild-type, there is an increase in the expression of genes which encode enzymes involved in glutathione S-transferase activity (AFUA_6G09690), glutathione reduction (AFUA_3G08660), polyamine biosynthesis (AFUA_8G06540) and ornithine de-carboxylation (AFUA_7G08450). *gliG* showed the highest increase in expression, and could be due to gliotoxin influence on the *gli* cluster as mentioned earlier. Unlike ATCC46645, which showed three genes with decreased expression, Δ*gliT* has twelve genes with a significant decrease in expression, seven of which encode glutathione transferases. The remaining are involved in glutathione synthesis (AFUA_5G06610) and glutathione degradation (AFUA_3G05450, AFUA_4G13580 and AFUA_7G04760). These results suggest glutathione biosynthesis genes are dysregulated in response to gliotoxin with genes involved in glutathione salvage and glutathione synthesis being equally affected in Δ*gliT* and to a lesser extent wild type cells.

5.3.4 Oxidative stress related proteins

Previous results from this study have shown gliotoxin induces oxidative stress in *A. fumigatus*. Results presented in section 5.3.3 have shown that gliotoxin alters the expression of genes involved in glutathione biosynthesis, a radical scavenger and key component of the OS response (Alton Meister 1988; Izawa *et al.,* 1995) . One key difference between wild-type and Δ*gliT* +/- gliotoxin, is the altered expression of genes which are involved in the OS response. An increase in the expression of relatively few OS related genes is seen in ATCC46645 +/- gliotoxin with catalase-peroxidase (AFUA_8G01670), thioredoxin reductase (AFUA_4G12990), a putative peptidyl-prolyl cis-trans isomerise (AFUA_2G02050) which has orthologs seen to accumulate during DNA replication stress and Hsp 60 (AFUA_2G09290) all showing a significant increase

in their expression upon gliotoxin addition. Two genes had a decrease in their respective expressions: a putative catalase (AFUA_2g18030) and AFUA_5G10270 which has orthologs with mRNA binding and stress response functions.

Unlike ATCC46645, Δ*gliT* shows a decrease in the expression of manganese super oxide dismutase (AFUA_1G14550) and a simultaneous increase in the expression of a copper-zinc superoxide dismutase (AFUA_6G07210), both are involved in hydrogen peroxide dis-mutation and are located in different parts of the cell. A decrease in the expression of a mycelia catalase (AFUA_3G02270), two thioredoxins (AFUA_3G14970 and AFUA_8G01090), thioredoxin-peroxidase (AFUA_5G01440), oxido-reductase (AFUA_2G04320), p-nitroreductase (AFUA_5G09910) and AFUA_7G06420 which has orthologs with NADPH oxid-oreductase activity, were all seen in Δ*gliT* +/- gliotoxin. Similar to wild type, there is increased expression of the thioredoxin reductase (AFUA_4G12990), peptidyl-prolyl cis-trans isomerise (AFUA_2G02050) and Hsp60 (AFUA_2G09290). Contrary to this, there is a significant increase in the expression of a sulphate reductase with thioredoxin activity (AFUA_3G06540) and a disulphide oxido-reductase (AFUA_4G05950) which may have increased expression to compensate for *gliT* loss fulfilling its oxido-reductase activity, albeit less efficiently.

5.3.5 Ribosomal biogenesis

Chapter 5 highlighted the dysregulation of certain protein biosynthesis and processing components had in the presence of gliotoxin. At the transcriptomic level this is still the case, with Table 5.2 showing the top 20 genes to be differentially regulated out of a total number of 62. The majority of genes listed in Table 5.3 have a significant increase in their expression indicating gliotoxin induces a comprehensive response in this pathway. Although most of the genes are up-regulated in both ATCC46645 and Δ*gliT* +/- gliotoxin, only in Δ*gliT* are all ribosomal related genes up-regulated. Secondly, the level of up-regulation is significantly higher in Δ*gliT* when compared to ATCC46645 + gliotoxin, suggesting in the absence of *gliT* there is a greater demand for the expression of these genes than in wild-type cells.

5.3.6 Leucine/valine and isoleucine degradation

Different enzymes involved in the leucine/valine and isoleucine degradation pathway were found to be differentially expressed in protein lysates extracted from cells treated with gliotoxin. As seen in Table 5.3, gliotoxin appears to induce a decrease in the expression of the majority of genes involved in this pathway. There are some exceptions, such as AFUA_7G01720 which shows increased expression in both ATCC46645 and Δ*gliT* +/- gliotoxin. This encodes an enzyme which catalyses the formation of acetyl-acetate and acetyl CoA which is utilised in the citrate cycle.

There is also significantly increased expression of the hydroxymethylglutaryL-CoA synthase (AFUA_8G07210) in Δ*gliT* + gliotoxin when compared to ATCC46645 + gliotoxin, suggesting an increased need for acetyL-CoA biosynthesis related genes to be up-regulated in the presence of gliotoxin once *gliT* is no longer present. The reduction of so many genes involved in this pathway could result in an increased availability of these amino acids for subsequent translation. This is further supported by the fact two enzymes involved in leucine/valine and isoleucine biosynthesis (AFUA_1G15780 and AFUA_2G10420) were found to be up-regulated in Δ*gliT* in response to gliotoxin.

5.3.7 Gliotoxin biosynthetic cluster

Schrettl *et al.,,* showed addition of gliotoxin induced increased expression of genes involved in gliotoxin biosynthesis (Schrettl *et al.,* 2010). Gliotoxin exposure has also been demonstrated to induce an up-regulation of gliotoxin specific proteins in *A. fumigatus* (Schrettl *et al.,* 2010). Un-surprisingly, there is a significant increase in the regulation of genes of the *gli* cluster, ranging from 3-3102 fold. The dramatic increase in expression of *gliM* (AFUA_6G09680) may suggest a role in the detoxification of gliotoxin, explaining why it is so highly up-regulated. Interestingly, the corresponding expression levels in Δ*gliT* +/- gliotoxin are relatively low when compared to ATCC46645 +/- gliotoxin, and are significantly decreased when Δ*gliT* + gliotoxin is

compared to ATCC46645 + gliotoxin. This could suggest *gliT* presence is necessary for such high amounts of expression of the *gli* cluster. Unlike ATCC46645 +/- gliotoxin, Δ*gliT* +/- gliotoxin shows no increase in the expression of the clusters' transcriptional regulator *gliZ* (AFUA_6G09630), or of the L-amino-cyclopropane-1-carboxylic acid *gliI* (AFUA_6G09640). Surprisingly, there is a significant decrease in the expression of the dipeptidase *gliJ* (AFUA_6G09650).

5.3.8 L-tyrosine degradation

Addition of gliotoxin alters expression of different gene clusters in *A. fumigatus* as seen in Section 5.3.7. The L-tyrosine degradation pathway consists of a six gene cluster of (Schmaler-ripcke *et al.,* 2009). In both ATCC46645 +/- gliotoxin and Δ*gliT* +/- gliotoxin all six of these genes have a significant decrease in their expression. Interestingly, these same genes are significantly lower in Δ*gliT* + gliotoxin when compared to ATCC46645 + gliotoxin. These genes encode enzymes involved in the degradation of L-tyrosine into acetoacetate and fumarate, components of the citrate cycle. These same genes have been identified in encoding enzymes involved in an alternative melanin, pyomelanin, biosynthetic process in *A. fumigatus* (Schmaler-Ripcke *et al.,* 2009). Melanin and pyomelanin are two types of pigments produced in abundance in conidia and also possess a role in the oxidative stress response (Nosanchuk & Casadevall 2003).

5.3.9 DHN-melanin biosynthesis

Biosynthesis of dihyroxynaphthalene (DHN)-melanin is carried out via a six gene cluster located on chromosome 2. DHN-melanin is an important pigment utilised in conidia in its cell wall. It has also been demonstrated to be important in virulence acting as a defence mechanism against host reactive oxygen species and adherence to epithelial cells. Both a multi-copper oxidase (AFUA_2G17540), also known as *abr1*, and conidial pigment biosynthesis protein (AFUA_2G17550) also known as *ayg1*, showed a significant increase in their respective expression in ATCC46645 +/-

gliotoxin. These two genes encode enzymes involved in the initial steps of DHN-melanin biosynthesis.

Contrary to this, Δ*gliT* +/- gliotoxin, shows a decrease in the expression of three genes in this pathway: a laccase (AFUA_2G17530) *abr2*, *ayg1* and scytalone dehydratase (AFUA_2G17580) *arp1*. Interestingly, no transcripts of *abr1* in Δ*gliT* + gliotoxin were found, which could be due to the gene being expressed but at levels too low to be detected. Bar *abr1*, all other genes in this cluster were significantly lower in Δ*gliT* + gliotoxin when compared to ATCC46645 + gliotoxin indicating the entire cluster is being down-regulated in Δ*gliT* in the presence of gliotoxin compared to wild-type.

5.3.10 Fumitremorgin B biosynthesis

Fumitremorgin B is a secondary metabolite produced in *A. fumigatus* and other filamentous fungi. It acts as a mycotoxin, which can inhibit microtubule formation and is an increasing problem in the food industry, encoded by a nine gene cluster located on chromosome 8 (Grundmann *et al.*, 2008). Both ATCC46645 +/- gliotoxin and Δ*gliT* +/- gliotoxin have a decrease in the expression of certain parts of this cluster.

In ATCC46645 +/- gliotoxin, four of the nine genes show a decrease in their expression. These include the clusters putative non-ribosmal peptide synthase (AFUA_8G00170) *ftmA*, cytochrome P450 (AFUA_8G00190) *ftmC*, o-methyltransferase (AFUA_8G0020) *ftmD* and brevianamide F prenyL-transferase (AFUA_8G00210) *ftmPT1*. These same genes are also decreased in Δ*gliT* +/- gliotoxin, however so are the non-heme F (II) and α-ketoglutarate-dependant dioxygenase (AFUA_8G00230) *ftmF*, putative cytochrome P450 (AFUA_8G00240) *ftmG*, putative prenyL-transferase (AFUA_8G00250) *ftmPT2* and a putative ankyrin repeat protein (AFUA_8G00260) *ftml*. Similar to *abr1* in section 5.3.10, another cytochrome P450 (AFUA_8G00220) *ftmE*, had no detectable levels of transcript in Δ*gliT* + gliotoxin which could mean that the levels are reduced to such a low level in this strain that they cannot be detected or that addition of gliotoxin in Δ*gliT* completely switches off this gene.

5.4. Quantitative PCR (qPCR) of *A. fumigatus gliT* and *gliZ* strains

Results shown in the previous section further highlight key pathways involved in the response to gliotoxin. Some of these results corroborate what has discussed in Chapter 4, with genes involved in glutathione metabolism and the SAM cycle being significantly dysregulated when challenged with gliotoxin. To supplement these results and verify the trends of gene expression seen here, qPCR was carried out on selected genes which showed altered expression in response to gliotoxin and/or strain background. Utilising cDNA from the mRNA extracted from mycelia of *A. fumigatus* strains exposed to 5 µg/ml gliotoxin, it is possible to quantify the number of transcripts of a given gene using specific primers and a fluorescent agent. The amount of fluorescence will be proportional to the amount of that transcript present in that sample.

Additionally, cDNA was also constructed from Δ*gliZ*^{293} and Δ*gliT*Δ*gliZ*^{293}exposed cells, to investigate how the expression of these genes may be affected in these strains compared to each other and ATCC46645 and Δ*gliT*^{46645} with the aim of further elucidating the difference in their respective response to gliotoxin exposure. *GliM* (AFUA_6G09680) and AFUA_2G11120 were two of the four genes selected as firstly both had relatively high increases in expression in the presence of gliotoxin, with *gliM* being the most up-regulated gene and AFUA_2G11120 being the fourth highest. Secondly both have been annotated with predicted methyltransferase activity and could be involved in bis-methylating gliotoxin thus their large expression values. *GliJ* (AFUA_6G09650) was also chosen as it had differential expression between ATCC46645 +/- gliotoxin and Δ*gliT* +/- gliotoxin, showing an increase in its expression in wild-type cells in the presence of gliotoxin, but a decrease in Δ*gliT*. This may imply *gliT* requirement for its regulation in this gliotoxin mediated response, which the other strains could help elucidate.

Lastly *laeA* (AFUA_1G14660) was chosen due to the fact it has a decrease in its expression in Δ*gliT* +/- gliotoxin. Also, its involvement as a transcriptional regulator of secondary metabolite biosynthesis could indicate if there is a similar response in the other mutant strains to gliotoxin and down-regulation of particular secondary metabolite clusters regulated by *laeA*. Each of these genes would help strengthen the results seen in

the transcriptomic data from section 5.3, while also illustrating if the same response is happening in the other *gli* mutants.

5.4.1 *GliM* and AFUA_2G11120 relative expression

Both *GliM* and AFUA_2G11120 are predicted methyL-transferases which are also highly up-regulated in response to gliotoxin. As seen in Figure 5.2 A (*GliM)* and B (AFUA_2G11120), the relative gene expression can be seen when compared to the household keeping gene *calm* to ensure that any rise is due to that strain and condition and not simply a rise in general transcription. Interestingly, no analysis could be carried out for *gliM* in MeOH treated cells. One reason for this could be that this method is not as accurate as RNA Seq and is unable to detect low levels of transcripts, which further suggests as it can be detected in gliotoxin treated cells that *gliM* is induced under gliotoxin presence and in its absence *gliM* expression is very low.

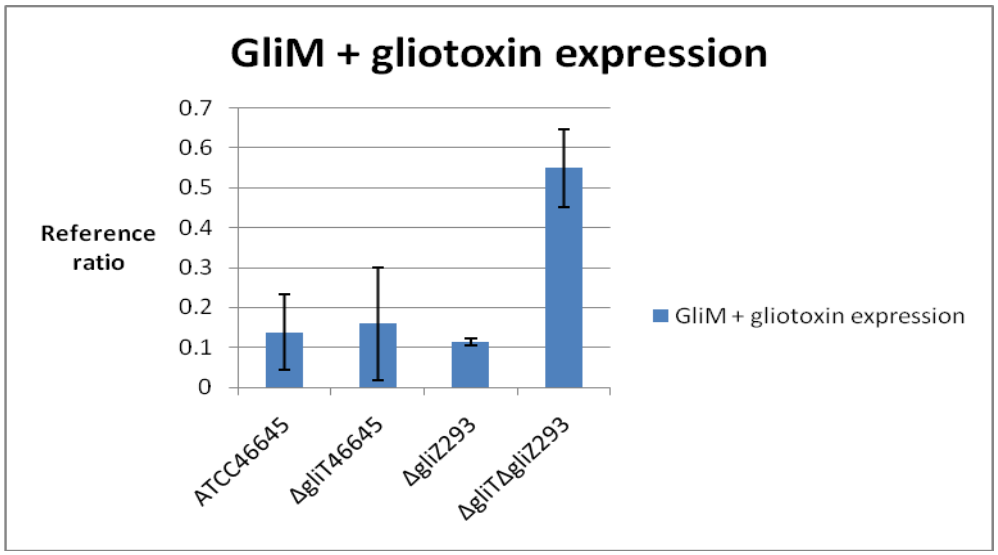

Figure 5.2 A Relative *gliM* expression in *A. fumigatus* strains ATCC46645, Δ*gliT*^{46645}, Δ*gliZ*^{293} and Δ*gliT*Δ*gliZ*^{293} in the presence of 5 µg/ml gliotoxin.

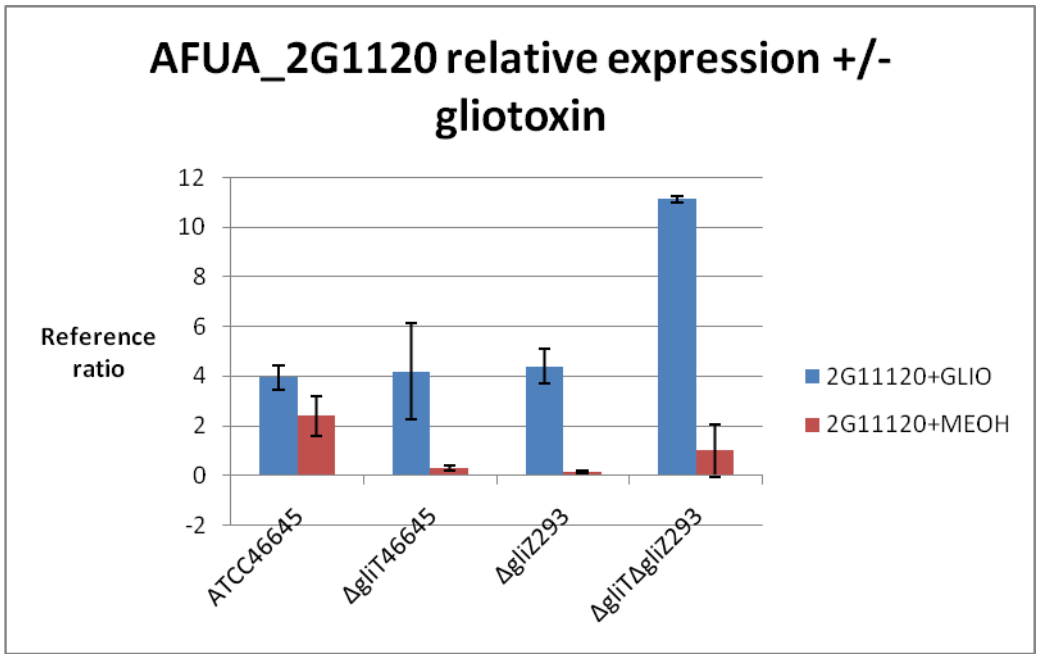

Figure 5.2 B Relative AFUA_2G11120 expression in *A. fumigatus* strains ATCC46645, Δ*gliT*^{46645}, Δ*gliZ*^{293} and Δ*gliT*Δ*gliZ*^{293} in the presence of methanol (MeOH) and 5 µg/ml gliotoxin (GLIO). The figures show mean ratio values of *GliM* and AFUA_2G11120 expression compared to the household keeping gene *calm* (reference ratio).

Δ*gliT*Δ*gliZ*^{293} has the highest expression of both *gliM* and AFUA_2G11120. Unlike *gliM*, AFUA_2G11120 is expressed under basal conditions and similar to what is seen in the transcriptomic results from Section 5.3, gliotoxin presence induces a significant increase in the expression of AFUA_2G11120.

5.4.2 g*liJ* relative expression

g*liJ* encodes a dipeptidase involved in gliotoxin structure formation. This could suggest *gliT* is necessary for the gliotoxin regulated increase in expression of all *gli* cluster genes. g*liJ* relative expression in *A. fumigatus* strains can be seen in Figure 5.3.

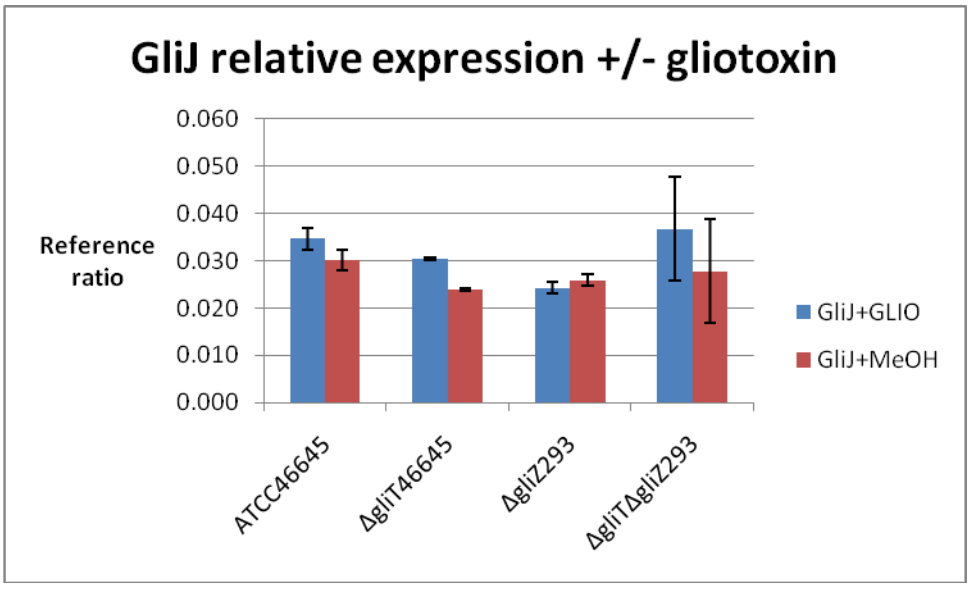

Figure 5.2 Relative *gliJ* expression in *A. fumigatus* strains ATCC46645, Δ*gliT*^{46645}, Δ*gliZ*^{293} and Δ*gliT*Δ*gliZ*^{293} in the presence of methanol (MeOH) and 5 µg/ml gliotoxin (GLIO). The figure shows mean ratio values of *gliJ* expression compared to the household keeping gene *calM* (reference ratio).

Contrary to what was seen in section 5.3, *gliJ* expression in Δ*gliT* is not lowered in response to gliotoxin exposure here. However, both the decrease in *gliJ* expression in Δ*gliT* + gliotoxin when compared to ATCC46645 + gliotoxin and the increase in its expression in ATCC46645 +/- gliotoxin are the same as what was described earlier, corroborating what was seen in the RNA Seq data.

5.4.3 *LaeA* relative expression

The control of secondary metabolites in cells is very important as many can be highly reactive and have adverese effects on the organism if not kept in check. One such way to do this is via various transcriptional regulators such as *laeA* which respond to various external and internal stimuli and responds accordingly in the regulation of their metabolites. The presence of gliotoxin appears to dysregulate secondary metabolites and gene clusters as shown in Section 5.3. As *laeA* is itself dysregulated in Δ*gliT* and has been described in previous work to influence many different secondary metabolites, its expression was examined here (Figure 5.4).

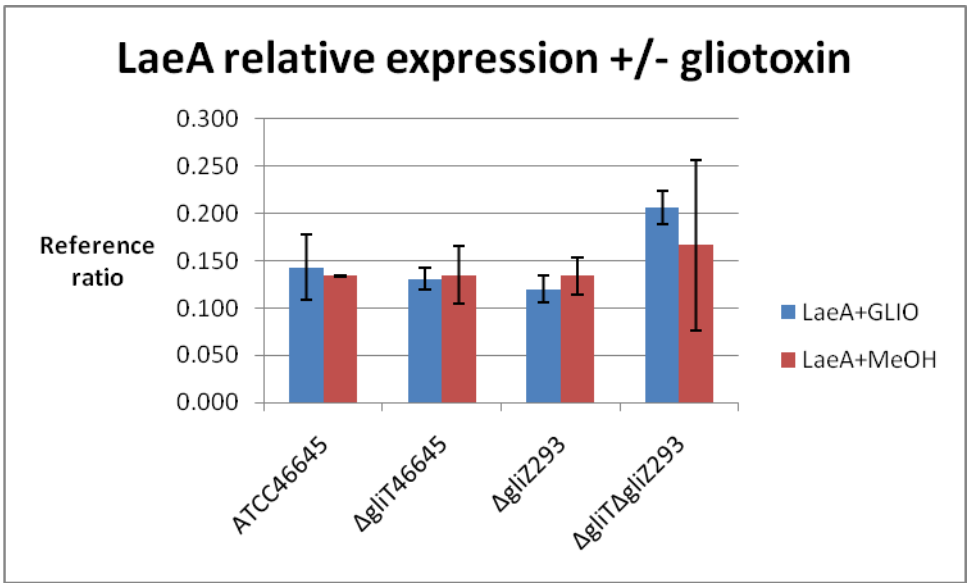

Figure 5.3 Relative *laeA* expression in *A. fumigatus* strains ATCC46645, Δ*gliT*^{46645}, Δ*gliZ*^{293} and Δ*gliT*Δ*gliZ*^{293} in the presence of methanol (MeOH) and 5 µg/ml gliotoxin (GLIO). The figure shows mean ratio values of *laeA* expression compared to the household keeping gene *calM* (reference ratio).

In Figure 5.3 it is hard to see if Δ*gliT* shows reduced expression of *laeA* as seen in the transcriptomics. This is common between MeOH vs gliotoxin treated samples, however any difference between individual strains is clear.

5.5. RNA Seq comparision of *A. fumigatus* Δ*gliT* and *S. cerevisiae* G600

To further elucidate gliotoxins mode of toxicity, the transcriptome response of Δ*gliT* was compared to a similar transcriptome study carried out in yeast (O'Brien, 2011). *S. cerevisiae* shows relative phenotypic sensitivity > 8 µg/ml gliotoxin (chapter 6), similar to Δ*gliT*. This work used two different concentrations of gliotoxin. 16 and 64 µg/ml to induce a response in the yeast compared to a methanol control. Selected pathways which were differentially regulated in Δ*gliT* were compared with orthologous pathways in *S. cerevisiae* cells treated with the lower, 16 µg/ml gliotoxin in order to uncover some similarities between these two gliotoxin sensitive strains.

Orthologs of genes from the different pathways listed in Table 5.2 were checked for significant up- and down- regulation (≥ 2 fold or ≤ 0.5 fold expression) in *S. cerevisiae* cells where applicable. In certain cases no orthology could be found due to certain genes not having been identified in yeast suggesting these evolved at a later time point.

Interestingly there are some similarities between the two fungi. Looking at the various genes differentially regulated in response to gliotoxin, the yeast transcriptome response appears to be more like Δ*gliT* than *A. fumigatus* wild-type. Table 5.4 lists genes differentially regulated in selected pathways in *A. fumigatus* ATCC46645, Δ*gliT* and *S. cerevisiae* in the presence of gliotoxin. Like Δ*gliT*, genes involved in L-cysteine, L-cystathionine, L-methionine and S-adenosyl methionine show significant increase in their expression in *S. cerevisiae* upon gliotoxin addition. There is also one gene found to have a significant decrease in expression in all three strains (YOR251c/TOM1) which encodes an enzyme involved in catalysing the formation of thio-sulfate and pyruvate from sulphite. Unlike Δ*gliT*, *S. cerevisiae* does not have an increase in the expression of S-adenosyl homocysteinase, presumably increased in Δ*gliT* to regulate the SAM cycle, suggesting this gene does not need to be significantly altered to maintain the SAM cycle in *S. cerevisiae*.

Similarly, genes involved in sulphur metabolism are also affected by gliotoxin presence in *S. cerevisiae* with significant expression of certain genes in the yeast which are also significantly altered in Δ*gliT*, and to a lesser extent ATCC46645, in a comparable fashion. In all three organisms, there is an increase in genes which encode enzymes involved in sulphide biosynthesis as well as a decrease in one gene involved in sulphite biosynthesis. Analogous to the L-cysteine and L-methionine metabolic pathway, *S. cerevisae*'s transcriptomic response to gliotoxin within the sulphur metabolic pathway is more akin to Δ*gliT* than ATCC46645 wild-type, with genes involved in L-cysteine and L-homocysteine having significant up-regulation.

Table 5.4 Mean expression values of genes differentially expressed in the presence of 5 µg/ml gliotoxin in ATCC46645 and Δ*gliT*^{46645} *A. fumigatus* strains and 16 µg/ml *S. cerevisiae*

Gene ID	Putative function	Fold change WT + glio/ WT + MeOH	Fold change Δ*gliT* + glio/ Δ*gliT* + MeOH	Fold change *S. cerevisae* + glio/ *S.cerevisae* + MeOH
Cysteine and methionine metabolism				
AFUA_5G02180/YLR303w	Cysteine synthase	0.771	2.914	5.5
AFUA_4G03950/YGL184c	Ortholog(s) have cystathionine beta-lyase activity	1.273	2.134	2
AFUA_7G01590/YFR055w	Has domain(s) with predicted catalytic activity, pyridoxal phosphate binding activity	0.824	3.450	4
AFUA_8G04340/YAL012w	Putative cystathionine gamma-lyase	0.756	0.285	4.06
AFUA_6G02490/AAT1	Has domain(s) with predicted pyridoxal phosphate binding, transaminase activity	0.963	2.774	2.65
AFUA_7G01370/YOR251c	Ortholog(s) have thiosulfate sulfurtransferase activity	0.452	0.473	0.48
AFUA_1G04160/AAT1	Has domain(s) with predicted pyridoxal phosphate binding, transaminase activity	0.261	0.060	2.65
AFUA_1G10130/YER	Putative adenosylhomocysteinase	1.287	3.530	2.75
AFUA_5G01500/YPL273w	Homocysteine S-methyltransferase activity	1.082	2.460	2.54

AFUA_4G07360/YER091c	Putative cobalamin-independent methionine synthase	0.903	4.112	2.87
AFUA_1G10630/YDR502c	Putative S-adenosylmethionine synthetase	1.011	2.480	3.8
AFUA_2G13630/YGL202w	Putative amino transferase	0.579	0.224	2

Sulphur metabolism				
AFUA_2G15590/YFR030w	Putative sulphite reductase	2.126	4.836	4.3
AFUA_6G08920/YJR137c	Assimilatory sulfite reductase	0.624	3.474	3.95
AFUA_4G03930/YLR303W	Putative cysteine synthase B	0.892	0.095	5.5
AFUA_5G02180YLR303W	Cysteine synthase (o-acetylserine (thiol)-lyase	0.771	2.914	5.5
AFUA_5G04250/YLR303W	Homocysteine synthase	0.490	0.888	5.5
AFUA_1G10820/YKL001c	Ortholog(s) have role in methionine metabolic process, sulfate assimilation and intracellular localization	1.734	2.859	7.44

Oxidative stress related proteins				
AFUA_1G14550/YHR008c	Putative manganese superoxide dismutase	0.789	0.037	0.36
AFUA_3G02270/YDR256c	Mycelial catalase	1.647	0.067	0.16
AFUA_2G18030/YDR256c	Putative catalase	0.212	0.836	0.16
AFUA_3G06540/YPR167C	Ortholog(s) have phosphoadenylyL-sulfate reductase (thioredoxin) activity	0.771	6.841	4.63
AFUA_5G01440/YLR109W	Ortholog(s) have thioredoxin peroxidase activity, role in cell redox homeostasis, cellular response to oxidative stress	0.580	0.264	2.29

AFUA_8G01670/YKR066C	Putative bifunctional catalase-peroxidase	3.096	1.095	0.319
AFUA_4G05950/YPLO59W	Ortholog(s) have disulfide oxidoreductase activity, role in cellular response to oxidative stress, response to osmotic stress	1.018	2.034	0.476
AFUA_2G04320/YHR179W	Has domain(s) with predicted FMN binding, oxidoreductase activity and role in oxidation-reduction process	1.439	0.161	2.92
AFUA_7G06420/YHR179W	Ortholog(s) have intracellular localization	1.162	0.406	2.92
AFUA_5G09910/YCL026C	Putative p-nitroreductase family protein	0.583	0.356	3.93

Translation and Ribosomal Biogenesis				
AFUA_1G05080/YLR340W	Putative 60S ribosomal protein P0	2.265	5.292	3.9
AFUA_1G05500/YOR369C	40S ribosomal protein S12	2.481	6.270	2.12
AFUA_1G12890/YPL131W	Putative 60S Ribosomal protein L5	2.181	6.717	4.16
AFUA_1G15730/YJL190C	40S ribosomal protein S22	2.495	5.754	4.06
AFUA_2G02150/YHL015W	Putative ribosomal protein S10	2.492	5.421	2.75
AFUA_2G09200/YGL030W	60S ribosomal protein L30	2.036	5.310	3.4
AFUA_2G10100/YDR382W	Allergen Asp f 8; putative ribosomal protein P2	2.326	7.066	2.22
AFUA_2G10300/YDR447C/ YML024W	40S ribosomal protein S17	2.404	5.068	3.03/3.19
AFUA_3G05600/YGL103W	60S ribosomal protein L27a	2.065	5.677	6.64
AFUA_3G06760/YDR500C	Ribosomal protein L37	2.231	5.823	3.05
AFUA_4G07730/YGR085C/ YPR102C	60S ribosomal protein L11	2.156	5.449	3.56/3.19
AFUA_5G03020/YBR031W	60S ribosomal protein L4	2.291	5.402	3.06
AFUA_5G05630/YOL127W	60S ribosomal protein L23	2.209	5.340	3.9

AFUA_5G06360/YFR031C/ YIL018W	60S ribosomal protein L8	2.232	5.715	4.67/5.67
AFUA_6G02440/YGL031C/ YGR148C	60s ribosomal protein L24	1.895	5.251	3.91/3.15
AFUA_6G11260/YGR034W	Ribosomal protein L26	2.026	5.199	4.66
AFUA_6G12660/YOR293W	40S ribosomal protein S10b	2.554	5.563	4.6
AFUA_6G13250/YLR406C	60S ribosomal protein L31e	2.164	5.294	5.12

5.6 Discussion

Gliotoxin induces a complex, global response affecting a large array of genes and pathways in *A. fumigatus*. This study focused on key pathways and genes which have been previously shown to be altered in response to gliotoxin either at the protein level or from different cell responses seen to be affected by gliotoxin. One such pathway is the cysteine and methionine metabolic pathway. This pathway is involved in the biosynthesis of key amino acids such as L-cysteine, L-methionine and L-homocysteine. It also feeds into other key pathways which appear to have some role in gliotoxin toxicity such as sulphur metabolism and glutathione metabolism. ATCC46645 appears to have a very different transcriptomic response when compared to Δ*gliT*, especially in the pathways listed in Table 5.3. The key difference between ATCC46645 wild-type and Δ*gliT*s' transcriptomic response to gliotoxin is seen in the cysteine and methionine metabolic pathway and the sulphur metabolic pathway where expression of genes involved in S-adenosyl methionine biosynthesis are altered. There is an increase in genes involved in L-homocysteine, L-cysteine and L-methionine biosynthesis, each required for the SAM cycle and subsequent S-adenoysl methionine biosynthesis. Interestingly, one of the few genes which have a decrease in its expression (AFUA_6G03740) is involved in S-adenosyl homocysteine biosynthesis (Kinehisa *et al.*,, 2004). Similarly, there is an increase in the expression in S-adenosyl homocysteine hydrolase (AFUA_1G10130) which encodes an enzyme which breaks down S-adenosyl homocysteine to L-homocysteine (Tehlivets *et al.*, 2004). It has been previously mentioned here that gliotoxin may induce an accumulation of L-homocysteine which can be toxic to cells when not kept in check (Fujita *et al.*, 2006). Alternatively, the regulation of S-adenosyl homocysteine levels could also be paramount, as this product has been shown to inhibit S-adenosyl methionine mediated S-methylation (Deguchi & Barchas 1971). If there is a corresponding increase in the translation of these enzymes, this altered expression of genes which maintain S-adenoysl homocysteine levels could be a method of preventing it inhibiting S-adenosyl methionine methylation, either of gliotoxin or other reactive intermediates which are produced in Δ*gliT* + gliotoxin. Additionally, when the *S. cerevisiae* transcriptome is compared to this, there is a

comparable trend in the altered expression of genes, suggesting a link between sensitivity to gliotoxin and these two strains.

This could imply that the ability to convert gliotoxin to the bis-methylated form is present in the yeast, however later in Chapter 6 this was found not to be the case. De-carboxylated S-adenosyl methionine acts as an aminopropyl donor in the biosynthesis of polyamines. In both ATCC46645 and Δ*gliT* + gliotoxin, AFUA_8G06540, a gene which encodes an enzyme involved in putrescine biosynthesis, a polyamine which, along with spermine and spermidine, has been demonstrated to be involved in sporulation and cell differentiation in *A. fumigatus* shows a significant increase in its expression (Guevara-Olvera *et al.,* 1993; López *et al.,* 1997).

The majority of genes involved in glutathione metabolism show a decrease in their expression in Δ*gliT* in response to gliotoxin. In both ATCC46645 and Δ*gliT* + gliotoxin, there is a common decrease in the expression of genes involved in glutathione biosynthesis and the γ-glutamyl cycle. Due to glutathiones' role in the oxidative stress response, it may have been hypothesised to have increased expression due to the production of super oxide radicals seen in chapter 3. However, Bernardo *et al.,*, demonstrated that gliotoxin influx occurred in a glutathione dependent manner suggesting higher levels of glutathione could result in greater gliotoxin influx into the cell (Bernardo *et al.,* 2003). In this case, reducing the expression of genes involved in glutathione biosynthesis and their subsequent enzymes would be advantageous to the cell. Interestingly, *S. cerevisiae* + gliotoxin does not show similar dysregulation of glutathione biosynthesis. A total of five genes were shown to be dysregulated in this pathway when the yeast is challenged with gliotoxin, four of which are involved in the oxidation/reduction of glutathione to its oxidised and reduced isoforms (Grant 2001). Three of these four genes show a significant decrease in their respective expression suggesting that in yeast, like *A. fumigatus*, the presence of gliotoxin alters genes involved in the regulation of glutathione biosynthesis, albeit in a different manner.

Both ATCC46645 and Δ*gliT* show high expression values for glutathione S-transferase, particularly *gliG*. In Schrettl *et al.,* exogenous gliotoxin

has been shown to up-regulate the expression of the genes in the gliotoxin biosynthetic cluster *gli* (Schrettl *et al.,* 2010). This significant increase in expression of *gliG*, is presumably due to this effect and not related, directly to the glutathione metabolic pathway. This is further supported by various S-transferases with significant decreases in their expression in response to gliotoxin.

One key difference between ATCC46645 and Δ*gliT* is the decrease in the expression of a *DUG1* ortholog, which is a key component of the γ-glutamyl cycle and glutathione degradation pathway (Ganguli *et al.,* 2007; Kaur *et al.,* 2009). A corresponding decrease in the expression of this enzyme would reduce the L-glycine and L-cysteine levels in the cell as they would still be contained within any glutathione being produced, this would impact further on glutathione biosynthesis and the levels of glutathione in Δ*gliT*. These results could imply that in the presence of gliotoxin, glutathione levels in the cell could be further reduced in Δ*gliT*, something which was seen in Schrettl *et al.,* in which the addition of exogenous glutathione (20 mM) to agarose plates containing gliotoxin (10 µg/ml) completely abolished the hypersensitive phenotype of the Δ*gliT* strain indicating a relationship between *gliT* and glutathione biosynthesis.

This proposed gliotoxin mediated reduction of glutathione in *A. fumigatus* was demonstrated in Carberry *et al.,*, in which they illustrated that addition of exogenous gliotoxin (5 µg/ml) resulted in a significant decrease in the glutathione levels in both ATCC26933 and Δ*gliT*^{26933} (Carberry *et al.,* 2012). Secondly, the glutathione levels were far lower in Δ*gliT* than the wild type upon gliotoxin addition, corroborating the above transcriptomic data. Together, these results demonstrate gliotoxin mediated reduction of *de novo* glutathione, presumably due to redox action with its disulphide bridge, as well as altering the expression of glutathione biosynthetic genes in *A. fumigatus* resulting in a further loss of glutathione.

As mentioned previously, glutathiones' primary role in the cell is acting as a radical scavenger in the oxidative stress response (Izawa *et al.,* 1995; Lee *et al.,* 2001). The expression of other oxidative stress related genes were also found to be altered in the presence of exogenous gliotoxin. Analogous to previous results, there is a clear difference in the expression of these genes between ATCC46645 and Δ*gliT*

+ gliotoxin. In ATCC46645, only six genes are differentially expressed, four of which are up-regulated. Most notable among these are a putative catalase (AFUA_2G18030), thioredoxin reductase (AFUA_4G12990) and a bi-functional catalase-peroxidase (AFUA_8G01670) (Goetz *et al.,* 2011; Abadio *et al.,* 2011; Paris *et al.,* 2003). Reduced expression of catalase may imply gliotoxin carrying out an anti-oxidant role as illustrated in Chapter 3.

An increase in the expression of the thioredoxin reductase could be to due to an increase in disulphide formation requiring further reduction to maintain the redox balance inside the cell. In Δ*gliT* there is a similar increase in the expression of this thioredoxin reductase indicating its expression is independent of *gliT* loss. Interestingly there is differential expression of two superoxide dismutases, AFUA_1G14550 (Sod3) and AFUA_6G07210 (Sod4) (Lambou *et al.,* 2010). The decrease in the expression of *sod3* which encodes a cytoplasmic superoxide dismutase and the contrasting increase in the expression of *sod4* a putative mitochondrial super-oxide dismutase suggests gliotoxin toxicity affecting these two locations in differing ways (Lambou *et al.,* 2010). The first could be due to gliotoxins' anti-oxidant potential while located in the cytoplasm while the second highlighting its affect on the redox status of the mitochondrion.

Contrary to this, *S. cerevisiae* shows no real comparison in the expression of orthologous genes, of which only three show a similar trend in expression compared to Δ*gliT* and none with ATCC46645. Instead it shows an increase in different oxidative stress related genes such as those with functions in oxidative/reduction reactions (AFUA_2G04320/YHR179W) and response to oxidative stress (AFUA_5G01440/YLR109W) (Niino *et al.,* 1995; Lee *et al.,* 1999). This indicates a difference in components of the OS response being affected in all three organisms, implying that although there are some clear similarities between both gliotoxin sensitive strains Δ*gliT* and *S. cerevisiae,* not all responses are affected in the same fashion. This could be due to the presence of un-related genes which are not present in the yeast, for example Δ*gliK* shows hypersensitivity when challenged with H_2O_2 implying some role in OS and could explain why genes which are differentially regulated in the yeast are not in *A. fumigatus* or Δ*gliT* (Gallagher *et al.,* 2012)

One clear result which shows similarity in its response to gliotoxin in all three strains is translation and ribosomal biogenesis genes which show a significant increase in expression. The expression levels of *S. cerevisiae* orthologs are similar to ATCC46645, while Δ*gliT* shows > 2 fold more expression than both. Gliotoxin presence induces an increase in genes involved in the synthesis of the ribosome, suggesting an increase in general translation. In Chapter 4 both 40 S ribosomal protein S4 (AFUA_3G06840) and 60S ribosomal protein L10 (AFUA_2G09210) show > 3 fold up-regulation in Δ*gliT*, while AF293 shows a 3.1 fold up-regulation of a translation elongation factor 2 subunit (AFUA_2G13530) corroborating an increase in the translational machinery in the cell upon gliotoxin addition (Grosse *et al.,* 2008; Asif *et al.,* 2010; Teutschbein *et al.,* 2010). This increase in translation could be due to various reasons, one could be the dysregulation of the L-cysteine and L-methionine biosynthetic pathways or any of the other pathways which are altered by gliotoxin altering the level of translation in the cell. This is further supported in *A. fumigatus* strains with concurrent decrease in the expression of the leucine/ valine and isoleucine degradation pathway. Increased translation would require an increase in amino acid biosynthesis and a corresponding decrease in amino acid degradation, the latter of which is seen in both ATCC46445 and Δ*gliT* in the presence of gliotoxin.

Gliotoxin increases the expression of genes within its own biosynthetic cluster *gli* (Schrettl *et al.,* 2010). This was demonstrated by Schrettl *et al.,* where addition of gliotoxin to ATCC46645 increased the expression of *gliT*, *A* and *G*. This is similar to what is seen here in table 5.3 with significant up-regulation of all genes of the *gli* cluster in ATCC46645 when challenged with gliotoxin. Interestingly this is not seen in Δ*gliT*. Four of thirteen genes show no increase in their expression, with two having decreased expression in the presence of gliotoxin. This would suggest that *gliT* is necessary for gliotoxin mediated expression of the *gli* cluster, as the transcriptional activator, *gliZ* (AFUA_6G09630) is un-altered compared to the control samples of Δ*gliT* when gliotoxin is added. Also, its expression is significantly decreased when Δ*gliT* + gliotoxin is compared to ATCC46445 + gliotoxin. Surprisingly all of the *gli* cluster genes are significantly decreased in Δ*gliT* in response to gliotoxin when compared with ATCC46645 + gliotoxin. This could

explain why no gliotoxin could be detected by Schrettl *et al.,,* as gliotoxin biosynthesis in this strain would be predicted, based on these results, to be much lower than wild-type cells. Other components of the *gli* cluster have been proposed as gliotoxin detoxification mechanisms such as *gliA* (AFUA_6G09710) and *gliM* (AFUA_6G09680), however there could be others source. As Δ*gliT* has a significant decrease in the expression of all *gli* cluster genes, any alternative gliotoxin detoxification mechanism which relies on other *gli* genes would be subsequently reduced and could be another explanation for Δ*gliT* hypersensitivity to gliotoxin.

Conidial pigmentation is controlled by the biosynthesis of different types of melanin: DHN melanin or the alternative pyomelanin (Schmaler-ripcke *et al.,* 2009; Valiante *et al.,* 2009). The former is synthesised via a seven gene cluster located on chromosome 2 while the latter is an alternative melanin used in conidial pigmentation first discovered by source *et al.,,* wherein a six gene cluster also located on chromosome 2 was found to alter the pigmentation of the fungus and also its sensitivity to different stressors. Melanins are high molecular weight pigment molecules, which also have a role in the OS response with DHN melanin shown to protect the cell from reactive oxygen species produced by host immune cells during infection source (Nosanchuk & Casadevall 2003). ATCC46645 and Δ*gliT* show a significant decrease in the expression of genes involved in pyomelanin biosynthesis when grown in the presence of gliotoxin. However, only ATCC46645 shows a simultaneous increase in the expression of two genes involved in the biosynthesis of DHN-melanin indicating that in the presence of gliotoxin, wild-type cells favour the biosynthesis of one type of melanin over the other. Δ*gliT* + gliotoxin shows a significant decrease in the expression of three of the six genes involved in this cluster meaning genes involved in the biosynthesis of both types of melanin are reduced which could result in lower concentrations of each being produced which could have a direct affect on Δ*gliT*s' ability to cope with reactive oxygen species.

Fumitremorgin B is a secondary metabolite which acts as a mycotoxin (Maiya *et al.,* 2006). Both ATCC46645 and Δ*gliT* show a significant decrease in the expression of components of this cluster, with all genes having a significant decrease in their expression in Δ*gliT* + gliotoxin. This could simply be a stress response, enabling the cell to conserve energy as biosynthesis of this secondary metabolite has

no direct advantage when the cell is undergoing gliotoxin induced stress. It could also imply gliotoxin has a regulatory role in the cell, altering the expression of certain metabolites at different time points which may interfere or which are no longer required after gliotoxin biosynthesis has occurred, usually 48 h after growth.

Gliotoxin induces a complex response in both *A. fumigatus* strains. It also has similar affects on the yeast *S. cerevisiae* which was seen to possess a similar response to gliotoxin as Δ*gliT*. This is particularly seen in the alteration of the cysteine and methionine metabolic pathway, notably the SAM cycle. Gliotoxin appears to affect this and some other metabolic pathways in a similar fashion in sensitive strains highlighting the importance of the role *gliT* has in *A. fumigatus* gliotoxin detoxification. This is further supported by the resistance which can be induced in *S. cerevisiae* when *A. fumigatus gliT* is transformed into yeast under a constitutive promoter as demonstrated by Schrettl *et al.,* (2010) The dysregulation of the SAM cycle could imply a role of this pathway in gliotoxin detoxification which is only beneficial in the presence of *gliT*, thus why Δ*gliT* and *S. cerevisiae*s sensitivity to gliotoxin is abolished when *gliT* is being expressed.

Loss of *gliT* has a dramatic affect on the transcriptomic response to gliotoxin in this strain, particularly in the regulation of *gli* cluster genes (Schrettl *et al.,* 2010). The significant decrease in their respective expression may further highlight why Δ*gliT* is so sensitive to gliotoxin as other components of the cluster could be necessary along with *gliT* for complete gliotoxin detoxification. One such gene is *gliA* which is the putative gliotoxin transporter (Gardiner & Howlett 2005). Reduced expression of this gene and the membrane protein it encodes would result in a corresponding decrease or complete abolishment of gliotoxin efflux from the cell which may then accumulate in the cell. If this was the case any alternative gliotoxin detoxification mechanisms, such as gliotoxin methylation, would naturally be up-regulated which is suggested here by the increased expression of the SAM cycle related genes and SAM cycle related enzymes as demonstrated in Chapter 4.

Chapter 6

Phenotypic response of *Saccharomyces cerevisiae* to gliotoxin

6.1. Oxidative Stress Response in *Saccharomyces cerevisiae*

The production of harmful reactive oxygen species (ROS) is a by-product of respiration and can cause damage to important cell components (Storz, *et al.,* 1987). To protect against these various ROS, organisms can employ both enzymatic and non-enzymatic means to help defend against increasing oxidative stress (OS) conditions (Kugel & Jones 1994). Eukaryotes can employ many types of cell responses to tackle the potential harm caused by different types of OS such as the biosynthesis of superoxide dismutases, and glutathione which help attenuate oxidative stress (Finkel & Holbrook 2000; Izawa *et al.,* 1995; Jamieson 1998).

Superoxide dismutases are required by the cell to aid in the OS response in dismutating O_2^- into molecular oxygen and hydrogen peroxide (Steinman 1980). There are two superoxide dismutases in yeast: Sod1p which is located in the cytosol and Sod2 which is located in the mitochondrion (Culotta *et al.,* 1995). In cells lacking *SOD1*, they exhibit increased sensitivity to OS inducers including H_2O_2, and diamide highlighting its role in the OS response (Jamieson 1998; Muller 1996).

The tri-peptide glutathione is the most abundant thiol found in the cell (Meister & Anderson 1983) and has been found to be instrumental in the OS response (Grant *et al.,* 1996). It can exist in one of two natural forms, a mono-thiol form commonly referred to as GSH or reduced glutathione, and a disulphide form whereby the two sulphur moieties covalently bind to each other via the formation of a disulphide bridge commonly referred to GSSG or oxidised glutathione (Meister 1988; Grant *et al.,* 1996; Lee *et al.,* 2001), only reverting back to the reduced form via a NADPH-dependent reaction requiring the glutathione specific reductase Glr1 (Grant *et al.,* 1996).

The importance of these two molecules can be seen in the regulation of the intracellular ratio of GSH:GSSG which is maintained *de novo* with a higher percentage of GSH to GSSG (Muller, 1996). In cells where the GSSG form is more abundant than the reduced form, is indicative of oxidative stress and an indicator of the oxidative state of the cell (Muller 1996; Garcia *et al.,* 2011). While increased levels of GSH predisposes cells to become more sensitive to reducing stress e.g. when exposed to reducing agents like dithiothreitol (Grant *et al.,* 1997).

Glutathione is produced in yeast via two ATP-dependent steps. The first is carried out by γ-glutamylcysteine synthetase (*GSH1*), forming the dipeptide γ-glutamylcysteine from glutamate and cysteine. In the last step glycine is added via glutathione synthetase (*GSH2*) producing glutathione (Lee *et al.,* 2001; Grant *et al.,* 1997). Glutathione biosynthesis is heavily regulated in order to maintain the GSH:GSSG ratio as seen by *GSH1* being negatively regulated by increasing levels of glutathione (Huang *et al.,* 1988, Meister *et al.,* 1988).

Glutathione acts as a radical scavenger of the cell via the oxidising of its free thiol found within its sulphydryl moiety (Meister 1988; Izawa *et al.,* 1995). *Δgsh1* strains show subsequent auxotrophy on non-glutathione containing media, however this is not the case in Δ*gsh2* strains which can still grow in the absence of glutathione due to an accumulation of the γ-glutamylcysteine (Wheeler *et al.,*2002). These strains also showed increased susceptibility to oxidative stress inducers such as H_2O_2 (Lee *et al.,* 2001; Izawa *et al.,* 1995), dipyridyl disulphide (López-Mirabel *et al.,* 2007) and heavy metal stress (Gales *et al.,* 2008). This is mainly caused by an inability to deal with mitochondrial dysregulation and a build up of endogenous ROS (Meister and Anderson 1983, Grant and Dawes 1996).

During OS there is an increase in the oxidised form of GSSG (Grant *et al.,* 1996). This can be due to interaction of the reduced form with ROS, via interactions with glutathione peroxidases (Izawa *et al.,* 1995) or via protein modification in the form of glutathionylation (Garcia *et al.,* 2011). In the mitochondrion, H_2O_2 is scavenged by glutathione peroxidases where it is reduced to H_2O and O_2, with GSH acting as an electron donor (Garcia *et al.,* 2011). Glutathione also modifies proteins via their free thiols, as seen in the mitochondrion where proteins are reversibly bound to GSH protecting the protein from oxidative damage (Garcia *et al.,* 2011). This is achieved by GSSG migrating to the mitochondrion during OS, as glutathione is not produced in the mitochondrion, and is then reduced via thioredoxin, glutathione reductase and NADPH presence (Garcia *et al.,* 2011; Yang *et al.,* 2010).

There are two key transcription factors associated with glutathione biosynthesis and regulation: *yap1*and *met4* (Wheeler *et al.,*2002 & 2003). Yap1 is a transcription factor which is up-regulated during OS, particularly H_2O_2 presence (Agnés *et al.,* 2000).

Yap1 has two key domains which are required for its regulatory function: an N-terminus Nuclear Localisation Signal which tags it for nuclear import, and a C-terminus Nuclear Export Signal (Kuge & Jones 1997). Yap1 migrates to and from the nucleus under non-stress conditions, however during OS induced by the presence of H_2O_2 or the thiol oxidant diamide, the protein accumulates within the nucleus after forming a di-sulphide bridge via a glutathione peroxidase, Gpx3, preventing its export via the exportin Crm1 (Kuge *et al.,* 2001; Delauney *et al.,* 2002; Kuge *et al.,* 1998). However, Yap1 accumulation has also been seen under different OS without the necessity of this conformational change which was shown to be dispensable in the presence of diamide (Lee *et al.,* 2013). Once accumulated in the nucleus Yap1 has been found to increase the regulation of key cell response genes such as *GLR1* (glutathione reductase), *TRR1* (thioredoxin reductase) and *GSH1*(γ-glutamylcysteine synthetase) to name a few (Grant *et al.,* 1996; Wu & Moye-Rowley 1994).

Δ*yap1* strains demonstrate increased sensitivity to OS, especially H_2O_2 induced stress (Schnell *et al.,* 1992) due to its role as the transcriptional regulator of a regulon consisting of 32 H_2O_2 inducible proteins alone (Lee *et al.,* 2013).

Met4 on the other hand is involved in the regulation of genes involved in the biosynthesis of amino acids which contain sulphur, heavy metal response and glutathione metabolism (Thomas & Surdin-kerjan 1997; Wheeler *et al.,* 2003). Δ*met4* strains are auxotrophic for L-methionine, SAM and L-homocysteine (Wheeler *et al.,* 2002; Wheeler *et al.,* 2003). Interestingly in Δ*gsh2* strains, Met4 has been demonstrated to induce the *gsh1* promoter, a process which can be later inhibited by the presence of GSH, or in the case of a Δ*gsh1* where no GSH is produced, the addition of exogenous GSH (Wheeler *et al.,* 2002).

The non-ribosomal peptide, fungal secondary metabolite gliotoxin, produced in certain fungi namely *Aspergilli spp.* and *Gliocladium spp.* (Scharf *et al.,* 2011), has been shown previously to have anti-fungal and cytotoxic properties towards both fungi and animal cells respectively (Herrick 1945; Sutton *et al.,* 1994). Due to the presence of a trans-molecular di-sulphide bridge, gliotoxin is a redox active molecule, cycling between an oxidised and reduced form, instilling it the ability to alter the oxidative state of cells and inducing toxicity (Waring *et al.,* 1995; Cramer *et al.,* 2006; Gardiner &

Howlett 2005). A genome-wide yeast deletion screen carried out by Chamilos *et al.,* identified important gene components of the oxidative stress response and other key cellular pathways to be affected by gliotoxin challenge (Chamilos *et al.,* 2008). However, as demonstrated in this study, additional strains with altered phenotypic responses to gliotoxin were identified which were originally overlooked.

A gene targeted approach was utilised here to further assess the response of *S. cerevisiae* to gliotoxin. With the aim to identify key targets of gliotoxin toxicity and to elucidate how gliotoxin induces its toxicity in this model organism.

6.2 Growth response of *S. cerevisiae* mutants to gliotoxin

Many studies have implicated gliotoxins' toxicity with the induction of OS and production of ROS (Waring 1990; Waring *et al.,* 1995; Carberry *et al.,* 2012). Being able to cycle between an oxidised and reduced form makes this highly likely, as would its ability to interact with the free thiols of proteins in the cell (Waring *et al.,* 1995). Previous work on the proteomic response to gliotoxin in *A. fumigatus* has identified an increase in protein expression of Sod1p in response to gliotoxin and a reduced expression of Ctt1p implicating gliotoxin induced alteration of the OS response (Carberry *et al.,* 2012). Results from previous chapters have illustrated gliotoxin does induce a significant increase in the levels of superoxide production, as well as dysregulating genes and proteins involved in the OS response (Chapters 3-5).

In a genome wide study carried out by Chamilos *et al.,* (2008) using *S. cerevisiae* mutants exposed to exogenous gliotoxin, identified 3 strains which exhibited increased sensitivity to gliotoxin and 10 with increased resistance (Chamilos *et al.,* 2008). Of these strains one was found to also be involved in the sulphur and methionine biosynthesis pathway, *CYS3*. *CYS3* encodes cystathionine γ-lyase, an enzyme involved in catalysing the formation of L-cysteine from L-homocysteine (Figure 6.1) (Hiraishi & Miyake 2008).

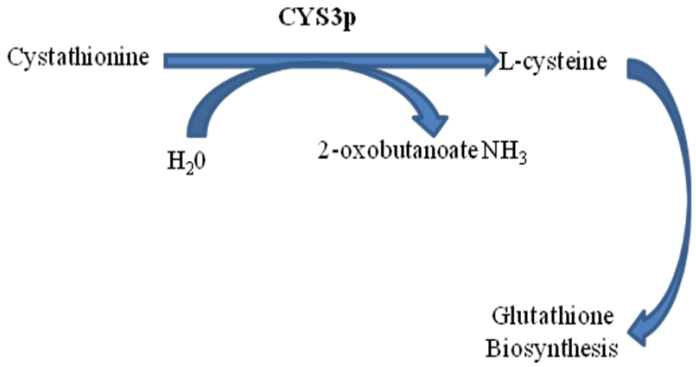

Figure 6.1 Cystathionine γ-lyase activity

Previous results demonstrated that gliotoxin exposure induces oxidative stress on the cell. Causing dysregulation to parts of the L-cysteine and L-methionine metabolic pathway and sulphur pathways (Chapter 5), as well as affecting glutathione biosynthesis and the SAM cycle (Chapter 4 and 5). Using a gene targeted approach, *S. cerevisiae* deletion strains were screened on gliotoxin Figure. 6.2 A and B.

Gliotoxin exposure (8 µg/ml) elicits a sensitive phenotype in both Δ*sod1* and Δ*yap1* on SC media. Both are involved in the OS response further corroborating gliotoxin induction of OS on the cell. However, when this is compared to other strains lacking important OS response genes such as Δ*ctt1* (Figure 6.2 A and B), gliotoxin exposure elicits a wild-type phenotype. Similarly, the response of other OS response mutant strains such as Δ*trx2*, which encodes thioredoxin an important OS repair protein and sulphur metabolism regulator (Kugel & Jones 1994), Δ*gsh2* which encodes glutathione synthetase the last enzyme involved in glutathione biosynthesis (Grant *et al.,* 1997), Δ*glr1* which encodes a glutathione reductase which is important in the reduction of oxidised glutathione (GSSG) to form GSH and helps maintain the *de novo* GSH levels (Grant *et al.,* 1996; Muller 1996; Østergaard *et al.,* 2004) and Δ*skn7* which encodes an important transcription factor involved in the OS response (Jamieson 1998; Auesukaree *et al.,* 2009) educe a wild-type phenotype when exposed to gliotoxin (O'Brien 2011).

Δ*gsh1* shows increased resistance to gliotoxin (Figure 6.2 B). *GSH1* encodes the rate limiting step in the formation of GSH and loss of this gene has been demonstrated to have a corresponding abolishment of GSH biosynthesis (Greenberg & Demple 1986; Lee *et al.*, 2001) Due to the role in the OS response, loss of GSH may be expected to induce sensitivity when the cell is exposed to gliotoxin, yet the opposite was seen here. This suggests low to null levels of GSH is advantageous when exposed to gliotoxin.

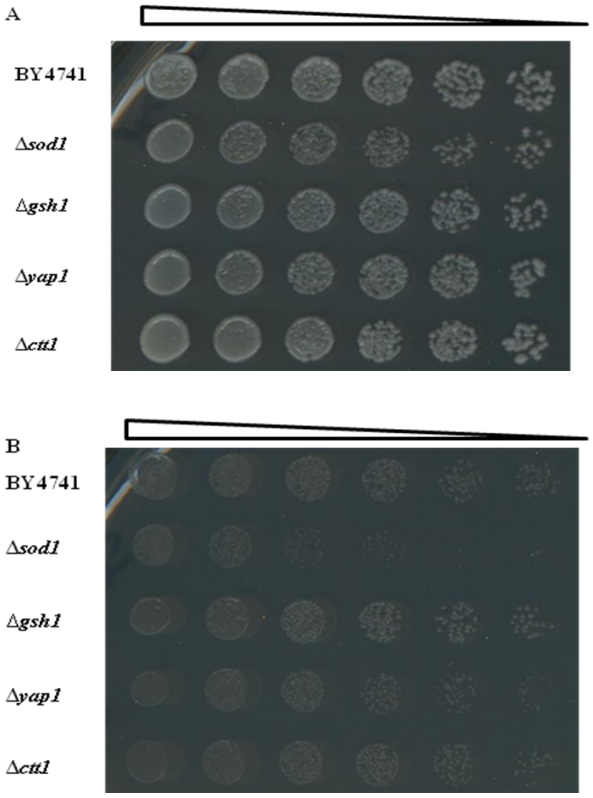

Figure 6.2 A and B Growth analysis of *S. cerevisiae* strains grown on synthetic complete media (SC) with or without gliotoxin. Comparative growth analysis assay using strains BY4741a, Δ*gsh1*, Δ*yap1* and Δ*ctt1*. (A) Strains grown on SC media. (B) Strains grown on SC media with 8 µg/ml gliotoxin added.

When the growth response of Δ*gsh1* is compared with strains lacking genes involved in glutathione biosynthesis Δ*gsh2* elicits a wild-type response (Figure 6.3 C and D) while Δ*cys3* elicits a sensitive growth response (Figure 6.3 A and B).

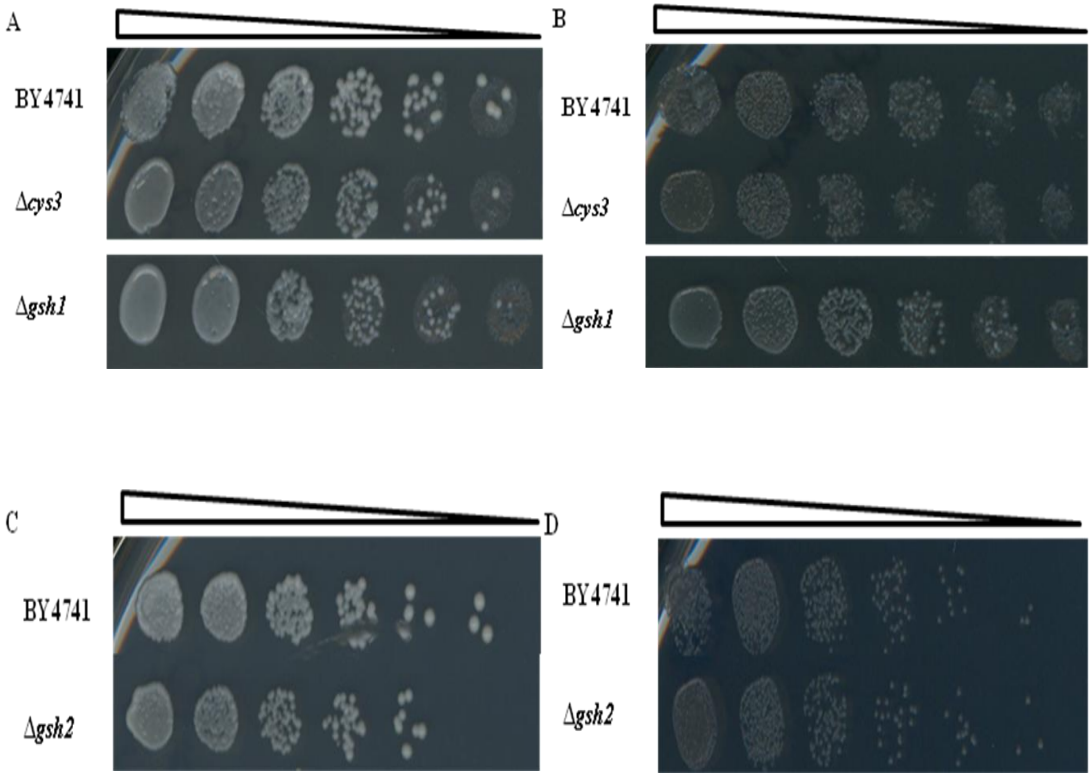

Figure 6.3 A-D Growth analysis of *S. cerevisiae* strains grown on synthetic complete media (SC) with or without gliotoxin. Comparative growth analysis assay using strains BY4741a, Δ*cys3*, Δ*gsh1*, and Δ*gsh2*. (A) Strains BY4741a, *Δcys3* and Δ*gsh1* grown on SC media. (B) Strains BY4741a, *Δcys3* and Δ*gsh1* with 8 µg/ml gliotoxin added. (C) Strains BY4741a, and Δ*gsh2* grown on SC media. (D) Strains BY4741a, and Δ*gsh2* grown on SC media with 8 µg/ml gliotoxin added

In Figure 6.4, each of the key genes involved in glutathione biosynthesis is illustrated. Cys3p is involved in the enzymatic breakdown of l-homocysteine to l-cysteine which later becomes part of the tri-peptide of glutathione.

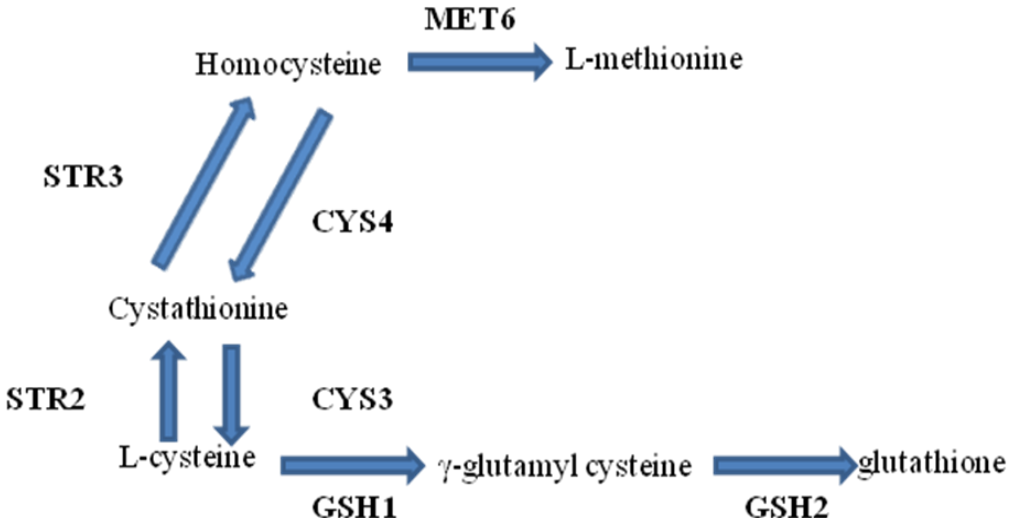

Figure 6.4 Glutathione biosynthesis pathway

Δ*cys3* is sensitive to gliotoxin however Δ*cys4* elicits a wild-type phenotype (Figure 6.5 A and B). Loss of *CYS3* may cause an alteration in the L-cysteine levels which in itself could induce stress via the alteration of GSH levels *in vivo*. As Δ*gsh1* is resistant to gliotoxin, it is un-likely that an alteration to glutathione biosynthesis due to the absence of *CYS3* is responsible for this sensitivity. Previously it has been demonstrated that loss of *CYS3* results in subsequent auxotrophy for L-cysteine (Cherest *et al.*, 1993) requiring cysteine to be present in the media for optimum growth. This could explain the weaker growth of this strain seen on SC media plates without gliotoxin, presumably due to low L-cysteine levels in the media (Figure 6.5 A).

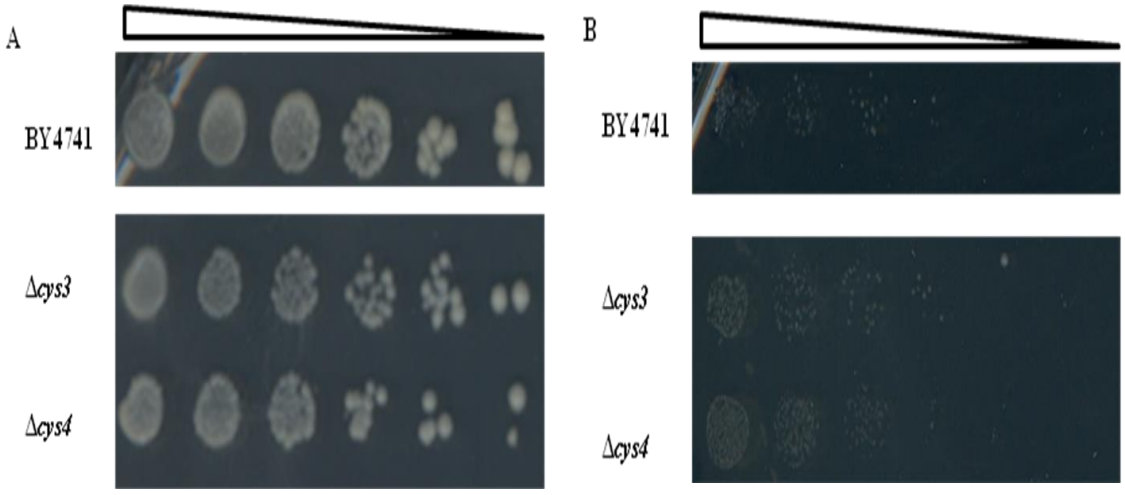

Figure 6.5 A and B Growth analysis of *S. cerevisiae* strains grown on synthetic complete media (SC) with or without gliotoxin. Comparative growth analysis assay using strains BY4741a, Δ*cys3* and Δ*cys4*. (A) Strains BY4741a, *Δcys3* and Δ*cys4* grown on SC media. (B) Strains BY4741a, *Δcys3* and Δ*cys4* with 8 µg/ml gliotoxin added.

As seen in Figure 6.3 D, Δ*gsh2* elicits a wild-type phenotype when challenged with gliotoxin. Gsh2p catalyses the last step in glutathione formation. Strains lacking *GSH2* have been shown to possess low to null levels of glutathione yet can compensate by over expressing *GSH1* and the biosynthesis of γ-glutamyl cysteine (Jamieson 1998; Wheeler *et al.*, 2002). As Δ*gsh2* cells possess naturally lower levels of glutathione than wild-type cells, loss of glutathione biosynthesis alone may not necessarily confer resistance to gliotoxin. All other strains used and tested on gliotoxin not mentioned here elicited a wild-type phenotype.

6.3 Oxidative stress response in *S. cerevisiae*

As seen in Chapter 3, gliotoxin induces an increase in the production of ROS. This is further corroborated in Chapters 4 and 5 where gliotoxin challenge results in subsequent dysregulation of OS related genes and proteins. To further elucidate the

affect gliotoxin has on the OS response, yeast deletion strains lacking genes involved in the OS response were exposed to H_2O_2 and gliotoxin. *S. cerevisiae* was employed due to the ready availability of mutants in this model organism, a well characterised OS response and a fully sequenced genome. Mid-exponential cells were serially diluted before being transferred onto minimal media agarose plates containing different concentrations of H_2O_2 (0-3 mM). Results for 0 (A), 2 (B) and 3 (C) mM H_2O_2 can be seen in figure 6.7 A-C, 1 mM not included as it is very similar to what is seen on 2 mM plates.

In Figure 6.6, all strains elicit a wild-type response when grown on SC media. However this changes once H_2O_2 is added whereby a dramatic change can be seen. On 2 mM H_2O_2 (Figure 6.6 B) SC plates, Δ*yap1* becomes hypersensitive with very little growth seen and no growth visible on 3 mM H_2O_2 (Figure 6.6 C). As mentioned previously, Yap1pis a transcription factor which regulates the expression of many OS response genes (Agnés *et al.,* 2000; Kugel & Jones 1994) . In Δ*yap1* this would no longer be occurring and once exposed to H_2O_2, lack of this Yap1 mediated OS response would result in the cells being vulnerable to ROS and oxidative damage. This has been demonstrated in other studies in which Δ*yap1* was seen to be highly sensitive to ROS generated by different OS inducing compounds e.g. H_2O_2 (Draculic *et al.,* 2000; Auesukaree *et al.,* 2009; López-Mirabel *et al.,* 2007) .

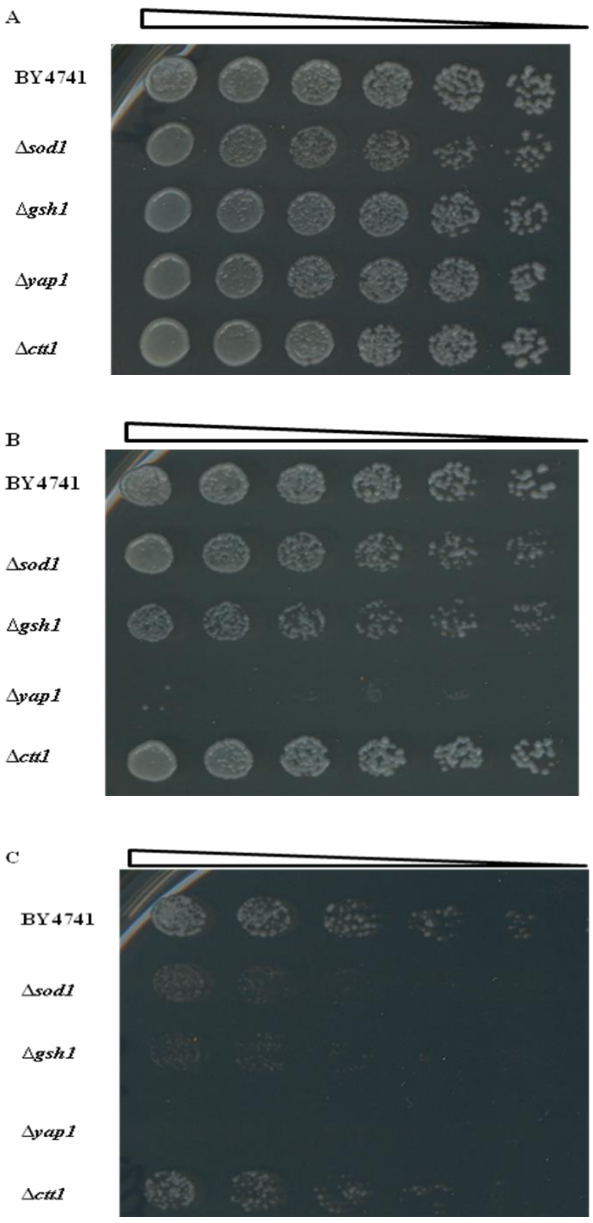

Figure 6.6 A-C Growth analysis of *S. cerevisiae* strains grown on synthetic complete media (SC) with or without H_2O_2. Comparative growth analysis assay using strains BY4741a, Δ*gsh1*, Δ*yap1* and Δ*ctt1*. (A) Strains grown on SC media. (B) Strains grown on SC media with 2 mM H_2O_2 added. (C) Strains grown on SC media with 3 mM H_2O_2 added.

SOD1, *GSH1* and *CTT1* are also involved in the OS response (Bermingham-McDonogh *et al.*, 1988; Jamieson 1998; Drakulic *et al.*, 2005). Sod1 is a superoxide

dismutase involved in the dismutating the superoxide radical and hydroxyl radical to molecular oxygen and hydrogen peroxide. The latter of which can serve as a signalling molecule activating Yap1 nuclear accumulation and subsequent transcriptional activation of OS response genes (Agnés *et al.,* 2000; Kuge *et al.,* 2001). Sensitivity to H_2O_2 is not seen until 3 mM H_2O_2 (Figure 6.6 C) in Δ*sod1,* indicating loss of this gene is not paramount in the OS response to H_2O_2. In yeast there are many forms of enzymatic and non-enzymatic means to alleviate ROS and OS (Finkel & Holbrook 2000; Jamieson 1998). In a Δ*sod1* strain these other defence mechanisms could be compensating for the loss of Sod1 helping to tackle the OS until the concentration of H_2O_2 becomes too much and begins to overwhelm them ultimately resulting in the strains eliciting a sensitive phenotype.

GSH is involved in scavenging free radicals inside the cell which can cause OS and facilitates their removal from the cell (Izawa *et al.,* 1995). It also has many other roles in metal stress tolerance and S-glutathionylation of proteins (Wheeler *et al.,* 2003; Yang *et al.,* 2010) . In Figure 6.6 B, Δ*gsh1* is somewhat sensitive to 2 mM H_2O_2, showing greater sensitivity to the highest concentration of 3 mM H_2O_2 (Figure 6.6 C). In other works, Δ*gsh1* has been demonstrated to have increased sensitivity to a variety of compounds such as nickel, menadione plumagin and ethanol (Bishop *et al.,* 2007; Stephen & Jamieson 1996; Yoshikawa *et al.,* 2009) presumably due to the loss of GSH and its role in the OS response. *GSH1* encodes the rate limiting enzyme involved in the biosynthesis of the tri-peptide glutathione. Glutathione cycles between a reduced GSH form and an oxidised GSSG form, with the former being the most abundant in the cell, which aids in maintain the redox state of the cell (Grant 2001; Wheeler *et al.,* 2003) . Loss of *GSH1* would result in the loss of glutathione biosynthesis, its free radical scavenging ability and its ability to maintain the redox state of the cell. However, like a Δ*sod1* strain, other OS response mechanisms could be compensating for the loss of *GSH1* and helping to attenuate ROS production *de novo*.

CTT1, encodes a catalase which catalyses the breakdown of H_2O_2 into water and molecular oxygen (Jamieson 1998). Loss of *CTT1* does not elicit sensitivity in Δ*ctt1* on 3 mM H_2O_2 (Figure. 6.6 C) suggesting other mechanisms may be compensating for its absence e.g. presence of another catalase Cta1 (Petrova *et al.,* 2004).

In Δ*sod1* and Δ*ctt1* H_2O_2 could be detoxified via other OS response mechanisms such as glutathione peroxidases e.g. Gpx1 and Gpx2, which catalyse the breakdown of H_2O_2 to water via the reduction of oxidised GPX proteins in the presence of H_2O_2 and GSH resulting the formation of GSSG (Figure 6.7) (Inoue *et al.*, 1999) .

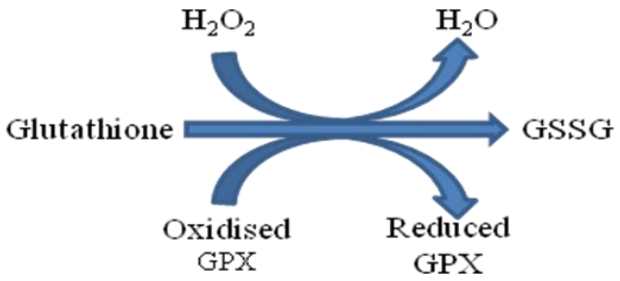

Figure 6.7 Breakdown of H_2O_2 by glutathione and glutathione peroxidases

6.4 Gliotoxin and H_2O_2 growth comparison

H_2O_2 is a known OS inducer, causing a rise in the production of ROS and oxidative damage in the cell (Collinson & Dawes 1992; Davies *et al.*, 1994; Finkel & Holbrook 2000). It also acts as a signalling molecule in the cell inducing an OS response (Agnés *et al.*, 2000; Dantas *et al.*, 2010) via activation of Yap1 nuclear localisation and subsequent transcriptional activation of OS response genes. This is enabled by the aforementioned di-sulphide formation in Yap1 inducing transcriptional function and activation of OS response genes (Kugel & Jones 1994; Agnés *et al.*, 2000; Kuge *et al.*, 2001).

As seen in Section 6.2, gliotoxin affects some major components of the OS response but not all as certain strain are un-perturbed by H_2O_2 presence. H_2O_2 appears to have a similar effect on yeast mutant strains as gliotoxin exposure, implying both H_2O_2 and gliotoxin could be having a similar effect on the cell, or at least effecting similar components of the OS response.

H_2O_2 has been implemented as a pre-treatment in many studies experimenting with its effect in alleviating chemically induced cellular stress (Collinson & Dawes 1992; Davies *et al.*, 1995; Park *et al.*, 1997). Davies *et al.*, demonstrated that 0.4 mM

H_2O_2 was sufficient in inhibiting growth of *S. cerevisiae* cells, yet when cells were pre-exposed to lower H_2O_2 concentrations and then re-exposed to the higher concentration, growth response significantly improved (Davies *et al.,* 1995). Similarly, pre-treatment with other toxins have been shown to help induce resistance in *S. cerevisiae* to hydrogen peroxide whereby 50 µg/ml cyclo-hexamide pre-exposure increased growth on a lethal dose of H_2O_2 (Collinson & Dawes 1992) underlining the potential signalling roles certain toxins have in inducing particular stress responses.

Co-addition of gliotoxin and H_2O_2 was seen to alleviate H_2O_2 toxicity in a gliotoxin concentration dependent manner in *A. fumigatus* strains (Gallagher *et al.,* 2012). Gliotoxin mediated attenuation of H_2O_2 was tested in *S. cerevisiae* strains grown on SC agarose plates containing similar concentrations of H_2O_2, gliotoxin and a combination of both (Figure 6.8 A-D).

Both 1 mM H_2O_2 (Figure. 6.8 B) and 8 µg/ml gliotoxin (Figure 6.8 C) elicit different degrees of sensitivity in certain yeast strains further supporting gliotoxin affecting similar biological pathways as H_2O_2. Contrary to this, H_2O_2 challenge induces sensitivity in Δ*gsh1* while this same strain is resistant to gliotoxin, highlighting how glutathione is necessary in the H_2O_2 stress response, but its absence is advantageous during gliotoxin exposure.

When both chemicals are added together, the attenuation of gliotoxin toxicity is not seen (Figure 6.8 D) as seen in *A. fumigatus* (chapter 3). Instead, addition of H_2O_2 has a synergistic effect, potentiating gliotoxin toxicity and resulting in inhibiting growth of all strains including the wild-type. This dramatic decrease in cell growth could be caused by an inability to respond to both H_2O_2 and gliotoxin. As can be seen in Figure 6.9 B, growth is relatively un-perturbed in the wild-type in the presence of 1 mM H_2O_2, less so in the presence of gliotoxin (Figure 6.8 C). On co-addition plates wild-type cells are unable to tolerate the toxicity of both H_2O_2 and gliotoxin eliciting a sensitive phenotype. H_2O_2 has been noted to reduce the thiol content as part of the OS response to peroxide stress via oxidation of free thiols (Winterbourn & Metodiewa, 1999). Gliotoxin has also been shown to lower the *de novo* glutathione pool, (Bernardo *et al.,* 2001). With the addition of these two, there would be an increasing oxidative state inside the cell due to the oxidation of different thiols found in the cell via H_2O_2 and

gliotoxin as well as increased formation of ROS which may explain this increased sensitivity.

The apparent inability of gliotoxin to alleviate H_2O_2 toxicity in *S. cerevisiae* could be due to the presence of different or more complex defensive mechanisms present in *A. fumigatus* which are absent in yeast such as gliotoxin induction of the *gli* biosynthetic cluster etc. In *S. cerevisiae*, any increase in the OS response induced by gliotoxin exposure does not outweigh the combinatory toxic effect of both chemicals.

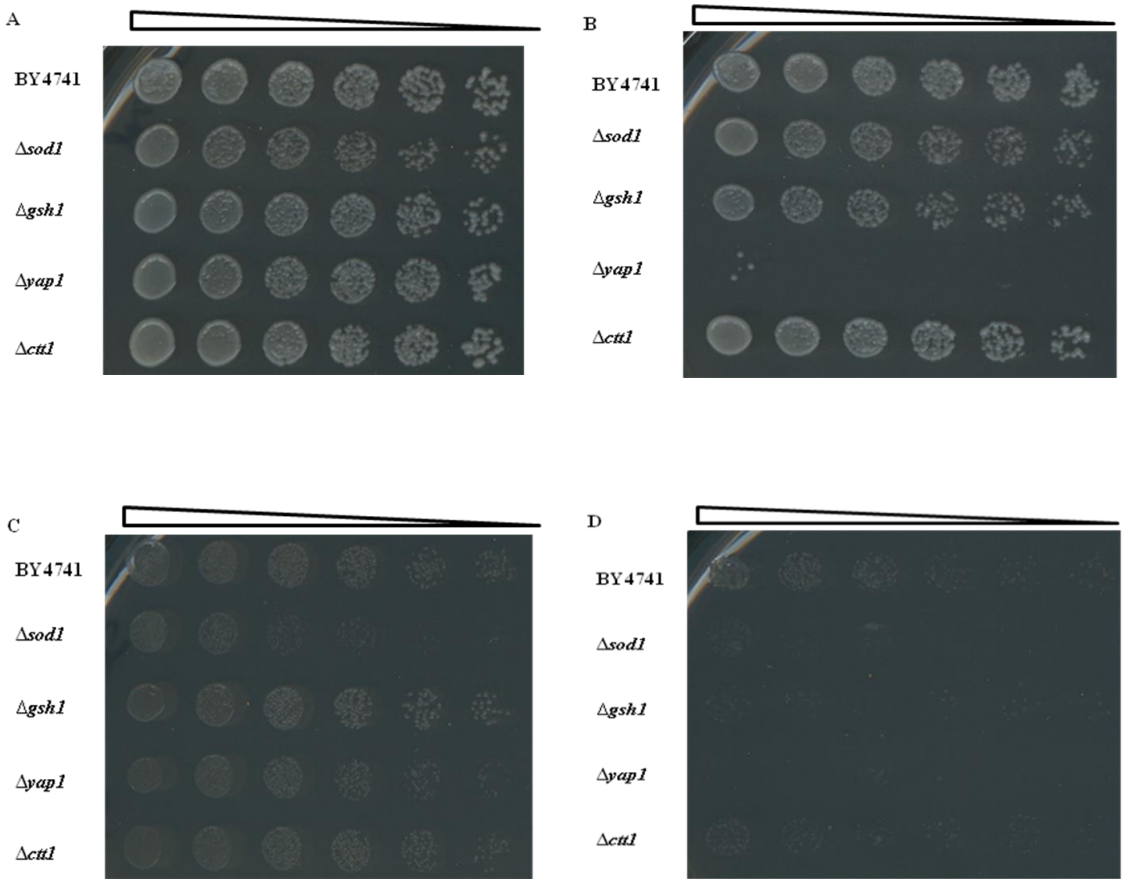

Figure 6.8 A-D Growth analysis of *S. cerevisiae* strains grown on synthetic complete media (SC) with or without gliotoxin and/or H_2O_2. Comparative growth analysis assay using strains BY4741a, Δ*sod1*, Δ*gsh1*, Δ*yap1* and Δ*ctt1*. (A) Strains grown on SC media. (B) Strains grown on SC media with 1 mM H_2O_2 added. (C) Strains grown on SC media with 8 µg/ml gliotoxin added. (D) Strains grown on SC media with 1 mM H_2O_2 and 8 µg/ml gliotoxin added.

6.5 Influence of glutathione on *S. cerevisiae* response to gliotoxin

Glutathione has been shown to be important in facilitating gliotoxin transport into the cell (Bernardo *et al.*, 2003). It acts as an important anti-oxidant in the OS response for a variety of different stresses, with depletion of *de novo* glutathione pools being lethal to the cell (Lee *et al.*, 2001; Cameron & Pakrasi 2010) . However, from Section 6.2 loss of *GSH1* elicits resistance to gliotoxin exposure indicating that glutathione or some related product may be exacerbating gliotoxin toxicity potentially through the facilitation of gliotoxin influx into the cell. With this in mind yeast strains were exposed to glutathione depleting conditions via the addition of the thiol-reductant diamide and CDNB.

6.5.1 Influence of diamide on *S. cerevisiae* and gliotoxin exposure

Diamide is a cell permeable thiol oxidant which has been shown to oxidise cysteine residues within Yap1 nuclear export domain disabling its ability to interact with Crm1p and subsequently its efflux from the nucleus facilitating Yap1 mediated regulation of OS response genes (Gulshan *et al.*, 2011). It also acts as a GSH scavenger, oxidising GSH to its oxidised isoform GSSG, reducing the *in vivo* GSH pool (Kower and Kower 1995; Sato *et al.*, 1995; Carberry *et al.*, 2012). Cells with reduced levels of GSH are naturally resistant to diamide as GSH presence is a pre-requisite for diamide toxicity, thus preventing alteration of the oxidative state of the cell due to rising GSSG levels (Kower and Kower, 1995). To examine the relationship between glutathione levels and the growth response of *S. cerevisiae* to gliotoxin, cells were exposed to a range of diamide concentrations (Figure 6.9 A-C) to identify *S. cerevisiae* strains which were resistant and thus possessed naturally lower levels of glutathione. These were then exposed to gliotoxin (Figure 6.9 D) and a combination of both gliotoxin and diamide (Figure 6.9 E and F) to examine if diamide mediated alteration of the *in vivo* glutathione levels subsequently improved yeast growth response to gliotoxin.

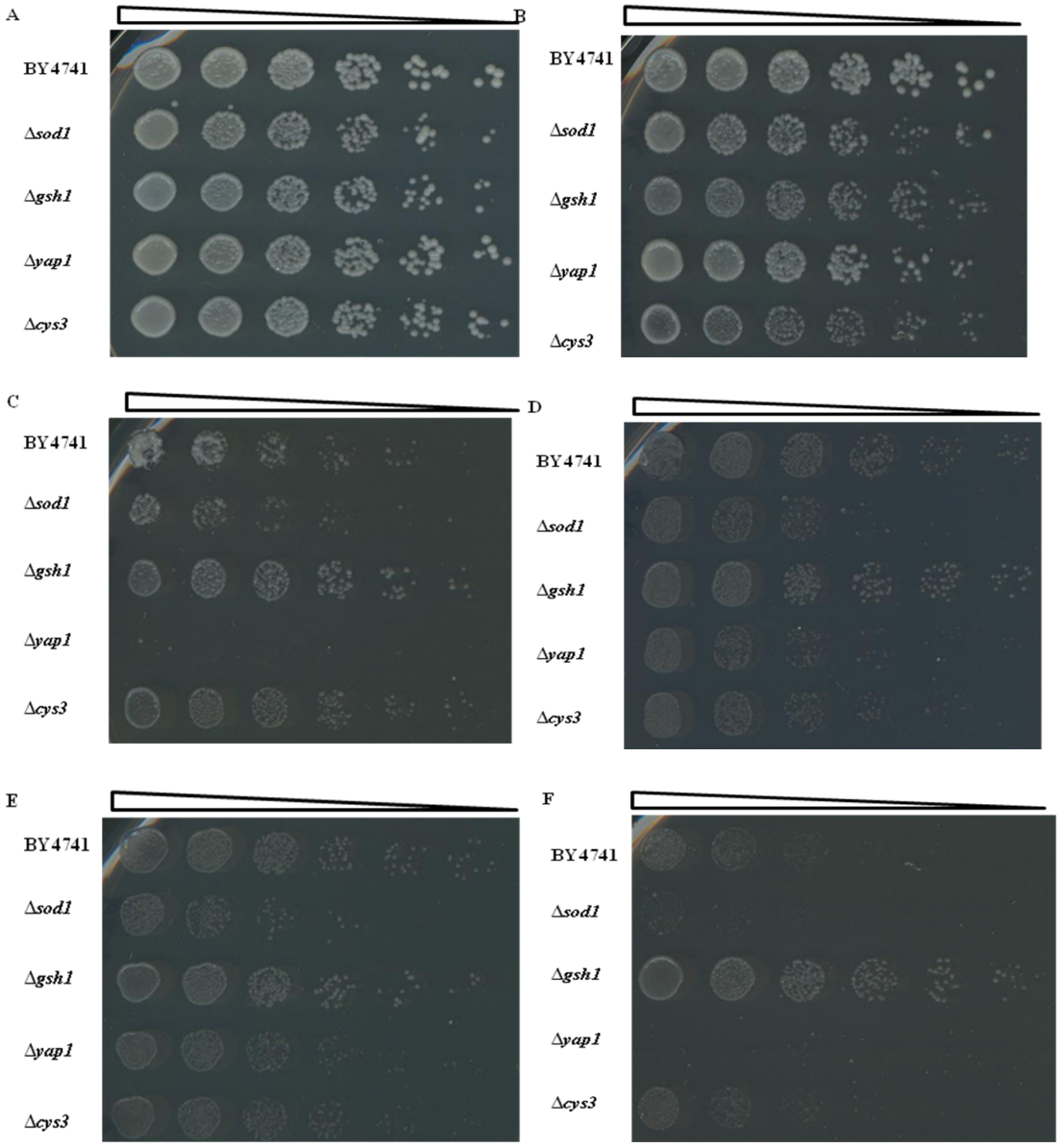

Figure 6.9 A-F Growth analysis of *S. cerevisiae* strains grown on synthetic complete media (SC) with or without gliotoxin and or diamide. Comparative growth analysis assay using strains BY4741a, Δ*sod1*, Δ*gsh1*, Δ*yap1* and Δ*cys31*. (A) Strains grown on SC media. (B) Strains grown on SC media with 1 mM diamide added. (C) Strains grown on SC media with 2 mM diamide added. (D) Strains grown on SC media with 8 µg/ml gliotoxin added. (E) Strains grown on SC media with 1 mM diamide and 8 µg/ml gliotoxin added. (F) Strains grown on SC media with 2 mM diamide and 8 µg/ml gliotoxin added.

In Figure 6.9 B, 2 mM diamide elicits a sensitive phenotype in both Δ*sod1* and Δ*yap1*. As both are involved in OS response, any increase in OS by diamide toxicity would be potentiated by the loss of each respective gene. Δ*yap1*s' augmented sensitivity when compared to Δ*sod1* could be due to Yap1 transcriptional positive regulation of OS response genes. One such gene, *GLR1* could alleviate diamide stress via its glutathione reductase role maintaining GSSG and GSH levels and subsequently the oxidative state of the cell (Lee *et al.*, 2001; Muller 1996)

Gsh1 and Cys3 are both involved in glutathione biosynthesis. Loss of these genes educes a resistant phenotype when exposed to diamide, indicating they may possess low levels of glutathione (Grant *et al.,* 1997; Bernardo *et al.,* 2003; Piccirillo *et al.,* 2009). Lower levels of glutathione, reduces the risk of diamide mediated oxidisation of GSH to GSSG and subsequent OS. When Δ*gsh1* and Δ*cys3* growth on 8 µg/ml gliotoxin is compared to this, Δ*cys3* has an increased sensitive phenotype while Δ*gsh1* shows an increased resistant phenotype compared to the wild type BY4741. This altered response seen in the phenotype of Δ*cys3* on diamide versus gliotoxin suggests that low glutathione levels, presumably responsible for its resistance to diamide, is insufficient to aid with its growth in the presence of gliotoxin.

When these same cells are exposed to a combination of both 1 mM diamide and 8 µg/ml gliotoxin (Figure. 6.9 E) there is some improvement in growth when compared to gliotoxin alone, however only in strains Δ*yap1* and Δ*cys3*. Wild-type, Δ*sod1*, and Δ*gsh1* show no significant difference in their respective growth response in the presence of both diamide and gliotoxin when compared to gliotoxin alone demonstrating addition of diamide is not advantageous in these strains; while in Δ*yap1*, and to a lesser extent Δ*cys3*, it does. Any benefit caused by diamide presence must not out-weigh gliotoxin toxicity in wild-type, Δ*sod1* or Δ*gsh1* strains.

6.5.2 Influence of 1-Chloro-2,4 di-nitro benzene on *S. cerevisiae* growth response on gliotoxin.

CDNB is a benzene derivative which has been shown to reduce the *in vivo* glutathione pools by conjugating to the free thiol of GSH (Izawa *et al.,* 1995) and inhibiting thioredoxin reductase and glutathione reductase which are both required in protecting against oxidative stress and re-formation of GSH from GSSG (Holmgren 1989; Grant 2001). CDNB is non-toxic to *S. cerevisiae* as seen in Figure 6.10 A with no change in the growth when compared to un-exposed cells (Izawa *et al.,* 1995; Trotter & Grant 2002a). Inoculated cultures were incubated with CDNB prior to transferral to minimal media plates in an attempt, to artificially reduce the intra-cellular levels of GSH in *S. cerevisiae* strains to examine if their respective growth could be improved to gliotoxin exposure once GSH was depleted (Figure 6.10 A-C).

In Figure 6.10 A, the addition of CDNB (0.08 M) had no adverse effects on cells when grown on minimal media. When exposed to 8 µg/ml gliotoxin (Figure. 6.10 B), this was not the case for Δ*sod1* + CDNB, where pre-incubation with CDNB potentiated gliotoxin toxicity increasing Δ*sod1* + CDNB sensitivity. Δ*sod1* has a hypersensitive phenotype when exposed to gliotoxin, presumably due to the loss of an important OS response gene. When there is a simultaneous reduction in glutathione due to CDNB pre-exposure, gliotoxin toxicity is exacerbated in the Δ*sod1* +CDNB strain, as two key OS responses no longer exist and its inability to tackle OS stress inflicted by gliotoxin presence is intensified.

In Figure 6.10 B, BY4741 + CDNB and Δ*yap1* + CDNB show an improvement in growth when compared to wild type and Δ*yap1* un-exposed cells respectively. This CDNB required augmentation of growth, improves growth on higher concentrations of gliotoxin (16 µg/ml) (Figure 6.10 C). Very little growth of the Δ*yap1* +CDNB can be seen while none is visible for Δ*yap1*. This along with the increased resistance of the BY4741 + CDNB demonstrates CDNBs' ability to improve growth of certain strains when exposed to gliotoxin via the reduction of glutathione levels inside the cell, further corroborating a relationship between glutathione presence and gliotoxin toxicity.

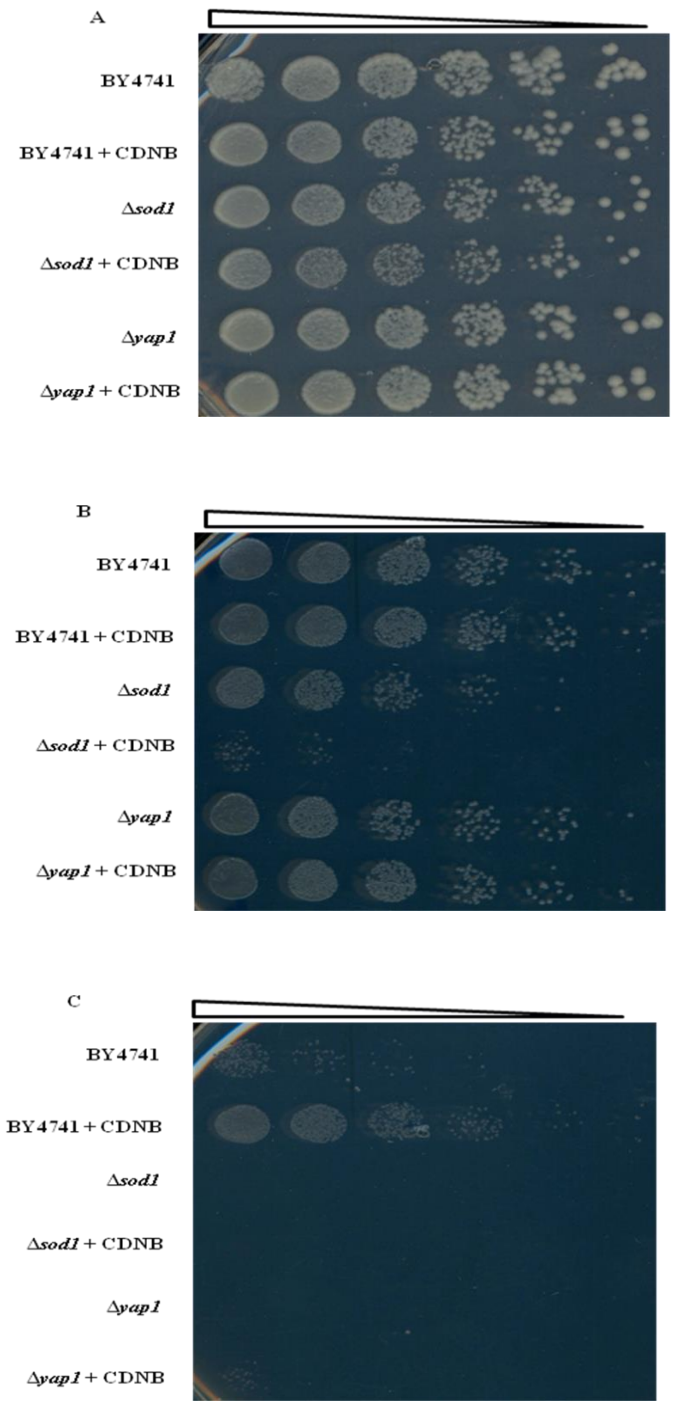

Figure 6.10 A-C Growth analysis of *S. cerevisiae* strains exposed with or without CDNB and grown on synthetic complete media (SC) with or without gliotoxin. Comparative growth analysis assay using strains BY4741a, BY4741a + CDNB Δ*sod1*, Δ*sod1* + CDNB, Δ*yap1* and Δ*yap1* + CDNB. (A) Strains grown on SC media. (B)

Strains grown on SC media with 8 µg/ml gliotoxin added. (C) Strains grown on SC media with 16 µg/ml gliotoxin added.

6.6 Glutathione quantification in *S. cerevisiae*

From the previous sections glutathione appears to play some role in the cells response to gliotoxin toxicity, with diminished levels of glutathione providing resistance to gliotoxin exposure. To verify this, *S. cerevisiae* lysates were created from minimal media and used to quantify the glutathione content of specific strains. As glutathione exists in two forms, a reduced GSH and oxidised GSSG, it's important to measure both to ascertain the redox state of the cell (Meister 1988; Drakulic *et al.,* 2005; Østergaard *et al.,* 2004).

The ratio of GSH:GSSG is pushed in favour of the reduced form (Meister 1988; Grant *et al.,* 1996) with a proportional increase in both indicative of increased redox stress in that cell (Trotter & Grant 2002a; Gales *et al.,* 2008). As can be seen in Figure 6.11, there is clear difference in the glutathione content of *S. cerevisiae* strains which may explain their different growth responses to gliotoxin exposure. The wild-type strain BY4741a exhibits almost equal levels of GSH:GSSG suggesting some form of OS is occurring, perhaps due to being grown on minimal media. Δ*sod1* shows negligible levels of glutathione under these same conditions with its GSSG content being slightly less than BY4741a. Indicating all GSH being produced is being oxidised into the GSSG form presumably due to its anti ROS role in the cell and at this time point (24 hours) and has not yet been reduced back to GSH. Δ*yap1* possess significantly greater ($P = 0.002$) GSSG:GSH levels, when compared to wild-type. This reduced glutathione level could be due to reduced expression of *GLR1* and *GSH*, both of which are transcriptionally regulated by Yap1 which is no longer present in this strain (Lee *et al.,* 2013).

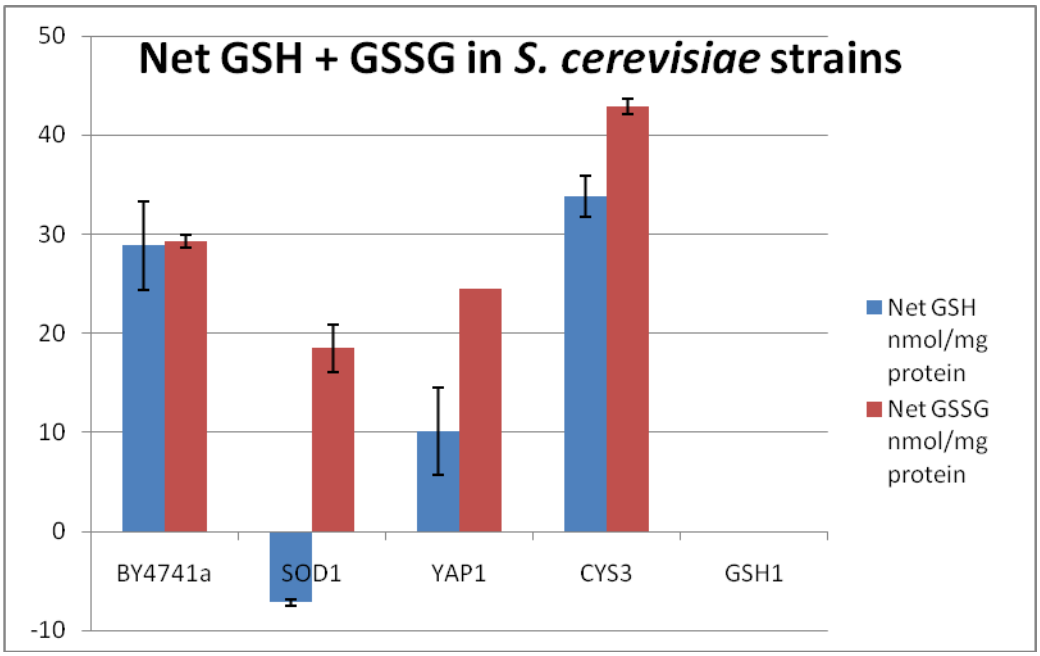

Figure 6.11 Glutathione quantification in *S. cerevisiae* strains Net GSH and GSSG levels were quantified using protein lysates of *S. cerevisiae* strains BY4741a, Δ*sod1*, Δ*yap1*, Δ*cys3* and Δ*gsh1* grown in minimal media.

Δ*cys3* shows GSH levels comparable to those of BY4741a, however the levels of GSSG are significantly higher ($p = 0.004$). As the GSH levels are not altered compared to wild type, loss of Δ*cys3* does not appear to be vital in the formation of glutathione, presumably due to the availability of l-cysteine in the media which can be taken up by the cell and used to synthesise glutathione. Its increased GSSG levels suggest increase in GSH oxidation as part of its role in the OS response. Although loss of Δ*cys3* may not significantly alter the glutathione levels inside the cell, this increase in GSSG could be caused by loss of other *CYS3* activity such as a subsequent rise in l-cystathionine which has been seen to result in homocysteine accumulation which can be toxic to cells (Fujita *et al.*, 2006).

No measurable quantities of GSH or GSSG could be detected in the Δ*gsh1* strain, confirming its pivotal role in glutathione biosynthesis. Since all gliotoxin plate assays were carried out on similar media, the glutathione levels shown in figure 6.11, depict the cells glutathione level prior to being exposed to gliotoxin.

In cells where GSH and GSSG are absent i.e. Δ*gsh1*, we see resistance in the presence of gliotoxin highlighting that complete absence of glutathione is advantageous when exposed to gliotoxin. Δ*cys3* sensitivity to gliotoxin could be due to its significantly higher levels of GSSG seen Figure 6.11. Alongside this, gliotoxin redox cycling would further dysregulate the oxidative state of the cell inducing stress. Similarly in Δ*yap1* and Δ*sod1*, which show high GSSG:GSH levels, gliotoxin could increase the GSSG levels in the cell by its own mediated by GSH. However the sensitivity seen in Δ*sod1* and Δ*yap1* is more likely a combination of the altered glutathione levels in these strains and the role their respective genes play in the OS response.

6.7 Metformins' influence on *S. cerevisiae* growth in response to gliotoxin exposure

Metformin is a compound primarily used in the treatment of type-2 diabetes whereby it reduces plasma concentrations of glucose helping reduce hypoglycaemia and promote less weight gain when compared to similar treatments (Nosadini *et al.,* 1987; Li *et al.,* 1999; Mäkimattila *et al.,* 1999). Although the exact mechanism of its functionality is not yet fully elucidated, it has been found to be important in other treatments such as reducing cancer (Dowling *et al.,* 2011) and in delaying the ageing of rodents and nematodes (Anisimov *et al.,* 2011; Onken & Driscoll 2010; Cabreiro *et al.,* 2013).

In a most recent study, Cabreiro *et al.,* (2013) found that *C.* elegans feeding on *E.* coli which were pre-exposed to metformin (100 mM), helped increase lifespan by 36 %. They found this increase in lifespan was specific to *E. coli* exposed to metformin and was not seen in *C. elegans* plus metformin alone, indicating it was due to some modification of the *E. coli* themselves which was affecting the *C. elegans* ageing (Cabreiro *et al.,* 2013). Looking closer into the metabolic affects after metformin exposure, it was found metformin exposure disrupted folate metabolism by inhibiting methionine synthase causing a subsequent accumulation of 5-methyl tetrahydrofolate, reduction in homocysteine and an increase in the s-adenosyl homocysteine levels (33%) and s-adenosylmethionine (86%) (Cabreiro *et al.,* 2013).

From previous results in *S. cerevisiae*, the accumulation of L-homocysteine due to gliotoxin exposure could explain the sensitivity of certain strains. Using metformin, L-homocysteine levels could be artificially reduced in these strains and thus help promote growth on gliotoxin. However as seen in Figure 6.12 B, exposure to 100 mM metformin increases sensitivity of Δ*sod1* and Δ*gsh1* when compared to plates with no metformin added (Figure 6.12 A) suggesting an alteration of the SAM cycle potentiates gliotoxin toxicity in these strains. When grown on minimal media plates containing 8 µg/ml gliotoxin and 100 mM metformin (Figure. 6.12 D) the growth of all strains is reduced when compared to 8 µg/ml gliotoxin alone (Figure. 6.12 C) indicating presence of metformin does not help promote growth in the presence of gliotoxin, but potentiates it due to some alteration of methionine biosynthesis.

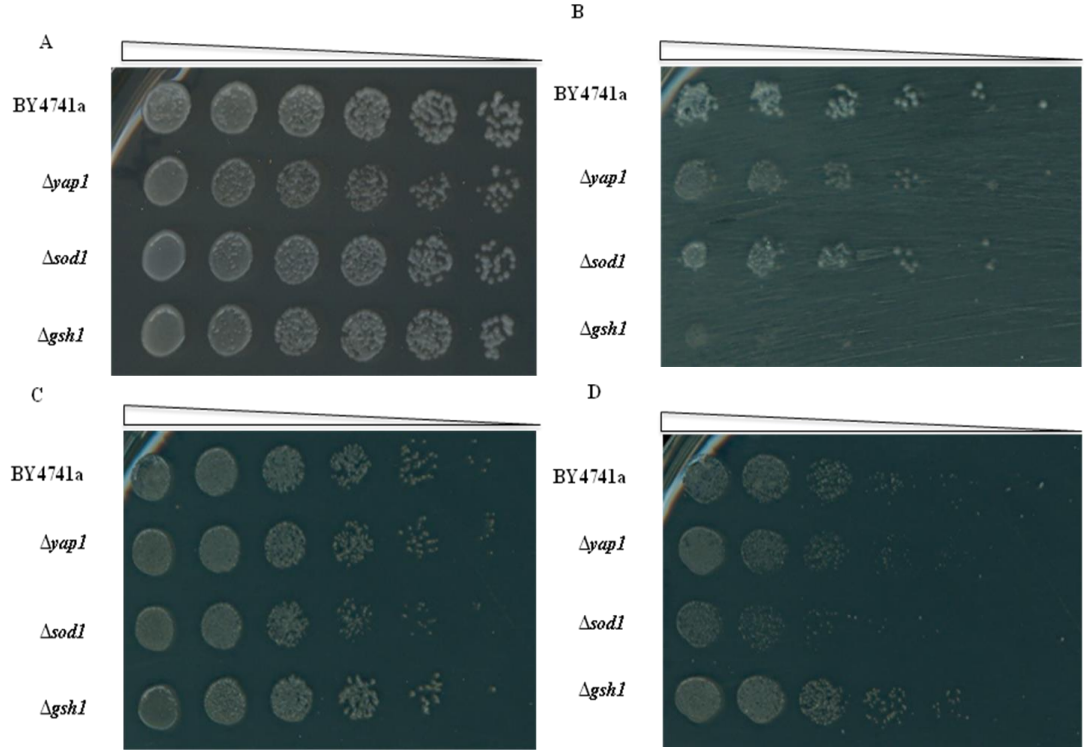

Figure 6.12 A-D Growth analysis of *S. cerevisiae* strains grown on synthetic complete media (SC) with or without gliotoxin and/or 100 mM metformin. Comparative growth analysis assay using strains BY4741a, Δ*yap1*, Δ*sod1* and Δ*gsh1*. (A) Strains grown on SC media. (B) Strains grown on SC media with 100 mM metformin added. (C) Strains grown on SC media with 8 µg/ml gliotoxin added. (D) Strains grown on SC media with 100 mM metformin and 8 µg/ml gliotoxin added

6.8 Comparison of RNA Sequence analysis and phenotypic response to gliotoxin in *S. cerevisiae*

RNA sequence analysis is one form of investigative study which can highlight key areas which are differentially regulated at the transcript level in response to a specific stimulus. Using the *S. cerevisiae* strain G600 exposed to two concentrations of gliotoxin (16 µg/ml and 64 µg/ml respectively were chosen in this study to compare a concentration which inhibited the growth of 50 % of a population and a higher concentration which causes >90 % inhibtion of *S. cerevisiae* growth) O'Brien (2011) carried a full transcriptomic study on the yeasts response to gliotoxin exposure. In the presence of gliotoxin, it was found ribosome biogenesis, protein biosynthesis and stress response genes were found to be the most common biological processes which were found to have >2 fold up-regulation, while carbohydrate metabolism, transport and mitochondrion organisation were found to be the most common biological processes with > 2 fold down-regulation (O'Brien 2011).

This data allowed for further examination of genes involved in gliotoxin tolerance at the transcript level. From this work it was clear that gliotoxin exposure caused a subsequent up-regulation of genes involved in methionine biosynthesis. In table 6.2, genes involved in methionine biosynthesis, glutathione biosynthesis and oxidative stress are differentially regulated when exposed to gliotoxin

Table 6.1 Transcript Up and Down regulation in response to 16 µg/ml gliotoxin exposure in *S. cerevisiae* vs. *S. cerevisiae* control

Gene Name	>1.5 fold up-regulation	>1.5 fold down-regulation
GSH1	**ø**	**Ø**
GSH2	**ø**	**Ø**
CYS3	**4**	**-**
CYS4	**1.55**	**-**
STR3	**4**	**-**
STR2	**-**	**1.8**

SOD1	**ø**	**Ø**
YAP1	**ø**	**ø**
CTT1	**-**	**3.55**
GPX1	**-**	**5.85**
GPX2	**-**	**1.55**
MET6	**2.89**	**-**
SAM2	**3.88**	**-**
SAM1	**1.82**	**-**

ø= no significant up/down regulation

Genes involved in the OS response i.e. *YAP1, SOD1* show no differential regulation in response to gliotoxin exposure, indicating any OS stress induced by gliotoxin exposure does not affect these genes at the transcript level, perhaps due to an 'intact' OS stress response. However, there is a significant down-regulation of genes involved in hydrogen peroxide stress i.e. *CTT1, GPX1* and GPX*2,* corroborating results seen in plate assays using mutant strains exposed to gliotoxin whereby they showed no significant change in their growth response demonstrating how these genes are dispensable in the presence of gliotoxin and gliotoxin stress. This result further depicts gliotoxin acting as an anti-oxidant *in vivo* explaining why these and other OS response genes are significantly down-regulated when compared to the control condition.

Similar to gliotoxin plate assays, *CYS3* is significantly up-regulated in response to gliotoxin. Loss of *CYS3* results in a sensitive phenotype when challenged with gliotoxin. The significant up-regulation of *CYS3* and *CYS4* would suggest there is a demand for an increase in the transcription of genes which encode enzymes that catalyse the formation of L-cysteine a precursor of GSH biosynthesis. However, as a corresponding increase in *gsh1* and g*sh2* was not seen during these conditions, suggesting this significant increase in the expression of c*ys3* and *cys4* may not be directly linked to glutathione biosynthesis.

Additionally, there appears to be a simultaneous dysregulation of genes which are involved in different parts in the SAM biosynthesis cycle as seen in Figure 6.13.

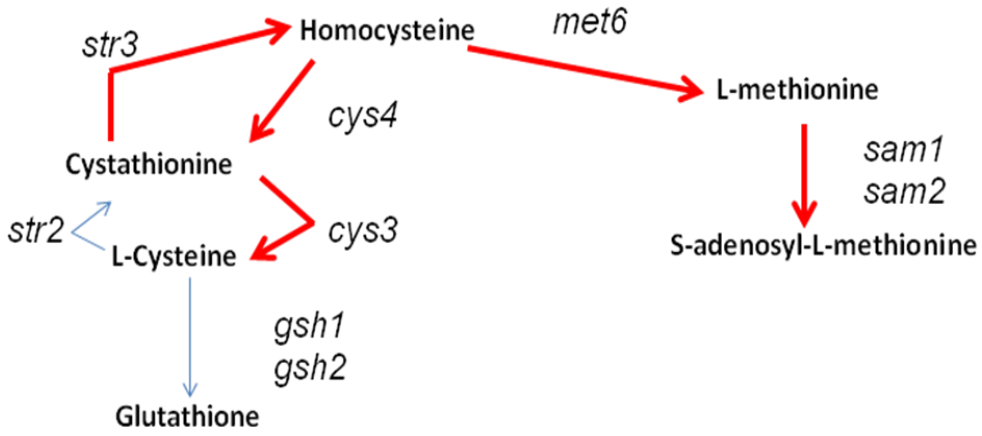

Figure 6.13 Representation of S-adenosyl Biosynthesis in *S. cerevisiae* Figure gives, genes italicised in their respective positions in this pathway. Red arrows depict significant transcript up-regulation, and blue depicting significant transcript down-regulation in response to 16 µg/ml gliotoxin exposure.

From Figure 6.13, there is significant up-regulation in genes which encode enzymes that catalyse the key preceding steps in SAM biosynthesis suggesting its role in gliotoxin stress. As mentioned previously, SAM is an essential molecule found in all cells, with *SAM1* and *SAM2* type genes being highly conserved eukaryotes (Lu 2000). SAM acts as a methyl donor in transulfuration reactions whereby it donates its methyl group to a methyl acceptor and is transformed into SAH (Mato *et al.*, 1997). This type of reaction is important in the OS response (Luo & Levine 2009) via the methylation of key OS response proteins which is a requirement of their function, and in the biosynthesis of polyamines which themselves play an important role in the stress response both directly via their interaction with ROS and in protecting important molecular components of the cell such as DNA and RNA (Finkelstein 1990). With the large increase in expression of genes in the SAM biosynthesis pathway, a corresponding increase in translation of the respective proteins may be of benefit in this regard i.e. SAMs role in the cellular stress response.

As mentioned previously, gliotoxin has an analogue in the form of Bis methyl gliotoxin which has been isolated from patients suffering from IA and found to more abundant than gliotoxin (Domingo *et al.*, 2012). It was hypothesised that this form of gliotoxin was actually a product of gliotoxin de-toxification, with each of the two methyl moieties being donated via SAM dependant methylation. However, this metabolite wasn't discovered in *S. cerevisiae* (section 6.9).

6.9 Bis-methyl-gliotoxin detection in *S. cerevisiae*

In section 6.8, transcriptomic evidence highlighted dysregulation of the SAM cycle, similar to what was seen in *A. fumigatus* (Chapter 5). This may indicate a role for this pathway in tackling gliotoxin toxicity, presumably via its role in the OS response or by modifying gliotoxin. As mentioned previously, any modification of gliotoxins disulphide bridge would be advantageous in attenuating gliotoxin toxicity. Similarly Bm-GT has been hypothesised as a product of gliotoxin detoxification and would require the SAM cycle in its biosynthesis. *S. cerevisiae* culture supernatants from cells exposed to gliotoxin showed no Bis methyl gliotoxin (m/z 357) to be produced indicating this mechanism of gliotoxin modification is not present in yeast and could go towards in explain its sensitivity (Figure. 6.14).

A

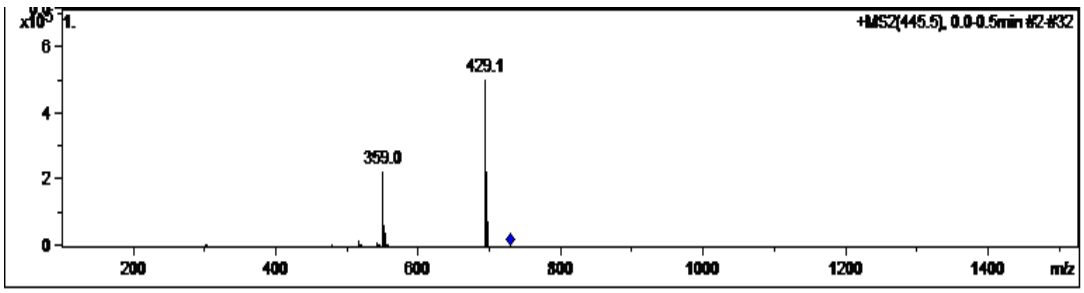

Figure 6.14 LC-MS detection of gliotoxin exposed *S. cerevisiae* culture supernatants Two un-associated peaks are found where the 357 Bm-GT should be detected if present

6.10 Discussion

Gliotoxin is a potent anti-fungal and cytotoxic toxin (Herrick 1945; Waring *et al.,* 1995; Sutton & Waring 1996). Gliotoxin toxicity is facilitated by the presence of an intra-molecular di-sulphide bridge which has been attributed to inactivating proteins via conjugation of their free thiols, resulting in the formation of ROS and subsequent OS and the disruption of the NADPH oxidase complex important in neutrophilic oxidase burst killing (Waring *et al.,* 1995; Carberry *et al.,* 2012; Tsunawaki *et al.,* 2004).

To further elucidate the effects gliotoxin toxicity has on a eukaryotic cell, the tractable yeast model *S. cerevisiae* was employed. The growth of *S. cerevisiae* strains were assessed on known oxidative stress inducers such as H_2O_2 and diamide and compared to their respective growth on gliotoxin.

In Figure 6.6 B, 2 mM H_2O_2 elicits a hypersensitive phenotype in Δ*yap1* presumably due to the loss of Yap1p transcriptional regulation of key OS response genes (Kugel & Jones 1994; Agnés *et al.,* 2000; Kuge *et al.,* 2001). On 3 mM H_2O_2 (Figure. 6.6 C) Δ*gsh1* and Δ*sod1* possess a sensitive phenotype indicating at these higher concentrations loss of either Δ*gsh1* or Δ*sod1* leaves the cell vulnerable to H_2O_2 induced stress.

When challenged with gliotoxin (Figure.6.2 B) Δ*sod1*& Δ*yap1* possess a sensitivity suggesting gliotoxin is inducing some kind of OS on the cell, as illustrated previously (Chapter 3, Section 4.5.3). Interestingly, no difference in growth could be seen in other strains involved in the OS response such as Δ*gsh2*, Δ*ctt1* or Δ*glr1* suggesting these genes are either not involved in detoxifying the ROS induced by gliotoxin exposure or are not imperative in that response due to some form of compensatory mechanism.

In a genome wide screen of various *S. cerevisiae* mutants lacking particular genes by Chamilos *et al.,* (2008), Δ*cys3* was found to be sensitive to gliotoxin exposure, which was corroborated in this work. However, the sensitivity of Δ*yap*1 and Δ*sod*1 or the resistance repeatedly seen of the Δ*gsh1* strain were not identified. As Δ*gsh1* is lacking in glutathione (Lee *et al.,* 2001) this result implies reduced glutathione levels helps protect *S. cerevisiae* from gliotoxin toxicity.

Glutathione is synthesised via two enzymes: γ-glutamyl cysteine synthetase (*GSH1)* and glutathione synthetase (*GSH2*) whereby *GSH1* is the rate limiting step (Ohtake *et al.,* 1990; Jamieson 1998; Wheeler *et al.,* 2002). Δ*gsh2* has been shown to have reduced glutathione levels yet resulting in the over expression of *GSH1* via Met4p positive regulation (Wheeler *et al.,* 2002). Once challenged with gliotoxin Δ*gsh2* shows no inhibition in growth demonstrating that low levels of glutathione in Δ*gsh2* does not elicit gliotoxin resistance. This may suggest that only null levels of glutathione are advantageous when exposed to gliotoxin or that absence of γ-glutamyl cysteine could induce the resistance seen Δ*gsh1*.

Both Δ*yap1* and Δ*sod1* are sensitive to 2 mM diamide (Figure. 6.9 C) presumably due to the induction of OS. Δ*cys3* and Δ*gsh1* are resistant to diamide exposure (Figure. 6.9 C) as is Δ*gsh2* (Trotter & Grant 2002b). Resistance to diamide suggests low levels of glutathione in the cell. As each of these are involved in different stages of glutathione biosynthesis, their resistance could be due to altered glutathione levels *in vivo* and subsequent reduction in diamides' ability to oxidise glutathione thus attenuating stress (Boyland & Chasseaud 1967; Lee *et al.,* 2001; Wheeler *et al.,* 2002). This result further suggests that low glutathione levels are not sufficient to instil resistance to gliotoxin as Δ*cys3* is sensitive to gliotoxin, yet has low glutathione levels. When challenged with both gliotoxin (8 µg/ml) and diamide (1 mM) (Figure 6.9 E) only Δ*yap1* shows improved growth while in remaining strains co-addition of diamide and gliotoxin elicits a wild-type phenotype (Figure 6.9 E).

Pre-exposure to CDNB educes improved growth of wild-type and Δ*yap1* resulting in growth on higher gliotoxin concentrations (16 µg/ml, Figure 6.10 C). CDNB specifically scavenges glutathione, depleting intracellular levels (Izawa *et al.,* 1995; Wheeler *et al.,* 2003) further supporting the hypothesis that loss of glutathione is important in gliotoxin toxicity. The increased sensitivity seen in Δ*sod1* + CDNB would suggest that loss of Sod1p and depleted levels of glutathione only exacerbate gliotoxin toxicity. Addition of CDNB and loss of *SOD1* potentiates the sensitivity seen in Δ*sod1* upon exposure to gliotoxin. This could suggest loss of both glutathione and *SOD1* leaves the cell vulnerable to OS induced by gliotoxin toxicity.

The GSH:GSSG ratio is highly regulated in order to maintain the redox state of the cell, with the reduced form found in greater amounts (50:1) creating a reduced environment inside the cell (Meister 1988; Drakulic *et al.,* 2005). During the course of this work, it was hypothesised that glutathione levels influenced gliotoxin toxicity with null levels of glutathione resulting in resistance. This can be seen in Δ*gsh1* which showed no measurable levels of GSH or GSSG due to the loss of the γ-glutamyl cysteine synthetase gene, and is subsequently, highly resistant to gliotoxin exposure. This is further supported by the sensitivity seen in Δ*cys3* when challenged with gliotoxin exposure and its corresponding altered levels of GSSG which might lead to this sensitivity. Loss of Δ*sod1* and Δ*yap1* respectively, results in a reduction in GSH and GSSG levels when compared to BY4741a wild type. Each possesses higher levels of GSSG compared to their respective GSH levels which is indicative of some underlying OS occurring. This increase in endogenous stress, in combination with gliotoxin toxicity would result in increase in ROS subsequently inhibiting growth, as seen in figure 6.2 B. The GSH:GSSG ratio seen in Figure 6.11 for BY4741a wild-type is almost equal and not what would be expected as a higher level of reduced glutathione is maintained within the cell (Muller 1996; Drakulic *et al.,* 2005). This could be attributed to growth on minimal media and the availability of resources inducing nutritional stress already inside the cell.

Metformin has been shown previously to influence the methionine biosynthesis cycle which in turn can influence the glutathione biosynthesis pathway due to L-cysteine availability from homocysteine (Cabreiro *et al.,* 2013; Ohtake *et al.,* 1990). Interestingly addition of metformin (Figure 6.12 B) increases the sensitivity of all strains, notably Δ*gsh1* and Δ*yap1*. Once added in combination with gliotoxin, the sensitivity induced by metformin is still present in Δ*gsh1* halting the resistance seen when grown on gliotoxin alone (Figure 6.12 C). This does not necessarily imply that metformin addition induces sensitivity of Δ*gsh1* to gliotoxin, as Δ*gsh1* does not show further sensitivity on metformin and gliotoxin when compared to metformin alone.

From this body of work a key role for glutathione absence has been identified which instils resistance to gliotoxin exposure in Δ*gsh1*. Altered levels of glutathione

and the loss of OS response genes also underlie sensitivity seen in different *S. cerevisiae* strains once challenged with gliotoxin, highlighting gliotoxins' ability to induce some form of ROS, presumably in the form of the superoxide radical due to its redox cycling ability and its transport facilitated by reduced glutathione (Bernardo *et al.*, 2003; Sutton & Waring 1996) . The absence of Bm-GT in *S. cerevisiae* culture supernatants may explain its sensitivity to this fungal secondary metabolite and may also support its role as a detoxification mechanism of gliotoxin in *A. fumigatus* which is not present in yeast.

Chapter 7

Discussion

7.1 Thesis Discussion

Gliotoxin is an important secondary metabolite which further mediates invasive aspergillosis in immuno-compromised individuals (Sutton & Waring 1996). Although gliotoxins' chemical structure and biosynthetic cluster have been characterised, a lot has yet to be elucidated about the genes involved in its biosynthesis. This work depicts the characterisation of two genes, *gliT* and *gliZ*, found within the gliotoxin biosynthetic cluster *gli*, in the human opportunistic pathogen *Aspergillus fumigatus.* It describes the dysregulation of two key cellular pathways which appear to have separate roles in gliotoxin toxicity and gliotoxin detoxification, highlighting a novel relationship between gliotoxin and two molecules found within these different pathways. A secondary role for gliotoxin is also demonstrated, suggesting gliotoxin may in fact be an accidental toxin possessing an additional role as an anti-oxidant in *A. fumigatus*

GliZ encodes a Zn2Cys6 bi-nuclear transcriptional regulator of the *gli* cluster (Bok *et al.,* 2006). In Δ*gliZ* gliotoxin biosynthesis is completely abolished, however *gliT* has been shown to be expressed (Bok *et al.,* 2006; Schrettl *et al.,* 2010). Δ*gliZ* shows no sensitivity to gliotoxin, presumably due to the independent regulation of *gliT* which, along with other *gli* cluster genes, has been noted to increase in the presence of exogenous gliotoxin (Cramer *et al.,* 2006), further highlighting its role in self protection against gliotoxin presence (Bok *et al.,* 2006). As mentioned, *gliT* is involved in self protection against gliotoxin toxicity acting as a gliotoxin oxido-reductase reducing the trans-molecular di-sulphide bridge which is imperative in gliotoxin toxicity. Loss of *gliT* results in hypersensitivity to relatively low levels of gliotoxin (Schrettl *et al.,* 2010). Similar to Δ*gliZ*, no gliotoxin could be detected in Δ*gliT* culture supernatants, suggesting gliotoxin biosynthesis is abolished, or that gliotoxin efflux is inhibited.

Δ*gliT*Δ*gliZ* was created to characterise the phenotypic response in *A. fumigatus* when the *gli* cluster was completely silenced. Interestingly, exposure to gliotoxin elicited a sensitive phenotype, however this response was not as sensitive as Δ*gliT*. This led to the hypothesis that some gliotoxin biosynthesis may be occurring in Δ*gliT* eliciting a hypersensitive phenotype to exogenous gliotoxin. Evidence can be found in

the transcriptome response to gliotoxin in Δ*gliT*. A significant increase in expression of almost all *gli* genes could result in the formation of endogenous gliotoxin, or gliotoxin related intermediates, may have the potential to potentiate exogenous gliotoxin toxicity and subsequent Δ*gliT* sensitivity. An intermediate with a mass of 279.076 m/z was found to be unique to Δ*gliT* supernatants (Schrettl *et al.,* 2010). Although this was later found to not induce any sensitivity, this suggests different metabolites are being produced in this strain which may be deleterious. Secondly, Δ*gliT*Δ*gliZ* is not as sensitive as Δ*gliT* presumably due to the absence of these intermediates as the *gli* cluster is completely silenced. Instead, Δ*gliT*Δ*gliZ* sensitivity to exogenous gliotoxin, is due to the loss of the *gliT* self protective mechanism, explaining why it's more sensitive than Δ*gliZ* which still expresses *gliT*. Accumulation of endogenous *gli* related products and other factors which will be discussed later, can be attributed to the hyper-sensitivity seen in Δ*gliT*.

Gliotoxin exists in either a di-sulphide oxidised form or a reduced di-thiol form. This di-thiol form has been demonstrated to be methylated to form bismethyl gliotoxin (bm-gt) which has previously been shown to exist at either greater or equi-molar concentrations than gliotoxin (Domingo *et al.,* 2012). Bm-gt is a more stable compound than gliotoxin, and due to its non-reactive nature, has been hypothesised as a product of gliotoxin detoxification (Waring & Beaver 1996). Bm-gt synthesis may be differentially regulated in the absence of *gliT* and *gliZ* in an attempt to reduce gliotoxin toxicity. This hypothesis is supported by the many observations made in chapters 3, 4 and 5. In summary, s-adenosyl-L-methionine acts as the primary methyl donor in methylation reactions, presumably in bm-gt formation. Genes and enzymes involved in the s-adenosyl-l-methionine biosynthesis cycle (SAM) were found to be dysregulated in response to gliotoxin, most probably in an attempt to influence bm-gt biosynthesis. This suggests that bm-gt biosynthesis may be up-regulated in these strains which could potentially be deleterious if not properly maintained.

Accumulation of by-products, namely l-homocysteine, has been demonstrated to be toxic if allowed to accumulate within the cell. This suggests an increase in the regulation of the SAM cycle brings with it the risk of these products accumulating if not properly regulated. Evidence for this occurring can be found in chapter 4 with the

identification of s-adenosyl homocysteinease in *gliT* and *gliZ* mutants exposed to gliotoxin compared to wild-type. This enzyme was found to have decreased expression in all *gliT* and *gliZ* mutant strains suggesting the L-homocysteine levels are being altered in response to gliotoxin. Two isoforms of this same enzyme was later identified in Δ*gliT* +/- gliotoxin, one which was down-regulated, same location as previous identifications, and the other which was up-regulated which was unique to this comparison, further suggesting l-homocysteine levels are significantly altered in this mutant compared to the other two. Alongside the aforementioned factors affecting *ΔgliT* sensitivity, this work provides evidence that l-homocysteine levels could also be a major factor facilitating its sensitivity to gliotoxin.

Additionally, Met H/D cobalamin L-methionine synthase was identified to be differentially regulated in Δ*gliZ* and Δ*gliT*Δ*gliZ* when compared to wild-type cells exposed to gliotoxin. Similarly to s-adenosyl homocysteinase, this enzyme is also involved in the SAM cycle utilised in the biosynthesis of L-methionine. Altered expression of both these enzymes may suggest that components of the SAM cycle may be induced by components of the *gli* cluster which are now silenced in these strains thus this enzyme is now being repressed. This is supported by the fact this enzyme was not identified in Δ*gliT* as it can still express these *gli* genes. Furthermore, it may also explain why only identify the up-regulated s-adenoysl homocysteinease isoform in Δ*gliT* protein lysates and not Δ*gliZ* or Δ*gliT*Δ*gliZ* +/- gliotoxin.

The dysregulation in the SAM cycle could also be a mechanism linked to gliotoxin toxicity. This is supported by the observations made in chapter 6 wherein cellular pathways, notably the SAM cycle, were altered in a similar fashion in both the yeast *S. cerevisiae* and Δ*gliT* when exposed to gliotoxin. Additionally, *S. cerevisiae* was shown to be unable to bis methylate gliotoxin suggesting this pathway is naturally up-regulated in fungi sensitive to gliotoxin and its role in modifying gliotoxin could be a later adaptation evolved by the fungus.

Throughout this work, glutathione levels have been hypothesised to be linked with gliotoxin susceptibility. This is supported by the fact that gliotoxin has been shown

to transport freely into mammalian cells in a glutathione dependent manner (Bernardo *et al.*, 2003) highlighting the relationship between gliotoxin and glutathione. Additionally in *S. cerevisiae*, complete absence of glutathione confers resistance to gliotoxin exposure in Δ*gsh1* (chapter 6). This suggests that the absence of glutathione is advantageous to cells and that high glutathione levels may be deleterious. This was demonstrated in Carberry *et al.*, where Δ*gliT* was found to have significantly higher GSH levels when grown in AMM media and subsequent sensitivity to gliotoxin exposure (Carberry *et al.*, 2012).

In yeast low to null levels of glutathione may reduce the influx of gliotoxin into the cell thus preventing it from having an effect. While in *A. fumigatus* this may not be the case due to the presence of a putative gliotoxin transporter protein gliA. Which may actively pump gliotoxin in and out of the cell regardless of the glutathione levels in the cell.

Gliotoxin has been previously demonstrated to be a potent anti-fungal agent inhibiting growth of many different fungi (Waring *et al.*, 1995). However, based on results shown here, it is unclear if this is its only role in the cell and whether it may in fact be an anti-oxidant molecule in *A. fumigatus*. Support for this can be seen in chapter 3 where co-addition of 15 μg/ml gliotoxin attenuates ROS production in cells challenged with 5 mM H_2O_2. Also Choi *et al.*, noted that gliotoxin actively targeted the thioredoxin system, accelerating the oxidation of NADPH and subsequent reduction of H_2O_2 to water and molecular oxygen (Choi *et al.*, 2007). This suggests gliotoxin has a dual function in the cell or that its toxic affect on other fungal cells is serendipitous.

Interestingly, co-addition of gliotoxin and H_2O_2 in agarose plates was found to elicit a wild-type phenotype in Δ*gliT*, with the hypersensitivity to gliotoxin previously seen on gliotoxin only plates completely disappearing. This indicates H_2O_2 chemically substitutes for *gliT* loss, presumably through the reaction found in Choi *et al.*, whereby gliotoxin is oxidised facilitating its efflux from the cell.

The findings presented here highlight many key issues involved in gliotoxin biosynthesis and gliotoxin toxicity. As described by Schrettl *et al.*, *gliT* is essential in

the self protection against gliotoxin. However, silencing of the *gli* cluster, including *gliT*, does not elicit a similarly sensitive phenotype. This suggests loss of *gliT* alone may not explicate Δ*gliT*s' sensitivity to gliotoxin but the involvement of various other factors such as biosynthesis and subsequent accumulation of reduced gliotoxin, inability to produce bm-gt, accumulation of *gli* cluster intermediates and accumulation of L-homocysteine. This highlights some of the effects gliotoxin may be inducing in non gliotoxin producing cells as illustrated in *S. cerevisiae* with exogenous gliotoxin addition inducing a similar dysregulation of the SAM cycle as in Δ*gliT*.

The identification of S-adenosyl homocysteinase common to all *gliT* and *gliZ* mutants responding to gliotoxin implies that the alteration of the *gli* cluster results in the dysregulation of components of the SAM cycle which may potentiate gliotoxin toxicity within these strains and could help explain particular phenotypes seen in these respective strain genotypic backgrounds.

This work has contributed to the characterisation of *gli* cluster mutants, highlighting key cellular pathways involved in gliotoxin tolerance and toxicity. Additionally, this work stresses the need for further work in elucidating the mechanisms involved in gliotoxin biosynthesis and the endogenous machinery utilised for its detoxification which could be employed as potential cellular targets.

From this body of work, the components of secondary metabolite regulation and biosynthesis, particularly in the case of gliotoxin, can be seen to not always be linear but can in fact be quite complex. This may also be the case in other secondary metabolite clusters, especially those with clustered genes orthologous to those of the *A. fumigatus gli* cluster. Secondly, gliotoxin and similar ETP molecules could fulfil multiple functions within a particular organsims, as demonstrated here with gliotoxin performing an anti-oxidant role in the presence of H_2O_2, and it may be the case that these other secondary metabolites could have a similar dual function which has yet to be characterised.

7.2 Future Work

Work presented here has raised many key questions with regard to gliotoxin biosynthesis and means of gliotoxin toxicity in *A. fumigatus* and *S. cerevisiae*. These include the LC-MS identification of Bm-GT production in *gliT*, *gliZ* mutants. The ability to produce Bm-GT may be a by-product of gliotoxin detoxification and could be impaired in *A. fumigatus* strains which exhibit a sensitive phenotype to gliotoxin. Based on the similarities of *A. fumigatus* Δ*gliT* and *S. cerevisiae* transcriptome and phenotypic response to exogenous gliotoxin, Bm-GT may be abolished in Δ*gliT*.

Secondly, the quantification of L-homocysteine and SAH from *A. fumigatus* lysates could help corroborate the hypothesis made throughout this body of work that gliotoxin dysregulates the SAM cycle inducing toxicity by inducing accumulation of one or both of these molecules which are toxic at high levels in the cell. *A. fumigatus* lysates exposed and un-exposed to gliotoxin could illustrate a rise in the level of L-homocysteine or SAH and could be expected to have a greater affect in *A. fumigatus* and yeast strain which elicit a sensitive phenotype.

Glutathione levels have been demonstrated to play an important factor in the response to gliotoxin in *S. cerevisiae* and *A. fumigatus*. Low to null levels of GSH has been illustrated to be advantageous to *S. cerevisiae* Δ*gsh1* eliciting a resistant phenotype to gliotoxin. Similarly the addition of GSH reducing chemicals, i.e. CDNB, was shown to significantly improve growth of certain *S. cerevisiae* strains when challenged with exogenous gliotoxin. Additionally, the GSH levels in *A. fumigatus* were found to be altered un unstressed *gliT*, *gliZ* mutant strains and was suggested to be a factor in their respective sensitivities to exogenous gliotoxin exposure. To further corroborate this, *A. fumigatus* gene deletions of gene involved in GSH biosynthesis should be examined to test if low to null GSH levels are as vital in *A. fumigatus* as they are in *S. cerevisiae*.

Lastly, proteomic analysis of the *A. fumigatus* response to exogenous gliotoxin identified one key enzyme found to be shared in all *A. fumigatus gliT*, *gliZ* mutant strains. S-adenosyl homocysteinease is involved in the hydration of SAH to form L-homocysteine, and its expression is significantly decreased in Δ*gliT*, Δ*gliZ* and

Δ*gliT*Δ*gliZ* when compared to *A. fumigatus* AF293 wild type. This is further evidence of gliotoxin alteration of the SAM cycle and suggests accumulation of L-homocysteine. It may be of interest to influence the levels of L-homocysteine by either addition of L-homocysteine or other product which will be used to produce L-homocysteine, e.g., L-cystathionine, directly into the media. Or by creating a gene deletion of methionine synthase which methylates L-homocysteine to produce L-methionine, thus reducing the L-homocysteine levels. Either could increase L-homocysteine levels inside the cell and potentially augment gliotoxin toxicity.

This work highlights key areas for future studies which will help further elucidate the means of gliotoxin toxicity and biosynthesis in *A. fumigatus* and its effects on other fungi.

Chapter 8

References

Abadio, A.K.R., Kioshima, E.S., Teixeira, M.M., Martins, N.F., Maigret, B. & Felipe, M.S.S., (2011). Comparative genomics allowed the identification of drug targets against human fungal pathogens. *BMC Genomics*, **12**(1), p.75.

Agnés, D., Isnard, A. & Toledano, M.B., (**2000**). H_2O_2 sensing through oxidation of the Yap1 transcription factor. *EMBO Journal*, **19**(19), pp.5157–5166.

Aguilaniu, H., Semb, H., Nystro, T., Hernebring, M. & Brole, G., (2006). Elimination of damaged proteins during differentiation of embryonic stem cells. *PNAS*, **103**(20), pp.1–6.

Akashi, T., Kanbe, T. & Tanaka, K., (**1994**). The role of the cytoskeleton in the polarized growth of the germ tube in *Candida albicans*. *Microbiology*, **140**(2), pp.271–280.

Alberts, A.W., Chen, J., Kuron, G., Hunt, V., Huff, J., Hoffman, C., Rothrock, J., Lopez, M., Joshuat, H., Harrist, E., Patchettt, A., Monaghan, R., Currie, S., Stapley, E., Albers-Schonber, G., Hensens, O., Hirshfield, J., Hoogsteen, K., Liescht, J. & Springer, J., (1980). Mevinolin : A highly potent competitive inhibitor of hydroxymethylglutaryl-coenzyme A reductase and a cholesterol-lowering agent. *PNAS*, **77**(7), pp.3957–3961.

Albrecht, D., Guthke, R., Brakhage, A.A., *et al.*, (**2010**). Integrative analysis of the heat shock response in *Aspergillus fumigatus*. *BMC Genomics*, **11**(32), pp.1–17.

Aliaa, R.E.-S., (**2008**). Control of root-rot diseases of *Phaseolus vulgaris* using gliotoxin. *Malaysian Journal of Microbiology*, **4**(1), pp.40–43.

Aljofan, M., Sganga, M.L., Lo, M.K., Rootes, C.L., Porotto, M., Meyer, A.G., Saubern, S., Moscona, A. & Mungall, B.A., (2009). Antiviral activity of gliotoxin , gentian violet and brilliant green against Nipah and Hendra virus in vitro. *Virology Journal*, **13**, pp.1–13.

Alton Meister, (**1988**). Glutathione metabolism and its selective modification. *The Journal of Biological Chemistry*, **263**(33), pp.17205–17208.

Amitani, R., Taylor, G., Elezis, E.-N., Llewellyn-jones, C., Mitchell, J., Kuze, F., Cole, P.J. & Wilson, Robert (1995). Purification and characterization of factors produced by *Aspergillus fumigatus* which affect human ciliated respiratory epithelium. *Microbiology*, **63**(9), pp.3266–3271.

Angelova, M.B., Pashova, S.B., Spasova, B.K., Vassilev, S.V. & Slokoska, L.S., (2005). Oxidative stress response of filamentous fungi induced by hydrogen peroxide and paraquat. *Mycology Research*, **109**(2), pp.150–158.

Anisimov, V.N., Berstein, L.M., Popovich, I.G., Zabezhinski, M.A., Egormin, A.P., Piskunova, T.S., Semenchenko, A.V., Tyndyk, M.L., Yurova, M.N., Kovalenko, I.G. & Poroshina, T.E., (2011). If started early in life , metformin treatment increases life-span and postpones tumors in female SHR mice. *Aging*, **3**(2), pp.148–157.

Arellano, M. et al., (**2002**). Tea3p is a cell end marker activating polarized growth in *Schizosaccharomyces pombe*. *Current Biology*, **12**(9), pp.751–756.

Arnaud, M.B., Cerqueira, G.C., Inglis, D.O., Skrzypek, M.S., Binkley, J., Chibucos, M.C., Crabtree, J., Howarth, C., Orvis, J., Shah, P., Wymore, F., Binkley, G., Miyasato, S.R., Simison, M., Sherlock, G. & Wortman, J.R., (2011). The Aspergillus Genome Database (AspGD): recent developments in comprehensive multispecies curation, comparative genomics and community resources. *Nucleic Acids Research*, **40**(Database), pp.653–659.

Arst Jr, H. & Penalva, M.A., (**2003**). pH regulation in *Aspergillus* and parallels with higher eukaryotic regulatory systems. *Trends in genetics*, **19**(4), pp.224–231.

Arvanitis, M., Glavis-bloom, J. & Mylonakis, E., (**2013**). Invertebrate models of fungal infection. *BBA - Molecular Basis of Disease*, **1832**(9), pp.1378–1383.

Asif, A.R., Oellerich, M., Amstrong, V.W., Riemenschneider, B., Monod, M. & Reichard, U., (2006). Proteome of conidial surface associated proteins of

Aspergillus fumigatus reflecting potential vaccine candidates and allergens research articles. *Journal of Proteome Research*, **5**(1), pp.954 – 962.

Asif, A.R., Oellerich, M., Amstrong, V.W., *et al.*, (**2010**). Analysis of the cellular *Aspergillus fumigatus* proteome that reacts with sera from rabbits developing an acquired immunity after experimental aspergillosis. *Electrophoresis*, **31**(12), pp.1947–58.

Askew, D.S., (**2008**). *Aspergillus fumigatus*: virulence genes in a street-smart mold. *Current Opinion in Microbiology*, **11**(4), pp.331–7.

Auesukaree, C., Damnernsawad, A., Kruatrachue, M., Pokethitiyook, P., Boonchird, C. & Kaneko, Y., (2009). Genome-wide identification of genes involved in tolerance to various environmental stresses in *Saccharomyces cerevisiae*. *Journal of Applied Genetics*, **50**(3), pp.301–310.

Axelsson, V., Pikkarainen, K. & Forsby, A., (**2006**). Glutathione intensifies gliotoxin-induced cytotoxicity in human neuroblastoma SH-SY5Y cells. *Cell Biology and Toxicology*, **22**(2), pp.127–136.

Bachem, C.W.B., Hoeven, R.S.V.D., Bruijn, S.M.D., Vreugdenhil, D., Zabeau, M. & Visser, R.G. F., (1996). Visualization of differential gene expression using a novel method of RNA fingerprinting based on AFLP: Analysis of gene expression during potato tuber development. *The Plant Journal*, **9**(5), pp.745–753.

Balbo, A. & Bozzaro, S., (**2006**). Cloning of *Dictyostelium* eIF6 (p27BBP) and mapping its nucle(ol)ar localization subdomains. *European journal of cell biology*, **85**(9-10), pp.1069–78.

Balibar, C.J. & Walsh, C.T., (**2006**). GliP, a multimodular nonribosomal peptide synthetase in *Aspergillus fumigatus*, makes the diketopiperazine scaffold of gliotoxin . *Biochemistry*, (18), pp.15029–15038.

Bannister, J. V, Bannister, W.H. & Rotilio, G., (**1987**). Aspects of the structure, function, and applications of superoxide dismutase. *Critical Reviews in Biochemistry and Molecular Biology*, **22**(2), pp.111–180.

Barker, B., Kroll, K., Vödisch, M., Mazurie, A., Kniemeyer, O. & Cramer, R.A., (2012). Transcriptomic and proteomic analyses of the *Aspergillus fumigatus* hypoxia response using an oxygen-controlled fermenter. *BMC Genomics*, **13**(1), p.62.

Barrientos A., (2003). Yeast models of human mitochondrial disease. *IUBMB Life*, **55**(2), pp.83:95

Basten, E.J.W., Visser, J. & Schaap, P.J., (**2001**). Lysine aminopeptidase of *Aspergillus niger*. *Microbiology*, **147**, pp.2045–2050.

Bayram, Ö., Krappmann, S., Ni, M., Bok, J.W., Helmstaedt, K., Valerius, O., Braus-Stromeyer, S., Kwon, N.-J., Keller, N.P., Yu, J.-H. & Braus, G.H., (2008). VelB / VeA / LaeA complex coordinates light signal with fungal development. *Science*, **320**, pp.1504–1506.

Bell, M., Johnson, J., Wilde, B. & Woodward, R.B., (1958). The structure of gliotoxin. *The Journal of the American Chemical Society*, **80**(4), pp.1001–1001.

Bellí, N., Marın, S., Sanchis, V. & Ramos, A.J., (2004). Influence of water activity and temperature on growth of isolates of *Aspergillus* section Nigri obtained from grapes. *The Journal of Food Microbiology*, **96**(1), pp.19 – 27.

Bermingham-mcdonogh, O., Gralla, E.B. & Valentine, J.S., (**1988**). The copper , zinc-superoxide dismutase gene of *Saccharomyces cerevisiae* : Cloning , sequencing , and biological activity. *Genetics*, **85**(July), pp.4789–4793.

Bernardo, P.H., Chai, C.L.L., Deeble, G.J., Liu, X.-M. & Waring, P., (2001). Evidence for gliotoxin ± glutathione conjugate adducts. *Bioorganic and Meidicianl Chemistry Letters*, **11**, pp.483–485.

Bernardo, P.H., Brasch, N., Chai, C.L.L. & Waring, P., (2003). A novel redox mechanism for the glutathione-dependent reversible uptake of a fungal toxin in cells. *The Journal of Biological Chemistry*, **278**(47), pp.46549–46555.

Bhadauria, V., Popescu, L. & Zhao, W., (**2007**). Fungal transcriptomics. *Microbiological Research*, **162**, pp.285–298.

Bishop, A.L., Rab, F.A., Sumner, E.R., Avery, S.V., (2007). Phenotypic heterogeneity can enhance rare-cell survival in " stress-sensitive " yeast populations. *Molecular Microbiology*, **63**(December 2006), pp.507–520.

Blaiseau, P. & Thomas, D., (**1998**). Multiple transcriptional activation complexes tether the yeast activator Met4 to DNA. *The EMBO Journal*, **17**(21), pp.6327–6336.

Blatzer, M., Barker, B.M., Willger, S.D., Beckmann, N., Blosser, S.J., Cornish, J.E., Mazurie, A., Grahl, N., Haas, H. & Cramer, R.A., (2011). SREBP coordinates iron and ergosterol homeostasis to mediate triazole drug and hypoxia responses in the human fungal pathogen *Aspergillus fumigatus*. *PLoS Genetics*, **7**(12).

Bok, J.W., Chung, D., Balajee, S.A., Marr, K.A., Andes, D., Nielsen, K.F., Frisvad, J.C., Kirby, K.A. & Keller, N.P., (2006). GliZ , a transcriptional regulator of gliotoxin biosynthesis, contributes to *Aspergillus fumigatus* virulence. *Infection and Immunity*, **74**(12), pp.6761–6768.

Bok, J.W., Balajee, S.A., Marr, K.A., Nielsen, K.F., Frisvad, J.C. & Keller, N.P., (2005). LaeA , a regulator of morphogenetic fungal virulence factors. *Eukaryotic Cell*, **4**(9), pp.1574–1582.

Bok, J.W., Noordermeer, D., Kale, S.P. & Keller, N.P., (2006). Secondary metabolic gene cluster silencing in *Aspergillus nidulans*. *Molecular Microbiology*, **61**(6), pp.1636–1645.

Bok, J.W. & Keller, N.P., (**2004**). LaeA , a regulator of secondary metabolism in *Aspergillus spp*. *Eukaryotic Cell*, **3**(2), pp.527–535.

Botstein, D., Chervitz, S.A. & Cherry, J.M., (**2011**). Yeast as a model organism. *Science*, **277**(5330), pp.1259–1260.

Bové J., Prou D., Perier C., & Prxedborski S., (2005). Toxin-induced models of Parkinson's disease. *NeuroRx*, **2**(3), pp484-494.

Boyland, B.Y.E. & Chasseaud, A.L.F., (**1967**). Enzyme-catalysed conjugations of glutathione with unsaturated compounds. *Biochemical Journal*, **104**, pp.95–102.

Bozza, S., Gaziano, R., Lipford, G.B., Montagnoli, C., Bacci, A., Di, P., Kurup, V.P., Wagner, H. & Romani, L., (2002). Vaccination of mice against invasive aspergillosis with recombinant *Aspergillus* proteins and CpG oligodeoxynucleotides as adjuvants. *Microbes and Infection*, **4**(13), pp.1281–1290.

Brakhage, A.A., Schuemann, J., Bergmann, S., Scherlach, K., Schroeckh, V. & Hertweck, C., (2008). Activation of fungal silent gene clusters: A new avenue to drug discovery. *Nature Compounds as Drugs*, **66**, pp.1–12.

Brakhage, A.A. & Langfelder, K., (**2002**). Menacing Mold: The Molecular Biology of *Aspergillus fumigatus*. *Annual Reviews Microbiology*, **56**, pp.433–455.

Brakhage, A.A. & Schroeckh, V., (**2011**). Fungal secondary metabolites – Strategies to activate silent gene clusters. *Fungal Genetics and Biology*, **48**(1), pp.15–22.

Brennan, L., Hewage, C., Malthouse, J.P.G. & McBean, G.J., (2004). Gliotoxins disrupt alanine metabolism and glutathione production in C6 glioma cells: a 13C NMR spectroscopic study. *Neurochemistry international*, **45**(8), pp.1155–65.

Brennan, M., Thomas, D.Y., Whiteway, M. & Kavanagh, K., (2002). Correlation between virulence of *Candida albicans* mutants in mice and *Galleria mellonella* larvae. *FEMS Immunology and Medical Microbiology*, **34**, pp.153–157.

Brenner, S., Johnson, M., Bridgham, J., Golda, G., Lloyd, D.H., Johnson, D., Luo, S., Mccurdy, S., Foy, M., Ewan, M., Roth, R., George, D., Eletr, S., Albrecht, G., Vermaas, E., Williams, S.R., Moon, K., Burcham, T., Pallas, M., Dubridge, R.B., Kirchner, J., Fearon, K., Mao, J. & Corcoran, K., (2000). Gene expression analysis by massively parallel signature sequencing (MPSS) on microbead arrays. *Nature Biotechnology*, **18**(June), pp. 1021

Brookman, J.L. & Denning, D.W., (**2000**). Molecular genetics in *Aspergillus fumigatus*. *Current Opinion in Microbiology*, **3**(5), pp.468–474.

Brookman, J.L., Ratcliffe, N.A. & Rowley, A.F., (**1989**). Studies on the activation of the prophenoloxidase system of insects by bacterial cell wall components. *Insect Biochemistry*, **19**(1), pp.47–57.

Bruneau, J., Magnin, T., Tagat, E., Legrand, R., Bernard, M., Diaquin, M., Fudali, C., Latgé, J.-P., (2001). Proteome analysis of *Aspergillus fumigatus* identifies glycosylphosphatidylinositol-anchored proteins associated to the cell wall biosynthesis. *Electrophoresis*, **22**, pp.2812–2823.

Bruns, S., Seidler, M.,Albrecht, D., Salvenmoser, S., Remme, N., Hertweck, C., Brakhage, A., Kniemeyer, O. & Müller, F.-M.C., (2010). Functional genomic profiling of *Aspergillus fumigatus* biofilm reveals enhanced production of the mycotoxin gliotoxin. *Proteomics*, **10**(17), pp.3097–107.

Cabiscol, E., Piulats, E., Echave, P., Herrero, E. & Ros, J., (2000). Oxidative stress promotes specific protein damage in *Saccharomyces cerevisiae*. *Biochemistry*, **275**(35), pp.27393–27398.

Cabral, M.G., Viegas, C., Teixeira, M.C. & Sá-Correia, I., (2003). Toxicity of chlorinated phenoxyacetic acid herbicides in the experimental eukaryotic model *Saccharomyces cerevisiae*: role of pH and of growth phase and size of the yeast cell population. *Chemosphere*, **51**(1), pp.47–54.

Cabreiro, F., Au, C., Leung, K.-Y., Vergara-irigaray, N., Cocheme, H.M., Tahereh, N., Weinove, D., Schuster, E., Greene, N.D.E. & Gems, D., (2013). Metformin retards aging in *C. elegans* by altering microbial folate and methionine metabolism. *Cell*, **153**(1), pp.228–239.

Cagas, S.E., Jain, M.R., Li, H., Perlin, D.S., (2011). The proteomic signature of *Aspergillus fumigatus* during early development.*Molecular & Cellular Proteomics*, **10**(1), pp.1–20.

Calera, A., Paris, S., Monod, M., Hamilton, A.J., Debeaupuis, J.-P., Diaquin, M. & Lo, R., (1997). Cloning and disruption of the antigenic catalase gene of *Aspergillus fumigatus*. *Microbiology*, **65**(11), pp.4718–4724.

Cameron, J.C. & Pakrasi, H.B., (**2010**). Essential role of glutathione in acclimation to environmental and redox perturbations in the cyanobacterium *Synechocystis sp.* PCC 6803. *Plant physiology*, **63130**(314).

Cantoni, G.L., (**1951**). Methylation of nicotinamide with a soluble enzyme system from rat liver. *The FASEB Journal*, **1**(189), pp.203–216.

Caprariello, A., Mangla, S., Miller, R.H. & Selkirk, S.M., (2013). Apoptosis of oligodendrocytes in the CNS results in rapid focal demyelination. *Annual Neurobiology*, **72**(3), pp.395–405.

Carberry, S., Neville, C.M., Kavanagh, K. *et al.*, (**2006**). Analysis of major intracellular proteins of *Aspergillus fumigatus* by MALDI mass spectrometry: identification and characterisation of an elongation factor 1B protein with glutathione transferase activity. *Biochemical and biophysical research communications*, **341**(4), pp.1096–104.

Carberry, S., Molloy, E., Hammel, S., O'Keeffe, G., *et al.*, (**2012**). Gliotoxin effects on fungal growth: mechanisms and exploitation. *Fungal genetics and biology : FG & B*, **49**(4), pp.302–12.

Carr, P.D., Tuckwell, D., Hey, P.M., Simon, L., D'Enfert, C., Birch, M., Oliver, J.D. & Bromley, M.J., (2010). The transposon impala is activated by low temperatures: use of a controlled transposition system to identify genes critical for viability of *Aspergillus fumigatus*. *Eukaryotic cell*, **9**(3), pp.438–48.

Chabane, S., Sarfati, J., Ibrahim-Granet, O., Du, C., Schmidt, C., Mouyna, I., Prevost, M.-C., Calderone, R. & Latgé, J.-P., (2006). Glycosylphosphatidylinositol-anchored Ecm33p influences conidial cell wall biosynthesis in *Aspergillus fumigatus*. *Applied and Environmental Microbiology*, **72**(5), pp.3259–3267.

Chamilos, G. et al., (**2008**). Genomewide screening for genes associated with gliotoxin resistance and sensitivity in *Saccharomyces cerevisiae*. *Antimicrobial Agents and Chemotherapy*, **52**(4), pp.1325–1329.

Chattopadhyay, M.K., Tabor, C.W. & Tabor, H., (**2002**). Polyamines protect *Escherichia coli* cells from the toxic effect of oxygen. *PNAS*, **100**(5), pp.2261–2265.

Chazalet, V., Debeaupuis, J.-P., Sarfati, J., Lortholary, J., Ribaud, P., Shah, P., Thien, H.V., Gluckman, E., Brücker, G., Latgé, J.-P., Chazalet, R.I.E., Cornet, M. & Thien, H.V.U., (1998). Molecular typing of environmental and patient isolates of *Aspergillus fumigatus* from various hospital settings. *Journal of Clinical Microbiology*, **36**(6), pp.1494–1500.

Cherest, H., Thomas, D. & Kerjan, Y.S., (**1993**). Cysteine biosynthesis in *Saccharomyces cerevisiae* occurs through the transsulfuration pathway which has been built up by enzyme recruitment. *Journal of Bacteriology*, **175**(17), pp.5366–5374.

Chiang, P.K., Gordon, R.K., Tal, J., Zeng, G.C., Doctor, B.P., Pardhasaradhi, K. & Mc Cann, P.P., (1996). S-adenosylmethionine methylation. *The FASEB Journal*, **10**(4), pp.471–480.

Choi, H.S., Shim, J.S., Kim, J.-A., Kang, S.W. & Kwon, H.J., (2007). Discovery of gliotoxin as a new small molecule targeting thioredoxin redox system. *Biochemical and biophysical research communications*, **359**(3), pp.523–8.

Cock, P.J.A., Antao, T., Chang, J.T., Chapman, B.A., Cox, C.J., Dalke, A., Friedberg, I., Hamelryck, T. & Kauff, F., (2009). Biopython : freely available Python tools for computational molecular biology and bioinformatics. *Bioinformatics*, **25**(11), pp.1422–1423.

Coleman, J.O.D. & Randall, R., (**1997**). Detoxification of xenobiotics in plant cells by glutathione conjugation and vacuolar compartmentalization : a fluorescent assay using monochlorobimane. *Plant, Cell and Environment*, **20**(4), pp.449–460.

Collinson, L. & Dawes, I.W., (**1992**). Inducibility of the response of yeast cells to peroxide stress. *Journal of General Microbiology*, **138**, pp.329–335.

Cosper, M.M., Cosper, N.J., Hong, W.E.I., Shokes, J.E., Broderick, W.E., Broderick, J.B., Johnson, M.K. & Scott, R.A., (2003). Structural studies of the interaction of S-adenosylmethionine with the [4Fe-4S] clusters in biotin synthase and pyruvate formate-lyase activating enzyme. *Protein Science*, **12**(1), pp.1573–1577.

Cotgreave, I.A. & Gerdes, R.G., (**1998**). Recent trends in glutathione biochemistry — glutathione–protein interactions: A molecular link between oxidative stress and cell proliferation? *Biochemical and Biophysical Research Communications*, **9**(242), pp.1–9.

Cotter, G., Doyle, S. & Kavanagh, K., (**2000**). Development of an insect model for the in vivo pathogenicity testing of yeasts. *FEMS Immunology and Medical Microbiology*, **27**(2), pp.163–169.

Couillault, C., Fourquet, P., Pophillat, M. & Ewbank, J.J., (2012). A UPR-independent infection-specific role for a BiP / GRP78 protein in the control of

antimicrobial peptide expression in *C. elegans* epidermis. *Virulence*, **3**(3), pp.299–308.

Cramer, R.A., Gamcsik, M.P., Brooking, R.M., Najvar, L.K., Kirkpatrick, W.R., Patterson, T.F., Balibar, C.J., Graybill, J.R., Perfect, J.R., Abraham, S.N. & Steinbach, W.J., (2006). Disruption of a non-ribosomal peptide synthetase in *Aspergillus fumigatus* eliminates gliotoxin production. *Eukaryotic Cell*, **5**(6), pp.972–980.

Culotta, V.C., Joh, H.-D., Lin, S.-J., Slekar, K.H. & Strain, J., (1995). A physiological role for *Saccharomyces cerevisiae* copper /zinc superoxide dismutase in copper buffering. *The Journal of Biological Chemistry*, **270**(50), pp.29991–29997.

Dagenais, T.R.T. & Keller, N., (**2009**). Pathogenesis of *Aspergillus fumigatus* in Invasive Aspergillosis. *Clinical Microbiology Reviews*, **22**(3), pp.447–465.

Dantas, S., Patterson, M.J., Smith, D.A., Maccallum, D.M., Erwig, L.P., Morgan, B.A. & Quinn, J., (2010). Thioredoxin regulates multiple hydrogen peroxide-induced signalling pathways in *Candida albicans*. *Molecular and Cellular Biology*, **30**(19), pp.4550–4563.

Davies, J., Lowry, C. & Davies, K., (**1995**). Transient adaptation to oxidative stress in *Archives of Biochemistry and Biophysics*, **317**(1), pp.1–6.

Davies, K.J.A. & Delsignores, M.E., (**1987**). Protein damage and degradation by Oxygen Radicals 111. *The Journal of Biological Chemistry*, **262**(20), pp.9908–9913.

Davis, C., Carberry, S., Schrettl, M., Singh, I., Stephens, J.C., Barry, S.M., Kavanagh, K., Challis, G.L., Brougham, D. & Doyle, S., (2011). The role of glutathione S-transferase GliG in gliotoxin biosynthesis in *Aspergillus fumigatus*. *Chemistry & biology*, **18**(4), pp.542–52. Available at: http://www.ncbi.nlm.nih.gov/pubmed/21513890 [Accessed May 7, 2011].

Deguchi, T. & Barchas, J., (**1971**). Inhibition of transmethylations of biogenic amines by S-Adenosyl-L-homocysteine: enhancement of transmethylation by adenosyl-L-homocysteinase. *The Journal of Biological Chemistry*, **246**, pp.3175–3181.

Delaney, J.R., Ahmed, U., Chou, A., Carr, D., Murakami, C.J., Sutphin, G.L., An, E.H., Fletcher, M., Higgins, S., Jelic, M., Klum, S., Muller, B., Peng, Z.J., Rai, D., Ros, V., Singh, M., Wende, H.V., Kennedy, K. & Kaeberlein, M., (2013). Stress profiling of longevity mutants identifies Afg3 as a mitochondrial determinant of cytoplasmic mRNA translation and ageing. *Aging Cell*, **12**, pp.156–166.

Delaunay, A., Pflieger, D., Barrault, M.-B., Vinh, J. & Toledano, M.B., (2002). A thiol peroxidase is an H_2O_2 receptor and redox-transducer in gene activation. *Cell*, **111**(4), pp.471–81.

Demain, A.L. & Elander, R.P., (**1999**). The β-lactam antibiotics : past , present , and future. *Antonie van Leeuwenhoek*, **75**, pp.5–19.

Denikus, N., Orfaniotou, F., Wulf, G., Lehmann, P.F., Monod, M. & Reichard, U., (2005). Fungal antigens expressed during Invasive Aspergillosis. , **73**(8), pp.4704–4713.

DeWitte-Orr, S.J. & Bols, N.C., (**2005**). Gliotoxin-induced cytotoxicity in three salmonid cell lines : Cell death by apoptosis and necrosis. *Comparative Biochemistry and Physiology*, **141**(2), pp.157 – 167.

Dhingra, S., Andes, D. & Calvo, A.M., (**2012**). VeA regulates conidiation, gliotoxin production, and protease activity in the opportunistic human pathogen *Aspergillus fumigatus*. *Eukaryotic Cell*, **11**(12), pp.1531–1543.

Dhingra, S., Lind, A.L., Lin, H.-C., Tang, Y., Rokas, A. & Calvo, A.M., (2013). The fumagillin gene cluster , an example of hundreds of genes under veA Control in *Aspergillus fumigatus*. *PLoS ONE*, **8**(10), pp.1–16.

Diwakar, L. & Ravindranath, V., (**2007a**). Inhibition of cystathionine-gamma-lyase leads to loss of glutathione and aggravation of mitochondrial dysfunction mediated by excitatory amino acid in the CNS. *Neurochemistry international*, **50**(2), pp.418–26. Available at: http://www.ncbi.nlm.nih.gov/pubmed/17095121

Do, J.H., Yamaguchi, R. & Miyano, S., (**2009**). Exploring temporal transcription regulation structure of *Aspergillus fumigatus* in heat shock by state space model. *BMC Genomics*, **10**(306), pp.1–16.

Domingo, M.P., Colmenarejo, C., Martínez-lostao, L., Müllbacher, A., Jarne, C., Revillo, M.J., Delgado, P., Roc, L., Meis, J.F., Rezusta, A., Pardo, J. & Gálvez, E.M., (2012). Bis (methyl) gliotoxin proves to be a more stable and reliable marker for invasive aspergillosis than gliotoxin and suitable for use in diagnosis . *Diagnostic Microbiology and Infectious Disease*, **73**(1), pp.57–64.

Dowling, R.J.O., Goodwin, P.J. & Stambolic, V., (**2011**). Understanding the benefit of metformin use in cancer treatment. *BMC Medicine*, **9**(1), p.33.

Draculic, T, Dawes, I.W. & Grant, C.M., (**2000**). A single glutaredoxin or thioredoxin gene is essential for viability in the yeast *Saccharomyces cerevisiae*. *Molecular microbiology*, **36**(5), pp.1167–74.

Drakulic, T., Temple, M.D., Guido, R., Jarolim, S., Breitenbach, M., Attfield, P.V. & Dawes, I.W., (2005). Involvement of oxidative stress response genes in redox homeostasis , the level of reactive oxygen species , and ageing in *Saccharomyces cerevisiae*. *FEMS Yeast Research*, **5**, pp.1215–1228.

Egan, M.J., Mcclintock, M.A. & Reck-peterson, S.L., (**2012**). Microtubule-based transport in filamentous fungi. *Current Opinion in Microbiology*, **15**(6), pp.637–645. Available at: http://dx.doi.org/10.1016/j.mib.2012.10.003.

Eloranta, T. & Kajander, E.O., (**1984**). Catabolism and lability of S-adenosyl-L-methionine in rat liver extracts. *Biochemical Journal*, **224**(1), pp.137–144.

De Enfert, C., (**1996**). Selection of multiple disruption events in *Aspergillus fumigatus* using the orotidine-5-decarboxylase gene, *pyrG*, as a unique transformation marker. *Current Genetics*, **30**(1), pp.76–82.

Feder, M.E. & Walser, J., (**2005**). The biological limitations of transcriptomics in elucidating stress and stress responses. *Journal of Evolutionary Biology*, **18**(4), pp.901–910.

Fedorova, N.D., Khaldi, N., Joardar, V.S., Maiti, R., Amedeo, P., Anderson, M.J., Crabtree, J., Silva, J.C., Badger, J.H., Albarraq, A., Angiuoli, S., Bussey, H., Bowyer, P., Cotty, P.J., Dyer, P.S., Egan, A., Galens, K.,Fraser-Liggett , C.M., Haas, B.J., Inman, J.M., Kent, R., Lemieux, S., Orvis, J., Roemer, T., Ronning, C.M., Sundaram, J.P., Sutton, G., Venter, J.C., White, O.R., Whitty, B.R., Youngman, P., Wolfe, K.H., Goldman, G.H., Wortman, J.R., Jiang, B., Denning, D.W. & Nierman, W.C., (2008). Genomic islands in the pathogenic filamentous fungus *Aspergillus fumigatus*. *PLoS Genetics*, **4**(4), pp.1–13.

Ferreira, M.E.D.S., Malavazi, I., Savoldi, M., Brakhage, A., Helena, M., Goldman, S., Kim, H.S., Nierman, W.C. & Goldman, G.H., (2006). Transcriptome analysis of *Aspergillus fumigatus* exposed to voriconazole. *Current Genetics*, **50**(1), pp.32–44.

Finkel, T. & Holbrook, N.J., (**2000**). Oxidants, oxidative stress and the biology of ageing. *Nature*, **408**(November), pp.239–247.

Finkelstein, J.D. & Martin, J.J., (**1990**). Methionine metabolism in mammals. *Journal of Biological Chemistry*, **259**(15), pp.9508–9513.

Fonseca, R.R., Johnson, W.E., Brien, S.J.O., Vasconcelos, V. & Antunes, A., (2010). Molecular evolution and the role of oxidative stress in the expansion and functional diversification of cytosolic glutathione transferases. *BMC evolutionary biology*, **10**, p.281.

Fordi, S. & Friedman, L., (**1967**). Experimental study of the pathogenicity of *Aspergilli* for mice. *Journal of Bacteriology*, **94**(4), pp.928–933.

Forseth, Ry Roger, Fox, E.M., Chung, D., Howlett, B.J., et al., (**2011**). Identification of cryptic products of the gliotoxin gene cluster using NMR-based comparative metabolomics and a model for gliotoxin biosynthesis. *Journal of the American Chemical Society*, **133**(25), pp. 9678-9681.

Fox, E.M. & Howlett, B.J., (**2008**). Secondary metabolism : regulation and role in fungal biology. *Current Opinion in Microbiology*, **11**(6), pp.481–487.

Fraczek, M.G., Rashid, R., Denson, M., Denning, D.W. & Bowyer, P., (2010). *Aspergillus fumigatus* allergen expression is coordinately regulated in response to hydrogen peroxide and cyclic AMP. *Clinical and Molecular Allergy*, **8**(15), pp.1–11.

Frazzon, J., Fick, J.R. & Dean, D.R., (**2002**). Biosynthesis of iron-sulphur clusters is a complex and highly conserved process. *Biochemical Society transactions*, **30**(4), pp.680–5.

Fredriksson, Å., Ballesteros, M., Dukan, S. & Nystro, T., (2005). Defense against protein carbonylation by DnaK / DnaJ and proteases of the heat shock regulon. *Journal of Bacteriology*, **187**(12), pp.4207–4213.

Friedal, H.A., Goa, K.L. & Benfield, P., (**1989**). S-adenosyl-l-methionine. A review of its pharmacological properties and therapeutic potential in liver dysfunction and affective disorders in relation to its physiological in cell metabolism. *Drugs*, **38**(3), pp.389–416.

Fujita, Y., Ukena, E., Iefuji, H. & Giga-Hama, Y., (2006). Homocysteine accumulation causes a defect in purine biosynthesis : further characterization of *Schizosaccharomyces pombe* methionine auxotrophs. *Microbiology*, **152**(2), pp.397–404.

Galagan, J.E., Calvo, S.E., Cuomo, C., Ma, L.-J., Wortman, J.R., Batzoglou, S., Spevak, C.C., Clutterbuck, J., Kapitonov, V., Jurka, J., Scazzocchio, C., Farman, M., Butler, J., Purcell, S., Harris, S., Braus, G.H., Draht, O., Busch, S., Enfert, C.D., Bouchier, C., Goldman, G.H., Denning, D.W., Caddick, M., Hynes, M., Paoletti, M., Fischer, R., Miller, B., Dyer, P., Sachs, M.S., Osmani, S.A. & Birren, B.W., (2005). Sequencing of *Aspergillus nidulans* and comparative analysis with *A . fumigatus* and *A . oryzae*. *Nature*, **438**, pp.1105–1115.

Gales, G., Penninckx, M., Block, J.-C. & Leroy, P., (2008). Role of glutathione metabolism status in the definition of some cellular parameters and oxidative stress tolerance of *Saccharomyces cerevisiae* cells growing as biofilms. *FEMS Yeast Research*, **8**, pp. 667-675.

Gallagher, L., Owens, R.A., Dolan, S.K., Keeffe, G.O., Schrettl, M., Kavanagh, K., Jones, G.W. & Doyle, S., (2012). The *Aspergillus fumigatus* protein GliK protects against oxidative stress and is essential for gliotoxin biosynthesis. *Eukaryotic Cell*, **11**(10), pp.1226 –1238.

Ganguli, D., Kumar, C. & Bachhawat, A.K., (**2007**). The alternative pathway of glutathione degradation is mediated by a novel protein complex involving three new genes in Saccharomyces cerevisiae. *Genetics*, **175**(3), pp.1137–51.

Garcia, J., Han, D., Sancheti, Harsh Yap, L.P., Kaplowitz, N. & Cadenas, E., (2010). Regulation of mitochondrial glutathione redox status and protein glutathionylation by respiratory substrates. *The Journal of biological chemistry*, **285**(51), pp. 39646-39654..

Gardiner, D.M., Cozijnsen, A.J., Wilson, L.M., Pedras, M.S.C. & Howlett, B.J., (2004). The sirodesmin biosynthetic gene cluster of the plant pathogenic fungus Leptosphaeria maculans. *Molecular Microbiology*, **53**, pp.1307–1318.

Gardiner, D.M. & Howlett, B.J., (**2005**). Bioinformatic and expression analysis of the putative gliotoxin biosynthetic gene cluster of *Aspergillus fumigatus*. *FEMS Microbiology Letters*, **248**, pp.241–248.

Gardiner, D.M., Jarvis, R.S. & Howlett, B.J., (**2005**). The ABC transporter gene in the sirodesmin biosynthetic gene cluster of Leptosphaeria maculans is not essential for sirodesmin production but facilitates self-protection. *Fungal Genetics and Biology*, **42**, pp.257–263.

Gardiner, D.M., Waring, P. & Howlett, B., (**2005**). Review The epipolythiodioxopiperazine (ETP) class of fungal toxins : distribution , mode of action , functions and biosynthesis. *Microbiology*, **151**, pp.1021–1032.

Gautam, P., Shankar, J., Madan, T., Sirdeshmukh, R., Sundaram, C.S., Gade, W.N., Basir, S.F. & Sarma, P.U., (**2008**). Proteomic and transcriptomic analysis of *Aspergillus fumigatus* on exposure to amphotericin B. *Antimicrobial agents and chemotherapy*, **52**(12), pp.4220–7.

Gerken, T. & Walsh, C.T., (**2013**). Cloning and sequencing of the chaetocin biosynthetic gene cluster. *ChemBioChem*, **10**, pp.1–4.

Gibreel, T.M. & Upton, M., (**2013**). Synthetic epidermicin NI01 can protect *Galleria mellonella* larvae from infection with *Staphylococcus aureus. Journal of Antimicrobial Chemotherapy*, **68**(10), pp. 2269-2273.

Gill, S.S. & Tuteja, N., (**2010**). Reactive oxygen species and antioxidant machinery in abiotic stress tolerance in crop plants. *Plant Physiology and Biochemistry*, **48**(12), pp. 909-930.

Goetz, K.E., Coyle, C.M., Cheng, J.Z., Connor, S.E.O. & Panaccione, D.G., (2011). Ergot cluster-encoded catalase is required for synthesis of chanoclavine-I in *Aspergillus fumigatus*. *Current Genetics*, **57**(3), pp.201–211.

Goujon, M., Mcwilliam, H., Li, W., Valentin, F., Squizzato, S., Paern, J. & Lopez, R., (2010). A new bioinformatics analysis tools framework at EMBL – EBI. *Nucleic Acids Research*, **38**(2), pp.695–699.

Grant, C.M., Collinson, L.P., Roe, J.-Hye., Dawes, I.W., (1996). Yeast glutathione reductase is required for protection against oxidative stress and is a target gene for yAP-1 transcriptional regulation. *Molecular Microbiology*, **21**, pp.171–179.

Grant, C.M., Maciver, F.H. & Dawes, I.W., (**1997**). Glutathione synthetase is dispensable for growth under both normal and oxidative stress conditions in the yeast *Saccharomyces cerevisiae* due to an accumulation of the dipeptide γ-glutamylcysteine. *Molecular Biology of the Cell*, **8**(September), pp.1699–1707.

Grant, C.M, (**2001**). MicroReview Role of the glutathione / glutaredoxin and thioredoxin systems in yeast growth and response to stress conditions. *Molecular Microbiology*, **39**(3), pp.533–541.

Greenberg, J.T. & Demple, B., (**1986**). Glutathione in *Escherichia coli* is dispensable for resistance to H_2O_2 and gamma radiation. *Journal of Bacterioology*, **168**(2), pp.1026–1029.

Griffin, T.J., Gygi, S.P., Ideker, T., Ristţ, B., Eng, J., Hood, L. & Aebersold, R., (2002). Complementary profiling of gene expression at the transcriptome and proteome levels in *Saccharomyces cerevisiae*. *Molecular & Cellular Proteomics*, **1**(4), pp.323–333.

Grigat, M. & Ja, Y., (**2012**). Multiple histone deacetylases are recruited by corepressor Sin3 and contribute to gene repression mediated by Opi1 regulator of phospholipid biosynthesis in the yeast *Saccharomyces cerevisiae*. *Molecular Genetics and Genomics*, pp.461–472.

Groopman, J.D., Cain, L.G. & Kensler, T.W., (**1988**). Aflatoxin exposure in human populations: Measurements and relationship to cancer. *Critical Reviews in Toxicology*, **19**(2), pp.113–145.

Groot, M.J.L. De., Daran-lapujade, P., Van, B., Knijnenburg, T.A., Hulster, E.A.F.De., Marcel, J., Reinders, T., Pronk, J.T., Heck, A.J.R. & Slijper, M., (2007). Quantitative proteomics and transcriptomics of anaerobic and aerobic yeast

cultures reveals post- transcriptional regulation of key cellular processes. *Microbiology*, **153**(11), pp.3864–3878.

Groot, P.W.J. De., Brandt, B.W., Horiuchi, H., Ram, A.F.J., Koster, C.G.De. & Klis, F.M., (2009). Comprehensive genomic analysis of cell wall genes in *Aspergillus nidulans*. *Fungal Genetics and Biology*, **46**(1), pp.S72–S81.

Gross, U., Nieger, M. & Brase, S., (**2010**). A unified strategy targeting the thiodiketopiperazine mycotoxins, exserohilone, gliotoxin, the epicoccins, the epicorazines, rostratin A and aranotin. *Chemistry*, **16**(38), pp.11624 – 11631.

Grosse, C., Heinekamp, T., Kniemeyer, O., Gehrke, A. & Brakhage, A., (**2008**). Protein kinase A regulates growth, sporulation, and pigment formation in *Aspergillus fumigatus*. *Applied and Environmental Microbiology*, **74**(15), pp.4923–33.

Grundmann, A. et al., (**2008**). FtmPT2 , an N-prenyltransferase from *Aspergillus fumigatus*, catalyses the last step in the biosynthesis of fumitremorgin B. *ChemBioChem*, **9**(13), pp.2059 – 2063.

Guevara-Olvera, L., Calvo-Mendez, C. & Ruiz-Herrera, J., (**1993**). The role of polyamine metabolism in dimorphism of *Yarrowia lipolytica*. *Journal of General Microbiology*, **193**(3), pp.485–493.

Gulshan, K., Lee, S.S. & Moye-Rowley, W.S., (2011). Differential oxidant tolerance determined by the key transcription factor *YAP1* is controlled by levles of the YAP1-binding protein, YBP1 *Journal of Biological Chemistry*, **286**(39), pp. 34071-34081.

Harding, H.P., Zhang, Y., Zeng, H., Novoa, I., Lu, P.D., Calfon, M., Sadri, N., Yun, Chi., Popko, B., Paules, R., Stojdl, D.F., Bell, J.C., Hettmann, T., Leiden, J.M. & Ron, D., (2003). An integrated stress response regulates amino acid metabolism and resistance to oxidative stress. *Molecular Cell*, **11**(3), pp.619–633.

Hartmann, T., Cairns, T.C., Olbermann, P., Morschhäuser, J., Bignell, E. & Krappmann, S., (2011). Oligopeptide transport and regulation of extracellular proteolysis are required for growth of *Aspergillus fumigatus* on complex substrates but not for virulence. *Molecular microbiology*, **82**(4), pp.917–35.

Hatabu, T., Hagiwara, M., Taguchi, N., Kiyozawa, M., Suzuki, M., Kano, S. & Sato, K., (2006). *Plasmodium falciparum*: The fungal metabolite gliotoxin inhibits proteasome proteolytic activity and exerts a plasmodicidal effect on *P. falciparum*. *Experimental Parasitology*, **112**, pp.179–183.

Hayes, J.D., Flanagan, J.U. & Jowsey, I.R., (**2005**). Glutathione transferases. *Annual Review Pharmicology and Toxicology*, **45**, pp.51–88.

Heemskerk, J., Tobin, A.J. & Ravina, B., (**2002**). From chemical to drug : neurodegeneration drug screening and the ethics of clinical trials. *Nature Neuroscience*, **5**, pp.1027–1029.

Hegde, P., Qi, R., Abernathy, K., Gay, C., Gaspard, R., Hughes, J.E., Snesrud, E., Lee, N. & Quackenbush, J., (2000). BioFeature a concise guide to cDNA microarray analysis. *Biotechniques*, **29**(3), pp.548–562.

Herrick, J.A., (**1945**). Effects of gliotoxin on *Trichophyton gypseum*. *The Ohio Journal of Science*, **45**(2), pp.45–46.

Hertweck, C., (**2009**). Hidden biosynthetic treasures brought to light. *Nature Chemical Biology*, **5**, pp.450–452.

Hiraishi, H., Miyake, T. & Ono, B., (**2008**). Transcriptional regulation of *Saccharomyces cerevisiae CYS3* encoding cystathionine gamma-lyase. *Current genetics*, **53**(4), pp.225–34.

Hoffmann, J.A., (**1995**). Innate immunity of insects. *Current Opinion in Immunology*, **7**(1), pp.4–10.

Holding, K.J., Dworkin, M.S., Wan, P.-C.T., Hanson, D.L., Klevens, R.M., Jones, J.L. & Sullivan, P.S., (2000). Aspergillosis among people infected with human immunodeficiency virus: incidence and survival. *Clinical Infectious Diseases*, **31**(1), pp.1253–1257.

Holdom, M.D., Hay, R.J. & Hamilton, A.J., (**1995**). Purification, N-terminal amino acid sequence and partial characterisation of a Cu, Zn superoxide dismutase from the pathogenic fungus *Aspergillus fumigatus*. *Free Radical Research*, **22**(6), pp.519–531.

Holdom, M.D., Hay, R.J. & Hamilton, A.J., (**1996**). The Cu , Zn superoxide dismutases of *Aspergillus flavus*, *Aspergillus niger*, *Aspergillus nidulans*, and *Aspergillus terreus*: purification and biochemical comparison with the *Aspergillus fumigatus* Cu , Zn superoxide dismutase. *Infection and Immunity*, **64**(8), pp.3326–3332.

Holmgren, A., (**1989**). Thioredoxin and glutaredoxin systems. *The Journal of Biological Chemistry*, **264**(24), pp.13963–13966.

Horio, T. & Oakley, B.R., (**2005**). The role of microtubules in rapid hyphal tip growth of *Aspregillud nidulans*. *Molecular Biology of the Cell*, **16**(2), pp.918 –926.

Howell, C.R. & Stipanovic, R.D., (**1995**). Mechanisms in the biocontrol of *Rhizoctonia solani*-Induced cotton seedling disease by *Gliocladium virens*: Antibiosis. *Phyopathology*, **85**, pp.469–472.

Hurne, A.M., Chai, C.L.L. & Waring, P., (**2000**). Inactivation of rabbit muscle creatine kinase by reversible formation of an internal disulfide bond induced by the fungal toxin gliotoxin. *The Journal of Biological Chemistry*, **275**, pp.25202–25206.

Husson, A., Brasse-Lagnel, C., Fairand, A., Renouf, S. & Lavoinne, A., (2003). Argininosuccinate synthetase from the urea cycle to the citrulline-NO cycle. *European Journal of Biochemistry*, **270**(9), pp.1887–1899.

Hwang, C., Rhie, G., Oh, J.-H. & Huh, W.-K., (2002). Copper- and zinc-containing superoxide dismutase (Cu / ZnSOD) is required for the protection of *Candida albicans* against oxidative stresses and the expression of its full. *Microbiology*, **148**(11), pp.3705–3713.

Ibrahim-granet, O. & Enfert, C.D., (**1995**). The *Aspergillus fumigatus* gene *mepB* encodes an 82 kDa intracellular metalloproteinase structurally related to mammalian thimet oligopeptidases. *Micriobiology*, **143**(7), pp.2247–2253.

Ibrahim-Granet, O., Dubourdeau, M., Latgé, J.-P., Ave, P., Huerre, M., Brakhage, A. & Brock, M., (2007). Methylcitrate synthase from *Aspergillus fumigatus* is essential for manifestation of invasive aspergillosis. *Cellular Microbiology*, **10** (1), pp. 134-148.

Inoue, Y., Matsuda, T., Sugiyama, I. & Kimura, A., (1999). Genetic analysis of glutathione peroxidase in oxidative stress response of *Saccharomyces cerevisiae*. *The Journal of Biological Chemistry*, **274**, pp.27002–27009.

Iouk, T.L., Aitchison, J.D., Maguire, S. & Wozniak, R.W., (2001). Rrb1p , a yeast nuclear WD-repeat protein involved in the regulation of ribosome biosynthesis. *Molecular and Cellular Biology*, **21**(4), pp.1260–1271.

Izawa, S., Inoue, Y. & Kimura, A., (**1995**). Oxidative stress response in yeast : effect of glutathione on adaptation to hydrogen peroxide stress in *Saccharomyces cerevisiae*. *FEBS Letters*, **368**, pp.73–76.

Jacob, C., Giles, G.I., Giles, N.M. & Sies, H., (2003). Sulfur and selenium: The role of oxidation state in protein structure and function. *Angewadte Chemie*, **42**(39), pp.4742 – 4758.

Jain, R., Valiante, V., Remme, N., Docimo, T., Heinekamp, T., Hertweck, C., Gershenzon, J., Haas, H., Brakhage, A. & Schiller, F., (2011). The MAP kinase MpkA controls cell wall integrity , oxidative stress response , gliotoxin production

and iron adaptation in *Aspergillus fumigatus*. *Molecular Microbiology*, **82**(1), pp. 39-53.

Jamieson, D.J., (**1998**). Oxidative stress responses of the yeast *Saccharomyces cerevisiae*. *Yeast*, **1527**, pp.1511–1527.

Johannessen, L.N., Nilsen, A.M. & L, M., (**2005**). The mycotoxins citrinin and gliotoxin differentially affect production of the pro-inflammatory cytokines tumour necrosis factor-a and interleukin-6 , and the anti-inflammatory cytokine interleukin-10. *Clinical and Experimental Allergy*, **35**(6), pp.782–789.

Johnson, J.I., Decker, S., Zaharevitz, D., Rubinstein, L.V., Venditti, J.M., Schepartz, S., Kalyandrug, S. & Christian, M., (2001). Relationships between drug activity in NCI preclinical *in vitro* and *in vivo* models and early clinical trials. *British Journal of Cancer*, **84**, pp.1424–1431.

Johnson, J.R., Bruce, W.F. & Dutcher, J.D., (**1943**). Gliotoxin, the antibiotic principle of *Gliocladium fimbriatum*. *ACS Publications*, **65**(10), pp.2005–2009.

Jones, R.W. & Hancock, J.G., (**1988**). Mechanism of gliotoxin action and factors mediating gliotoxin Sensitivity. *Journal of General Microbiology*, **134**, pp.2067–2075.

Kacprzak, M.M., Lewandowska, I., Matthews, R.G. & Paszewski, A., (2003). Transcriptional regulation of methionine synthase by homocysteine and choline in *Aspergillus nidulans*. *Biochemistry*, **376**(2), pp.517–524.

Kamei, K. & Watanabe, A., (**2005**). *Aspergillus* mycotoxins and their effect on the host. *Medical Mycology*, **43**, pp.95–99.

Kamencic, H., Lyon, A., Paterson, P.G. & Juurlink, Bernhard, H.J., (2000). Monochlorobimane fluorometric method to measure tissue glutathione. *Analytical Biochemistry*, **37**, pp.35–37.

Kanehisa M., Goto S., Kawashima S., Okuno Y. & Hattori M., (2004). The KEGG resource for deciphering the genome. *Nucleic Acids Rsearch,* **32**, pp. 277-280

Kandil, S., Brennan, L. & Mcbean, G.J., (**2010**). Glutathione depletion causes a JNK and p38 MAPK -mediated increase in expression of cystathionine- g -lyase and upregulation of the transsulfuration pathway in C6 glioma cells. *Neurochemistry International*, **56**(4), pp.611–619.

Kandpal, R.P., Saviola, B. & Felton, J., (**2009**). The era of 'omics' unlimited. *Biotechniques*, **46**(4), pp.351–355.

Kauadji, M., (**1990**). Gliotoxin: uncommon 1H couplings and revised H- and 13C-NMR Assignments. *Journal of Natural Products*, **53**(3), pp.717–719.

Kaur, H., Kumar, C., Junot, C., Toledano, M.B. & Bachhawat, A.K., (2009). Dug1p Is a Cys-Gly peptidase of the gamma-glutamyl cycle of *Saccharomyces cerevisiae* and represents a novel family of Cys-Gly peptidases. *The Journal of biological chemistry*, **284**(21), pp.14493–502.

Kavanagh, K. & Reeves, E.P., (**2004**). Exploiting the potential of insects for *in vivo* pathogenicity testing of microbial pathogens. *FEMS Microbiology Reviews*, **28**(1), pp.101–112.

Keesey, J.K., Bigelis, R. & Fink, G.R., (**1979**). The product of the *his4* gene cluster in of the *his4* gene cluster in *Saccharomyces cerevisiae*. *The Journal of Biological Chemistry*, **254**(15), pp.7427–7433.

Keller, N.P., Turner, G. & Bennett, J.W., (**2005**). Fungal secondary metabolism-from biochemistry to genomics. *Microbiology*, **3**, pp.937–947.

Kersey, P., Hermjakob, H. & Apweiler, R., (**2000**). VARSPLIC : alternatively-spliced protein sequences derived from SWISS-PROT and. *Bioinformatics*, **16**(11), pp.1048–1049.

Khaldi, N., Seifuddin, F.T., Turner, G., Haft, D., Nierman, W.C., Wolfe, K.H. & Fedorova, N.D., (2011). SMURF:Genomic Mapping of fungal secondary metabolite clusters. *Fungal Genetics and Biology*, **47**(9), pp.736–741.

Kim, J.H., Campbell, B.C., Yu, J., Mahoney, N., Chan, K.L., Molyneux, R.J., Bhatnagar, D. & Cleveland, T.E., (2005). Examination of fungal stress response genes using *Saccharomyces cerevisiae* as a model system : targeting genes affecting aflatoxin biosynthesis by *Aspergillus flavus*. *Applied Microbial Biotechnology*, **67**(6), pp.807–815.

Kim, K., Yamashita, A., Wear, M.A., Maéda, Y. & Cooper, J.A., (2004). Capping protein binding to actin in yeast : biochemical mechanism and physiological relevance. *The Journal of Cell Biology*, **164**(4), pp.567–580.

Kim, K., Brown, K.M., Harris, P.V., Langston, J.A. & Cherry, J.R., (2007). A proteomics strategy to discover glucosidases from *Aspergillus fumigatus* with two-dimensional PAGE in-gel activity assay and tandem mass spectrometry research articles. *Journal of Proteome Research*, **6**(12), pp.4749–4757.

Kispal, G., Steiner, H., Court, D.A., Rolinski, B. Lill, R., (1996). Cell biology and metabolism: Mitochondrial and cytosolic branched-chain amino acid transaminases from Yeast, homologs of the myc oncogene-regulated Eca39 Protein. *The Journal of Biological Chemistry*, **271**(40), pp.24458–24464.

Klein, M., Mamnun, Y.M., Eggmann, T., Schu, C., Wolfger, H., Martinoia, E. & Kuchler, K., (2007). The ATP-binding cassette (ABC) transporter Bpt1p mediates vacuolar sequestration of glutathione conjugates in yeast. *FEBS Letters*, **520**(1-3), pp.63–67.

Kniemeyer, O., Lessing, F. & Brakhage, A.A., (**2009**). Proteome analysis for pathogenicity and new diagnostic markers for *Aspergillus fumigatus*. *Natural Product Research*, **47**(Supplement I), pp.248–254.

Kodzius, R., Kojima, M., Nishiyori, H., Nakamura, M., Fukuda, S., Tagami, M., Sasaki, D., Imamura, K., Kai, C., Harbers, M., Hayashizaki, Y. & Carninci, P., (2006). CAGE : cap analysis of gene expression. *Nature Methods*, **3**(3), pp.211–222.

Kosower, N.S., Kosower, E.M., Wertheim, B. & Correa, W.S., (1969). Diamide, a new reagent for the intracellular oxidation of glutathione to disulfide. *Biochemical and Biophysical Research Communications*, **37**(4), pp.593–596.

Krappmann, S. & Braus, G.H., (**2005**). Deletion and allelic exchange of the *Aspergillus fumigatus veA* Locus via a novel recyclable marker module. *Eukaryotic Cell*, **4**(7), pp.1298–1307.

Krappmann, S., Sasse, C. & Braus, G.H., (**2006**). Gene targeting in *Aspergillus fumigatus* by homologous recombination is facilitated in a non-homologous end-joining-deficient genetic background. *Eukaryotic Cell*, **5**(1), pp.212–215.

Kredich, N.M. & Hershfield, M.S., (**1979**). S-adenosylhomocysteine toxicity in normal and adeonsine kinase-deficient lymphoblasts of human origin. *PNAS*, **76**(5), pp.2450–2454.

Kubodera, T., Yamashita, N. & Nishimura, A., (**2000**). Pyrithiamine resistance gene (*ptrA*) of *Aspergillus oryzae*: Cloning, characterisation and application as a dominant selectable marker for transformation. *Bioscience, Biotechnology and Biochemistry*, **64**(7), pp.1416–1421.

Kuge, S., Toda, T., Iizuka, N. & Nomoto, A., (1998). Crm1 (XpoI) dependent nuclear export of the budding yeast transcription factor yAP-1 is sensitive to oxidative stress. *Genes to Cells*, **1**, pp.521–532.

Kuge, S., Arita, M., Murayama, A., Maeta, K., Izawa, S., Inoue, Y. & Nomoto, A., (2001). Regulation of the Yeast Yap1p nuclear export signal is mediated by redox signal-induced reversible disulfide bond formation. *Molecular and Cellular Biology*, **21**(18), pp.6139–6150.

Kuge, S. & Jones, N., (**1994**). YAP1 dependent activation of TRX2 is essential for the response of *Saccharomyces cerevisiae* to oxidative stress by hydroperoxides. *EMBO Journal*, **13**(3), pp.655–664.

Kuge, S. & Jones, N., (**1997**). Regulation of yAP-1 nuclear localization in response to oxidative stress. *The EMBO Journal*, **16**(7), pp.1710–1720.

Kupfahl, C., Heinekamp, T., Geginat, G., Ruppert, T., Härtl, A., Hof, H. & Brakhage, A.A., (2006). Deletion of the *gliP* gene of *Aspergillus fumigatus* results in loss of gliotoxin production but has no effect on virulence of the fungus in a low-dose mouse infection model. *Molecular Microbiology*, **62**(August), pp.292–302.

Kupfahl, C., Michalka, A., Lass-Flörl, C., et al., (**2008**). Gliotoxin production by clinical and environmental *Aspergillus fumigatus* strains. *International Journal Of Medical Microbiology*, **298**, pp.319–327.

Kuwayama, H., Obara, S., Morio, T., Katoh, M., Urushihara, H. & Tanaka, Y., (2002). PCR-mediated generation of a gene disruption construct without the use of DNA ligase and plasmid vectors. *Nucleic Acids Research*, **30**(2), pp.2–6.

Kweon, Y., Paik, Y.-H., Schnabl, B., Qian, T., Lemasters, J.J. & Brenner, D.A., (2003). Gliotoxin-mediated apoptosis of activated human hepatic stellate cells. *Journal of Hepatology*, **39**(1), pp.38–46.

Kwon-Chung, K.J. & Sugui, J.A., (**2009**). What do we know about the role of gliotoxin in the pathobiology of *Aspergillus fumigatus*? *Molecular Microbiology*, **47**(Suppl 1), pp.1–12.

Lamarre, C., Lemay, J.-D., Deslauriers, N. & Bourbonnais, Y., (2001). *Candida albicans* expresses an unusual cytoplasmic manganese- containing superoxide dismutase (*SOD3* gene product) upon the entry and during the stationary phase. *The Journal of Biological Chemistry*, **276**(47), pp.43784–43791.

Lamarre, C., Sokol, S., Debeaupuis, J.-P., Henry, C., Lacroix, C., Glaser, P., Coppée, J.-Y., François, J.-M. & Latgé, J.-P., (2008). Transcriptomic analysis of the exit from dormancy of *Aspergillus fumigatus* conidia. *BMC Genomics*, **15**, pp.1–15.

Lambou, K., Lamarre, C., Beau, R., Dufour, N. & Latge, J.-P., (2010). Functional analysis of the superoxide dismutase family in *Aspergillus fumigatus*. *Molecular Microbiology*, **75**, pp.910–923.

Lamoth, F., Juvvadi, P.R., Fortwendel, J.R. & Steinbach, W.J., (2012). Heat shock protein 90 is required for conidiation and cell wall Integrity in *Aspergillus fumigatus*. *Eukaryotic Cell*, **11**(11), pp.1324 –1332.

Larin, N.M., Copping, M.P., Herbst-Later, R.H., Roberts, B. & Wenham, R.B.M., (1965). Antiviral activity of gliotoxin. *Chemotheraopia*, **10**, pp.12–23.

Latge, J., (**2001**). The pathobiology of *Aspergillus fumigatus*. *Trends in Microbiology*, **9**(8), pp.382–389.

Latgé, J., (**1999**). *Aspergillus fumigatus* and Aspergillosis *Microbiology Reviews*, **12**(2), pp.310–350.

Lee, J., Spector, D., Labarre, J., Toledano, M.B. & Godon, C., (1999). A New Antioxidant with Alkyl Hydroperoxide Defense Properties in Yeast. *The Journal of Biological Chemistry*, **274**(8), pp.4537–4544.

Lee, J C., Stra, M.J., Jang, T.-Y., Higgins, V.J., Grant, C.M. & Dawes, I.W., (2001). The essential and ancillary role of glutathione in *Saccharomyces cerevisiae* analysed using a grande *gsh1* disruptant strain. *FEMS yeast research*, **1**(1), pp.57–65.

Lee, J., Godon, C., Spector, D., Garin, J., Toledano, M.B., Lagniel, G. & Labarre, J., (2013). Yap1 and Skn7 control two specialized oxidative stress response regulons in Yeast. *The Journal of Biological Chemistry*, **274**(23), pp. 16040-16046

Lemaitre, B., Nicolas, E., Michaut, L., Reichhart, J.-M. & Hoffmann, J.A., (1996). The dorsoventral regulatory gene cassette spatzle/Toll/cactus controls the potent antifungal response in *Drosophila* adults. *Cell*, **86**, pp.973–983.

Lessing, F., Kniemeyer, O., Wozniok, I., Loeffler, J., Kurzai, O., Haertl, A. & Brakhage, A. (**2007**). The *Aspergillus fumigatus* transcriptional regulator AfYap1 represents the major regulator for defense against reactive oxygen intermediates but is dispensable for pathogenicity in an intranasal mouse infection model. *Eukaryotic cell*, **6**(12), pp.2290–302.

Li, B., Forseth, R.R., Bowers, A.A., Schroeder, F.C. & Walsh, C.T., (2012). A backup plan for self-protection: S-methylation of holomycin biosynthetic intermediates in *Streptomyces clavuligerus*. *ChemBioChem*, **13**(1), pp.2521 – 2526.

Li, C.L., Pan, C.Y., Lu, J.M., Zhu, Y., Wang, J.H., Deng, X.X., Xia, F.C., Wang, H.Z. & Wang, H.Y., (1999). Effect of metformin on patients with impaired glucose tolerance. *Diabetic Medicine*, **16**, pp.477–481.

Li, K. Ouyang, H., Lü, Y., Liang, J., Wilson, I.B.H. & Jin, C., (2011). Repression of N-glycosylation triggers the unfolded protein response (UPR) and overexpression of cell wall protein and chitin in *Aspergillus fumigatus*. *Microbiology*, **157**(Pt 7), pp.1968–79.

Li, X., Kim, S.-K., Nam, K.W., Kang, J.S. & Choi, H.D., (2006). A new antibacterial dioxopiperazine alkaloid related to gliotoxin from a marine isolate of the fungus *Pseudallescheria*. *Natural Product Sciences*, **59**(4), pp.248–250.

Liang, P. & Pardee, A.B., (**1992**). Differential display of eukaryotic messenger RNA by means of polymerase chain reaction. *Science*, **257**(5072), pp.967–971.

Lin, S., Schranz, J. & Teutsch, S.M., (**2001**). Aspergillosis case-fatality rate: Systematic review of the literature. *Clinical Infectious Diseases*, **32**(3), pp.358–366.

Lo, K. & Johnson, A.W., (2009). Reengineering ribosome export. *Molecular Biology of the Cell*, **20**, pp.1545–1554.

Van Loon, A.P.G.M., Pesold-hurt, B. & Schatz, G., (**1986**). A yeast mutant lacking mitochondrial manganese-superoxide dismutase is hypersensitive to oxygen. *PNAS*, **83**(11), pp.3820–3824.

López, M.C., García, S., Ruiz-Herrera, J. & Dominguez, A., (1997). The ornithine decarboxylase gene from *Candida albicans*. Sequence analysis and expression during dimorphism. *Current Genetics*, **32**(2), pp.108–114.

López-Mirabel, H.R., Thorsen, M., Kielland-Brandt, M.C., Toledano, M.B. & Winther, J.R., (2007). Cytoplasmic glutathione redox status determines survival upon exposure to the thiol-oxidant 4 , 4 0 -dipyridyl disulphide. *FEMS Yeast Research*, **7**, pp.391–403.

Losada, L., Ajayi, O., Frisvad, J.C., Yu, J. & Nierman, W.C., (2009). Effect of competition on the production and activity of secondary metabolites in *Aspergillus* species. *Medical Mycology*, **47**, pp.88–96.

Low, C. & Rotstein, C., (**2011**). Emerging fungal infections in immunocompromised patients. *Medicine*, **8**, pp.1–8.

Lu, S.C., (**2000**). S-adenosylmethionine. *International Journal of Biochemistry*, **32**, pp.391–395.

Lu, X., Sun, J., Nimtz, M., Wissing, J., Zeng, A.-P. & Rinas, U. (2010). The intra- and extracellular proteome of *Aspergillus niger* growing on defined medium with xylose or maltose as carbon substrate. *Microbial Cell Factories*, **9**(23), pp.1–13.

Luo, S. & Levine, R.L., (**2009**). Methionine in proteins defends against oxidative stress. *The FASEB Journal*, **23**(2), pp.464–472.

Mabey, J.E., Anderson, M.J., Giles, P.F., Miller, C.J., Attwood, T.K., Paton, N.W., Robson, G.D., Oliver, S.G., Denning, D.W., (2004). CADRE : the Central

Aspergillus Data REpository. *Nucleic Acids Research*, **32** (Database issue), pp.401–405.

Machida, M., Asai, K., Sano, M., Tanaka, T., Kumagai, T., Terai, G., Kusumoto, K., Arima, T., Akita, O., Kashiwagi, Y., Abe, K., Gomi, K., Horiuchi, H., Kitamoto, K., Kobayashi, T., Takeuchi, M., Denning, D.W., Galagan, J.E., Nierman, W.C., Yu, J., Archer, D.B., Bennett, J.W., Hosoyama, A., Ichinomiya, M., Igarashi, R., Iwashita, K., Juvvadi, P.R., Maruyama, J., Nagasaki, H., Nakajima, T., Oda, K., Okada, K. & Paulsen, I., (2005). Genome sequencing and analysis of *Aspergillus oryzae*. *Nature*, **438**, pp.1–3.

Mahoney, N., Chan, K.L. & Molyneux, R.J., (**2010**). Chemosensitization of aflatoxigenic fungi to antimycin A and strobilurin using salicylaldehyde, a volatile natural compound targeting cellular antioxidation system. *Micropathologia*, **171**(4), pp. 291-298

Maiya, S. et al., Grundmann, A., Li, S.-M. & Turner, G., (2006). The fumitremorgin gene cluster of *Aspergillus fumigatus*: identification of a gene encoding brevianamide F synthetase. *ChemBioChem*, **7**(7), pp.1062 – 1069.

Mäkimattila, S., Nikkilä, K. & Yki-Jarvinen, H., (**1999**). Causes of weight gain during insulin therapy with and without metformin in patients with Type II diabetes mellitus. *Diabetologia*, **42**, pp.406–412.

Marui, J., Yoshimi, A., Hagiwara, D., Fujii-Watanabe, Y.,Oda, K., Koike, H., Tamano, K., Ishii, Tomoko. & Sano, M., (2010). Use of the *Aspergillus oryzae* actin gene promoter in a novel reporter system for exploring antifungal compounds and their target genes. *Applied Microbiology*, **87**(5), pp.1829–1840.

Marui, J. & Sawaki, M.M., (**2012**). Comparison of expression and enzymatic properties of *Aspergillus oryzae* lysine aminopeptidases ApsA and ApsB. *World Journal of Microbiology and Biotechnology*, **28**(8), pp.2643–2650.

Maruyama, J., Juvvadi, P.R., Ishi, K. & Kitamoto, K., (2005). Three-dimensional image analysis of plugging at the septal pore by Woronin body during hypotonic shock inducing hyphal tip bursting in the filamentous fungus *Aspergillus oryzae. Biochemical and Biophysical Research Communications*, **331**, pp.1081–1088.

Mato, J. et al., Alvarez, L., Ortis, P. & Pajares, M., (1997). S-adenosylmethionine synthesis : Molecular mechanisms and clinical implications. *Pharmocoligal Therapeutics*, **73**(3), pp.265–280.

Mayer, M.P. & Bukau, B., (**2005**). Cellular and molecular life sciences Hsp70 chaperones : Cellular functions and molecular mechanism. *Cellular and Molecular Life Sciences*, **62**, pp.670– 684.

Mc Goldrick, S., O'Sullivan, S.M. & Sheehan, D., (**2005**). Glutathione transferase-like proteins encoded in genomes of yeasts and fungi : insights into evolution of a multifunctional protein superfamily. *FEMS Microbiology Letters*, **242**, pp.1–12.

Mc Cammon, M.T. & Parks, L.W., (**1981a**). Inhibition of sterol transmethylation by S-adenosylhomocysteine analogs. *Journal of Bacteriology*, **145**(1), pp.106–112.

Mc Cord, J.M. & Fridovich, I., (**1969**). An enzymatic function for erythrocuprein. *The Journal of Biological Chemistry*, **244**(22), pp.6049–6055.

McDonagh, A., Fedorova, N.D., Crabtree, J., Yu, Y., Kim, S., Chen, D., Loss, O., Cairns, T., Goldman, G., Armstrong-James, D., Haynes, K., Haas, H., Schrettl, M., May, Gregory Nierman, W.C. & Bignell, E., (2008). Sub-telomere directed gene expression during initiation of invasive aspergillosis. *PLoS pathogens*, **4**(9), p.e1000154.

Meyer, V., (**2008**). Genetic engineering of filamentous fungi — Progress , obstacles and future trends. *Biotechnology Advances*, **26**(2), pp.177 – 185.

Miralles-Barrachine, O., Savoye, G., Belmonte-Zalar, L., Hochain, P., Ducrotté, P., Hecketsweiler, B. Lerebours, E. & Déchelotte, P., (1999). Low levels of

glutathione in endoscopic biopsies of patients with Crohn's colitis: the role of malnutrition. *Clinical Nutrition*, **18**, pp.313–317.

Mitsuguchi, H., Seshime, Y., Fujii, I. & Shibuya, M., (2009). Biosynthesis of steroidal antibiotic fusidanes: Functional analysis of oxidosqualene cyclase and subsequent tailoring enzymes from *Aspergillus fumigatus*. *JACS*, **131**(7), pp.6402–6411.

Montibus, M., Pinson-Gadais, L., Richard-Forget, F., Barreau, C. & Ponts, N., (2013). Coupling of transcriptional response to oxidative stress and secondary metabolism regulation in filamentous fungi. *Critical Reviews in Microbiology*, pp.1–14.

Morgan, B.A., Banks, G.R., Toone, W. M., Raitt, D., Kuge, S. & Johnston, L.H., (1997). The Skn7 response regulator controls gene expression in the oxidative stress response of the budding yeast *Saccharomyces cerevisiae*. *The EMBO Journal*, **16**(5), pp.1035–1044.

Moss, R.B., (**2002**). Allergic Bronchopulmonary Aspergillosis. *Clinical Reviews in Allergy and Immunology*, **23**(1), pp.87–104.

Mowlds, P., Coates, C., Renwick, J. & Kavanagh, K., (2010). Dose-dependent cellular and humoral responses in *Galleria mellonella* larvae following b-glucan inoculation. *Microbes and Infection*, **12**(2), pp.146–153.

Mowlds, P. & Kavanagh, K., (**2008**). Effect of pre-incubation temperature on susceptibility of *Galleria mellonella* larvae to infection by *Candida albicans*. *Mycopathologia*, **165**, pp.5–12.

Moye-Rowley, W.S., (**2003**). Regulation of the Transcriptional Response to Oxidative Stress in Fungi : Similarities and Differences. *Eukaryotic Cell*, **2**(3), pp.381–389.

Mukherjee, K., Altincicek, B., Hain, T., Domann, E., Vilcinskas, A. & Chakraborty, T., (2010). *Galleria mellonella* as a model system for studying *Listeria*. *Applied and Environmental Microbiology*, **76**(1), pp.310–317.

Mullbacher, A. & Eichner, R.D., (**1984**). Immunosuppression *in vitro* by a metabolite of a human pathogenic fungus. *Immunology*, **81**(June), pp.3835–3837.

Muller, E.G.D., (**1996**). A glutathione reductase mutant of yeast accumulates high levels of oxidized glutathione and requires thioredoxin for growth. *Molecular Biology of the Cell*, **7**(November), pp.1805–1813.

Mutoh, N. & Kitajima, S., (**2007**). Accelerated chronological aging of a mutant fission yeast deficient in both glutathione and superoxide dismutase having Cu and Zn as cofactors and its enhancement by Sir2 deficiency. *Bioscience, Biotechnology, and Biochemistry*, **71**(11), pp.2841–2844.

Nagalakshmi, U., Wang, Z., Waern, K., Shou, C., Raha, D., Gerstein, M. & Snyder, M., (2008). The transcriptional landscape of the yeast genome defined by RNA sequencing. *Science*, **320**(5881), pp.1344–1349.

Narasimha, G., Sridevi, A., Buddolla, V., Subhosh, C.M. & Rajasekhar, R.B., (2006). Nutrient effects on production of cellulolytic enzymes by *Aspergillus niger*. *African Journal of Biotechnology*, **5**(5), pp.472–476.

Nestelbacher, R., Laun, P., Vondráková, D., Pichová, A.,Schüller, C. & Breitenbach, M., (2000). The influence of oxygen toxicity on yeast mother cell-specific aging. *Experimental gerontology*, **35**(1), pp.63–70.

Nielsen, M.L., Albersen, L., Lettier, G., Nielson, J.B. & Mortensen, U.H., (2006). Efficient PCR-based gene targeting with a recyclable marker for *Aspergillus nidulans*. *Fungal Genetics and Biology*, **43**(1), pp.54–64.

Nierman, W.C., Pain, A., Anderson, M.J., Wortman, J.R., Kim, H.S., Arroyo, J., Berriman, M., Abe, K., Archer, D.B., Bermejo, C., Bennett, J., Bowyer, P., Chen, D., Collins, M., Coulsen, R., Davies, R., Dyer, P.S., Farman, M., Fedorova, N., Fedorova, N., Feldblyum, T.V., Fischer, R., Fosker, N., Fraser, A., Garcı, J.L., Goble, A., Goldman, G.H., Gomi, K., Griffith-Jones, S., Gwilliam, R., Garcı, M.J., Keller, N., Khouri, H., Kitamoto, K., Kobayashi, T.,

Konzack, S., Kulkarni, R., Li, W., Lord, A., Lu, C., Majoros, W.H., May, G.S., Miller, B.L., Mohamoud, Y., Molina, M., Monod, M., Mouyna, I., Mulligan, S., Murphy, L., Neil, S.O., Paulsen, I., Pen, M.A., Pertea, M., Price, C., Pritchard, B.L., Quail, M.A., Rabbinowitsch, E., Rawlins, N., Rajandream, M.-A., Reichard, U., Renauld, H., Robson, G.D., Rodr, J.M., Saunders, D., Seeger, K., Salzberg, S.L., Sanchez, Mi., Sa, J.C., Fraser, C., Galagan, J.E., Asai, K., Machida, M., Hall, N. & Barrell, B., (2005). Genomic sequence of the pathogenic and allergenic filamentous fungus *Aspergillus fumigatus*. *Nature*, **438**, pp.1151–1156.

Nigam, S. Sarma, P.V., Ghosh, P.C. & Sarma, P.U., (2001). Characterization of *Aspergillus fumigatus* protein disulfide isomerase family gene. *Gene*, **281**(1-2), pp.143–50.

Niino, Y.S., Chakraborty, S., Brown, B.J. & Massey, V., (1995). A new old yellow enzyme of *Saccahromyces cerevisiae*. *The Journal of Biological Chemistry*, **270**(5), pp.1983–1991.

Nishida, H., Motoyama, T., Suzuki, Y., Yamamoto, S., Aburatani, H., *et al*., (**2010**). Genome-wide maps of mononucleosomes and dinucleosomes containing hyperacetylated histones of *Aspergillus fumigatus*. *PloS one*, **5**(3), p.e9916.

Nishikawa, S., Fewell, S.W., Kato, Y., Brodsky, J.L. & Endo, T., (2001). Molecular chaperones in the yeast endoplasmic reticulum maintain the solubility of proteins for retrotranslocation and degradation. *The Journal of Cell Biology*, **153**(5), pp.1061–1069.

Noma, A., Sakaguchi, Y. & Suzuki, T., (**2009**). Mechanistic characterization of the sulfur-relay system for eukaryotic 2-thiouridine biogenesis at tRNA wobble positions. *Nucleic Acids Research*, **37**(4), pp.1335–1352.

Norman, B.Y. & Meldrum, U., (**1930**). The behaviour of glutathione in yeast. *Biochemistry Journal*, **24**(5), pp. 1421-1427

Nosanchuk, J.D. & Casadevall, A., (**2003**). Microreview The contribution of melanin to microbial pathogenesis. *Cellular Microbiology*, **5**(4), pp.203–223.

Nystro, T., (**2005**). Role of oxidative carbonylation in protein quality control and senescence. *EMBO Journal*, **24**(7), pp.1311–1317.

O' Gorman, M., Fuller, H.T. & Dyer, P.S., (**2009**). Discovery of a sexual cycle in the opportunistic fungal pathogen *Aspergillus fumigatus*. *Nature*, **457**, pp.4–8.

Oh, Y.T., Ahn, C.-S., Jeong, Y.J., Kim, J.G., Ro, H.-S.,Han, K.-H., Lee, C.-W. & Kim, J.W., (2013). *Aspergillus nidulans* translationally controlled tumor protein has a role in the balance between asexual and sexual differentiation and normal hyphal branching. *FEMS Microbiology Letters*, **343**(1), pp.20–25.

O'Hanlon, K.A., Cairns, T., Stack, D., Schrettl, M., Bignell, E.M., Kavanagh, K., Miggin, M., O'Keeffe, G., Larsen, T.O. & Doyle, S., (2011). Targeted disruption of non-ribosomal peptide synthetase *pes3* augments the virulence of *Aspergillus fumigatus*. *Infection and Immunity*, **79**(10), pp.3978–3992.

Ohtake, Y., Satou, A. & Yabuuchi, S., (**1990**). Isolation and characterization of glutathione biosynthesis-deficient mutants in *Saccharomyces cerevisiae. Agriculture, Biology and Chemistry*, **54**(12), pp.3145–3150.

Onken, B. & Driscoll, M., (**2010**). Metformin induces a dietary restriction–like state and the oxidative stress response to extend *C. elegans* healthspan via AMPK, LKB1 and SKN-1. *PLoS ONE*, **5**(1), pp.1–13.

Ono, B., Shirahige, Y., Nanjoh, A., Andou, N. & Ohue, H., (1988). Cysteine biosynthesis in *Saccharomyces cerevisiae*: Mutation that confers cystathionine 3-synthase deficiency. *Journal of Bacteriology*, **170**(12), pp.5883–5889.

Oosthuizen, J.L., Gomez, P., Ruan, J., Hackett, T.L., Moore, M.M., Knight, D. a, *et al.*, (**2011**). Dual organism transcriptomics of airway epithelial cells interacting with conidia of *Aspergillus fumigatus*. *PloS one*, **6**(5), p.e20527.

Østergaard, H., Tachibana, C. & Winther, J.R., (**2004**). Monitoring disulfide bond formation in the eukaryotic cytosol. *The Journal of Cell Biology*, **166**(3) pp.337–345.

Pagano, L., Giremenia, C., Mele, L., Ricci, P., Tosti, M.E., Nosari, A., Buelli, M., Picardi, M., Allione, B., Corvatta, L., D'Antonio, D., Montillo, M., Melillo, L., Chierchini, A., Cenacchi, A., Tonso, A., Cudillo, L., Candoni, A., Savignano, C., Bonini, A., Martino, P. & Favero, A.D., (2001). Infections caused by filamentous fungi in patients with hematologic malignancies. *Clinical Infectious Diseases*, **86**(8), pp.862–870.

Pahl, H.L., Kraub, B., Schulze-osthoff, K., Decker, T., Traenckner, E.B.-M., Vogt, M., Myersfl, C., Parks, T., Warring, P., Miihlbacher, A., Czernilofsky, A.-P. & Baeuerle, P.A., (1996). The immunosuppressive fungal metabolite gliotoxin specifically inhibits transcription factor Nf-kappaB. *The Journal of Experimental Medicine*, **183**(4), pp.1829–1840.

Pandey, A., Golla, R., Yoon, H., Dancis, A. & Pain, D., (2012). Persulfide formation on mitochondrial cysteine desulfurase: Enzyme activation by a eukaryote-specific interacting protein and Fe-S cluster synthesis. *Biochemical Journal*, **448** (2), pp. 171-187

Papakostas, G.I., Mischoulon, D., Shyu, I. & Fava, M., (2010). Methionine (SAMe) augmentation of serotonin reuptake inhibitors for antidepressant nonresponders with major depressive disorder: a double-blind, randomized clinical trial. *Psychiatry: Interpersonal and Biological Processes*, **167**(8), pp.942–948.

Paris, S., Wysong, D., Debeaupuis, J.-P., Shibuya, K., Philippe, B., Diamond, R.D. & Latgé, J-P., (2003). Catalases of *Aspergillus fumigatus*. *Infection and Immunity*, **71**(6), pp.3551–3562.

Park, J., Grant, C.M. Attfield, P.V., Dawes, I.W., (1997). The freeze-thaw stress response of the yeast *Saccharomyces cerevisiae* is growth phase specific and is

controlled by nutritional state via the RAS-cyclic AMP signal transduction pathway. *Microbiology*, **63**(10), pp.3818–3824.

Park, H., Bayram, Ö., Braus, G.H., Kim, S.C. & Yu, J.-H., (2012). Characterization of the velvet regulators in *Aspergillus fumigatus*. *Molecular Microbiology*, **86**(4), pp.937–953.

Paugam, A., Creuzet, C., Dupouy-Camet, J. & Roisín, M.P., (2002). *In vitro* effects of gliotoxin, a natural proteasome inhibitor , on the infectivity and proteolytic activity of *Toxoplasma gondii*. *Parisitology Research*, **88**(8), pp.785–787.

Perrin, R.M., Fedorova, N.D., Bok, J.W., Jr, R.A.C., Wortman, J.R., Kim, H Stanley, et al., (**2007**). Transcriptional regulation of chemical diversity in *Aspergillus fumigatus* by LaeA. *PLoS Pathogens*, **3**(4), pp.508–517.

Petrova, V.Y., Drescher, D., Kujumdzieva, A.V. & Schmitt, M.J., (2004). Dual targeting of yeast catalase A to peroxisomes and mitochondria. *Journal of Biochemistry*, **400**, pp.393–400.

Philippe, B., Ibrahim-Granet, O., Prévost, M C., Gougerot-Pocidalo, M.A., Perez, M.S., Meeren, A.V.D. & Latgé, J.P., (2003). Killing of *Aspergillus fumigatus* by alveolar macrophages is mediated by reactive oxidant intermediates *Infection and Immunity*, **71**(6), pp.3034–3042.

Piccirillo, S., Filomeni, G., Rotilio, G., Ciriolo, M.R. & Bru, B., (2009). Redox mechanisms involved in the selective activation of Nrf2-mediated resistance versus p53-dependent apoptosis in adenocarcinoma cells. *Journal of Biological Chemistry*, **284**(40), pp.27721–27723.

Piper, P.W., Byrne, K., Praekelt, U.M., Meacock, P., Récnacq, M. & Boucherie, H., (1994). Induction of major heat-shock proteins of *Saccharomyces cerevisiae*, including plasma membrane Hsp30, by ethanol levels above a critical threshold. *Microbiology*, **140**, pp.3031–3038.

Pompella, A., Visvikis, A., Paolicchi, A., Tata, V. & Casini, A.F., (2003). The changing faces of glutathione , a cellular protagonist. *Biochemical Pharmacology*, **66**(8), pp.1499–1503.

Post, M.J., Gastl, G. & Invasive, D.N., (**2007**). Invasive fungal infections in allogeneic and autologous stem cell transplant recipients: a single-center study of 166 transplanted patients. *Transplant Infectious Disease*, **9**(3), pp.189–195.

Pray, L., (2008). L.H. Hartwell's yeast: A model organism for studying somatic mutations and cancer. *Nature Education*, **1**(1), pp. 183.

Puri, A., Ahmad, A. & Panda, B.P., (**2010**). Development of an HPTLC-based diagnostic method for invasive aspergillosis. *Biomedical chromatography : BMC*, **24**(8), pp.887–92.

Pusztahelyi, T., Klement, É., Szajli, E., Klem, J., Miskei, M., Karányi, Z., Emri, T., Kovács, S., Orosz, G., Kovács, K.L., Medzihradszky, K.F., Prade, R.A. & Pócsi, I., (2011). Comparison of transcriptional and translational changes caused by long-term menadione exposure in *Aspergillus nidulans*. *Fungal Genetics and Biology*, **48**(2), pp.92–103.

Quazi, F. & Aitken, S.M., (**2009**). Characterization of the S289A, D mutants of yeast cystathionine β-synthase . *BBA - Proteins and Proteomics*, **1794**(6), pp.892–897.

Raasi, S. & Wolf, D.H., (**2007**). Ubiquitin receptors and ERAD : A network of pathways to the proteasome. *Seminars in Cell & Developmental Biology*, **18**, pp.780–791.

Raggam, R.B., Salzer, H.J.F., Marth, E., Heiling, B., Paulitsch, A.H. & Buzina, W., (2011). Molecular detection and characterisation of fungal heat shock protein 60. *Mycoses*, **54**(5), pp.e394–9.

Rateb, M.E. & Ebel, R., (**2011**). Secondary metabolites of fungi from marine habitats . *Natural Products*, **28**(11), pp.290–344.

Reeves, E.P., Messina, C.G.M., Doyle, S. & Kavanagh, K., (2004). Correlation between gliotoxin production and virulence of *Aspergillus fumigatus* in *Galleria mellonella*. *Mycopathologia*, **158**(1), pp.73–79.

Reeves, E.P., Reiber, K., Neville, C., Scheibner, O. & Kavanagh, K., (2006). A nonribosomal peptide synthetase (*Pes1*) confers protection against oxidative stress in *Aspergillus fumigatus*. *FEBS Journal*, **273**(13), pp.3038–3053.

Renwick, J., Daly, P., Reeves, E.P. & Kavanagh, K., (2007). Susceptibility of larvae of *Galleria mellonella* to infection by *Aspergillus fumigatus* is dependent upon stage of conidial germination. *Medical Mycology*, **161**(6), pp.377–384.

Renwick, J., Reeves, E.P., Wientjes, F.B. & Kavanagh, K., (2006b). Translocation of proteins homologous to human neutrophil p47 phox and p67 phox to the cell membrane in activated hemocytes of *Galleria mellonella*. *Developmental and Comparative Immunology*, **31**(4), pp.347–359.

Rinnerthaler, M., Jarolim, S., Heeren, G., Palle, E., Perju, S., Klinger, H., Bogengruber, E., Madeo, F., Braun, R.J., Breitenbach-koller, L., Breitenbach, Mi. & Laun, P., (2006). MMI1 (YKL056c , TMA19), the yeast orthologue of the translationally controlled tumor protein (TCTP) has apoptotic functions and interacts with both microtubules and mitochondria. *Biochemica et Biophysica Acta*, **1757**(5-6), pp.631 – 638.

Rodrigues-Pousada, C.A., Nevitt, T., Menezes, R., Azevedo, D., Pereira, J. & Amaral, C., (2004). Yeast activator proteins and stress response: An overview. *FEBS letters*, **567**(1), pp.80–5.

Rowan, R., Moran, C., Mccann, M. & Kavanagh, K., (2009). Use of *Galleria mellonella* larvae to evaluate the *in vivo* anti-fungal activity of [Ag_2 (mal)$(phen)_3$]. *Biometals*, **2**, pp.461–467.

Roy, H., Ling, J., Alfonzo, J. & Ibba, M., (2005). Loss of editing activity during the evolution of mitochondrial phenylalanyl-tRNA synthetase. *Journal of Biological Chemistry*, **280**(46), pp.38186–38192.

Ruiz-Díez, B., (**2002**). Strategies for the transformation of filamentous fungi. *Journal of Applied Microbiology*, **92**(2), pp.189–195.

Salazar, M., Vongsangnak, W., Panagiotou, G., Andersen, M.R. & Nielsen, J. (2009). Uncovering transcriptional regulation of glycerol metabolism in *Aspergilli* through genome-wide gene expression data analysis. *Molecular genetics and genomics : MGG*, **282**(6), pp.571–86.

Sarker S., **Perlstein E.O., Pineau S., Cordenier A., Maglathlin R.L., Webster J.A., Lewis T.A., O'Kane C.J., Schreiber S.L. & Rubinsztein D.C., (2007).** Small molecules enhance autophagy and reduce toxicity in Huntington's disease models. *Nat Chem Biol*, **3**(6), pp331-338.

Sato, N., Iwata, S., Nakamura, K., Hori, T., Mori, K. & Yodoi, J., (1995). Thiol-mediated redox regulation of apoptosis. *The Journal of Immunology*, **154**(7), pp.3194–3203.

Sato, I., Shimizu, M., Hoshino, T. & Takaya, N., (2013). The glutathione system of *Aspergillus nidulans* involves a fungus-specific glutathione S-transferase. *Journal of Biological Chemistry*, **284**(12), pp.8042–8053.

Schafer, F.Q. & Buettner, G.R., (**2001**). Redox environment of the cell as viewed through the redox state of the glutathione disulfide/glutathione couple. *Free Radical Biology and Medicine*, **30**(11), pp.1191–1212.

Scharf, D.H., Remme, N., Heinekamp, T., Hortschansky, P., Brakhage, A. & Hertweck, C., (2010). Transannular disulfide formation in gliotoxin biosynthesis and its role in self-resistance of the human pathogen *Aspergillus fumigatus*. , (8), pp.10136–10141.

Scharf, D.H., Heinekamp, T., Remme, N., Hortschansky, P., Brakhage, A. & Hertweck, C., (2011). Biosynthesis and function of gliotoxin in *Aspergillus fumigatus*. *Applied Microbiology*, **2005**.

Scharf, D.H., Chankhamjon, P., Scherlach, K., Heinekamp, T., Roth, M., Brakhage, A. & Hertweck, C., (2012). Epidithiol Formation by an Unprecedented Twin Carbon – Sulfur Lyase in the Gliotoxin Pathway. *Natural Sulfur Compounds*, **51**, pp.10064 –10068.

Scharf, D.H., Chankhamjon, P., Scherlach, K., Heinekamp, T., Willing, K., Brakhage, A. & Hertweck, C., (2013). Epidithiodiketopiperazine biosynthesis: A four-enzyme cascade converts glutathione conjugates into transannular disulfide bridges. *Angewadte Chemie*, **52**, pp.11092 –11095.

Schimel, J., Balser, T.C. & Wallenstein, M., (**2007**). Microbial stress-response physiology and its implications for ecosystem function. *Microbial Ecology*, **88**(6), pp.1386–1394.

Schmaler-ripcke, J., Sugareva, V., Gebhardt, P., Winkler, R., Kniemeyer, O., Heinekamp, T. & Brakhage, A., (2009). Production of Pyomelanin , a second type of melanin , via the tyrosine degradation pathway in *Aspergillus fumigatus* □. *Applied and Environmental Microbiology*, **75**(2), pp.493–503.

Schrettl, M., Bignell, E., Kragl, C., Joechl, C., Rogers, T., Herbert, N.A., Haynes, K. & Haas, H., (2004). Assimilation is essential for *Aspergillus fumigatus* virulence. *The Journal of Experimental Medicine*, **200**(9), pp.1–7.

Schrettl, M., Beckmann, N., Varga, J., Heinekamp, T., Jacobsen, I.D., Jöchl, C., *et al*., (**2010**). HapX-mediated adaption to iron starvation is crucial for virulence of *Aspergillus fumigatus*. *PLoS pathogens*, **6**(9), p.e1001124.

Schrettl, M., Carberry, S., Kavanagh, K., Haas, H., Jones, G.W., O'Brien, J., *et al*., (**2010**). Self-protection against gliotoxin--a component of the gliotoxin

biosynthetic cluster, GliT, completely protects *Aspergillus fumigatus* against exogenous gliotoxin. *PLoS pathogens*, **6**(6), p.e1000952.

Schulz, B., Boyle, C., Draeger, S., Ro, A.-K. & Krohn, K., (2002). Endophytic fungi : a source of novel biologically active secondary metabolites. *Mycology Research*, **106**(9), pp.996–1004.

Seed, K.D. & Dennis, J.J., (**2008**). Development of *Galleria mellonella* as an alternative infection model for the *Burkholderia cepacia* complex. *Infection and Immunity*, **76**(3), pp.1267–1275.

Seymourt, I.J. & Piper, P.W., (**1999**). Stress induction of HSP30, the plasma membrane heat shock protein gene of *Saccharomyces cerevisiae*, appears not to use known stress-regulate transcription factors. *Microbiology*, **145**, pp.231–239.

Sha, W., Martins, A.M., Laubenbacher, R., Mendes, P. & Shulaev, V., (2013). The genome-wide early temporal response of *Saccharomyces cerevisiae* to oxidative stress induced by cumene hydroperoxide. *PLoS ONE*, **8**(9), pp.1–15.

Sharma, D. & Masison, D.C., (**2008**). Functionally redundant isoforms of a yeast Hsp70 chaperone subfamily have different anti-prion effects. *Genetics*, **179**(3), pp.1301–1311.

Sharma, M., Soni, R., Nazir, A., Oberoi, H.S. & Chadha, B.S., (2011). Evaluation of glycosyl hydrolases in the secretome of *Aspergillus fumigatus* and saccharification of alkali-treated rice straw. *Applied biochemistry and biotechnology*, **163**(5), pp.577–91.

Sheppard, D.C., Rieg, G., Chiang, L.Y., Filler, S.G., Edwards, J.E. & Ibrahim, A.S., (2004). Novel inhalational murine model of invasive pulmonary Aspergillosis. *Antimicrobial Agents and Chemotherapy*, **48**(5), pp.1908–1911.

Sherif, R. & Segal, B.H., (**2012**). Pulmonary Aspergillosis: clinical presentation, diagnositc tests, management and complications. *Current Opinion in Pulmonary Medicine*, **16**(3), pp.242–250.

Shimizu, M., Fujii, T., Masuo, S. & Takaya, N., (2010). Mechanism of *de novo* branched-chain amino acid synthesis as an alternative electron sink in hypoxic *Aspergillus nidulans* cells. *Applied and Environmental Microbiology*, **76**(5), pp.1507–1515.

Shwab, E.K., Bok, J.W., Tribus, M., Graessle, S. & Keller, N.P., (2007). Histone deacetylase activity regulates chemical diversity in *Aspergillus*. *Eukaryotic Cell*, **6**(9), pp.1656–1664.

Silberg, J.J., Tapley, T.L., Kevin, G.H. & Vickery, L.E., (2013). Enzyme catalysis and regulation: Regulation of the HscA ATPase reaction cycle by the co-chaperone HscB and the iron-sulfur cluster assembly protein IscU. *Biochemistry*, **279**(52), pp.53924–53931.

Sims, A.H., Gent, M.E., Lanthaler, K., D.-C., Nigel S. Oliver, S.G. & Robson, G.D., (2005). Transcriptome analysis of recombinant protein secretion by *Aspergillus nidulans* and the unfolded-protein response *in vivo*. *Applied and Environmental Microbiology*, **71**(5), pp.2737–2747.

Singh, B., Sharma, G.L., Oellerich, M., Kumar, R., Singh, S., Bhadoria, D.P., Katyal, A., Reichard, U. & Asif, A.R., (2010). Novel cytosolic allergens of *Aspergillus fumigatus* identified from germinating conidia research articles. *Journal of Proteome Research*, **9**(11) , pp.5530–5541.

Singhal, A., Arora, G., Sajid, A., Maji, A., Bhat, A., Virmani, R., Upadhyay, S., Nandicoori, V.K., Sengupta, S. & Singh, Y., (2013). Regulation of homocysteine metabolism by *Mycobacterium tuberculosis*. *Scientific Reports*, **3**(2264), pp.1–13.

Slater, J.L., Gregson, L., Denning, D.W. & Warn, P.A., (2011). Pathogenicity of *Aspergillus fumigatus* mutants assessed in *Galleria mellonella* matches that in mice. *Medical Mycology*, **49**(1), pp.107–113.

Slepneva, I.A., Glupov, V.V., Sergeeva, S.V. & Khramtsov, V.V., (1999). EPR detection of reactive oxygen species in hemolymph of *Galleria mellonella* and

Dendrolimus superans sibiricus (*Lepidoptera*) larvae. *Biochemical and Biophysical Research Communications*, **264**, pp.212–215.

Som, T. & Kolaparthit, V.S.R., (**1994**). Developmental decisions in *Aspergillus nidulans* are modulated by Ras activity. *Molecular and Cellular Biology*, **14**(8), pp.5333–5348.

Sørensen, L.M., Lametsch, R., Andersen, M.R., Nielsen, P.V. & Frisvad, J.C., (2009). Proteome analysis of *Aspergillus niger*: Lactate added in strach-containing medium can increase production of the mycotoxin fumonisin B_2 by modifiying acetyl-CoA metabolism*BMC Microbiology*, **9**(255), pp.1–20.

Spikes, S. Xu, R., Nguyen, C.K., Chamilos, G., Kontoyiannis, D.P., Jacobson, R.H., Ejzykowicz, D.E., Chiang, L.Y., Filler, S.G. & May, G.S., (2008). Gliotoxin production in *Aspergillus fumigatus* contributes to host-specific differences in virulence. *The Journal of infectious diseases*, **197**(3), pp.479–86.

Stanzani, M., Orciuolo, E., Lewis, R., Kontoyiannis, D.P., Martins, S.L.R., St.John, L.S. & Komanduri, K.V., (2005). *Aspergillus fumigatus* suppresses the human cellular immune response via gliotoxin-mediated apoptosis of monocytes. *Blood*, **105**(6), pp.2258–2265.

Steinman, H.M., (**1980**). The amino acid sequence of copper-zinc superoxide dismutase from bakers' Yeast. *The Journal of Biological Chemistry*, **255**(14), pp.6758–6765.

TunSugui, J., Pardo, J., Chang, Y.C., Zarember, K.A., Nardone, G., Galvez, E.M., Mu, A., Gallin, J.I., Simon, M.M. & Kwon-chung, K.J., (2007). Gliotoxin is a virulence factor of *Aspergillus fumigatus*: *gliP* deletion attenuates virulence in mice immunosuppressed with hydrocortisone. *Eukaryotic cell*, **6**(9), pp.1562–9.

Sugui, J., Kim, H. S., Zarember, K., Chang, Y.C., Gallin, J.I., Nierman, W.C. & Kwon-Chung, K.J., (2008). Genes differentially expressed in conidia and hyphae

of *Aspergillus fumigatus* upon exposure to human neutrophils. *PloS one*, **3**(7), p.e2655.

Suh, M.-J. Fedorova, N.D., Cagas, S.E., Hastings, S., Fleischmann, R.D., Peterson, S.N., Perlin, D.S., Nierman, W.C., Pieper, R. & Momany, M., (2012). Development stage-specific proteomic profiling uncovers small, lineage specific proteins most abundant in the *Aspergillus fumigatus* conidial proteome. *Proteome science*, **10**(1), p.30.

Suhadolnik, R.J. & Chenoweth, R.G., (**1958**). Biosynthesis of gliotoxin. 1.l incorporation of phenylalanine-1- and-2-C14. *Journal of the American Chemical Society*, **80**(2), pp.4391–4392.

Suliman, H.S. Sawyer, G.M., Appling, D.R. & Robertus, J.D., (2005). Purification and properties of cobalamin-independent methionine synthase from *Candida albicans* and *Saccharomyces cerevisiae*. *Archives of Biochemistry and Biophysics*, **441**(1), pp.56–63.

Sutton, P. Newcombe, N.R., Waring, P. & Mullbacher, A., (1994). *In vivo* immunosuppressive activity of gliotoxin, a metabolite produced by human pathogenic fungi. *Microbiology*, **62**(4), pp.1192–1198.

Sutton, P. & Waring, P., (**1996**). Exacerbation of invasive aspergillosis by the immunosuppressive fungal metabolite, gliotoxin. *Immunology and Cell Biology*, **74**, pp.318–322.

Tehlivets, O., Hasslacher, M. & Kohlwein, S.D., (**2004**). S-Adenosyl- L - homocysteine hydrolase in yeast : key enzyme of methylation metabolism and coordinated regulation with phospholipid synthesis. *FEBS Letters*, **577**, pp.501–506.

Terashima, H. Yabuki, N., Arisawa, M., Hamada, K. & Kitada, K., (2000). Up-regulation of genes encoding glycosylphosphatidylinositol (GPI) -attached proteins

in response to cell wall damage caused by disruption of FKS1 in *Saccharomyces cerevisiae*. *Molecular and General Genetics*, **264**, pp.64–74.

Teutschbein, J., Albrecht, D., Potsch, M., Guthke, R., Aimanianda, V., Latgé, J.-P. Brakhage, A. & Kniemeyer, O., (2010). Proteome profiling and functional classification of intracellular proteins from conidia of the human-pathogenic mold *Aspergillus fumigatus* research articles. *Journal of Proteome Research*, **9**(10), pp.3427–3442.

Thomas, D. & Surdin-kerjan, Y., (**1997**). Metabolism of sulfur amino acids in *Saccharomyces cerevisiae*. *Microbiology*, **61**(4), pp.503–532.

Thomson, G.R. & Patterson, T.F., (**2008**). Pulmonary Aspergillosis. *Critical Care*, **28**(2), pp.103–110.

Thorpe, G.W. Fong, C.S., Alic, N., Higgins, V.J. & Dawes, I.W., (2004). Cells have distinct mechanisms to maintain protection against different reactive oxygen species: oxidative-stress-response genes.*PNAS*, **101**(17), pp.6564–9.

Todorova, T.T. Petrova, V.Y., Vuilleumier, S. & Kujumdzieva, A.V., (2009). Response to different oxidants of *Saccharomyces cerevisiae ure2* mutant. *Archives of Microbiology*, **191**(11), pp.837–845.

Tomee, J.F.C. & Werf, T.S. Van Der, (**2001**). Pulmonary aspergillosis. *The Netherlands Journal of Medicine*, **59**(5), pp.244–258.

Trotter, E.W. & Grant, C.M., (**2002**). Thioredoxins are required for protection against a reductive stress in the yeast *Saccharomyces cerevisiae*. *Molecular Microbiology*, **46**, pp.869–878.

Tsunawaki, S. Yoshida, L.S., Nishida, S., Kobayashi, T. & Shimoyama, T., (2004). Fungal metabolite gliotoxin inhibits assembly of the human respiratory burst NADPH oxidase. *Infection and Immunity*, **72**(6), pp.3373–3382.

Tunnicliffe, H.E., (**1925**).The occurrence of quantitative estimation of glutathione in tissues. *Biochemistry Journal* **19** (2) pp. 194-198

Valiante, V. Zhang, L., Vogelstein, B. & Kinzler, K.W.., (2009). The MpkA MAP kinase module regulates cell wall integrity signalling and pyomelanin formation in *Aspergillus fumigatus*. *Fungal Genetics and Biology*, **46**(12), pp.909–918.

Velculescu, V.E. et al., (**1995**). Serial Analysis of Gene Expression. *Science*, **270**(5235), pp.484–487.

Vera, J.C., Wheat, C.W., Fescemyer, H.W., Frilander, M.J., Crawford, D.L., Hanski, I. & Marden, J.H.., (2008). Rapid transcriptome characterization for a non-model organism using 454 pyrosequencing. *Molecular Ecology*, **17**(7), pp.1636–1647.

Verweij, P.E. Oakley, K.L., Morrissey, J., Morrissey, G. & Denning, D.W., (1998). Efficacy of LY303366 against Amphotericin B-susceptible and -resistant *Aspergillus fumigatus* in a murine model of Invasive Aspergillosis. *Antimicrobial Agents and Chemotherapy*, **42**(4), pp.873–878.

Vödisch, M., Albrecht, D., Lessing, F., Schmidt, A.D., Winkler, R., Guthke, R., Brakhage, A. & Kniemeyer, O., (2009). Two-dimensional proteome reference maps for the human pathogenic filamentous fungus *Aspergillus fumigatus*. *Proteomics*, **9**(5), pp.1407–15.

Vödisch, M. Scherlach, K., Winkler, R., Hertweck, C., Braun, H.-P., Roth, M., Haas, H., Werner, E.R., Brakhage, A. & Kniemeyer, O (2011). Analysis of the *Aspergillus fumigatus* proteome reveals metabolic changes and the activation of the pseurotin A biosynthesis gene cluster in response to hypoxia. *Journal of proteome research*, **10**(5), pp.2508–24.

Walsh, C.T. Chen, H., Keating, T.A., Hubbard, B.K., Losey, H.C., Luo, L., Marshall, G.C., Miller, D.A. & Patel, H.M., (**2001**). Tailoring enzymes that

modify nonribosomal peptides during and after chain elongation on NRPS assembly lines. *Current Opinion in Chemical Biology*, **5**(5), pp.525–534.

Wang, Z., Gerstein, M. & Snyder, M., (**2009**). RNA-Seq: a revolutionary tool for transcriptomics. *Nature Reviews Genetics*, **10**(1), pp.57–63.

Waring, P. Eichner, R.D., Mullbacher, A. & Sjaarda, A., (**1988**). Gliotoxin induces apoptosis in macrophages unrelated to Its antiphagocytic properties. *The Journal of Biological Chemistry*, **263**(34), pp.18493–18499.

Waring, P., (**1990**). DNA Fragmentation Induced in Macrophages by Gliotoxin does not require protein synthesis and is preceded by raised inositol triphosphate levels. *Biochemistry*, **265**(24), pp.14476–14480.

Waring, P., Sjaarda, A. & Lin, Q.H., (**1995**). Gliotoxin inactivates alcohol dehydrogenase by either covalent modification or free radical damage mediated by redox cycling. *Biochemical Pharmacology*, **49**(9), pp.1195–1201.

Waring, P. & Beaver, J., (**1996**). Gliotoxin and Related Epipolythiodioxopiperazines. *Science*, **27**(8), pp.1311–1316.

Wartenberg, D., Lapp, K., Jacobsen, I.D., Dahse, H.-M., Kniemeyer, O., Heinekamp, T. & Brakhage, A., (**2011**). Secretome analysis of *Aspergillus fumigatus* reveals Asp-hemolysin as a major secreted protein. *International journal of medical microbiology : IJMM*, **301**(7), pp.602–11.

Wheeler, G.L. Quinn, K.A., Perrone, G., Dawes, I.W.& Grant, C.M., (**2002**). Glutathione regulates the expression of γ -glutamylcysteine synthetase via the Met4 transcription factor. *Molecular Microbiology*, pp.545–556.

Wheeler, G.L. Trotter, E.W., Dawes, I.W. & Grant, C.M., (**2003**). Coupling of the transcriptional regulation of glutathione biosynthesis to the availability of glutathione and methionine via the Met4 and Yap1 transcription factors. *Biochemistry*, **278**(50), pp.49920 –49928.

Wiese, S. Reidegeld, K.A., Meyer, H.E. & Warscheid, B., (**2007**). Protein labeling by iTRAQ : A new tool for quantitative mass spectrometry in proteome research. *Proteomics*, **7**(3), pp.340–350.

Winterbourn, C. & Metodiewa, D., (**1999**). Reactivity of biologically important thiol compunds with superoxide and hydrogen peroxide. *Science*, **27**(99), pp.322–328.

Winther, J.R., (**2007**). Cytoplasmic glutathione redox status determines survival upon exposure to the thiol-oxidant 4 , 4 0 -dipyridyl disulfide. *FEMS Yeast Research*, **7**, pp.391–403.

Wu, A. & Moye-rowleyl, W.S., (**1994**). *GSH1*, which encodes y-glutamylcysteine synthetase , is a target gene for yAP-i transcriptional regulation. *Molecular and Cellular Biology*, **14**(9), pp.5832–5839.

Wus, A. Wemmieq, J.A., Edgingtonqll, N.P., Guevaraq, J.L., Moye-rowleysqts, W.S. & Bank, D., (**1993**). Yeast bZip proteins mediate pleiotropic drug and metal resistance. *The Journal of Biological Chemistry* , **288**(25) pp 18850-18858

Xiao, P., Shin, K., Wang, T. & Yu, J., (**2010**). *Aspergillus fumigatus flbB* encodes two basic leucine zipper domain (bZIP) proteins required for proper asexual development and gliotoxin production. *Eukaryotic cell*, **9**(11), pp.1711–1723.

Yamada A., Kataoka T. & Nagai K. (2000). The fungal metabolite gliotoxin; immunosuppressive activity on CTL-mediated cytotoxicity. *Immunol* Lett, 71, 27-32

Yang, Y. et al., (**2010**). Oxidative stress inhibits vascular KATP channels by S-glutathionylation. *The Journal of biological chemistry*, **285**(49), pp 38461-38468

Yarunin, A., Govind, V., et al., (**2005**). Functional link between ribosome formation and biogenesis of iron – sulfur proteins. *EMBO Journal*, **24**(3), pp.580–588.

Yarunin, A., Panse, V.G., et al., (**2005**). Functional link between ribosome formation and biogenesis of iron-sulfur proteins. *The EMBO journal*, **24**(3), pp.580–8.

Yen, J.L. Flick, K., Papagiannis, C.V., Mathur, R., Tyrrell, A., Ouni, I., Kaake, R.M., Huang, L. & Kaiser, P., (**2012**). Article Signal-Induced disassembly of the SCF Ubiquitin Ligase complex by Cdc48 / p97. *Molecular Cell*, **48**(2), pp.288–297.

Yoshiga, T. Georgieva, T., Dunkov, B.C., Harizanova, N., Ralchev, K. & Law, J.H., (**1999**). *Drosophila melanogaster* transferrin and up-regulation on bacterial infection. *European Journal of Biochemistry*, **260**(2), pp.414–420.

Yoshikawa, K. Tanaka, T., Furusawa, C., Nagahisa, K. & Hirasawa, T., (**2009**). Comprehensive phenotypic analysis for identification of genes a affecting growth under ethanol stress in *Saccharomyces cerevisiae*. *FEMS Yeast Research*, **9**(1), pp.32–44.

Yost, F.J. & Fridovich, I., (**1973**). An Iron-containing Superoxide Dismutase from *Escherichia coli*. *Journal of Biological Chemistry*, **248**(14), pp.4905–4908.

Youn, H.-D. Kim, E., Roe, J., Hah, Y. & Kang, S., (**1996**). A novel nickel-containing superoxide dismutase from *Streptomyces spp* . *Biochemical Journal*, **318**, pp.889–896.

Yu, J. Hamari, Z., Han, K. & Seo, J., (**2004**). Double-joint PCR : a PCR-based molecular tool for gene manipulations in filamentous fungi. *Fungal Genetics and Biology*, **41**(11), pp.973–981.

Zalkinz, H. Paluh, J.L., Cleemputg, M.V., Moye, W.S. & Yanofskygll, C., (**1984**). Nucleotide sequence of *Saccharomyces cerevisiae* genes *TRPB* and *TRP3* encoding bifunctional anthranilate synthase : Indole-3-glycerol phosphate synthase *Journal of Biological Chemistry*, **259** (6), pp 3985-3992.

Zhang, L. Li, F. & Nie, L., (**2009**). Comparative proteomic analysis of an *Aspergillus fumigatus* mutant deficient in glucosidase I (AfCwh41). *Microbiology*, **155**(Pt 7), pp.2157–67.

Zhang, W., Li, F. & Nie, L., (**2010**). Integrating multiple " omics " analysis for microbial biology : application and methodologies. *Microbiology*, **156**, pp.287–301.

Zhao, Y. Paderu, P., Park, S., Senter, M. & Perlin, D.S., (**2012**). Expression turnover profiling o monitor the antifungal activities of Amphotericin B , voriconazole , and micafungin against *Aspergillus fumigatus*. *Antimicrobial Agents and Chemotherapy*, **56**(5), pp.2770–2772.

Zilberberg, M.D., Shorr, A.F. & Kollef, M.H., (**2008**). Secular Trends in Candidemia - Related Hospitalization in the United States , 2000 – 2005. *Infection Control and Hospital Epidemiology*, **29**(10), pp.978– 980.